Characterisation of the enterococcal sensor kinase $VanS_A$ and its ligand binding properties

By

Charlotte Sarah Hughes

A thesis submitted in partial fulfilment for the requirements for the degree of Doctor of Philosophy at the University of Central Lancashire

Approved May 2018

STUDENT DECLARATION FORM

Concurrent registration for two or more academic awards

I declare that while registered as a candidate for the research degree, I have not been a registered candidate or enrolled student for another award of the University or other academic or professional institution

_____

Material submitted for another award

I declare that no material contained in the thesis has been used in any other submission for an academic award and is solely my own work

_____

(state award and awarding body and list the material below):

Collaboration

Where a candidate's research programme is part of a collaborative project, the thesis must indicate in addition clearly the candidate's individual contribution and the extent of the collaboration. Please state below:

Signature of Candidate _____

Type of Award _____

School _____

ABSTRACT

The enterococci are a leading cause of Hospital-acquired infections (HAI) in the UK, with increasing numbers identified as resistant towards “last line” glycopeptide antibiotics (GPAs) vancomycin and teicoplanin. Of the two types of vancomycin resistance in enterococci, type A (vancomycin and teicoplanin resistant) rather than type B (vancomycin resistant, teicoplanin susceptible) is the most prominent in the UK and is the system that will described in this Thesis.

All vancomycin resistances in Gram-positive bacteria including the enterococci are controlled by a two-component signal transduction system (TCS). TCSs allow the organism to appropriately respond to external stimuli, and are composed of a membrane-bound sensor kinase and a partnered cytosolic regulator which upon stimulation by an activating ligand initiate appropriated adaptive responses by the bacteria. Type A vancomycin resistance in the enterococci is regulated by the $VanR_AS_A$ TCS composed of $VanS_A$ (the sensor) and $VanR_A$ (the partner regulator). The activating stimulus of $VanS_A$ is still unknown.

Following successful production of intact and active membrane sensor protein $VanS_A$, the structure and function effects of a range of candidate compounds (GPAs vancomycin and teicoplanin, peptidoglycan compounds, and sugars) were screened using biophysical approaches available at Beamline 23, Diamond Light Source Ltd, coupled with phosphorylation activity assays. Results identified GPAs as the only materials binding $VanS_A$ suggesting a change in the local tertiary structure of $VanS_A$ and roles for aromatic amino acids tryptophan and tyrosine in ligand recognition confirmed using circular dichroism, magnetic synchrotron radiation circular dichroism and fluorescence spectroscopy. Characterisation of the interaction revealed differences in the affinity of the two GPAs; 70 µM for vancomycin , and 30 µM for teicoplanin. Furthermore, only in the presence of vancomycin and teicoplanin were $VanS_A$ phosphorylation rates increased and longer-lived relative to $VanS_A$ alone, overall suggesting the roles of GPAs as the activating ligands for the onset of type A vancomycin resistance in the enterococci.

ACKNOWLEDGEMENTS

Firstly, I would like to thank my Parents for their endless support. For tolerating my emotions, attitudes and dramas. Truly without it I would not be where I am today.

To my family and friends, for being a “normal” escape away from the lab.

I would also like to thank my Supervisors Rohanah and Mary for their help and guidance throughout my studentship during dramas both in and out of the lab.

I would like to extend my thanks to everyone in the labs at the Biomedical Research Facility (UCLan), Diamond (especially Beamline staff on B23), MPL and RCaH for their help and being around for a gossip between experiments and keeping me sane during the waits of long incubation periods – you helped to make the long days bearable.

Finally, I would like to thank the University of Central Lancashire (UCLan) and Diamond Light Source for financial support for the duration of the studentship.

I have learned a lot, not only science but about myself and I am truly grateful for the opportunities I have been given.

LIST OF ABBREVIATIONS

Hospital-acquired infections (**HAI**)

Glycopeptide antibiotics (**GPAs**)

Two-component signal transduction system (**TCS**)

Vancomycin-resistant enterococci (**VRE**)

Minimal Inhibitory Concentration (**MIC**)

Histidine kinases (**HKs**)

Response regulator (**RR**)

Histidine protein kinase (**HPK**)

Membrane sensor kinase (**MSK**)

Adenosine Triphosphate (**ATP**)

Circular Dichroism (**CD**)

Synchrotron radiation circular dichroism (**SRCD**)

Magnetic synchrotron radiation circular dichroism (**MSRCD**)

Fluorescence spectroscopy (**Fluorescence**)

Dynamic light scattering (**DLS**)

Right circularly polarised (**RCP**)

Left circularly polarised (**LCP**)

Luria-Bertani (**LB**)

Isopropyl β-D-1-thiogalactopyranoside (**IPTG**)

Ethylenediaminetetraacetic acid (**EDTA**)

n-Dodecyl β-D-maltoside (**DDM**)

Molecular weight cut-off (**MWCO**)

Polyvinylidene difluoride (**PVDF**)

Size-Exclusion Chromatography Multi-Angle Light Scattering (**SEC-MALS**)

Sodium Dodecyl Sulfate Polyacrylamide Gel Electrophoresis (**SDS-PAGE**)

Bovine serum albumin (**BSA**)

Dynamic light scattering (**DLS**)

Polymerase chain reaction (**PCR**)

N-acetylmuramic acid (**NAM**)

N-acetylglucosamine (**NAG**)

D- Ala -D- Ala, Ala-D-γ-Glu-Lys-D-Ala-D-Ala (**pentapeptide**)

Phos-tag™ acrylamide (**PTA**)

Phos-tag™ Biotin BTL-111 (**PTB-111**)

Universal Kinase Assay Kit®, R & D systems (**R & D**)

Adenosine triphosphate (**ATP**)

Adenosine diphosphate (**ADP**)

TABLE OF CONTENTS
LIST OF TABLES

TABLE OF CONTENTS
LIST OF FIGURES

TABLE OF CONTENTS

CHAPTER 1:
INTRODUCTION

1.1. Overview of antibiotic resistance in Gram-positive bacteria

1.1.1. History of drug discovery and the development of antibacterial resistance within Gram-positive bacteria

Throughout the history of the discovery and clinical use of antibiotics, there has been a trend for the development of resistance within target organisms within a decade of the intensive use of an antibiotic best exemplified in the period after the 'Golden Age of Antibiotics' and the intensive use of penicillin during the 1940s and 1950s followed by the rise of penicillin resistant organisms during the 1960s. Current clinical concerns relate to emerging resistance towards the glycopeptide antibiotic (GPA) vancomycin. Commonly used during the 1970s-1980s due to its effectiveness against Gram-positive organisms which are often agents of post-operation inflammations (reviewed in Gerard D Wright, 2007); in addition to its effectiveness against emerging multi-resistant organisms, vancomycin was prescribed >100-fold more frequently during this period and into the millennia (Kirst, Thompson, & Nicas, 1998). This wide-spread application of vancomycin is considered a main factor in the development of vancomycin-resistant enterococci (VRE) (Gerding, 1997).

1.1.2. Overview of glycopeptide family of antibiotics mode of action

Vancomycin is a glycopeptide (GPA) which targets cell-wall component bridging and synthesis by targeting the terminal D-Ala-D-Ala dipeptide of the pentapeptide chains of peptidoglycan precursors (Fig. 1-1). High affinity hydrogen bonds are formed between vancomycin and peptidoglycan precursors (Pfeiffer 1981; Barna and Williams 1984; Liu *et al*. 1994), sequestering the peptidoglycan precursors and physically inhibiting transpeptidase and transglycosylase cross-linking for the formation of mature peptidoglycan cell walls (Courvalin 2006; Kahne *et al*. 2005; Nieto and Perkins 1971; Perkins and Nieto 1974; Reynolds 1989). Dimerisation of vancomycin (dimerisation domain shown in Fig. 1-1), which is thought to reduce the MIC (Minimal Inhibitory Concentration) by improving the entropic penalties for vancomycin:peptidoglycan complex formation as a dimer than

the monomeric form (Barna and Williams, 1984; Gerhard *et al.*, 1993; Loll *et al.*, 1998; Mackay *et al.*, 1994).

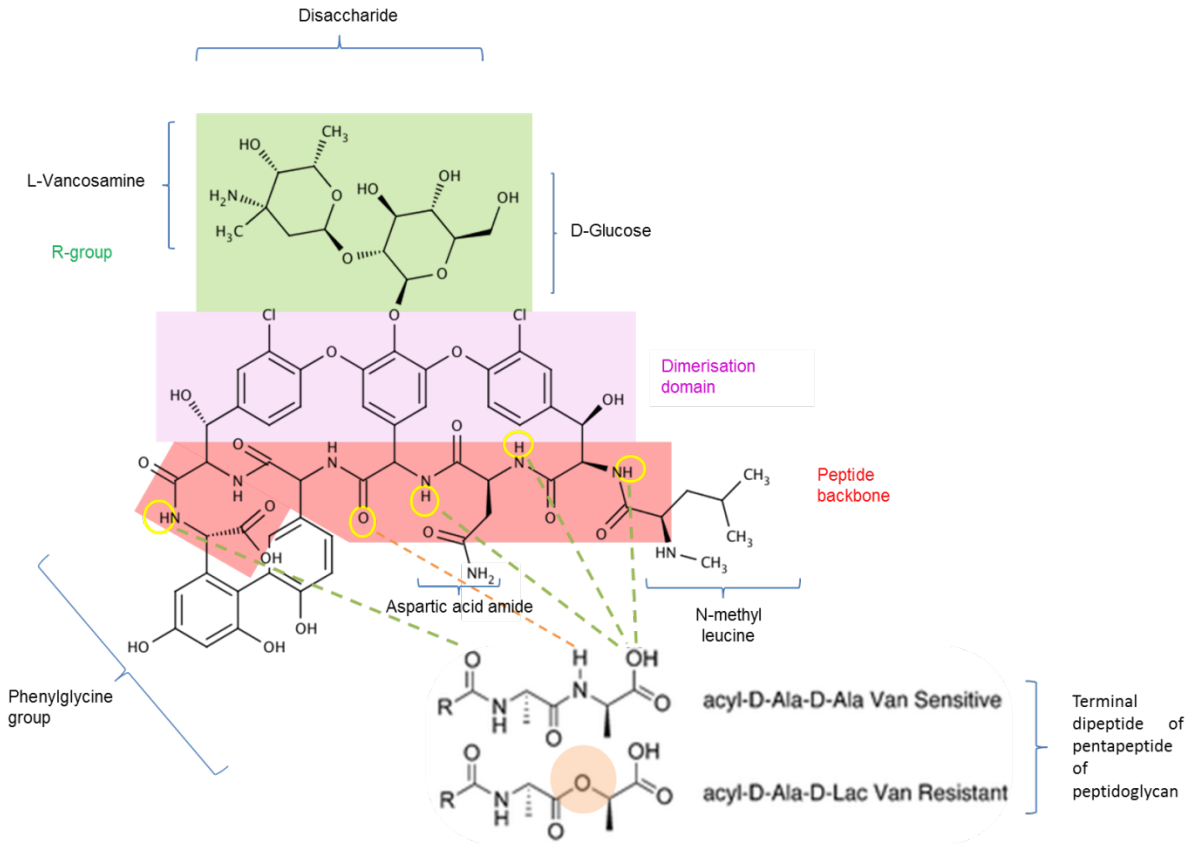

Figure 1-1: Structure of vancomycin-peptidoglycan complex.

Five hydrogen bonds (circled in yellow) form between vancomycin and D-ala-D-ala dipeptide of peptidoglycan precursors, leading to the formation of a complex which cannot be cross-linked into the cell wall. NH to O substitution (orange circle) resulting from the substitution of D-ala-D-ala with D-ala-D-lac or D-ala-D-ser in the terminal dipeptide of peptidoglycan precursors in vancomycin resistant strains causes a 1000-fold reduction in affinity of vancomycin for dipeptide target due to removal of one hydrogen bond acceptor (NH) and increasing electrostatic repulsion. The structure of vancomycin is also shown. Peptide backbone (red shading), dimerisation domain (purple shading). R-group (green) which varies within the glycopeptide group and is the name-giving group for vancomycin is composed of a disaccharide of L-vancosamine and D-glucose.

Teicoplanin, a member of the GPA family of antibiotics, is distinctly different to vancomycin. Discovered as a fermentation product from *Streptomyces teichomyceticus* (Parenti *et al*. 1978; Bardone *et al*. 1978), teicoplanin is a group of 9 isoforms (5 major, 4 minor) (Borghi *et al*. 1984; Borghi *et al*. 1989; Zanol *et al*. 1988). Clinically, teicoplanin is more effective than vancomycin due to its lower MIC towards streptococci and Gram-positive anaerobes (Greenwood, 1988) including enterococci (Y. C. Liu et al., 2011) with fewer reported side effects (Campoli-Richards, Brogden, & Faulds, 1990; Svetitsky, Leibovici, & Paul, 2009). As with other GPAs, teicoplanin activity was shown to involve the targeting of the terminal D-Ala-D-Ala dipeptide of peptidoglycan (Parenti 1986; Parenti *et al*. 1978) by formation of 5 hydrogen bonds in a manner similar to that described for vancomycin (Barna & Williams, 1984; Westwell, Gerhard, & Williams, 1995). Structurally, teicoplanins are distinct from other GPAs, attributed to the presence of a fatty acid chain (Fig. 1-2) and display differences in biological activity (Borghi *et al*. 1984). The presence of the fatty acid tail is thought to reduce the MIC and improve its potency by enabling insertion into the membrane (Beauregard, Williams, Gwynn, & Knowles, 1995).

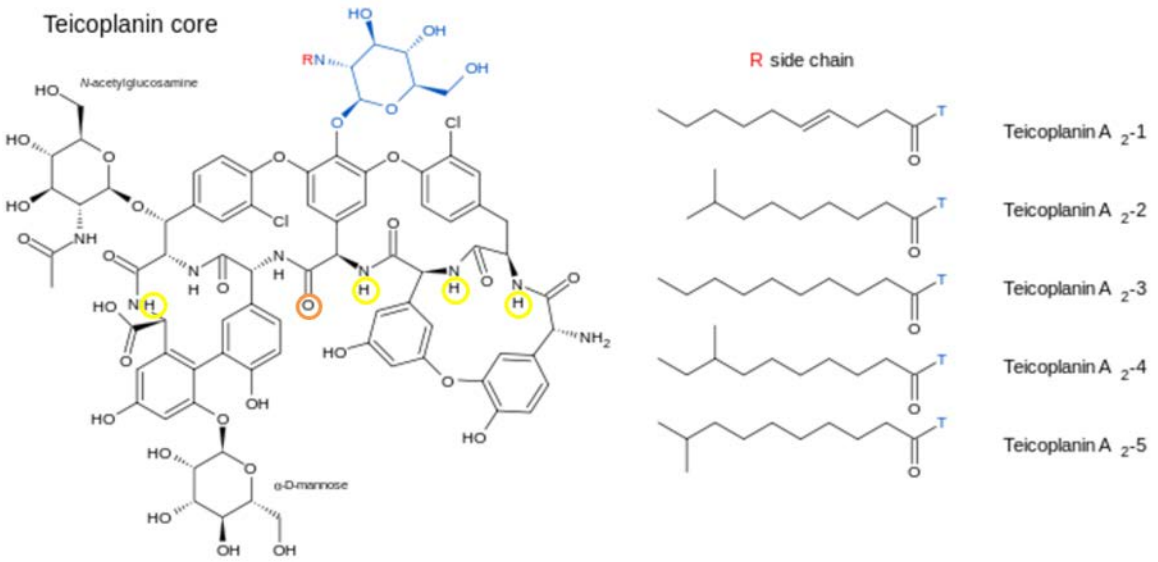

Figure 1-2: Structure of major teicoplanin compounds.

Teicoplanin core structure (left) including the β-D-glucosamine carbohydrate moiety (blue) to which the variable lipid R group is attached at (R). The R-group attached determines the class of teicoplanin compound. 5 groups which form hydrogen bonds to D-Ala-D-Ala are circled (yellow and organe). Loss of 1 hydrogen bond (orange) in type A vancomycin resistance due to the overhaul of peptidoglycan production from D-Ala-D-Ala to D-Ala-D-Lac results in a 1000-fold reduction in affinity for teicoplanin. Image adapted from https://www.drugbank.ca/drugs/DB06149.

1.1.3. Occurrence of resistance towards glycopeptide antibiotics in prokaryotes

Resistance towards some antibiotics (including β-lactams) in the enterococci are innate chromosomal features of these organisms (Hong *et al*. 2008; Cetinkaya *et al*. 2000; Hollenbeck and Rice 2012) which has resulted in the need to find alternative drug therapies against these organisms. GPAs are one of the few effective drugs against these organisms, however recently vancomycin-resistant enterococci (VRE) have emerged (Sievert et al., 2000).

Concerns regarding the frequency of GPA resistance transmission within the enterococci due to the encoding of such resistance genes on mobile genetic elements (including plasmids and transposons) (Hollenbeck and Rice 2012) increased as a result of fears (firstly due to the successful *in vitro* demonstration of transfer of vancomycin resistance genes from enterococci to staphylococci (Noble, Virani, & Cree, 1992) and eventual *in vivo* occurrence of cross-species spreading, the most notable being to Staphylococci (Chang et al., 2003; Hiramatsu, 1998) against which vancomycin is considered the 'Last-line' defence.

Vancomycin resistance is characterised differently for the staphylococci and the enterococci. In the enterococci, 6 types of vancomycin resistance exist which are characterised by the organisation of *van* genes (Fig. 1-6), with strains displaying different MICs towards vancomycin (Schwaber et al., 2003). So far one type of resistance has been characterised in the staphylococci (Srinivasan, Dick, & Perl, 2002); although resistance has been demonstrated in the staphylococci in the absence of vancomycin (Tenover, Biddle, & Lancaster, 2001; Whitener et al., 2004).

1.2. An overview of Two-Component Signal Transduction Systems (TCSs)

1.2.1. Overview of Two-Component system mechanism of action

The traditional layout for all Two-component signal transduction systems (TCSs), regardless of type comprises a membrane sensor histidine kinase (HK) and a partner response regulator (RR). The signal sensing component of TCSs is the membrane-spanning sensor kinase (Fig. 1-3), which belongs to the histidine protein kinase (HPK) family of proteins (Mitrophanov and Groisman, 2008) which are a diverse group of mainly membrane proteins that contribute to a variety of responses in the organism (West and Stock, 2001). Most HPKs function together with a partner response regulator (RR) component (Fig. 1-3) which is the effector DNA-binding component. Both have been suggested to be possible targets for the design of novel antibacterial drugs (Stephenson and Hoch, 2002).

The depiction of a two-component system below can be regarded as an over-simplification of the *in vivo* regulatory processes in prokaryotes. Recent studies abolish the simplistic view of a naive two-component system interacting alone for the regulation of downstream genes, but suggest a network of interactions for the regulation of genes, which indicates a more sophisticated regulatory mechanism, allowing the organism to specifically adapt to environmental input for optimum survival. This process involves the cross-talk of interacting HKs from other two-component systems (Sun, Birkey, & Hulett, 1996), but is not limited to input from Serine-Threonine Kinases (Lux and Shi 2005) Which together with recent findings revealing the existence of aspartate-less domain response regulators (Maule et al., 2015) has increased the complexity of the mechanisms regulating downstream gene activation.

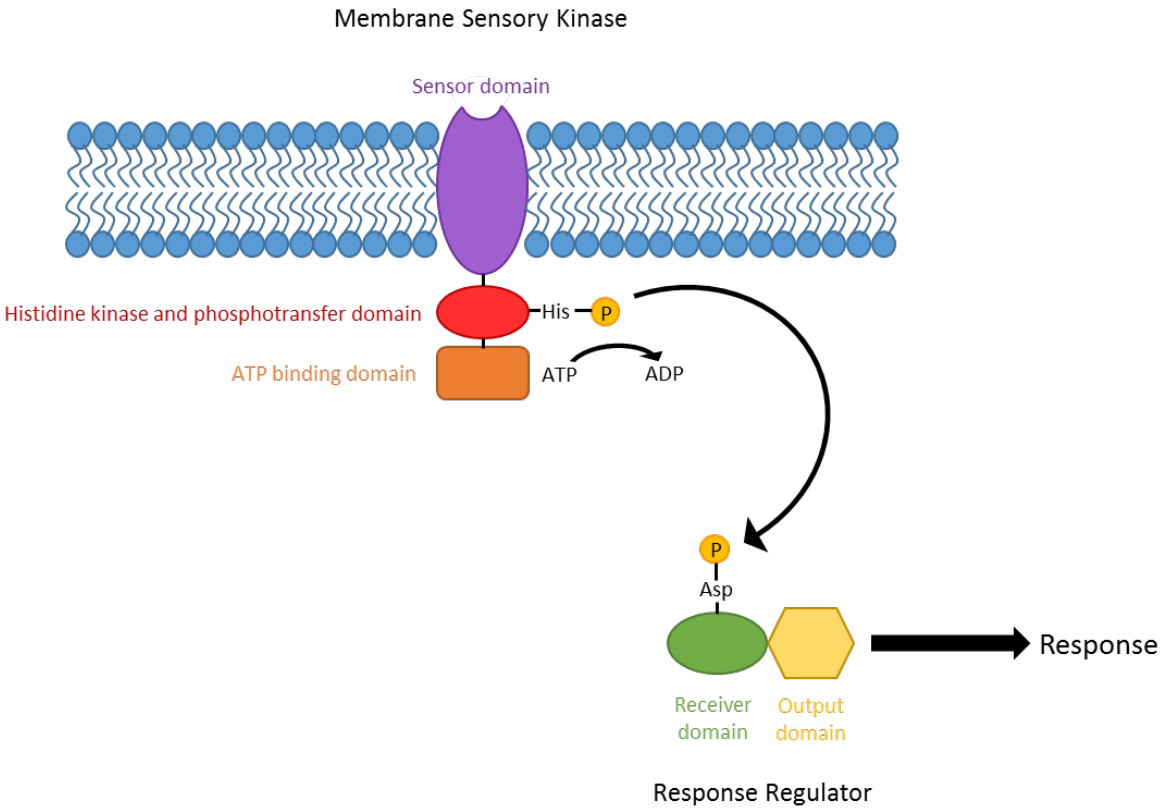

Figure 1-3: Traditional schematic diagram of a common two-component signal transduction system comprised of a Class 1 sensor kinase and partner response regulator.

The membrane sensor kinase binds ATP at the ATP-binding domain before activation of the autokinase activity of the membrane sensor kinase (MSK), where phosphorylation of a conserved histidine on the autokinase domain coincides with the hydrolysis of ATP to ADP. Phosphotransfer from the Histidine of the MSK to the aspartate of the receiver domain of the Response Regulator (RR) leads to a conformational change in the output domain of the RR, commonly resulting in the activation of the RRs as transcription factor by increasing its affinity for DNA.

Histidine phosphorylation was first discovered in 1962 (Boyer, Deluca, Ebner, Hultquist, & Peter, 1962), however it has taken more than 50 years for their biological significance in non-animal systems to be fully appreciated. Histidine exists in two tautomeric forms under basic and neutral conditions (Fig. 1-4) where either N1 or N3 of the imidazole ring are protonated (Puttick, Baker, & Delbaere, 2008) (Fig. 1-5). Phosphorylation occurs at the un-protonated nitrogen.

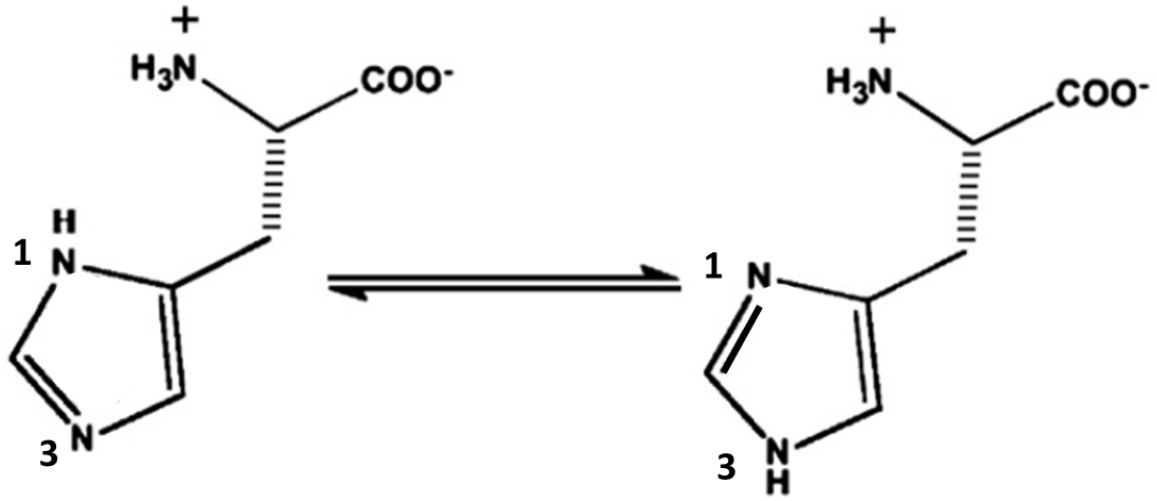

Figure 1-4: Tautomeric forms of free histidine under neutral and basic solution conditions. *Release of lone pair of electrons from either nitrogen (1 or 3) of the imidazole ring results in the production of 2 conjugate forms, i.e. the two conjugate forms of histidine. Figure from Puttick et al. (2007).*

Relative to other phosphorylated amino acids, phosphohistidine is relatively unstable. This instability stems from the N-P bond (especially under acidic conditions), and this has been one of the main bottlenecks for histidine phosphorylation research (Klumpp & Krieglstein, 2002). The phoshophistidine P-N bond is less stable (ΔG = ~12 kcal) than the C-O bond of phosphohydroxy amino acids (ΔG =~8 kcal) due to i) substantial delocalisation of electron density from the P-N bond by highly electronegative oxygens in the phosphate group; and ii) poor contribution of the nitrogen

lone pair of π electrons which differ in the energy levels to phosphorous d-orbital electrons (Attwood, Piggott, Zu, & Besant, 2007). Furthermore, the localisation of the nitrogen lone pair of electrons makes the nitrogen more basic, therefore protonation under acidic conditions becomes unfavourable and increases the leaving-group properties of the nitrogen (Fig. 1-5).

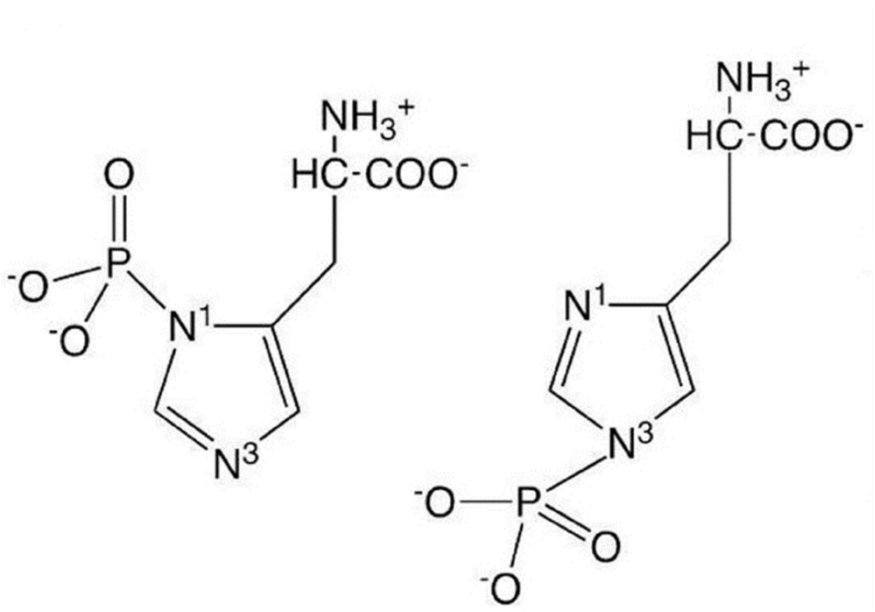

Figure 1-5: Two tautomeric forms of monophosphohistidine. *Depiction of the monophosphorylated tautomers of histidine which can either be phosphorylated on the 1- or 3- nitrogen of the imidazole ring. Image from* (Wieland & Attwood, 2015).

The acid lability of the phosphohistidine has made the study of these systems increasingly difficult. They are more common in prokaryotic (bacterial) systems rather than eukaryotic, and this phenomenon may be related to their rapid turn-over rates. Such activity would enable a quicker relay of information due to the transient nature of the phosphorylated bond compared to more stable, longer lived phosphorylation of hydroxyl groups of amino acids.

There are three classes of histidine kinases (HKs) which are characterised by organisation of domains; specifically the location of the ligand-binding domain (LBD) (Dutta, Qin, & Inouye, 1999; Maslennikov et al., 2010). Class 1 have an extracellular LBD, Class 2 have a membrane-embedded LBD, and Class 3 have cytosolic LBDs. Throughout this Thesis the activity of the Class 1 HK $VanS_A$ will be discussed,

1.2.2. Role of Two-Component systems in the regulation of advantageous phenotypes for bacterial survival

The successful survival of prokaryotic organisms in clinical environments, and their roles as pathogenic agents are due to the expression of virulence factors which code for genes that will favour pathogenic behaviours and lifestyle. Such behaviours include the ability of the organism to adhere to, and establish biofilms within the host (Hancock and Perego, 2004a, 2004b); the ability to produce proteases *(*Nakayama *et al.*, 2001, 2007; Thurlow *et al.*, 2010) and haemolysins *(*Haas *et al.,* 2002) increase their invasiveness. Regulation, activation, and production of many of these processes are mediated via two-component signal transduction systems (TCSs), which enable the organism to sense and respond to their environment (via ligands) (Hoch, 2000; Stock *et al.*, 2000; Mascher *et al.*, 2006; Gao *et al.*, 2007). TCSs are composed of membrane-spanning sensory kinases, and a complementary soluble response regulator protein which commonly has DNA binding and regulatory properties activated after phosphotransfer from the kinase (Fig. 1-3). In the case of *Enterococcus faecalis* possesses 17 TCSs (Hancock and Perego, 2004; Hancock and Perego, 2002) and the sensory kinases (SKs) have been overexpressed in *Escherichia coli* (Ma *et al.*, 2008).

HPKs of TCSs are able to interact with a variety of ligands (environmental and native; activating and inhibiting). Binding to the sensory kinase is the initiating step in the expression of downstream genes (Fig. 1-3), and subsequent intracellular interactions can further diversify the cellular response and resulting phenotype (Mitrophanov and Groisman, 2008; Gao *et al.*, 2007). Consequently, study and characterisation of such interactions are important for understanding the mechanism of activation and potential inhibition of such systems. However, little is known about the ligand:sensor kinase interaction, and this is mainly due to the difficulty in the purification of intact and functional membrane proteins (Kelly and Price, 2000). However, recent developments in the field with regards to the purification of intact membrane HPKs proteins (e.g. Ma *et al.*, 2008) have led to the possibility of furthering such research, with long-term aims of designing specific and effective anti-virulence drugs.

Further, TCSs commonly regulate advantageous phenotypes including resistance towards antibiotics, demonstrated in this Thesis through the investigation of the interactions of the membrane sensor kinase of the two-component system regulating type A vancomycin resistance (resistant toward both vancomycin and teicoplanin) in the enterococci.

1.3. Overview of vancomycin resistance in the enterococci

1.3.1. Mechanism of resistance towards glycopeptide antibiotics

There are 6 types of vancomycin resistance which are categorised by the sequence of *vanA* (Fig. 1-6) and differ in the level of resistance (Courvalin, 2006; Pootoolal *et al.*, 2002) (Table 1). The type A shows the highest level of resistance and is most common in the UK, and this shall be the topic of this Thesis. Type A vancomycin resistance in *E. faecium* is a high-level resistance mechanism that is most prominent in the UK (Werner *et al.*, 2013) and it was first discovered in strain BM4147, encoded on plasmid p1819 (Leclercq *et al.*, 1988). Genes required for vancomycin resistance are contained within the *van* operon and expression results in the production and incorporation of D-Ala-D-Lac or D-ala-D-ser (Table 1). In vancomycin-susceptible strains of enterococci, peptidoglycan is found to be in a transient state of continual renewal where only 7% of the pentapetide chains of the stem chains end with D-Ala-D-Ala terminal dipeptides (Patti, Kim, & Schaefer, 2008), thought to result from the activities of carboxypeptidases which leave D-Ala-D-Ala only on the nucleating structures for cell wall biosynthesis. The *vanA* operon consists of a conserved upstream $vanR_AS_A$ encoding the $VanR_AS_A$ two-component system which regulates the system, in addition to a downstream $vanH_AA_AX_AY_AZ_A$ operon encoding enzymes which cooperatively (1) synthesise D-Ala-D-Lac for dipeptide incorporation, and (2) remove D-Ala-D-Ala from early and late peptidoglycan precursors (Fig. 1-4) resulting in an overall overhaul of the incorporated peptidoglycan to D-Ala-D-Lac (Arthur, Molinas, & Courvalin, 1992; Hong et al., 2008). This terminal dipeptide of peptidoglycan has a 1000-fold reduced affinity for vancomycin (Wright and Walsh 1992) which permits the cell to produce mature cross-linked peptidoglycan. This mechanism differs from that displayed by vancomycin resistant staphylococci which rather than changing the terminal didpeptide of pepetidoglycan as occurs with VRE, instead synthesise and release excessive quantities of D-Ala-D-Ala terminating free peptidoglycan precursors into the surrounding environment to “mop-up” vancomycin in the local environment of the organism to prevent it reaching the target site (Sieradzki,

Roberts, Haber, & Tomasz, 1999); in addition to thickening of the peptidoglycan cell wall to reduce the effectiveness of vancomycin at causing cell lysis (Srinivasan *et al.*, 2002).

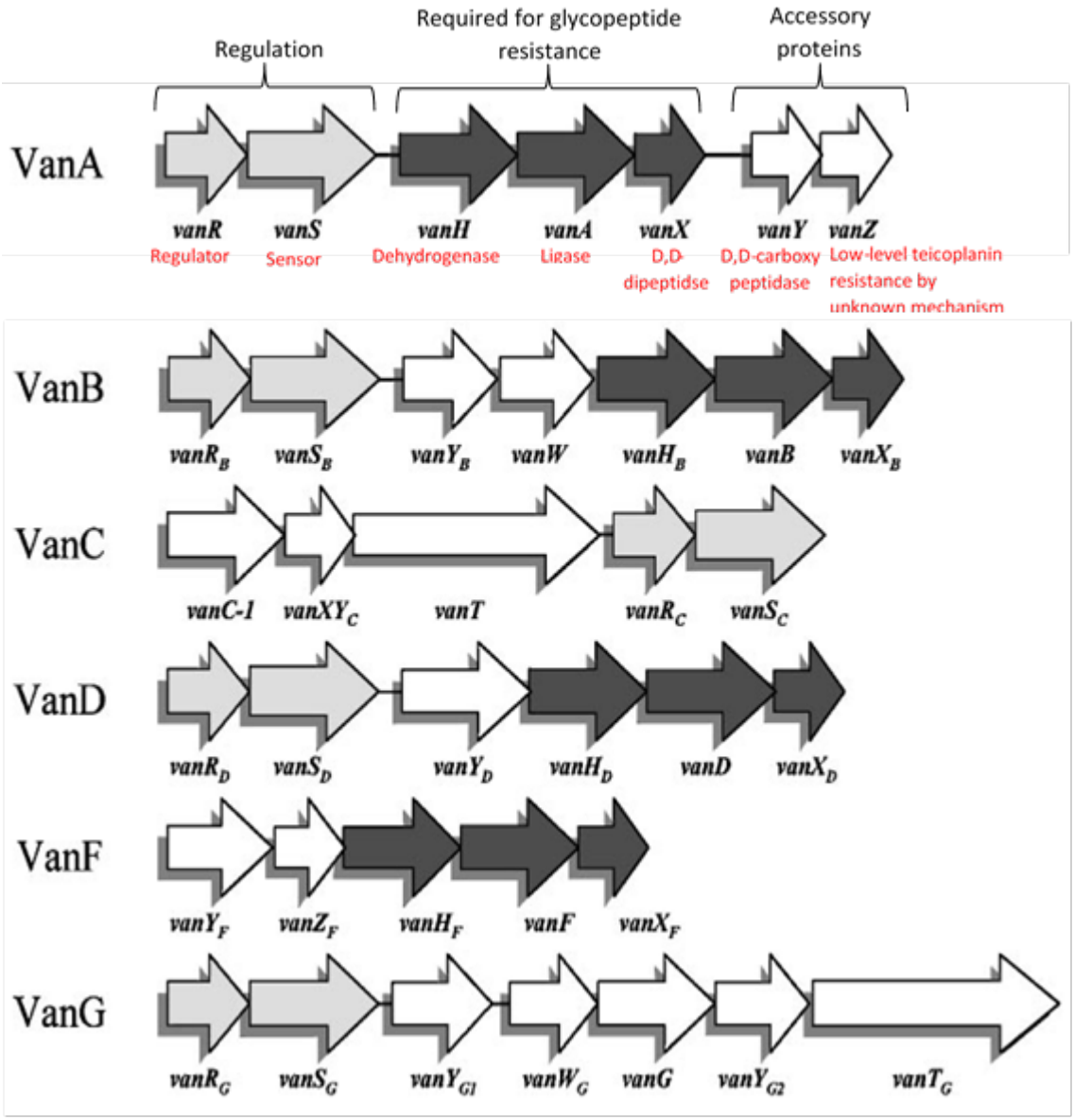

Figure 1-6: Arrangement of genes in the van operons of the different types of vancomycin resistance in enterococci. *The VanRS two-component system regulates downstream van genes and is encoded by upstream $vanR_A$ and $vanS_A$. Downstream van genes bring about the resistance phenotype by encoding for proteins with activities that result in the changing of the terminal dipeptide of the pentapeptide of peptidoglycan from D-ala-D-Ala to D-Ala-D-Lac. Adapted from Pootoolal et al., 2002.*

Strain Characteristic	Acquired resistance level, type					
	High, VanA	Variable, VanB	Moderate, VanD	Low		Intrinsic resistance, low level, type VanC1/C2/C3
				VanG	VanE	
MIC, mg/L						
Vancomycin	64-100	4-1000	64-128	16	8-32	2-32
Teicoplanin	16-512	0.5-1	4-64	0.5	0.5	0.5-1
Conjugation	Positive	Positive	Negative	Positive	Negative	Negative
Mobile element	Tn1546	Tn1547 or Tn1549	...	...	...	...
Expression	Inducible	Inducible	Constitutive	Inducible	Inducible	Constitutive Inducible
Location	Plasmid chromosome	Plasmid chromosome	Chromosome	Chromosome	Chromosome	Chromosome
Modified target	D-Ala-D-Lac	D-Ala-D-Lac	D-Ala-D-Lac	D-Ala-D-Ser	D-Ala-D-Ser	D-Ala-D-Ser

Table 1: Characteristics of different types of vancomycin resistant enterococci.

Characteristics for type A vancomycin resistance highlighted in red. Adapted from Courvalin, 2006.

1.3.2. The controversial identity of the ligand initiating the vancomycin resistance phenotype in the enterococci

$VanR_AS_A$, the TCS regulating type A vancomycin resistance in the enterococci is composed of a membrane sensor kinase, $VanS_A$, and a partner response regulator $VanR_A$. Interaction of the integral membrane sensory kinase, $VanS_A$, with an unknown ligand activates the response regulator component, $VanR_A$ (Fig. 1-7), for the expression of downstream vancomycin resistance genes in the $vanH_AA_AX_AY_AZ_A$ operon (Evers *et al.*, 1996). Autophosphorylation and phosphotransfer activities have been demonstrated *in vitro* using purified cytosolic portions of $VanS_A$ (G D Wright, Holman, & Walsh, 1993). Further studies provided insights into the phosphatase activity controlled feedback mechanism regulating the expression of the *vanA* operon, whereby activation by $VanR_A$~P initiates expression of both the $vanH_AA_AX_A$ resistance operon and the $vanR_AS_A$ operon encoding for the TCS proteins (Arthur et al., 1997) providing a mechanism for the up-regulation of the expression of the TCS proteins and downstream resistance genes. Together this suggests the need for binding of an activator to VanS to supress its phosphatase activity towards VanR for the induction of the *vanA* operon.

Currently, the nature of the inducer remains unknown and there are different theories for its identity; the antibiotic (Koteva *et al.*, 2010), the antibiotic-peptidoglycan precursor complex (Kwun *et al.*, 2013), or the accumulating peptidoglycan precursors as a result of vancomycin mode of action (Baptista, Depardieu, Courvalin, & Arthur, 1996).

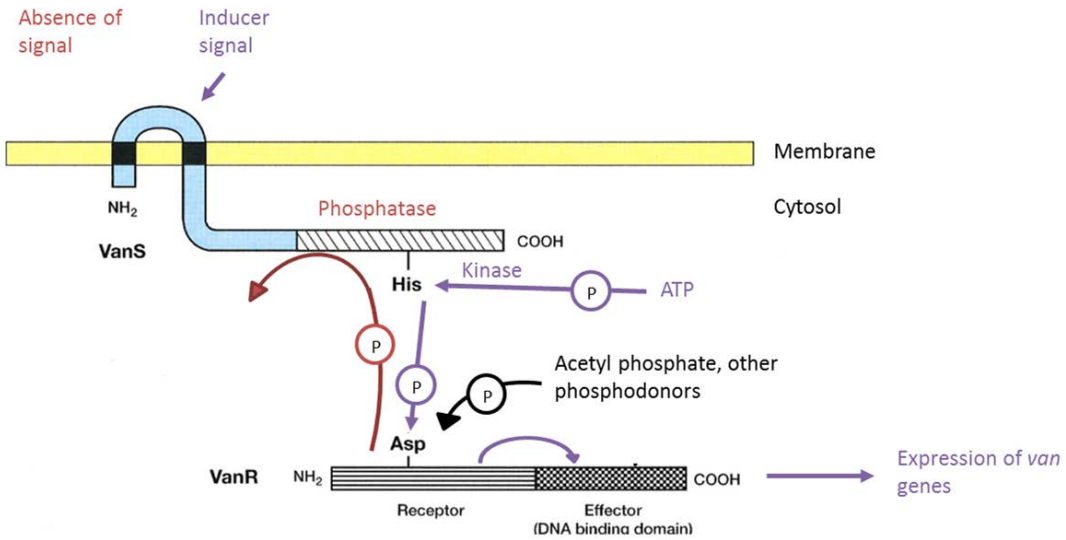

Figure 1-7: Schematic of the two-component system, $VanR_AS_A$, regulating the van operon for vancomycin resistance. *The $VanR_AS_A$ two-component system is composed of a membrane-bound histidine kinase and a cytoplasmic response regulator that acts as a transcriptional activator. Interaction of an unidentified ligand at the extracellular ligand binding domain of $VanS_A$ leads to the activation of the C-terminal cytoplasmic kinase domain of $VanS_A$, catalysing the ATP-dependent autophosphorylation of a conserved Histidine. Phosphotransfer from the phosho-Histidine to a conserved Aspartate in the receptor domain of $VanR_A$ leads to the activation of the effector domain of $VanR_A$, increasing its activity as a transcriptional activator. $VanS_A$ is also capable of affecting phosphatase activity towards $VanR_A$, therefore it can modulate the levels of $VanR_A$~P* (Hong et al., 2008). *Image adapted from Courvalin, 2006.*

1.4. Approaches that will be used to investigate the activities of the Membrane Sensor kinase $VanS_A$ of the two-component system regulating type A vancomycin resistance in the enterococci.

Genetic approaches applied for the *in vivo* determination of the activities of the downstream gene products in the *van* operon regulated by the $VanR_AS_A$ TCS (Pootoolal et al., 2002). These methods have identified the biological effects of the activation of the TCS and genetic approaches have been used for the monitoring of the roles and activities of downstream enzymes activated by the two-component system.

Throughout this Thesis, *in vitro* approaches will be used for the investigation of the structural and activity effects of ligand binding by $VanS_A$, the membrane histidine kinase receptor of the two-component receptor regulating type A vancomycin resistance in the enterococci.

1.4.1. Methods for the obtaining of pure and active membrane proteins for *in vitro* experimentation

Membrane proteins are abundant proteins within diverse living systems, and are predicted to be involved in many disease processes, making them ideal targets for disease pathology and drug discovery investigations. Study of these proteins has proven challenging due to the hydrophobic nature of these proteins which tends to produce low expression yields and the viscous nature of preparations due to the addition of detergent and other stabilising buffer components make the study of these proteins challenging. The biological importance of membrane proteins has led to a pressing necessity for the development of methods for the production of membrane proteins. Such methods were previously reported (Saidijam et al., 2003) describing universal methods for the purification of membrane proteins.

Though relatively difficult to overexpress in high yields due to the difficult nature of the proteins which can often be toxic to the cell and are therefore sequestered into inclusion bodies (Bannwarth and Schulz 2003), or the energy requirement for the expression of membrane proteins (Price, Wetmore, Deutschbauer, & Arkin, 2016), or increased packing of the cell membrane with proteins can be toxic to the cells (Rosano and Ceccarelli 2014); therefore optimisation for the expression of the protein of interest is required.

Heterologous expression of the entire genetic complement of enterococcal histidine sensor kinases (HKs) adapted from previously described methods (CA Potter, Ward, & Laguri, 2002; Christopher a. Potter, Jeong, Williamson, Henderson, & Phillips-Jones, 2006; Saidijam et al., 2003) has been described (Ma et al., 2008). Methods adapted from (Ma et al., 2008) were applied to work conducted in this Thesis for the overexpression and purification of $VanS_A$, the HK regulating type A vancomycin resistance in the enterococci. Employing the pTTQ vector (Stark, 1987) which is particularly useful for membrane protein expression, heterologous expression of HKs into *E. coli* membranes was performed.

Homogenous and pure protein preparations are desired for experimental use, especially in the case of highly sensitive biophysical approaches. Therefore tests to assess the quality of protein preparations will be conducted to ensure quality controls.

1.4.2. Methods investigating the activities of Two-component signal transduction systems (TCSs)

Classical methods used for the investigation of two-component signal transduction systems (TCSs) include *in vitro* activity assays that have been used for the elucidation of the phosphorylation activities of proteins of TCSs (Scharf, 2010) and determination of the effect of the presence of activating ligands and inhibitors on TCS activity (Ma et al., 2008, 2011; CA Potter et al., 2002; Christopher a. Potter et al., 2006).

In the case of the *van* operon the activities of the encoded proteins have been characterised, reviewed in Pootoolal *et al*., 2002, however the activating ligand(s) for $VanS_A$ have not been identified. Results Chapter 5 will describe different *in vitro* approaches used to investigate the phosphorylation activities of the HK $VanS_A$ of the $VanR_AS_A$ TCS regulating vancomycin resistance in the enterococci.

Many *in vitro* approaches investigating the phosphorylation activity of TCSs use radiolabelled ATP (Scharf, 2010), and although these routine approaches are highly sensitive, health and safety regulations may cause problems for attempts to implement these methods. Recent advances have seen the development of increased sensitivity non-radioactive alternatives to probe for protein phosphorylation (Kinoshita et al., 2012; Kinoshita, Kinoshita-Kikuta, Takiyama, & Koike, 2006; Wilke, Francis, & Carlson, 2012; Wu, 2011). The advantages of using such methods include the reduced health and safety concerns and the ability to routinely implement the methods in standard lab environments without the requirement of specialised equipment.

Most non-radioactive methods have been tested for their suitability against relatively stable serine/threonine and tyrosine phosphorylation sites (Kinoshita et al., 2012; Kinoshita, Kinoshita-Kikuta, & Koike, 2009; Kinoshita et al., 2006), and therefore there is a desire to test their compatibility with weaker and more transient histidine phosphorylation which is lacking in the literature. Here, the use of some of these methods for the investigations of the activities of proteins

of TCSs regulating vancomycin resistance in the enterococci will be presented and compared to the established method of radioactively labelled ATP.

1.4.3. Biophysical methods used in the Thesis for the investigation of the interactions of the sensor kinase regulating vancomycin resistance in the enterococci.

Biophysical methods including Circular dichroism (CD) using a xenon and synchrotron light sources, magnetic synchrotron radiation circular dichroism (MSRCD), Fluorescence spectroscopy (Fluorescence), UV absorbance spectroscopy, dynamic light scattering (DLS) will be used to characterise the protein-ligand interactions of $VanS_A$, the membrane receptor of the two-component system regulating vancomycin resistance in the enterococci. The data obtainable in addition to the advantages and disadvantages for each method will be discussed.

Circular Dichroism (CD) utilises the inherent differences in absorption of right circularly polarised (RCP) and left circularly polarised (LCP) light by chiral chromophores (S M Kelly, Jess, & Price, 2005). In the case of this Thesis, biological chromophores of proteins including the transitions of the peptide backbone and surface-exposed aromatic amino acids in the local tertiary structure will be investigated using the far- and near-UV regions respectively.

The availability of xenon and synchrotron light sources in addition to a variety of cell designs allows for the tailoring of assays to samples and the data to be obtained. The advantages of synchrotron light sources stem from the ten-times brighter light available over a wider range of far- and near- UV wavelengths compared to xenon sources. The high flux and highly collimated (low-level of divergent beam) nature of the micro-beam means higher signal:noise ratios are achievable (Javorfi, Hussain, Myatt, & Siligardi, 2010) in samples of comparatively small samples sizes, allowing for the application of the approach to samples of low abundance e.g. membrane proteins (Siligardi, Hussain, Patching, & Phillips-Jones, 2014).

The use of titration approaches using CD has been established for the determination of the dissociation constant for the interactions of the soluble protein ligand interactions and protein complex formation (Freeman, Pattenden, Drake, & Siligardi, 1998; Prodromou et al., 1999; Siligardi et al., 2002), and later applied to the determination of ligand binding for membrane proteins (Patching, Edara, & Ma, 2012; Siligardi et al., 2014) which itself is a challenging are due to the presence of added buffer components including glycerol and detergent. The field of membrane protein research is a challenging area. Titration approaches will be applied to CD, MSRCD, fluorescence and absorbance studies to quantitatively characterise the interactions of $VanS_A$ with binding ligands.

Thermal denaturation experiments can be used as additional tools for the determination of ligand binding by probing the stability of the protein of interest in different experimental condition, e.g. buffer, ligands, etc. Thermal denaturation approaches will be applied to monitor the thermodynamics of protein unfolding (Greenfield, 2007) for $VanS_A$.

Furthermore, magnetic synchrotron radiation circular dichroism (MSRCD) will be used to assess the interactions of tryptophan and tyrosine during ligand binding. During MSRCD, magnet-induced changes in the absorption of left- (LCP) and right- (RCP) polarised light, in addition to a strong polarisation of the electromagnetic transitions of tyrosine and tryptophan produces strong, distinct signals to enable monitoring of their interactions throughout an experiment, e.g. to monitor their roles during ligand binding.

Proteins with intrinsic fluorescence due to the presence of fluorophores including aromatic amino acids (tryptophan, tyrosine, and phenylalanine) and co-factors (e.g. NAD, FAD, FMN and porphyrin rings) can be monitored by fluorescence. Fluorescence spectroscopy is a very sensitive method, which requires comparatively little material therefore is a useful technique for investigations of systems where resources are limited, such as membrane proteins. However, the high sensitivity of the methods means factors including concentration are important to consider to prevent the

excessive absorbance of the excitation light ("inner filter" effect); especially during ligand binding and titration studies where the presence of ligands can cause distortions in the fluorescence emissions (Birdsall et al., 1983) due to increased net absorbance of the mixture in the presence of ligand which needs to be accounted for during analysis.

Dynamic Light Scattering (DLS) is a biophysical technique which can provide information about the size distribution and homogeneity of samples tested. In the case of proteins it can provide information on protein aggregation. Sensor kinases utilise dimerisation for their activity via transphosphorylation between kinase monomers before phosphotransfer to a partner response regulator (Stock et al., 2000), therefore assessment of the dimerisation of $VanS_A$ in the absence and presence of ligands will be conducted using DLS to test for the dimerisation phenomenon in the presence of screened ligands.

1.5. Aims

This Thesis aims to characterise $VanS_A$, the membrane sensor kinase of the two-component system regulating type A vancomycin resistance in a clinically relevant species of *Enterococcus faecium*.

Specifically, the aims will be:

1) To express and purify stable, active $VanS_A$ protein using the over-expression vector PTTQ18vanS_A in *E. coli* BL21 [DE3].
2) Using SRCD spectroscopy, investigate the structural effects of ligand binding on $VanS_A$ in the
    a. Far-UV to investigate the secondary structural effects of interaction
    b. Near-UV to investigate the involvement of surface-exposed aromatic residues of $VanS_A$
3) To investigate the activity changes which occur in $VanS_A$ upon ligand interaction, comparing different methods for the monitoring of phosphorylation of a protein.

CHAPTER 2:
EXPRESSION, PURIFICATION AND OPTIMISATION OF HIS_6-TAGGED $VANS_A$

2.1. Introduction

Current knowledge of the activities of the $VanR_AS_A$ two-component system regulating type A vancomycin resistance in the enterococci has been conducted in equivalent models using genetic approaches *in vivo* (Arthur *et al*., 1996), however the activating ligand for $VanS_A$ is yet to be determined. Throughout the following chapters, *in vitro* approaches are used to investigate the interactions of the membrane sensor kinase, $VanS_A$, of the two-component system, therefore it is necessary to overexpress, purify and verify pure and active $VanS_A$.

The purification and expression of membrane proteins is a difficult field due to their hydrophobic nature which often requires the use of detergents. Furthermore, factors including low yields, low-level expression due to the increased instability of the host's translation system, exclusion of expressed protein into inclusion bodies as a defensive mechanism towards the potential toxic nature of these membrane proteins stemming from the increased stress their expression causes in the cell membrane stability and the overall increased energy requirement for their expression have been reviewed extensively (Baneyx, 1999; Lin & Guidotti, 2009; Makrides, 1996; Sørensen & Mortensen, 2005; Stevens, 2000).

To counteract these problems, expression host and vector compatibility are principal factors which require optimisation (Schlegel, Hjelm, Baumgarten, Vikström, & de Gier, 2014) in addition to experimental conditions including growth and induction conditions. Common practices used to avert the undesirable effects of the overexpression of membrane proteins include longer induction periods at lower temperatures to enable a longer and slower production and insertion of the protein into the membrane, in addition to the use of expression vectors and host which are optimised for the expression of membrane proteins (Rosano & Ceccarelli, 2014). Conditions appropriate for the expression of membrane proteins have been outlined previously (Saidijam *et al*., 2003) and have been adapted for the expression of membrane sensor kinases for use in activity and structural studies (Ma *et al*., 2008). Expression conditions including Isopropyl β-D-1-thiogalactopyranoside

(IPTG) concentration, and induction time and temperature; and purification conditions including detergent screens are described. Adapted approaches will be used to produce pure, active and intact $VanS_A$ for use in experiments investigating its activities in response to ligand binding.

The $VanS_A$ gene described here is encoded in the pTTQ plasmid, a plasmid which has historically been particularly useful for the expression of membrane proteins (Stark, 1987) (Fig. 2-1). Compared to other plasmids, the pTTQ plasmid has a higher success rate for membrane protein expression (Surade *et al*., 2006). Furthermore, BL21 [DE3] *E. coli*, which are optimised hosts for membrane protein expression (Schlegel *et al*., 2014) will be used throughout experiments described in this Thesis.

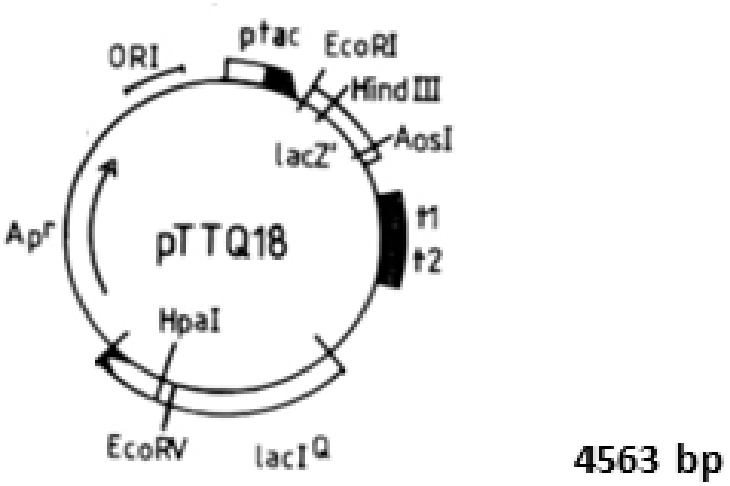

Figure 2-1: Schematic of the pTTQ18 plasmid. *Labelled are the tac promoter (ptac), rrnB terminator fragments (t1, t2), restriction sites (EcoRI, HindIII, AosI, EcoRV), inducible β-galactosidase gene (lacZ), lac repressor ($lacI^Q$). Figure adapted from Stark (1987).*

Post-expression, appropriate purification conditions are important in order to obtain sufficient quantities of active, soluble proteins. For example too high concentrations of detergent can have deleterious effects on protein stability and function (Ma *et al*., 2008); high glycerol concentrations

although cryoprotectant for the protein, may negatively affect the activity of the protein or be unsuitable for experimental conditions such as HPLC and protein crystallisation , not to mention protein concentration by BCA assay and other colorimetric tests like the R & D systems universal kinase assay kit which are described in this Thesis, therefore optimisation of the concentrations of these components will be undertaken to ensure protein stability and compatibility with experimental methods.

Within the field of biological research, there is a need for the production and use of biosimilar products. Pharmaceutical industries emphasise the importance for achieving biosimilar products, especially with products destined for consumers (Agostini, Canonica, & Maggi, 2015). Many soluble proteins are available to purchase, and these proteins are offered with a high level of quality control ensuring a fairly consistent level of biosimilarity between protein preparations.

Problems arise when preparing biological compounds such as membrane proteins from recombinant overexpression systems. Proteins are diverse biomolecules which are innately dynamic (Henzler-Wildman & Kern, 2007) and environmentally sensitive in nature (Ruckenstein & Shulgin, 2006; Talley & Alexov, 2010). Added to the fact that in recombinant-systems no cells will have identical experiences, and purification methods and conditions will inevitably change, such factors can result in non-biosimilar preps (Kuhlmann & Covic, 2006). In the lab, intra- and inter-batch differences may be more difficult to realise due to the often sophisticated and rigorous quality control tests performed on purchased proteins. These differences are rarely discussed but should be considered essential to obtain consistent and reliable results, especially when reporting differences in the presence of ligands as will be discussed here.

This Chapter will describe the optimisation steps undertaken for the successful production of pure intact and active $VanS_A$.

2.2. Working hypothesis

The expression and purification of $VanS_A$ can be optimised for the production of soluble, intact, active protein.

2.3. Methods

2.3.1. Small-scale overexpression and purification of $VanS_A$

10 ml of LB + 100 µg/ml carbenicillin inoculated with cells from a glycerol stock stored at -80 °C was grown overnight at 37 °C before centrifuging at 4000 x g (av) and resuspending in 1 ml of LB for use as a starter culture. 50 ml of media (M9 minimal, Luria-Bertani (LB), or 2TY) was inoculated with 50 µl of starter culture, growing cells in the presence of 100 µg/ml carbenicillin at 37 °C to OD_{600} (0.6) before induction of $VanS_A$ expression by addition of isopropyl β-D-1-thiogalactopyranoside (IPTG) in variable concentrations and either 30 °C or 37 °C for 3 hours. Cells were harvested by centrifugation at 4000 x g (av) for 5 minutes before storage at -80 °C.

2.3.2. Waterlysis *E. coli* BL21[DE3]

Cell pellets from 50 ml of culture stored at -80 °C thawed over ice were resuspended in 0.2 M Tris-HCl pH 8.0 and mixed by gentle agitation for 20 minutes at room temperature. To initiate cell lysis, 4.85 ml of 0.2 M Tris-HCl pH 8.0 containing 1 M sucrose and 1 mM EDTA was added (t = 0 minutes), followed by addition of 65 µl of lysozyme (10 mg/ml in 0.2 M Tris-HCl pH 8.0) at time=1.5 minutes and 9.6 ml sterile deionised water at t = 2 minutes. Sample mixed by agitation at room temperature for 20 minutes before sedimentation of spheroplasts at 38724 x g (av) for 20 min at 4 °C. Pelleted spheroplasts were resuspended in 15 ml sterile deionised water and incubated for 30 minutes at room temperature. Membranes were sedimented at 38724 x g (av) for 20 min at 4 °C. An additional 2 washing steps were performed using 0.2 mM Tris-HCl pH 8.0 to remove contaminant proteins (including soluble cytosolic proteins) from the membranes before resuspending in 500 µl of the final

buffer (0.1 M Na phosphate pH 7.2 containing 1 mM mercaptoethanol). Samples stored at -20 °C if not used immediately.

2.3.3. Medium-scale overexpression

6 X 1 L of LB was inoculated with 1 ml of started culture, growing cells in the presence of 100 µg/ml carbenicillin at 37 °C to OD_{600} (0.6) before induction of $VanS_A$ expression by addition of 1 mM IPTG. After induction for 3 hours at 30 °C cells were harvested at 8000 x g (av) for 10 minutes. Cells were washed in 10 mM Tris-HCl pH 8.0, 10 % glycerol, 0.5 mM EDTA and centrifuged at 8000 x g (av) before resuspending in 20 ml of the same buffer and storage at -80 °C.

2.3.4. Mixed membrane preparation of $VanS_A$

Thawed cell pellets from 6L of culture resuspended in 10 mM Tris-HCl pH 8.0, 10 % glycerol, 0.5 mM EDTA as described above were lysed by explosive decompression using a Benchtop cell disruptor (Constant Systems Ltd). Lysed cells were centrifuged at 12000 x g (av) for 40 minutes at 4 °C to remove cell debris, and the supernatant removed and ultracentrifuged at 131000 x g (av) for 2 hours at 4 °C. The supernatant was removed and the pellet washed and resuspended in 10 mM Tris-HCl pH 8.0 + 2 mM β-mercaptoethanol and ultracentrifuging at 131000 x g (av) for 1 hour at 4 °C. The wash step was repeated a further two times to remove contaminant proteins before resuspending the mixed membranes in 10 mM Tris-HCl pH 8.0 and storage at -80 °C.

2.3.5. Purification of $VanS_A$

Purification was conducted as described in Ma *et al*., (2008). Mixed membrane preparations were adjusted to 4 mg/ml for solubilisation in 10 mM HEPES pH 8.0, 20 % glycerol, 1 % n-Dodecyl β-D-maltoside (DDM), 20 mM imidazole pH 7.9, 2 mM β-mercaptoethanol for 4 hours at 4 °C with gentle agitation before ultracentrifugation at 131000 x g (av) for 40 minutes at 4 °C. Supernatant was incubated for 8 hours with Ni-NTA Agarose (Qaigen) pre-equilibrated with 10 mM HEPES pH 8.0, 20 mM imidazole pH 7.9, 20 % glycerol, 0.025 % DDM. Recovered resin was washed with Wash buffer (10 mM HEPES pH 8.0, 20 mM imidazole pH 7.9, 20 % glycerol, 0.025 % DDM) through a 30 ml column before eluting with 5 column volumes of Elute buffer (10 mM HEPES pH 8.0, 200 mM imidazole pH 7.9, 20 % glycerol, 0.025 % DDM), collecting in 1m fractions. Protein-containing fractions identified using BCA assay (see below) and A_{280} measurements (see below) were pooled and concentrated to 1 ml (Vivaspin®6 (100 kD MWCO)) before dialysing (Spectra/Por® Float-A-Lyzer® G2 (3.5-5 kDa)) into Exchange buffer (10 mM HEPES pH 8.0, 20 % glycerol, 0.025 % DDM).

2.3.6. Buffer optimisation

Protein was purified as described above. Pooled eluted protein was regularly dialysed into exchange buffer over 24 hours at 4 °C using Spectra/Por® float-A-Lyzer G2 3.5-5 kDa (Spectrum).

2.3.7. Sodium Dodecyl Sulfate Polyacrylamide Gel Electrophoresis (SDS-PAGE)

Samples prepared in NuPAGE® LDS sample buffer (ThermoFisher) (1X final concentration) and resolved through Novex®NuPage® pre-cast gels (4-12%) (ThermoFisher) using NuPAGE® MOPS SDS running buffer (ThermoFisher) buffer system prepared to a 1x concentration as per the manufacturer's instructions. Protein molecular weight calculated relative to Precision Plus Protein™ Dual Xtra Standards (BioRad) as molecular weight reference markers. Gel stained using InstantBlue® (Expedeon) and imaged using ImageQuant™ LAS 4000 (GE Healthcare Life Sciences).

2.3.8. Western Blotting

For Western blots, the gel was incubated in Transfer buffer (25 mM Tris, 200 mM glycine, 20 % methanol) + 10 mM EDTA (pH 8.0) for 10 minutes before incubating in Transfer buffer for 10 minutes, each step with gentle agitation. Blots were performed under standard conditions (90 V, 1 hour), the polyvinylidene difluoride (PVDF) membrane was blocked overnight in 10 % (w/v) milk in 1 X TBST (10 mM Tris HCl pH 7.5, 100 mM NaCl, 1 % (v/v) Tween 20). The membrane was probed with Anti-His_6 antibody HRP conjugate (INDIA) and developed by incubating with SuperSignal™ West Pico Chemiluminescent Substrate (Thermo Scientific) and exposing to film. Image acquisition using a ChemiDoc™ XRS+ (BioRad), and densiometry analysis preformed using ImageJ (Rasband, 1997; Schneider, Rasband, & Eliceiri, 2012).

2.3.9. Mass Spectrometry

LC-MS/MS performed at Advanced Proteomics Facility, Department of Biochemistry, University of Oxford.

Peptides re-suspended in 10% formic acid were separated on an Ultimate 3000 UHPLC system (Thermo Fischer Scientific) and electrosprayed directly into a QExactive mass spectrometer (Thermo Fischer Scientific) through an EASY-Spray nano-electrospray ion source (Thermo Fischer Scientific). The peptides were trapped on a C18 PepMap100 pre-column (300µm x 5mm,100Å, Thermo Fisher Scientific) using solvent A (0.1% Formic Acid in water) at a pressure of 500 bar. Peptides were separated on a PepMapRSLC C18 column (2um, 100Å, 75umx50cm, Thermo Fisher Scientific) using a linear gradient (length: 120 minutes, 7% to 28% solvent B (0.1% formic acid in acetonitrile), flow rate: 200 nL/min). The raw data was acquired on the mass spectrometer in a data-dependent mode (DDA). Full scan MS spectra were acquired in the Orbitrap (scan range 350-2000 m/z, resolution 70000, AGC target 3e6, maximum injection time 50 ms). After the MS scans, the 20 most intense peaks were selected for HCD fragmentation at 30% of normalised collision energy. HCD spectra were

also acquired in the Orbitrap (resolution 17500, AGC target 5e4, maximum injection time 120 ms) with first fixed mass at 180 m/z.

Raw MS data were processed by MaxQuant (version 1.5.0.35i) for peak detection and quantification. MS spectra were searched against a custom database using the Andromeda search engine with the following search parameters: full tryptic specificity, allowing two missed cleavage sites, fixed modification was set to carbamidomethyl(C) and the variable modification to acetylation (protein N-terminus), oxidation(M).

Mass spectra were recalibrated within MaxQuant with a precursor error tolerance of 50ppm and then re-searched with a mass tolerance of 5 ppm.

Fragment ion tolerance was set to 20ppm.

The search results were filtered with a false discovery rate (FDR) of 0.01 for proteins, peptides and peptide spectra matches (PSM).

2.3.10. Bioinformatics

2.3.10.1. RaptorX structure prediction (RaptorX)

Predicted amino acid sequence for $VanS_A$ was submitted to RaptorX (http://raptorx.uchicago.edu/about/). RaptorX predicts secondary and tertiary structure of submitted protein sequences without close homologs (<30 % sequence identity) in the Protein Data Bank (PDB) using conditional neural fields for protein threading and alignment of sequences in context with its environment (Peng & Xu, 2011).

2.3.10.2. TMPred

Amino acid sequence for $VanS_A$ was submitted to TMpred (http://embnet.vital-it.ch/software/TMPRED_form.html). TMPred uses an algorithm based on the statistical analysis of the database of transmembrane proteins, TMbase. It makes predictions of membrane-spanning regions and their orientation. Predictions are made using a combination of several weight-matrices for scoring (Hofmann & Stoffel, 1993).

2.3.10.3. TMHMM 2.0

Amino acid sequence for $VanS_A$ was submitted to TMHMM (http://www.cbs.dtu.dk/services/TMHMM-2.0/). The TMHMM prediction tool applies a hidden Markov model to predict membrane protein topology and discriminate between soluble and membrane proteins with high accuracy (Krogh, Larsson, von Heijne, & Sonnhammer, 2001).

2.3.11. BCA assay for protein determination

Assays performed using BCA Protein Assay Kit (Pierce). Standard curve with protein concentrations 0, 3.125, 6.25, 12.5, 18.75, 25 µg of bovine serum albumin (BSA) standard in the same conditions as the test samples were used to determine the unknown protein concentration of samples. Samples were regularly diluted 1/20 and 1/50 for protein concentration determination. 50 µl of sample mixed with 1 ml of BCA reagent (prepared 1:50 dilution of Reagent B (4% cupric sulfate): Reagent A (bicinchoninic acid) and incubated at 37 °C for 30 minutes before measuring A_{550}. A_{550} of samples of unknown protein concentration used to determine protein concentration from standard curve.

2.3.12. Protein concentration determination using A_{280}

Protein concentration determination using a P-class 330 nanophotometer (Implen). The Beer-Lambert law was applied using the calculated extinction coefficient (ε) 45770 M^{-1} cm^{-1} for $VanS_AHis_6$.

2.3.13. Circular Dichroism (CD)

Measurements were conducted using a Chirascan-Plus (Applied Photophysics).

Far-UV measurements (180-260 nm) collected using 0.5 mg/ml of $VanS_A$. Employing cylindrical cells with 0.2 mm pathlength, 4 scans were collected at 20 °C in 1 nm increments using 1 s integration and either 1nm bandwidth (CD). Data presented in molar extinction (Δε).

All samples were incubated at 20 °C for 30 minutes prior to data collection. All data was analysed using CDApps (Hussain *et al*., 2015) where the mean residue weight of $VanS_A$ was taken to be 113. Unless otherwise stated, all spectra presented are difference spectra where all relevant background buffers, ligands etc. have been subtracted. Data acquired when the HT of the detector (PMT) was equal to or greater than 600 V were excluded from the analyses.

Secondary structure estimations of $VanS_A$ were performed from data collected in the far-UV region using the CONTINLL algorithm (Provencher & Glockner, 1981; van Stokkum *et al*., 1990; Sreerama & Woody, 2000) and SMP 56 (43 soluble, 13 membrane) database.

See Chapter 3, section 3.3.1. for more information of the fundamentals of CD.

2.3.14. Dynamic light scattering (DLS)

70 µl of 0.5 mg/ml of $VanS_A$ in either 10 mM HEPES pH 8.0 only (—), or 10 mM HEPES pH 8.0, 10 % (v/v) glycerol, 0.025 % (w/v) DDM was analysed using Disposable Solvent Resistant Micro Cuvettes (ZEN0040, Malvern) in a Zetasizer Nano ZSP (Malvern).

See Chapter 3, section 3.3.5. for the fundamentals of DLS.

2.3.15. Size-Exclusion Chromatography Multi-Angle Light Scattering (SEC-MALS)

Performed using 0.1 mg of purified protein in final suspension buffer. A Superdex 200 Increase 5/150 GL column (GE Healthcare Life Sciences) was pre-equilibrated with ddH_2O overnight, followed by equilibration with running buffer containing 10 mM HEPES pH 8.0, 5 % glycerol, 0.025 % DDM before sample injection.

2.4. Results

2.4.1. Bioinformatics structural predictions of His_6-tagged $VanS_A$

Bioinformatics tools were used to predict the topology of the protein and to obtain information about the protein of interest that will aid in subsequent experimental designs. Transmembrane prediction tools (TMHMM (http://www.cbs.dtu.dk/services/TMHMM-2.0/) and TMpred (http://embnet.vital-it.ch/software/TMPRED_form.html) (Appendix 1.4 and 1.5, respectively)) identified an average region predicted to lie extracellular between the two transmembrane regions (Fig. 2-2) suggesting this region to be the extracellular sensory domain of $VanS_A$, i.e. the site of ligand binding. The predicted model for $VanS_A$ using RaptorX (Appendix) revealed a protruding loop in the extracellular direction which contained exposed tryptophan and tyrosine residues (Fig. 2-2) suggesting the possibility to monitor the interactions of these residues using synchrotron radiation circular dichroism (SRCD) in the near-UV region (260-310 nm).

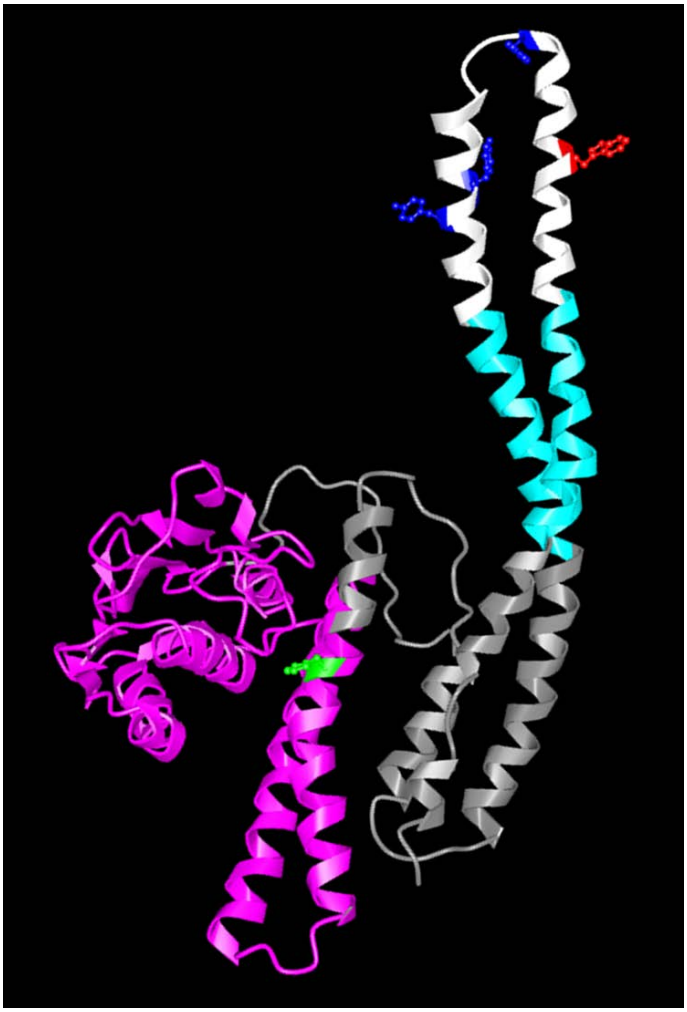

Figure 2-2: Model of 3D structure of $VanS_A$ predicted using Raptor. *Transmembrane α-helical regions predicted at residues 23-41 and 82-101 (cyan) are separated by the predicted extracellular sensory domain (42- 81) (TMHMM, TMpred, Appendix 1.4 and 1.5, respectively (white). α-helices, β-strands and loop secondary structures are displayed; as are the structures of the side chains of aromatic amino acids Trp (red) Tyr (blue) located in the predicted ligand binding domain. Kinase domain (http://www.uniprot.org/uniprot/Q06240) (magenta) is highlighted as is the structure of the conserved histidine (green) involved in phosphorylation. Remaining sequence of $VanS_A$ shown in grey. Predicted secondary structure composition 59 % Helix, 12 % Beta, 28 % C. Solvent accessibity 24 % Exposed, 59% Medium, 16% Buried. (raptorx.uchicago.edu) (Peng & Xu, 2011). Image obtained from the .pdb file of Raptor results using* https://www.ncbi.nlm.nih.gov/Structure/icn3d/full.html.

2.4.2. Optimisation of the overexpression of His-$_6$-tagged VanS$_A$ in *E. coli* BL21[DE3]

Adapting methods described in Ma *et al.*, 2008, and furthering work determining the optimum expression conditions for VanS$_A$ (Pogson, 2013) protein expression under various conditions (Table 2) were compared to determine the optimum conditions for the successful over-production of VanS$_A$ for use in downstream experiments. Two concentrations of IPTG were trialled. The concentrations chosen resulting from similarities in the concentration used during other studies (Ma 2008, find others - concentrations used for other pTTQ expression systems). 2 induction temperatures were chosen. 4 °C overnight (16 hrs) was not used as previous work did not show any considerable increase in the expression of HKs (Ma *et al*., 2008). Similarly, longer incubation times after the addition of IPTG was not used because previous work had not shown any benefits by way of improved expression yields with longer incubation periods. Again, although higher concentrations of IPTG could be used for induction, larger ranges were not used as the aim was to find the minimal concentration for maximum protein expression.

Media	[IPTG]	Induction temperature
M9	0 mM IPTG	30 °C induction
		37 °C induction
	0.5 mM IPTG	30 °C induction
		37 °C induction
	1 mM IPTG	30 °C induction
		37 °C induction
LB	0 mM IPTG	30 °C induction
		37 °C induction
	0.5 mM IPTG	30 °C induction
		37 °C induction
	1 mM IPTG	30 °C induction
		37 °C induction
2TY	0 mM IPTG	30 °C induction
		37 °C induction
	0.5 mM IPTG	30 °C induction
		37 °C induction
	1 mM IPTG	30 °C induction
		37 °C induction

Table 1: Induction conditions of E. coli cells harbouring the pTTQ_VanS$_A$ expression plasmid.

For all conditions, cells were grown at 37°C to the optimum OD_{600} for induction, at which point the appropriate concentration of IPTG was added and the temperature was changed where appropriate for induction for 3 hours before cell harvesting.

Cell growth differed in each media tested (Fig. 2-3). Cells grown in minimal media M9 took longer to reach the optimum OD_{600} for inducing compared to cells grown in rich-media (2TY) that reached the OD_{600} for induction earlier (Fig. 2-3). Furthermore, differences in the behaviour of the cells were observed post-induction for each media tested, the most notable being increased cell death upon addition on IPTG and induction of $VanS_A$ expression exhibited in cells grown in M9 media (Fig. 2-3A). Conversely, in conditions with higher nutrient media, cell growth was not affected as severely upon induction of $VanS_A$ expression, though growth was slower and reached stationary phase quicker upon induction with ITPG than in control conditions (Figs. 2-3B and 2-3C) contradicting previous findings (Pogson, 2013).

Together, these results suggest increased stress and energy expenditure as a result of induction of expression of plasmid-encoded protein negatively affected cell viability, further supported during monitoring of cell growth in 2TY media which showed cells reached stationary phase at lower population densities sooner with increasing IPTG concentration (Fig. 2-3C).

A.

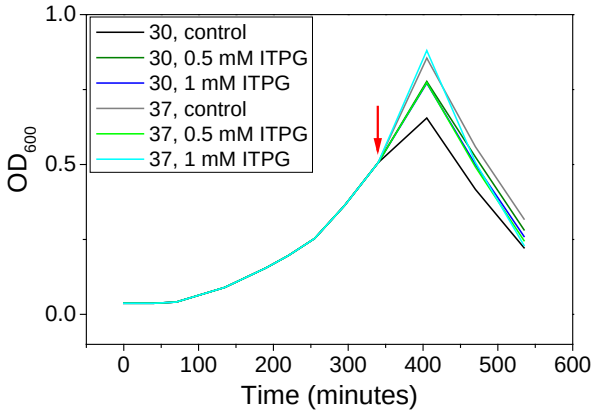

B.

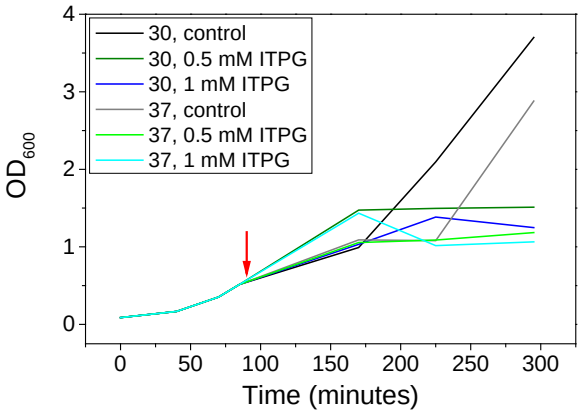

C.

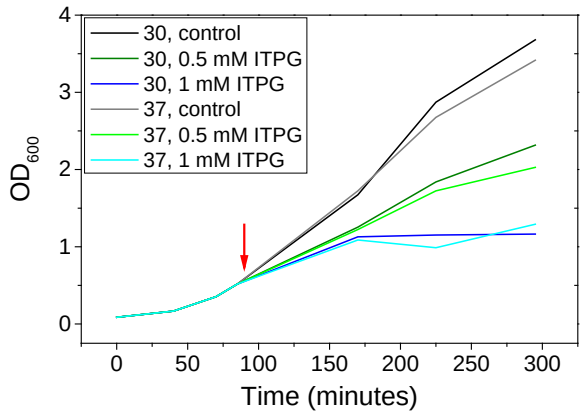

Figure 2-3: Growth curves for E. coli BL21[DE3] harbouring the pTTQ18 expression plasmid encoding VanS$_A$ under various induction conditions. *Expression of VanS$_A$ was induced as described in Methods in (A) M9 minimal media, (B) Luria-Bertani or (C) 2TY media, monitoring growth of cells via OD$_{600}$ throughout. After addition of IPTG, 1:4 dilutions monitored. OD$_{600}$ values plotted versus appropriate time point under each condition. Time-point for IPTG addition indicated by red arrow (↓).*

Using water lysis (see *Methods*), cell fractions (cytosolic, periplasmic, membrane) were prepared from cell pellets induced under different conditions (Table 2). Throughout all conditions tested $VanS_A$ (→) was present at the highest concentration in the membrane fractions confirming the expression and localisation of $VanS_A$ (Figs. 2-4, 2-5 and 2-6). Less intense bands were seen at lower molecular weights in all conditions tested (Figs. 2-4, 2-5 and 2-6), suggesting the presence of N-terminally truncated degradation products due to the confirmed presence of the C-terminal His_6-tag which was visualised using Western blots. Nevertheless, C-terminally truncated products may be present in the samples which cannot be confirmed by the same method but could be detected using N-terminal sequencing or Mass Spectrometry. These products could have resulted from imperfect or erroneous protein expression however it is more likely to be as a result of post-translational modifications rather than from translation or mRNA problems as fully intact full-length protein has been expressed in large proportions (Fig. 2-7) and confirmed by N-terminal sequencing (Fig. 2-9) and Mass Spectrometry (Fig. 2-10).

However, results showed only cells grown in M9 minimal media completely regulated $VanS_A$ expression indicative of the undesirable high energy expenditure involved in expression of plasmid-encoded $VanS_A$, presumably unfavourable for cell survival in already resource limited environments such as in minimal media; supported by growth curves recording cell death during induction of $VanS_A$ expression (Fig. 2-3A). However, although smaller quantities of $VanS_A$ was present in other cell compartments (periplasmic, cytosolic) during growth conditions tested in M9 minimal media, the low cell density and experimental time-course for a single experiment mean it is not a suitable solution for $VanS_A$ expression, especially for medium-scale grow-ups required to obtain sufficient material for downstream experiments. Increased cell density was observed in rich-media conditions during experiments monitoring cell growth under different growth conditions (Fig. 2-3). Comparison of protein expression resulting from the two induction temperatures in each condition showed higher yields were obtained at lower induction temperatures (30 °C) (Figs. 2-4, 2-5 and 2-6).

In the case of experimental longevity, ease of making LB or 2TY, and the fewer relatively inexpensive resources compared to M9 make these conditions more favourable. Furthermore, use of fewer resources is beneficial for the long-term aims of the project, therefore LB rather than 2TY is preferred. For conditions where yields could be improved, for example in lower IPTG concentrations, longer induction periods could be used, which would have to be optimised. Induction at higher temperature could be left for shorter induction times as under these conditions higher yields of protein may be possible. Furthermore lower induction temperatures for longer periods of time could be trialled.

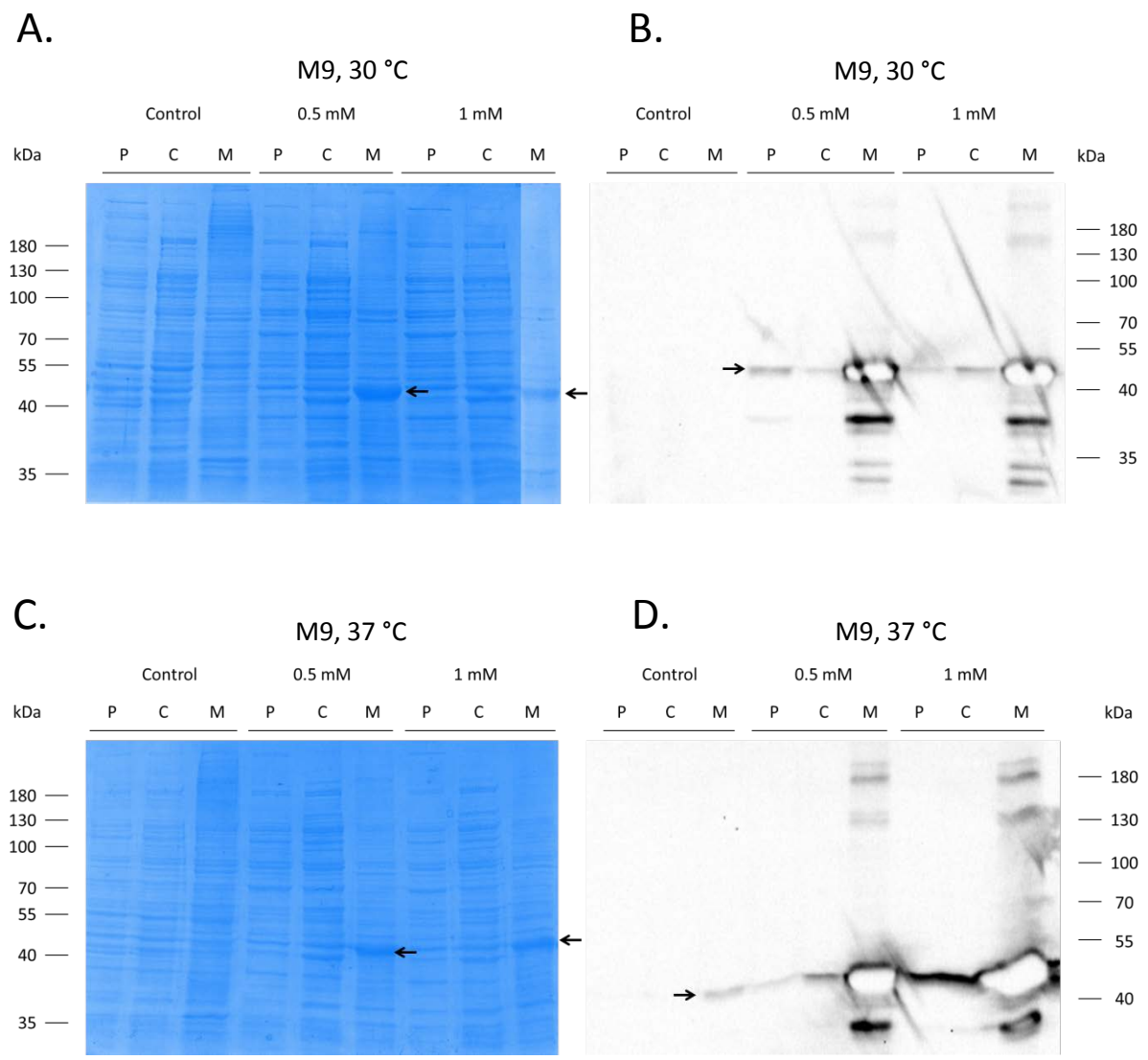

Figure 2-4: Expression trials of VanS$_A$ in M9 minimal media. *Expression trials of VanS$_A$ in M9 minimal media. Cells grown in M9 minimal media were induced with either (i) 0 (control), (ii) 0.5 mM or (iii) 1 mM IPTG at either (I) 30 °C or (II) 37 °C as described in Methods. Water lysis performed on cells as described in Methods. Samples of cell fractions containing 10 µg of total protein (determined by BCA assay, see Methods) were resolved using SDS-PAGE (5%/12%) as described in Methods. Gels were either Coomassie stained (A, C) or Western blotted for detection using Anti-His$_6$-HRP (B, D). Images collected using ChemiDoc XRS+ (BioRad), and analysed using ImageJ (Rasband, 1997; Schneider et al., 2012). Detected VanS$_A$ indicated by arrow (→).*

A. B.

LB, 30 °C LB, 30 °C

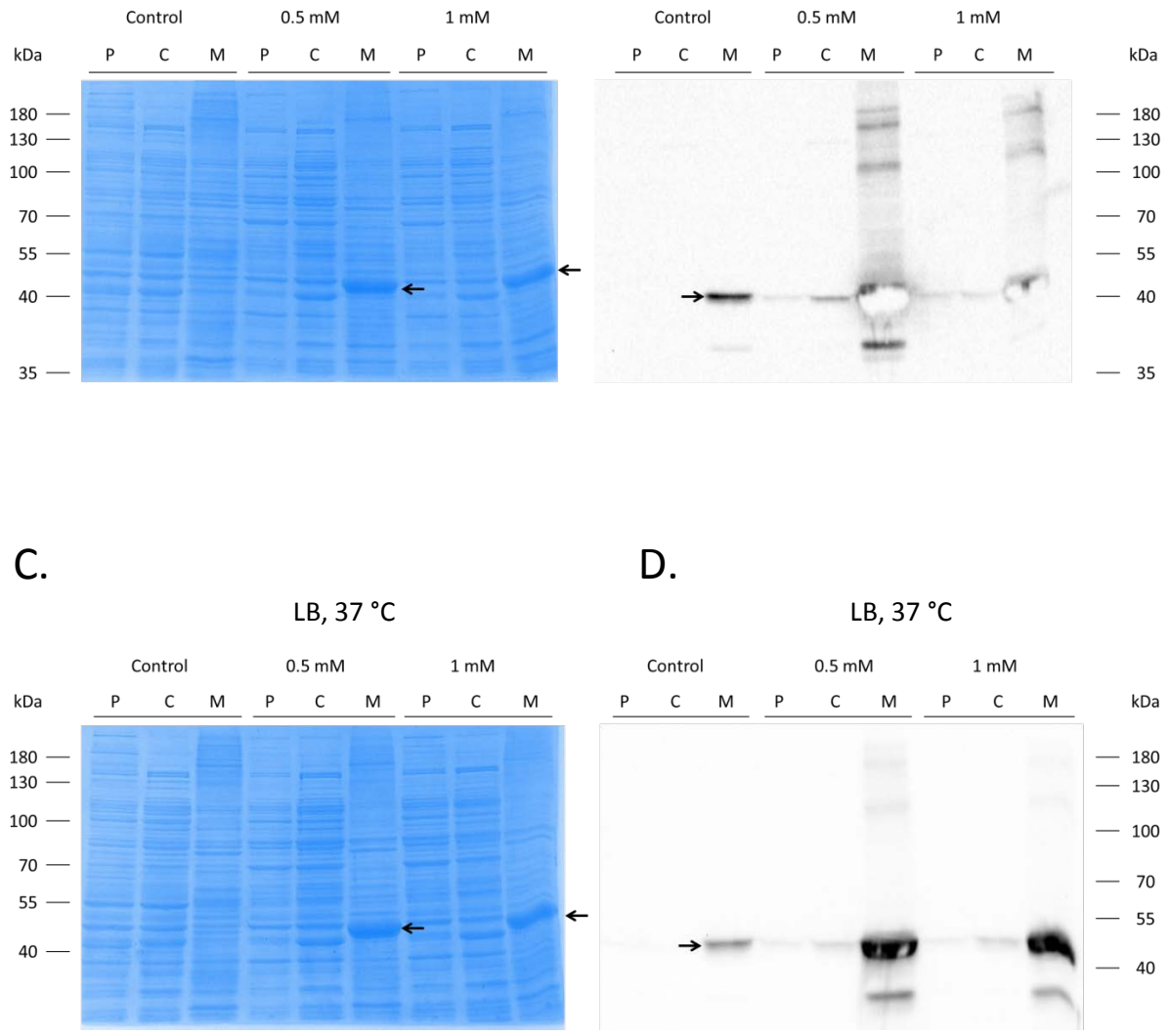

Figure 2-5: Expression trials of VanS$_A$ in LB media. *Cells grown in LB rich media were induced with either (i) 0 (control), (ii) 0.5 mM or (iii) 1 mM IPTG at either (I) 30 °C or (II) 37 °C as described in Methods. Water lysis performed on cells as described in Methods. Samples of cell fractions containing 10 µg of total protein were resolved using SDS-PAGE (5%/12%) as described in Methods. Gels were either Coomassie stained (A, C) or Western blotted for detection using Anti-His$_6$-HRP (B, D). Images collected using ChemiDoc XRS+ (BioRad), and analysed using ImageJ (Rasband, 1997; Schneider et al., 2012). Detected VanS$_A$ indicated by arrow (→).*

A.

2TY, 30 °C

B.

2TY, 30 °C

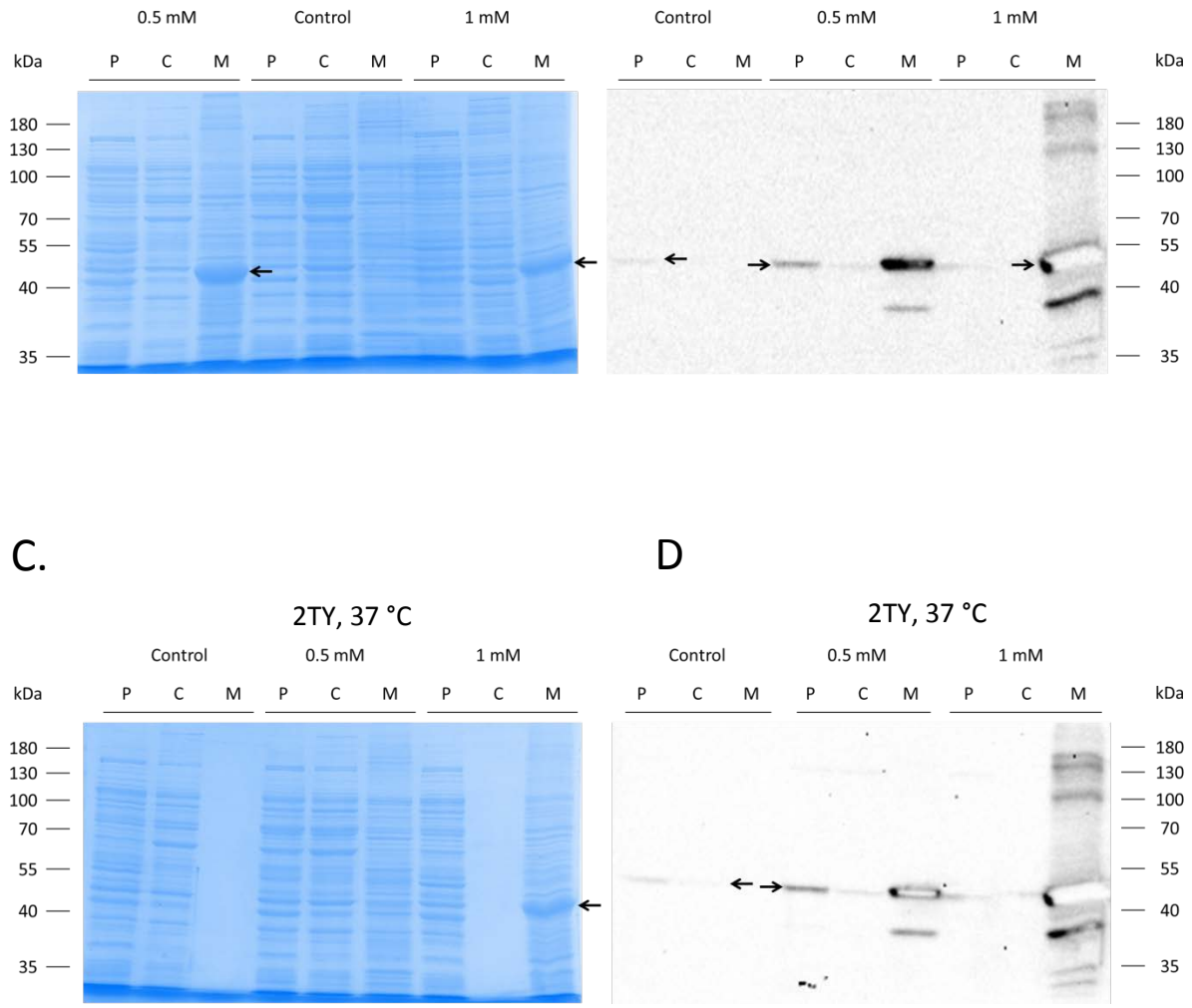

Figure 2-6: Expression trials of VanS$_A$ in 2TY media.

Cells grown in 2TY rich media were induced with either (i) 0 (control), (ii) 0.5 mM or (iii) 1 mM IPTG at either (I) 30 °C or (II) 37 °C as described in Methods. Water lysis performed on cells as described in Methods. Samples of cell fractions containing 10 µg of total protein were resolved using SDS-PAGE (5%/12%) as described in Methods. Gels were either Coomassie stained (A, C) or Western blotted for detection using Anti-His$_6$-HRP (B, D). Images collected using ChemiDoc XRS+ (BioRad), and analysed using ImageJ (Rasband, 1997; Schneider et al., 2012). Detected VanS$_A$ indicated by arrow (→).

2.4.3. Optimisation and confirmation of the purification of His-$_6$-tagged VanS$_A$

Once expression conditions for VanS$_A$ were optimised, similar optimisation approaches were taken to determine optimum conditions for the purification of VanS$_A$. A typical purification of VanS$_A$ is shown below (Fig. 2-7), demonstrating the presence of VanS$_A$ at each of the various stages of purification (↔) and the reduction in contaminating proteins throughout the purification process.

Fig. 2-7 shows a typical purification of VanS$_A$ (indicated by ↔). The final purification product (apparent molecular mass of ~43 kDa) was sufficiently pure (>90%) (Fig. 2-8) for downstream experiments. Western-blots and N-terminal sequencing confirmed the labelled band as VanS$_A$-His$_6$ (Figs. 2-8B and 2-9, respectively). The difference in the apparent mass of the band (43.4 kDa) from the predicted mass of VanS$_A$ (45764.79 Da) is typical of the previously described anomalous migration behaviour of membrane proteins in SDS-PAGE (Ma *et al*., 2008; Rath, Glibowicka, Nadeau, Chen, & Deber, 2009; Saidijam *et al*., 2003). Nevertheless, confirmation of the intact protein of the correct and full molecular mass (45774.91 Da) was obtainable by mass spectrometry (Fig. 2-10).

Additional bands were highlighted during Western blots of water lysis fractions (Figs. 2-4, 2-5 and 2-6) including lower molecular weight species potentially resulting from N-terminal degradation of VanS$_A$ and higher molecular weight species potentially from cross-reactivity of the antibody; all species disappear after purification, which was further confirmed by Mass Spectrometry results which showed no post-translational modification of the amino acid sequence for VanS$_A$ (Fig. 2-9B).

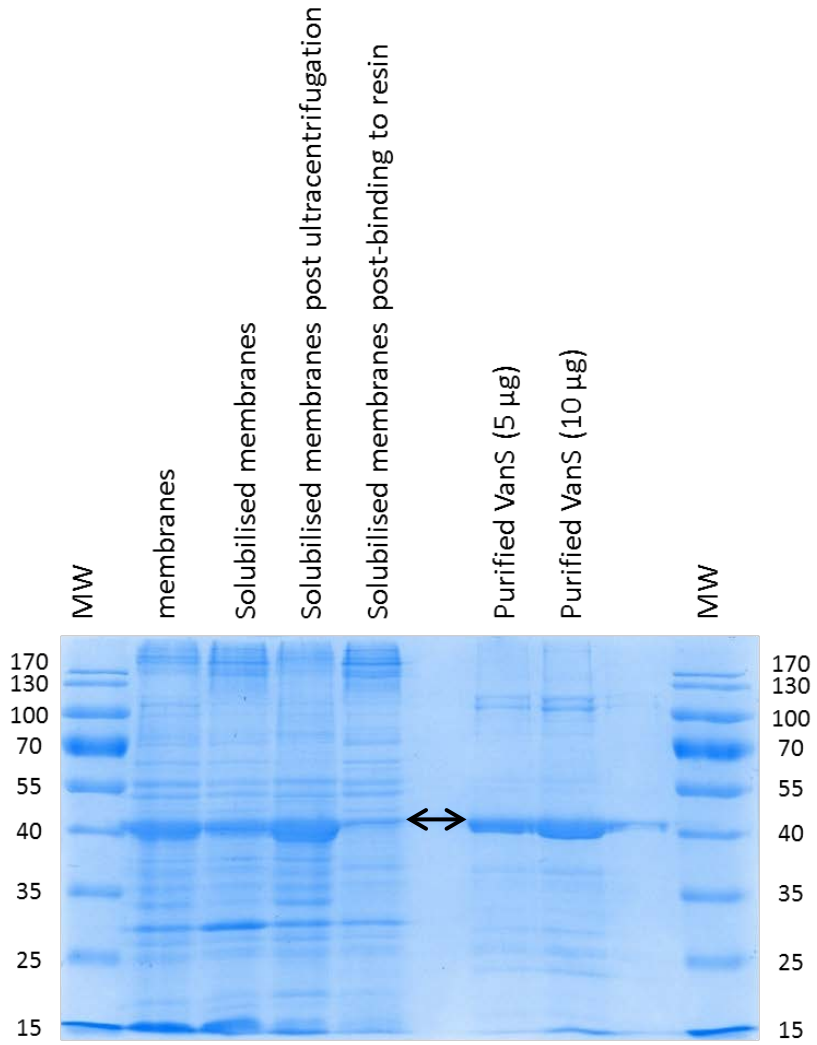

Figure 2-7: Purification of recombinant VanS$_A$. *SDS-PAGE of the final purified VanS$_A$ used in the SRCD and autophosphorylation experiments, and at various stages of the purification process. 5 and 10 µg of the final purified VanS$_A$, and 20 µg samples taken at various stages of protein purification process, were analysed by SDS-PAGE with a final concentration of 1X SDS-PAGE loading buffer in 15 ul total volume (n=6). VanS$_A$ is indicated by (↔). Molecular weight marker used is PageRuler™ (Fermentas) (10-170 kDa). Gel imaged using a ChemiDoc XRS+ (BioRad), and densitometry performed using ImageLab ™ (BioRad).*

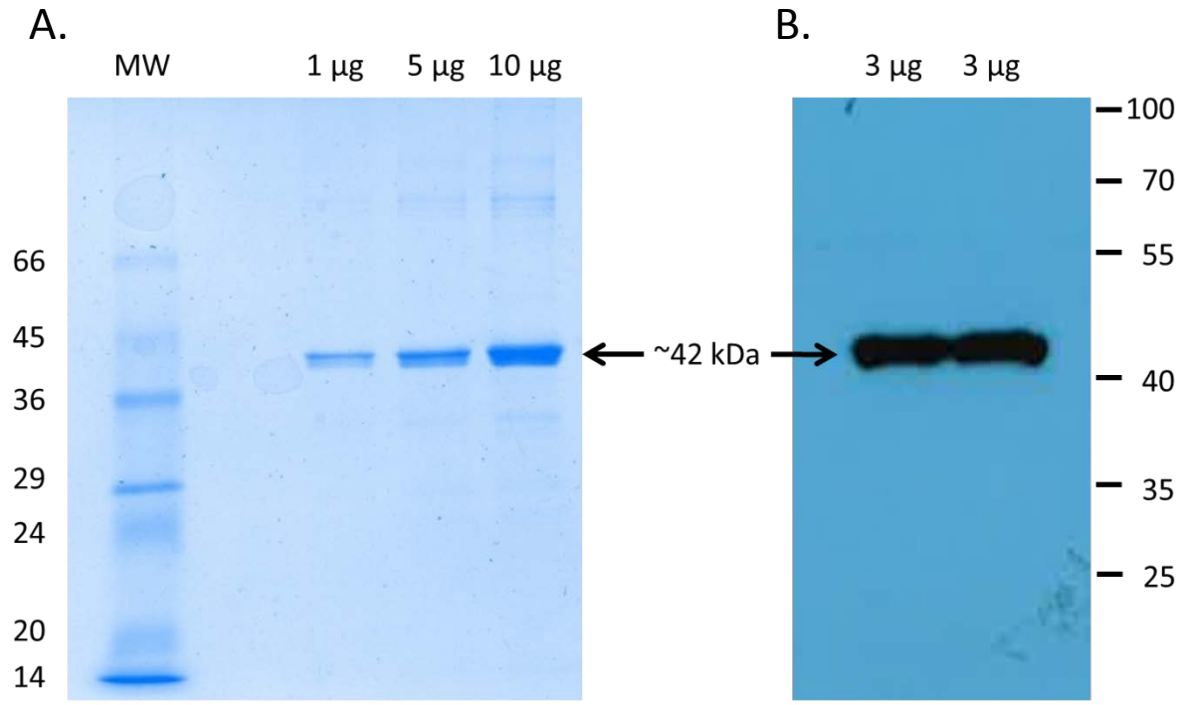

Figure 2-8: Coomassie-stained SDS-PAGE and Anti-His Western blot of purified VanS$_A$. *Purified VanS$_A$ (A) 1, 5, 10 µg; and (B) was resolved using SDS-PAGE electrophoresis through a 5%/12% SDS-acrylamide gel and (A) Coomassie stained using standard Coomassie stain as described in Methods, or (B) Western blotted under standard conditions described in Methods, probing using Anti-His$_6$ antibody (INDIA) and detection using SuperSignal West Pico Chemiluminescent Substrate (Thermo Scientific).*

N-terminal sequencing of purified VanS$_A$ confirmed the identity of the intensely stained protein band as VanS$_A$ as the N-terminal output matched the N-terminal portion of VanS$_A$ (Fig. 2-9). The predicted sequence incorporates the *EcoRI* cloning site, confirming the successful cloning and downstream overexpression and purification of the targeted VanS$_A$ protein, further confirmed by mass spectrometry which confirmed the expected amino acid sequence for VanS$_A$.

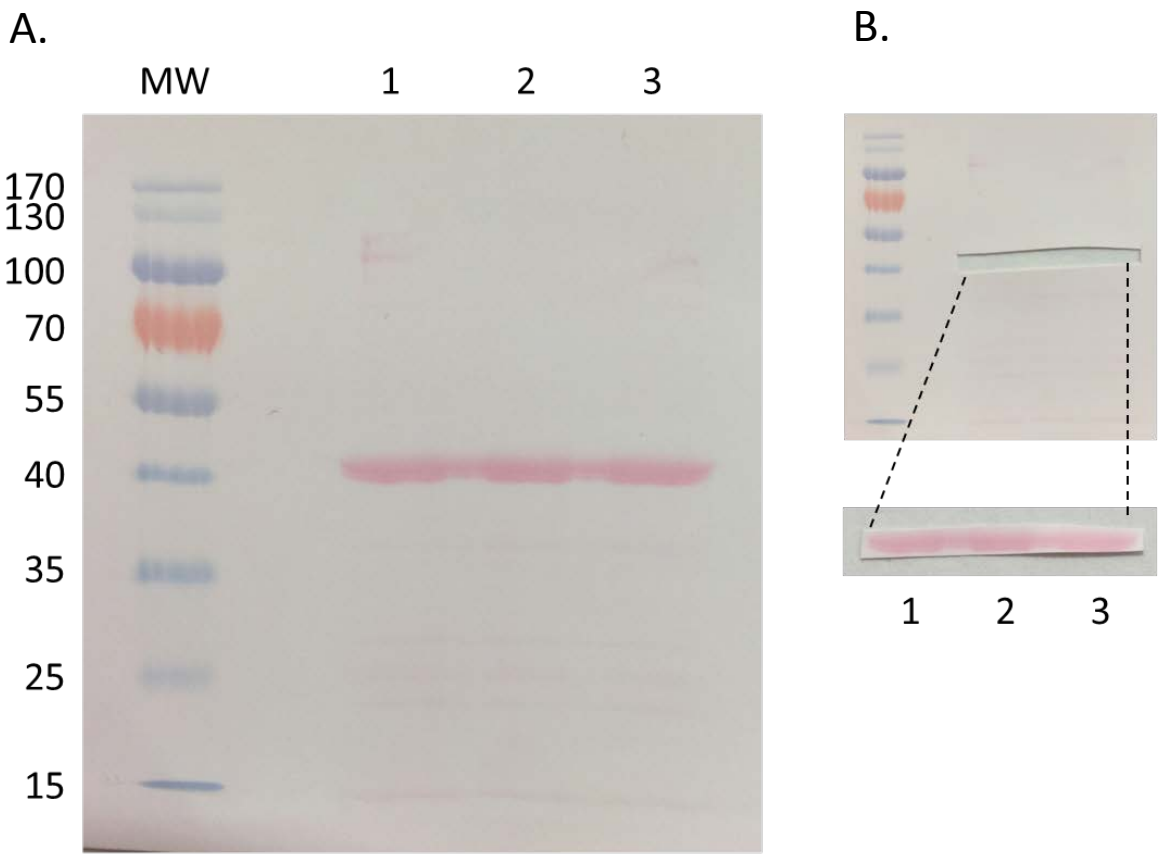

N-terminal sequencing:
N- M N S H M

His_6-tagged VanS amino acid sequence:
MNSHMVIKLKNKKNDYSKLERKLYMYIVAIVVVAIVFVLYIRSMIRGKLGDWILSILENKYDLNHLDAMKLYQYSIRNNID
IFIYVAIVISILILCRVMLSKFAKYFDEINTGIDVLIQNEDKQIELSAEMDVMEQKLNTLKRTLEKREQDAKLAEQRKNDVV
MYLAHDIKTPLTSIIGYLSLLDEAPDMPVDQKAKYVHITLDKAYRLEQLIDEFFEITRYNLQTITLTKTHIDLYYMLVQMTD
EFYPQLSAHGKQAVIHAPEDLTVSGDPDKLARVFNNILKNAAAYSEDNSIIDITAGLSGDVVSIEFKNTGSIPKDKLAAIFE
KFYRLDNARSSDTGGAGLGLAIAKEIIVQHGGQIYAESNDNYTTFRVELPAMPDLVDKRRSAAGGRGSHHHHHH

Figure 2-9: Protein-blotted PVDF membrane was stained using Ponceau S. *15 µg of purified His_6-tagged $VanS_A$ (lanes 1-3) was resolved using SDS-PAGE (5%/12%) before western-blotting onto PVDF membrane. The protein-blotted PVDF membrane was stained using Ponceau S (A) to visualise the band of interest before excising the bands of interest for analysis (B).*

A.

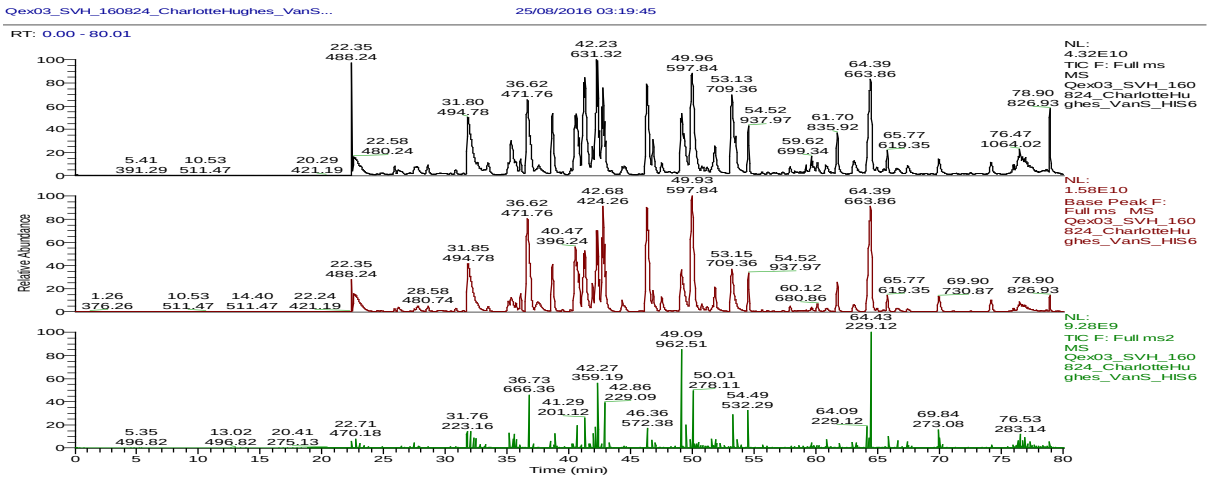

B.

Sequence	Mass	Start position	End position	Charges
MNSHMVIK	958.4728	1	8	2
NSHMVIK	827.4324	2	8	2
LGDWILSILENK	1399.771	49	60	2;3
YDLNHLDAMK	1218.57	61	70	2;3
YDLNHLDAMKLYQYSIR	2142.057	61	77	3;4
LYQYSIR	941.4971	71	77	2
VMLSKFAK	922.531	98	105	2
YFDEINTGIDVLIQNEDK	2125.022	106	123	2;3
QIELSAEMDVMEQK	1649.764	124	137	2;3
KNDVVMYLAHDIK	1544.802	159	171	2;3;4
NDVVMYLAHDIK	1416.707	160	171	2;3
TPLTSIIGYLSLLDEAPDMPVDQK	2615.34	172	195	2;3;4
AKYVHITLDK	1186.671	196	205	2;3
YVHITLDK	987.5389	198	205	1;2
YVHITLDKAYR	1377.741	198	208	3
LEQLIDEFFEITR	1651.846	209	221	2;3
YNLQTITLTK	1193.666	222	231	2;3
THIDLYYMLVQMTDEFYPQLSAHGK	2999.42	232	256	3;4;5
QAVIHAPEDLTVSGDPDK	1890.932	257	274	2;3
QAVIHAPEDLTVSGDPDKLAR	2231.155	257	277	3;4
VFNNILK	846.4963	278	284	2
NAAAYSEDNSIIDITAGLSGDVVSIEFK	2898.414	285	312	2;3
NTGSIPK	715.3865	313	319	1;2
DKLAAIFEK	1033.581	320	328	2
LAAIFEK	790.4589	322	328	2
LAAIFEKFYR	1256.692	322	331	2;3

FYRLDNAR	1053.536	329	336	2;3
LDNARSSDTGGAGLGLAIAK	1885.986	332	351	3
SSDTGGAGLGLAIAK	1316.694	337	351	2;3
SSDTGGAGLGLAIAKEIIVQHGGQIYAESNDNYTTFR	3852.892	337	373	4
EIIVQHGGQIYAESNDNYTTFR	2554.209	352	373	2;3;4
EIIVQHGGQIYAESNDNYTTFRVELPAMPDLVDK	3861.888	352	385	3;4
VELPAMPDLVDK	1325.69	374	385	2;3
VELPAMPDLVDKR	1481.791	374	386	2;3
GSHHHHHH	984.4175	394	401	2

Figure 2-10: Mass spectrometry results for $VanS_A$. *LC-MS/MS mass spectrometry of $VanS_A$ performed at the Advanced Proteomics Facility, Department of Biochemistry, University of Oxford as described in Methods. (A) Mass spectrometry spectrum for tryspin-digest fragments of $VanS_A$; (B) Table of fragment sequences identified using LC-MS/MS showing 35 unique peptides corresponding to the $VanS_A$ sequence with 78% of unique sequence coverage giving rise to the molecular weight of the $VanS_A$ 45.764 kDa.*

Conserved Histidine phosphorylated highlighted (Walsh, Fisher, Park, Prahalad, & Wu, 1996; Wright, Holman, & Walsh, 1993). *Predicted transmembrane regions highlighted. Predicted extracellular region (ligand binding domain) highlighted. Aromatic amino acids **tryptophan** and **tyrosine** lying in the predicted extracellular ligand binding domain.*

2.4.3.1. Optimisation of final buffer for $VanS_A$

Previous work (Pogson, 2013) determined final buffer conditions suitable for the purification of $VanS_A$ for use in synchrotron radiation circular dichroism experiments. However using the conditions described, solubility issues arose therefore buffer trials were conducted to determine the optimum conditions for the final buffer (Table 3). Factors such as salt, glycerol and detergent concentrations were considered as too high concentrations can affect the preparations suitability for downstream experiments. Different concentrations of DDM and glycerol were tested for their effect on the stability of $VanS_A$, in addition to the effect on downstream assay as too high concentrations of these components are often undesirable in downstream experimental designs, or may negatively affect the solubility and/or activity of the protein of interest (Neale *et al*., 2013).

The stability of $VanS_A$ in 10 mM HEPES pH 8.0, 20 % glycerol, 0.025 % DDM was compared to protein prepared in higher DDM concentration conditions (10 mM HEPES pH 8.0, 100 mM NaCl, 0.05 % DDM, 10 % glycerol). 0.025% DDM was used as the lowest concentration of DDM as this concentration is above the CMC (0.19 %) therefore was used as a concentration which is definitely above the CMC. The stability of $VanS_A$ in the lower concentrations of DDM and higher glycerol was greatly improved (with concentrations of 15-20 mg/ml achieved) compared to higher DDM concentration conditions (10 mM HEPES pH 8.0, 100 mM NaCl, 0.05 % DDM, 10 % glycerol in which 2-3 mg/ml could be achieved), with the protein remaining soluble and retaining structural integrity for several months when stored at 4°C compared to 1 month in higher DDM (Table 3). $VanS_A$ was stable in 10 mM HEPES pH 8.0 without additional DDM or glycerol and could be concentrated to 3-5 mg/ml (Table 3), though concentrations above 5 mg/ml were not tested for fears of precipitation in the addition of stabilising agents glycerol and detergent. Under these conditions $VanS_A$ retained its structural integrity and activity for over 1 month when stored at 4°C (Table 3). Furthermore, the presence of salt was argued not to affect the solubility of the protein as the addition of salt (to a maximum of 100 mM NaCl) was used with no negative influence on the solubility of $VanS_A$ in both

detergent concentration conditions (data not shown for lower detergent condition; **Fig**. 2-12 and Table 3 for higher detergent conditions).

By testing the solubility of precipitated protein pellet in different pH buffers the optimum pH for $VanS_A$ was found to be alkaline (> pH 8.0), with the pH 8.0 being the optimum (Fig. 2-11). At this pH, the protein remained soluble, and the pH was appropriate for use in other downstream experiments, such as activity assays which require a slightly alkaline pH due to the acid-lability of phospho-Histidine ATP (Attwood, Piggott, Zu, & Besant, 2007). Purification methods were adapted to suit the pH compatibility for the protein, and so all purification steps were carried out at pH 8.0. Once the protein was in an appropriate pH environment, the protein was stable for a long period of time and structurally sound (Table 3). This complements other work which showed the biosimilarity of protein preparations (see below).

During purification processes with the same ratios of washing buffer to resin (as described in *Methods*), it was found that purer preparations of protein were obtained when washing in HEPES buffer only, when no additional DDM or any glycerol were present. This could be due to the lack of components that may have a greater probability to bind to the column as a result of the increased viscosity when glycerol and DDM are present.

Buffer Components	Final concentration (mg/ml)	Appearance
10 mM HEPES pH 7.9, 0.05 % DDM, 5 % glycerol, 100 mM NaCl.	2 mg/ml	Clear. But a tendency to precipitate overnight, or within a short space of time.
50 mM NaPi pH 7.2, 0.05 % DDM, 100 mM NaCl.	—	Precipitated out of solution during buffer exchange.
10 mM HEPES pH 7.9, 0.05 % DDM, 10 % glycerol, 100 mM NaCl.	2 mg/ml	Clear
10 mM HEPES pH 8.0, 20 % glycerol, 0.025 % DDM.	16 mg/ml	Clear. Remains soluble for many months when stored at 4°C.
10 mm HEPES pH 8.0	2.5 mg/ml	Protein clear and soluble. Remained soluble for many months at 4°C.

**Precipitation was also observed using: 50 mM Tris/HCl pH 7.5, 100 mM NaCl, 0.05% DDM; 10 mM Tris/HCl pH 7.5, 25 mM NaCl, 0.05% DDM; 10 mM Tris/HCl pH 7.5, 100 mM NaCl, 0.05% DDM; 10 mM Tris/HCl pH 7.5, 300 mM NaCl, 0.05% DDM; 50 mM Tris/HCl pH 7.5, 300 mM NaCl, 0.05% DDM; 10 mM Tris/HCl pH 7.5, 5% glycerol (v/v), 100 mM NaCl, 0.05% DDM, 2 mM mercaptoethanol; 25 mM Tris/HCl pH 7.5, 5% glycerol (v/v), 100 mM NaCl, 0.05% DDM, 2 mM mercaptoethanol; 10 mM NaPi pH 7.2, 100 mM NaCl, 0.05% DDM; 10 mM NaPi pH 7.2, 25 mM NaCl, 0.05% DDM and 50 mM NaPi pH 7.2, 25 mM NaCl, 0.05% DDM.*

Table 2: Buffer components used for buffer optimisation of $VanS_A$.

Listed are the components of different buffer conditions trialled for $VanS_A$, and describing the appearance of the protein in each buffer condition.

A.

B.

Figure 2-11: Purified $VanS_A$ in different pH conditions.

$VanS_A$ preparations (1 mg/ml) in 10 mM HEPES, 20 % glycerol, 0.025 % DDM at either (A) pH 7.5 or (B) pH 8.0.

Most changes to the methods occurred post elution, during the final stages of preparation of the protein (the concentration and buffer exchange steps) with the final standardised method involving concentration of protein prior to buffer exchange before buffer exchange by dialysis. The advantages and disadvantages of the different methodologies tested during the optimisation of purification of $VanS_A$ are described in Table 4.

Methodology and timing	Advantages	Disadvantages
Buffer exchange using 100 kDa MWCO concentrator (Vivaspin)	Able to concentrate and buffer exchange in one step. Uses comparatively less buffer materials than dialysis.	Protein tended to precipitate out of solution. Takes a long time on a single piece of equipment which requires a lot of attention. Overall time consuming option.
Buffer exchange using dialysis tubing	Not as time-consuming as it can be left to buffer exchange overnight.	Requires a relatively larger volume of buffer components for efficient buffer exchange.
Concentrating prior to buffer exchange	Able to get the protein to a smaller volume and higher concentration when the protein is more stable. This means that dialysis should be more efficient and require fewer buffer changes and therefore reduce the waste from the process.	Often a long process due to the large volume of protein to be processed as a result of pooled elution fractions.
Concentrating after buffer exchange	Able to get the desired concentration of protein.	Possibility of precipitation.
Buffer exchange using a DG10 column (BioRad)	Easy to prepare. More economic and less time consuming as requires relatively less buffer materials	Requires concentration pre- and post- buffer exchange. Requires a specific volume of protein to be added to the

	for buffer exchange and can be left to flow through the column due to the stop-flow nature of the column.	column.

Table 3: Advantages and disadvantages of the use of alternative methods at different stages of the purification process.

2.4.4. Biosimilarity of purified $VanS_A$

When investigating protein form and function, especially when using sensitive techniques, such as Circular Dichroism (CD) to investigate structural features of proteins it is necessary to characterise the samples used (concentration, purity, etc.) (Kelly, Jess, & Price, 2005) for reliable data collection and analysis. An often overlooked area in protein research includes monitoring the biosimilarity of preparations as unaccounted differences in the starting materials (e.g. fold of protein or conformation of monitorable features such as aromatic side chains) when ignored may negate results.

The consistency of sample purity was monitored using SDS-PAGE, and the structure stability of the final protein produced was monitored using SRCD at different time point's post-final buffer exchange.

Higher detergent conditions (10 mM HEPES pH 8.0, 100 mM NaCl, 10 % glycerol, 0.05% DDM) resulted in the sustained instability of $VanS_A$ (Fig. 2-12) where protein required a 24 hour equilibration period for complete folding before using in any experiments. In buffer conditions containing lower concentrations of DDM (10 mM HEPES pH 8.0, 0.025 % DDM, 20 % glycerol), $VanS_A$ appeared more stable and did not appear to require the 24 hour stabilisation period (Fig. 2-12). Nonetheless the secondary structure estimations (SSE) from CD (Fig. 2-12B) did not match predictions form the amino acid sequence (Fig. 2-2) suggesting either errors in the prediction or indicating a potential incompatibility of the buffer for the protein.

SSE from these early batches of protein had lower helical content (Fig. 2-12) relative to homology predictions (Fig. 2-2) and subsequent batches presented later in the thesis (Fig. 3-9). It is possible that the methodology for these early preparations were not optimised for consistent folding of the protein, especially as later batches had increased helical content and were more comparable to homology predictions (Fig. 2-2). These later preparations used lower detergent concentrations, which could explain the differences. Detergent, although important for solubilisation out of the

membrane, can negatively affect folding (Gohon *et al*., 2011), stability (Yang *et al*., 2014) and solubility (Columbus *et al*., 2006) at high concentrations could negatively affect folding and solubility. In the cases presented here another possible explanation is the higher detergent conditions presented the formation of multimers (dimers), a state which could help to stabilise and encourage correct protein folding for the protein and explain the lack of helical folding in conditions not permitting their formation.

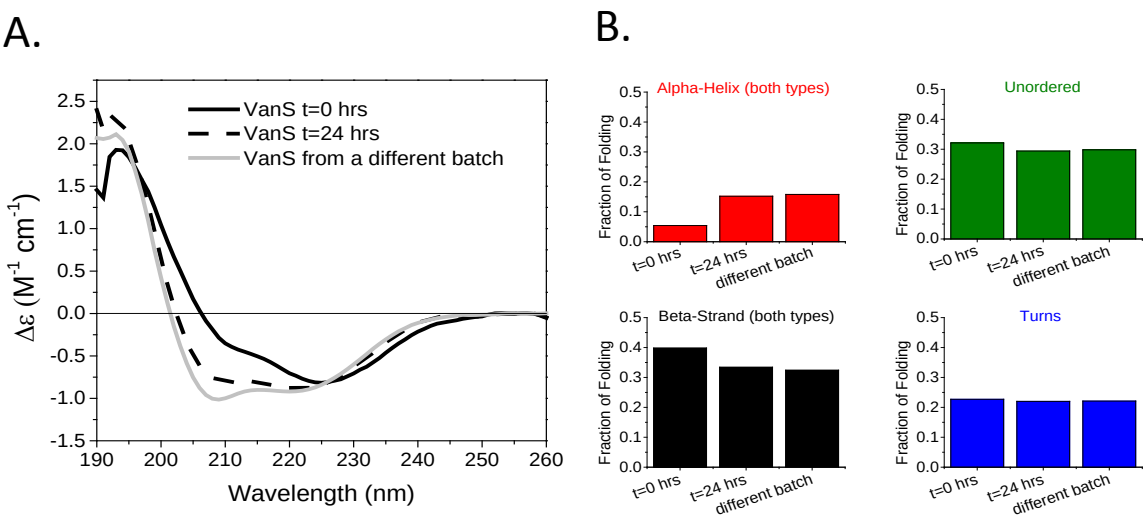

Figure 2-12: Difference spectra of $VanS_A$ at different time points post-final buffer exchange, from different batches.

(—) Protein in 10 mM HEPES pH 8.0, 0.05 % DDM, 10 % glycerol, 100 mM NaCl at t=0 hrs, defined as after buffer exchange by dialysis was complete; (···) Protein in 10 mM HEPES pH 8.0, 0.05 % DDM, 10 % glycerol, 100 mM NaCl at t=24 hrs, defined as 24 hours after buffer exchange complete; (—) Protein in 10 mM HEPES pH 8.0, 0.025 % DDM, 20 % glycerol at t=0 hrs, defined as 0 hours after buffer exchange complete.

2.4.5. Dimerisation and homogeneity studies of purified His_6-tagged $VanS_A$

2.4.5.1. Size-exclusion multi-angle light scattering (SEC-MALS) of detergent-solubilised $VanS_A$

SEC-MALS determines the molecular weight and size of molecules in solution from light scatter patterns created by the molecule of interest. Pairing the detection system to a size-exclusion column allows for the separation of species present in a sample and the determination of their size/weight in reference to a standard (commonly BSA). SEC-MALS can therefore be used as a method for the determination of the purity of a sample. Buffer subtraction during the analysis enables not only the determination of the homogeneity of a sample, but also the molecular weight when referenced to a standard, most commonly Bovine Serum Albumin (BSA).

A sloping yet flat baseline was observed for the buffer, indicative of light scattering from the detergent. A skewed Gaussian distribution was observed, which is weighted with larger retention volumes (Fig. 2-13) corresponding to higher molecular weight species.

Detergent micelles were retarded in the column for longer than $VanS_A$-DDM as predicted as lower weight species are retained in the column for longer than higher weight species and was shown to have a molecular weight of 12800 (±4500) Da (Fig. 2-13).

SEC-MALS studies revealed $VanS_A$ was present at a monomer with a molecular weight of 41510 (±931) Da, close to the predicted monomeric size of 45 kDa (Fig. 2- 13).

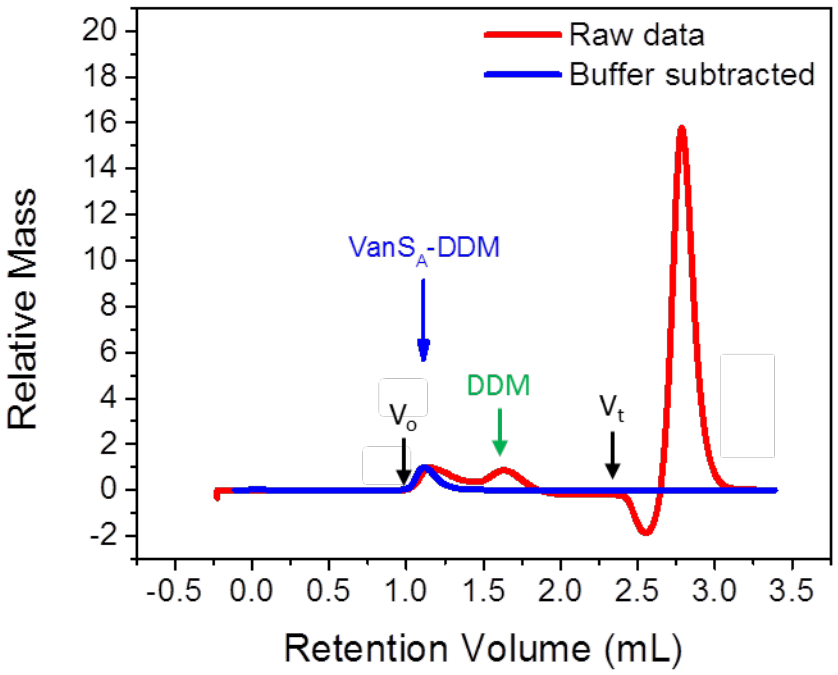

Figure 2-13: Spectrum of SEC-MALS datum for VanS$_A$.

A Superdex 200 Increase 5/150 GL column (GE Healthcare) was pre-equilibrated with 10 mM HEPES pH 8.0, 5% glycerol, 0.025% DDM before injection of 200 µl of VanS$_A$ (0.5 mg/ml) in 10 mM HEPES pH 8.0, 20 % glycerol, 0.025 % DDM using an ÄKTA pure system (GE Healthcare). Baseline set and the molecular weight calculated using data processing software (UNICORN 6, GE Healthcare). BSA as reference material was used to calibrate the instrument.

2.4.5.2. Dynamic light-scattering (DLS) of detergent-solubilised $VanS_A$

Similarly, DLS can be used to determine the homogeneity of a sample, and can therefore be used a method for the assessment of sample purity, homogeneity, and addition to as a method to screen for the effects of conditions and/or ligand/inhibitor binding studies.

DLS results showed the presence of detergent and glycerol resulted in a shift in the size distribution for $VanS_A$ (Fig. 2-14), presumably indicative of binding to $VanS_A$. Single skewed Gaussian peaks were observed for $VanS_A$ in each condition (Fig. 2-14) suggestive of non-homogenous preparations containing other species of different size which were present regardless of the addition or absence of glycerol or detergent. Only species smaller than the protein were detected buffer controls containing DDM and glycerol (fig. 2-14), presumably corresponding to the presence of detergent.

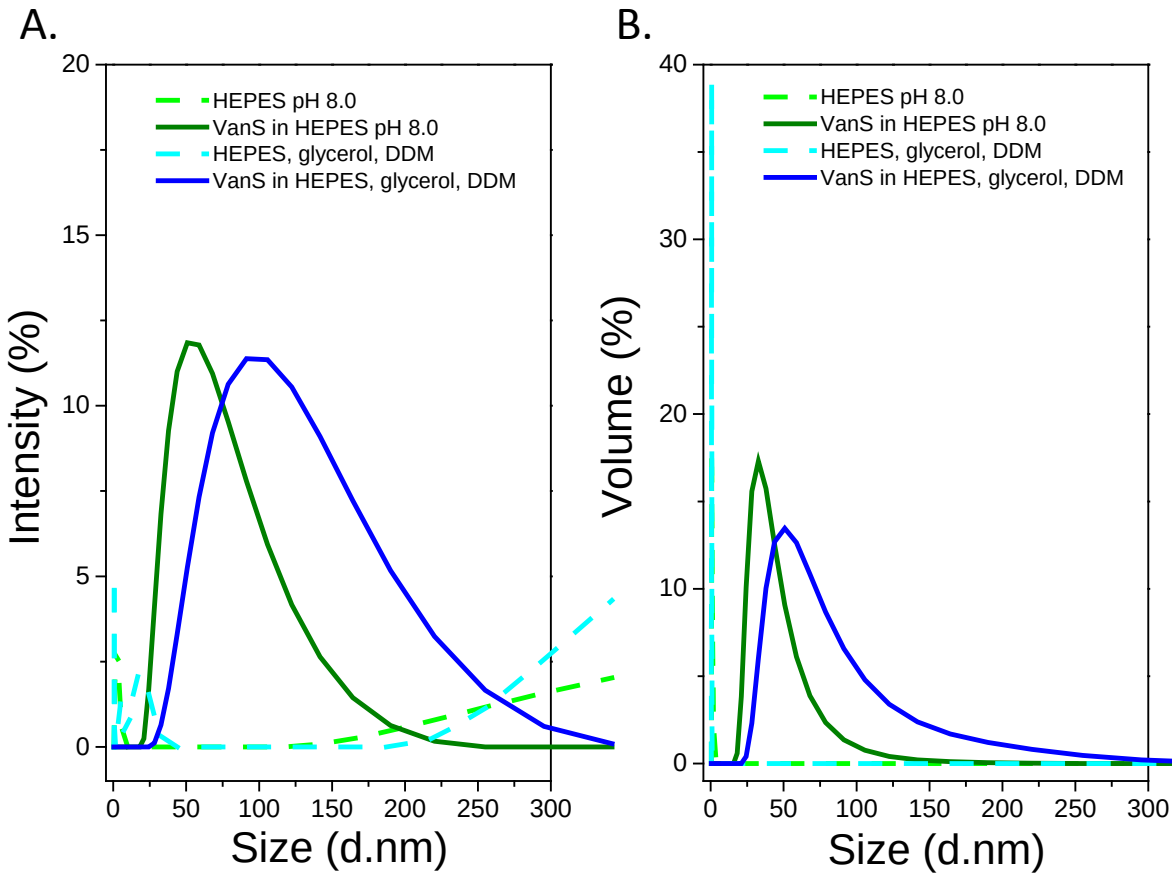

Figure 2-14: Comparison of the DLS spectrum for $VanS_A$ in different buffer conditions.

0.5 mg/ml of $VanS_A$ in either 10 mM HEPES pH 8.0 only (—), or 10 mM HEPES pH 8.0, 10 % (v/v) glycerol, 0.025 % (w/v) DDM (—), along with each respective buffer only (···,···) was analysed using Disposable Solvent Resistant Micro Cuvettes (ZEN0040, Malvern) in a Zetasizer Nano ZSP (Malvern), samples (70 µl) were analysed using pre-determined programme. (A) Intensity (%) and (B) volume (%) are shown.

2.5. Discussion

$VanS_A$ was found to successfully express and localise in *E. coli* inner membranes, with optimum expression conditions for use in downstream experiments identified as LB media, 1 mm IPTG, 30 °C induction temperature. The expression product was expressed as a fully intact product as mass spectrometry (Fig. 2-10) of the product closely matched the predicted molecular weight of the His_6-$VanS_A$, and the expression product was verified via N-terminal sequencing and Western blots (Figs. 2-9 and 2-8, respectively). Furthermore, purified $VanS_A$ was present as a homogenous monomeric preparation, regardless of final buffer conditions (Figs. 2-13, 2-14).

Optimum buffer conditions for $VanS_A$ were determined through buffer screens, including the determination of the optimum pH for $VanS_A$ which will be used in all purification processes. Results showed that lower concentrations of DDM were beneficial for $VanS_A$ stability (Table 2), supported by biosimilarity results showing a reduced equilibration period in lower DDM conditions (Fig. 2-12), in addition to enabling the concentrating of the final protein preparation to ~9-fold higher concentrations (Table 2).

In conditions containing higher concentrations of DDM, the protein was less stable and required an equilibration period before assays could be attempted. In conditions where the protein was in a lower concentration of DDM and higher concentration of glycerol, the protein was more stable and did not require the equilibration period described previously (Fig. 2-12). It could be that too high concentrations of detergent had deleterious effects on the stability of the protein due to the potential for detergent-mediated aggregation (Neale *et al.*, 2013). Glycerol of a well-known stabiliser of proteins (membrane and soluble) (Vagenende, Yap, & Trout, 2009) therefore it is not surprising that higher glycerol concentrations were beneficial for the protein.

Together these methods confirm the successful overproduction and purification of $VanS_A$ at purity suitable for use in downstream experiments after subsequent confirmation of the activity and structural integrity of the purified protein.

CHAPTER 3:
BIOPHYSICAL CHARACTERISATION OF LIGAND BINDING TO $VANS_A$

3.1. Introduction

Following confirmation of the purification of pure protein (Chapter 2) this Chapter describes the efforts made to identify binding species for $VanS_A$ which may affect the regulation of the expression of resistance genes (to be discussed in Chapter 4).

The activating ligand for $VanS_A$ is widely debated, with suggestions including the antibiotic itself (Koteva *et al.,* 2010), accumulating peptidoglycan precursors (Arthur & Quintiliani 2001), or the peptidoglycan-glycopeptide complex (Kwun *et al.,* 2013). Previous work identified vancomycin as a binding species to $VanS_A$ (Pogson 2013) therefore work described in this Chapter aims (i) to confirm and characterise vancomycin binding and (ii) investigate binding of other potential ligands including peptidoglycan components. This Chapter describes biophysical approaches including Circular Dichroism (CD), Magnetic Synchrotron Radiation Circular Dichroism (MSRCD), Fluorescence, Dynamic Light Scattering (DLS) employed to investigate the interactions of these suggested ligands for their interaction with $VanS_A$.

3.2. Working hypothesis

Biophysical methods shall be used to identify and characterise ligand(s) binding by $VanS_A$.

3.3. Methods

3.3.1. Synchrotron Radiation Circular Dichroism (SRCD) and Circular Dichroism

Circular dichroism spectroscopy relies on electromagnetic radiation which can be thought of as a travelling wave which can be described using equation *3.3.1-1.*

$$c = \nu\lambda \qquad \textbf{(Equation 3.3.1-1)}$$

Where c = velocity of light in a vacuum (m s^{-1}); ν = frequency (Hz); λ = wavelength defined as the distance between two successive peaks (mm).

In spectroscopy, the electromagnetic spectrum is characterised as light in terms of wavelength expressed in nanometres (nm). The UV region can be divided into the far- and near- UV (**Fig.** 3-1). Photons are absorbed at wavelengths where the energy of the incident photon matches the energy required for an electronic transition; the relationship is described in Equation *3.3.1-2*.

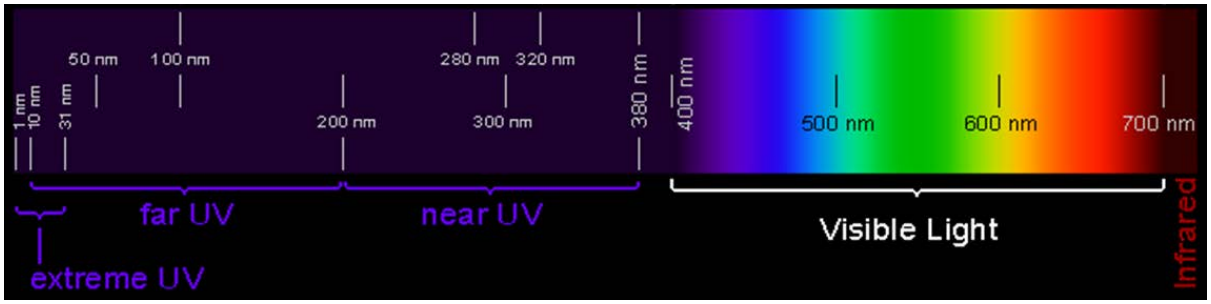

Figure 3-1: The UV and visible region of the electromagnetic spectrum. *Labelled are the UV region (1-380 nm), visible light (400-700 nm) and infrared light (starting from 700 nm). The UV region can be further divided into the extreme UV (1-31 nm), far UV (10-200 nm) and near UV (200-380 nm). Also shown are the visible regions (400-700 nm). Adapted*

from https://www.windows2universe.org/physical_science/magnetism/images/uv_spectrum_regions_big_gif_image.html.

$$E = h\,v \qquad \textit{(Equation 3.3.1-2)}$$

Where E = Energy (J); h = Planck's constant ($6.62607004 \times 10^{-34}$ J); v = frequency (s^{-1}).

Rearrangement using Equation *3.3.1-1* gives the expression in Equation *3.3.1-3.*

$$E = h\,\frac{c}{\lambda} \qquad \textit{(Equation 3.3.1-3)}$$

Where E = Energy (J); h = Planck's constant ($6.62607004 \times 10^{-34}$ J); c = velocity of light in a vacuum; λ = wavelength defined as the distance between two successive peaks.

Application of spectroscopic methods requires the consideration of experimental parameters in order to acquire relevant and experimentally sound data; the most important, the Beer-Lambert rule (*Equation 3.3.1-4*)

$$A = c.\,L.\,\varepsilon \qquad \textit{(Equation 3.3.1-4)}$$

Where A = absorbance; c = concentration ($mol.L^{-1}$); L = pathlength (cm^{-1}); ε =molar absorption of molecule at a specific wavelength ($L.mol^{-1}.cm^{-1}$). The ε is specific to the chromophore studied. In the case of proteins and peptides, ε_{280} can be calculated for proteins containing aromatic amino acids Trp/Try/Phe, and for non-aromatic-containing peptides the ε_{210}, which accounts for the peptide bond, can used.

Absorbance is therefore an important variable during data collection (as per *Equation 3.3.1-4* and *Equation 3.3.1-5)* which must not exceed an absolute limit of 1.5, with optimum values at 0.8 (Johnson 1985) in order to reduce excessive scattering of light and shielding of the absorbing properties of the materials studied. To achieve this, through application of the Beer-Lambert law (*Equation 3.3.1-4*) and accounting for the molar extinction coefficient of the chromophore of interest

(ε), pathlength and concentration of sample can be changed (*Equation 3.3.1-4*) to achieve optimum conditions. Pathlengths available at B23 range from 0.0002 to 0.02 cm for CaF_2 cells and 0.01 to 10 cm for quartz cells (http://www.diamond.ac.uk/Beamlines/Soft-Condensed-Matter/B23/status.html).

Sample preparation is extremely important as samples must be very homogenous and soluble, and in the case of protein solutions, free of aggregates in order to reduce light scattering which would reduce the absorbance of incident light towards the chromophores. Removal of aggregates by centrifugation and/or filtering are all worthwhile approaches during sample preparation. Furthermore, sample concentration determination is incredibly important (as a factor of the Beer-Lambert rule, *Equation 3.3.1-4*), more so after removal of aggregates. Spectroscopic rather than colorimetric approaches for concentration determination, e.g. in the case of proteins via the use of a nanophotometer are more desirable due to the increased specificity of absorbance at a specific wavelength (*See 2.3.9*).

Dichroism is defined as the differential absorbance of polarised light by a material, and is referred to Circular Dichroism when applied to the differential absorbance of left- (LCP) and right- (RCP) handed polarised light. Monitoring the differences in absorbance at different wavelengths (λ) is the basis of Circular Dichroism spectroscopy (*Equation 3.3.1-5*) (Fig. 3-2).

$$\Delta A(\lambda) = A(\lambda)_{LCP} - A(\lambda)_{RCP} \qquad \textbf{(Equation 3.3.1-5)}$$

Where λ = specific wavelength.

Throughout measurements, high signal:noise ratios are desirable in order to obtain reliable results. In order to achieve optimum experimental conditions for reliable data collection detector voltage must not exceed 600 mA or N. In order to achieve this, the following parameters (sample absorbance, pathlength, concentration, integration time, scan repeats, slit width) can be tuned as

per experiment (*Equation 3.3.1-6*), within the experimental set-up available at B23, and will be discussed below.

$$\frac{signal}{noise} = (Q.l.t)^{\frac{1}{2}} \qquad \textit{(Equation 3.3.1-6)}$$

Where *Q* = detector quantum efficiency; l = light intensity; *t* = time scale of the measurement.

Of these variables, *Q* and l are instrument dependent and customisable, although can be tuned for the bandwidth of incident light applied to the sample but not the source intensity (3.2 x 10^{12} photons s^{-1} $mm^{-2}$for B23, and 3.2 x 10^{11} for new Chirascan bulbs which degrades with age unlike light from synchrotron sources). The highly collimated micro-beam (0.15 mm^2) of synchrotron sources are characterised by less divergent incident light relative to benchtop CD instruments (100 mm^2). This results in greater light intensities upon the sample (Javorfi *et al.,* 2010) and therefore higher a signal:noise ratio is available using synchrotron light sources (Hussain *et al.,* 2016). The timescale of measurements are variable, and can be changed either by the length of time per measurement per wavelength (integration time) or the number of repeated scans (*Equation 3.3.1-7,* derived from rearrangement of *Equation 3.3.1-6*), both of which will improve the signal:noise ratio of the average scans.

$$n \propto \sqrt{s} \qquad \textit{(Equation 3.3.1-7)}$$

Where *n* = signal:noise ratio and *s* = number of scans.

Slit width changes the light intensity applied to the sample which is an important consideration for experiments, as increased light intensity improves the signal:noise ratio (*Equation 3.3.1-6*) however this can also lead to photo-instability and denaturation of samples (Longo *et al.,* 2015) which is more undesirable when monitoring the peptide backbone conformation in the far-UV region. Compromises must be made for data quality and sample stability. On Module B at B23, Diamond Light Source slit width is variable from either 0.5 or 1 mm (equivalent to 1.1 to 1.8 nm bandwidth), or

variable bandwidth in nm using the Chirascan™-Plus (Applied Photophysics) used in the data presented throughout this Thesis.

SRCD spectroscopy was carried out in a nitrogen-flushed chamber at beamline B23 at the Diamond Light Source Ltd, Oxfordshire as described in (Javorfi *et al.,* 2010; Siligardi *et al.,* 2014a). For Circular Dichroism studies, experiments were conducted using a Chirascan™-Plus (Applied Photophysics).

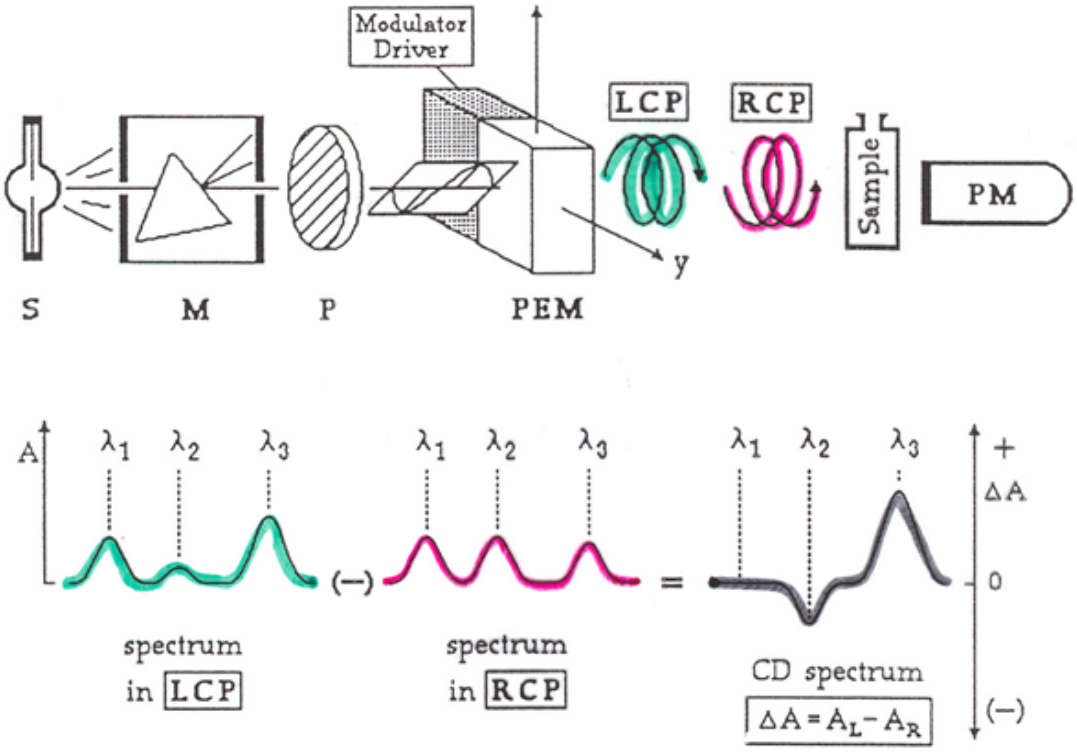

Figure 3-2: Schematic of a CD instrument. *Light from source (S) passes through a monochromator (M) to produce light of specific wavelength which is passed through a polariser which filters out light of different orientations to produce light in a single plane. The plane of polarised light of specific wavelength is passed through a photoelastic modulator orientated 45 ° to the beam resulting in the a 1 quarter-wave shift for one component of linearly polarised light to produce left- and right- circularly polarised light which is applied to the sample. Transmitted light is detected by the photomultiplier (PM), the final CD spectrum resulting from the differences in LCP and RCP light detected when passed through the sample. Image reproduced from Hussain & Siligardi 2016.*

Circular dichroism spectroscopy enables the monitoring of the absorbance of circularly polarised light of different wavelengths by chiral species. Many biological molecules including proteins and nucleotides exist in 2 "mirror-image" forms, left- and right- handed forms, which absorb left and right-handed circularly polarised light differently; this can be monitored using a circular dichroism spectrometer. In the case of proteins, the compounds monitored throughout this Chapter, transitions of the protein backbone and aromatic amino acids can be monitored in the far- and near-UV respectively.

3.3.1.1. Measurements in the far-UV region

In the far UV, transitions of the peptide bonds are monitored (stronger π→π* and weaker n→π* monitored at 190 nm and 220 nm, respectively) the intensity and energy of which are dependent on the ψ and ϕ angles of the peptide bond (Fig. 3-3).

As stated previously, absorption is related to the electronic transitions of molecules. Absorption in the far UV region (210 nm) of the peptide bond is ~30 times higher than chromophores in the near UV region (Anthis & Clore 2013), hence peptide bond transitions have higher molar absorption extinction coefficients than chromophores in the near UV region (e.g. aromatic side groups). Applying this to the Beer-Lambert law (Equation 3.3.1-4) shows why low concentrations of proteins can be used in the far-UV region (Kelly et al. 2005) as under experimental conditions of a fixed pathlength and fixed absorbance the molar extinction coefficient is inversely proportional to concentration (Equation 3.3.1.1-1).

$$\varepsilon = \frac{1}{c} \qquad \textbf{(Equation 3.3.1.1-1)}$$

When monitoring protein conformation in the far-UV region relatively low concentrations of sample are required due to the large extinction coefficient of the peptide bond chromophore monitored (Fig. 3-3).

Far-UV measurements (180-260 nm) were commonly collected using 0.5 mg/ml of $VanS_A$. Employing cylindrical cells with 0.2 mm pathlength, 4 scans were collected at 20 °C in 1 nm increments using 1 s integration and either 1 nm bandwidth (CD) or 1 mm slit width (equivalent to 1.8 nm bandwidth) (SRCD). Data presented in molar extinction (Δε). Measurements are obtainable in the <190 nm region in appropriate buffer conditions as absorbance from salt ions (e.g. Cl^-) common in protein buffers can interfere with reliable signal acquisition.

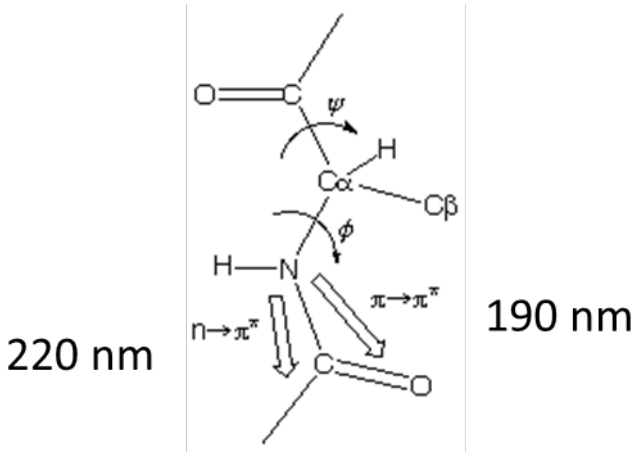

Figure 3-3: Representation of peptide bond monitored in the far-UV region using CD. *π→π* and n→π* bond transitions monitored at 190 nm and 220 nm respectively. Intensity dependent on the orientation of the peptide bonds and respective φ and ψ angles. Image adapted from http://www.proteinchemist.com/cd/cdspec.html*

3.3.1.1.1. Secondary structure estimations (SSE)

Characteristic spectral profiles are collected for the different secondary conformations of proteins when studied in the far-UV region (180-260 nm) (Fig. 3-4). From obtained spectra (of unknown secondary structure content) SSE can be made using a range of methods which commonly assume the spectrum of a protein is a single linear representation of the combined contributions of its secondary structural elements with "noise" variance (contributions from aromatic or prosthetic groups).

Generally, evaluation of conformation is by either of two methods which uses (1) polypeptide standards of known composition determined by X-ray scattering of films or IR in solution, or (2) spectra or proteins whose structure has been resolved using X-ray crystallography as standards. The standards are used as references which are compared to the unknown proteins using least squares analysis, ridge regression, singular value decomposition, single value decomposition with variable selection, the self-consistent method or neural network analysis (reviewed in Greenfield 2006b). Of these methods, least squares analysis programs, e.g. CONTIN, which keeps reference contributions low unless in good agreement with the raw data for the unknown and the theoretical best fit (Greenfield 2006).

Normalised mean residual standard deviation mean (NMRSD), is an estimator which accounting for the average of the square of deviations for which values closer to zero are preferred. It is the normalised square root of variance (standard deviation) which allows for comparisons between datasets and models, normalised by either the mean or the range, which in this case would be normalised to the average trace for the SSE therefore the closer to zero the better the estimate.

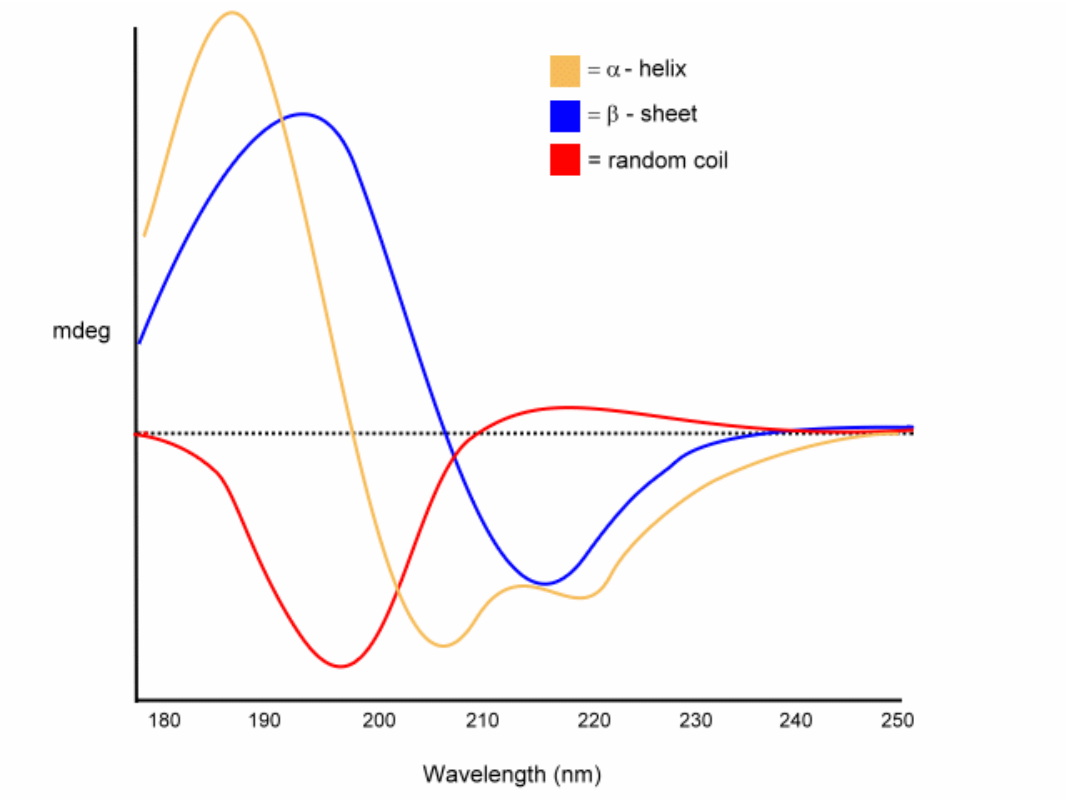

Figure 3-4: Spectra in the far-UV region for the common secondary structure components of proteins.

Image from http://www.proteinchemist.com/cd/cdspec.html. Where random coil means unordered structure.

Secondary structure estimations of $VanS_A$ were performed from data collected in the far-UV region using the CONTINLL algorithm (Provencher & Glockner, 1981; van Stokkum *et al.*,, 1990; Sreerama & Woody, 2000) and SMP 56 (43 soluble, 13 membrane) database.

3.3.1.2. Measurements in the near-UV region

The comparatively weak signals of aromatic amino acid chromophores monitored in the near-UV region (260-310 nm) means alternative strategies are applied to spectroscopic approaches. Often, longer signal accumulation time (integration time and scan repeats), longer pathlengths and higher concentrations are employed. The interferences from salts seen in the far-UV region are not applicable in the near-UV region. Furthermore photon flux is considered low enough at these wavelengths to not negatively affect protein stability.

In the near UV region chromophores including aromatic amino acids phenylalanine, tyrosine and tryptophan can be monitored in folded protein systems. Under these conditions a static aromatic ring is monitored in a chiral environment; during unfolding protein this chirality is lost and therefore cannot be monitored. Other properties which can be monitored in the near UV region include disulphide bonds and porphyrin ring systems.

Signals are dependent on the orientation of the chromophores with respect to global tertiary structure of the protein of interest; therefore signals are specific to the protein and batch producing a "fingerprint" for the protein of interest.

3.3.1.2.1. Qualitative measurements in the near-UV region

Near-UV measurements (260-350 nm) were collected using 1 mg/ml of protein and rectangular cells with 10 mm pathlength. Employing 2 nm bandwidth (CD) or 1 mm slit width (equivalent to 1.8 nm bandwidth); measurements were collected at 20 °C in 1 nm increments and 1 s integration time. Data presented in mean residue ellipticity (Kelly & Price, 2005).

3.3.1.2.2. Titrations in the near-UV region

Titration approaches using CD has been established for the determination of the dissociation constant for the interactions of the soluble protein ligand interactions and protein complex formation (Siligardi *et al.,* 2002; Freeman *et al.,* 1998; Prodromou *et al.,* 1999).

In the case of membrane proteins, the presence of added detergent, difficulties of handling commonly viscous membrane protein preparations, in addition to the relatively low yields of membrane proteins obtainable means the use of highly collimated beams from synchrotron light sources and the small aperture cells available at B23, Diamond Light Source are invaluable for the adaptation of these established titration approaches for membrane proteins (S. Patching *et al.,* 2012; Siligardi *et al.,* 2014b).

Titration experiments were performed as described previously (Siligardi *et al.,* 2002; S. G. Patching *et al.,* 2012). Following experimental plans designed using CDApps (Hussain *et al.,* 2015) ligand stock solutions were added incrementally in small volumes (not exceeding a limit of 15 % of the starting volume) to achieve protein:glycopeptide ratios of 1:0.3 to 1:11. Change in CD (mdeg) at a specific wavelength obtained during analysis using CDApps (Hussain *et al.,* 2015) was transferred to OriginPro® 9 for plotting against the corresponding concentration of ligand at each titration point and fitting with a Hill 1 function to determine the K_d for binding.

All samples were incubated at 20 °C for 30 minutes prior to data collection. All data was analysed using CDApps (Hussain *et al.,* 2015) where the mean residue weight of $VanS_A$ was taken to be 113. Unless otherwise stated, all spectra presented are difference spectra where all relevant background buffers, ligands etc. have been subtracted. Data acquired when the HT of the detector (PMT) was equal to or greater than 600 V were excluded from the analyses.

3.3.1.3. Temperature denaturation studies in the far UV region

Thermal denaturation of a protein of interest can lead to the establishment of the thermal stability of a protein of interest. Such experiments can either be manually executed or controlled by a script run by SpectralWorks Software (OLIS™). The temperature is controlled by a Quantum Peltier System (5-95° C) (Quantum Northwest, Inc) which pumps water heated/cooled to a specific value within a pre-determined tolerance into the cell holder. The sample is held at the specified temperature for a length of time (encoded in the script if using) before data collection.

Employing 0.5 mg/ml of $VanS_A$, measurements were routinely collected using a cylindrical cell of 0.2 mm pathlength in 1 nm increments using 1 s integration and 1 mm slit width (equivalent to 1.8 nm bandwidth) over a range of temperatures (20 °C - 95 °C, in 5 °C increments) in the absence and presence of ligands. Samples were incubated at the initial 20 ^{o}C for 30 minutes after ligand or solvent addition prior to acquisition of spectral data in the far-UV region (180-260 nm). At each temperature step reactions were incubated for 2 minutes prior to data collection (1 scan). A final scan was acquired post-temperature ramp after returning to 20 ^{o}C and incubation for 20 minutes before data acquisition. Data was analysed using CDApps (Hussain *et al.,* 2015) to obtain difference spectra where all controls (buffers, ligands, etc.) had been subtracted. Change in CD (mdeg) at a specific wavelength was transferred to OriginPro® 9 and plotted against the corresponding temperature for fitting to a Gibbs-Helmholtz equation derived from Boltzmann distribution (Singleton et al. 2016; Greenfield 2007) sigmoidal two-state denaturation curve to a Boltzmann distribution and the expression modified to include parameters for fitting of thermal denaturation data for the calculation of the melting temperature (T_m). Secondary structure estimations of $VanS_A$ were performed from data collected in the far-UV region using the CONTINLL algorithm (Provencher & Glockner, 1981; van Stokkum *et al.,*, 1990; Sreerama & Woody, 2000) and SMP 56 (43 soluble, 13 membrane) database.

3.3.1.4. Measurements in the near UV region

Measurements in the near-UV region (260-340 nm) were undertaken using 16-20 µM $VanS_A$ at 20 ^oC. Typically ligands such as vancomycin, teicoplanin (Targocid^R), Lipid II etc. were added in 2- or 5-fold molar excess. The total samples volumes were 70 µl and unless otherwise stated, 10 scans were acquired and the average spectrum presented. Spectral data was acquired in 1 nm increments using a 1 cm pathlength (2 mm × 2 mm aperture) and a 1 mm slit width, with a 1 s integration time.

3.3.2. Magnetic Synchrotron Radiation Circular Dichroism (MSRCD)

During MSRCD, the sample is held in a strong magnetic field applied parallel to the direction of the beam of light. In a compound in the absence of a magnetic field, the magnetic moments of orbiting electrons are cancelled out and the energy levels remain at equilibrium. In the presence of a magnetic field, the applied field induces a Zeeman effect, splitting the excited state into composite species of equal energy and opposite sign (Fig. 3-5). These species are absorbed to different extents by a material, and it is this difference which is monitored using MSRCD. For this reason, MSRCD can be applied to any chiral or non-chiral material as the asymmetry is induced by the magnetic field, and the resulting MSRCD is not directly related to the stereochemistry or CD of the material studied.

In the absence of a magnetic field the energy difference between ground and excited energy states are equal to wavelength (Fig. 3-5). The presence of a magnetic field leads to Zeeman splitting of the excited state into composite transitions of equal energy and opposite sign (Fig. 3-5) which are absorbed to different extents by materials which overall changes the final excitation wavelength and can be observed by a shift in λ_{max} (Fig. 3-5). Changes to the intensity of spectral peak can be influenced by the environment. Movement into more polar environments, e.g. movement from a buried to a solvent-exposed conformation, results in exposure to electron withdrawing groups which cause reductions in peak intensity and a blue-shift of λ_{max}. Movement to a more buried environment

and exposure to electron donating groups results in an increase in intensity and red-shift of λ_{max} (Djerassi *et al.* 1971; Barth *et al*. 1972; Longo *et al*. 2015).

In the case of biological materials, specifically proteins, aromatic amino acids contain polarisable electrons which give rise to MCD signals. MSRCD allows the monitoring of weak transitions of specific aromatic amino acids which can be masked during conventional CD studies. The strong polarisation of the electromagnetic transitions of tyrosine and tryptophan enables a clear distinction of signals for each amino acid and the potential to monitor their specific interactions (Hughes *et al.,* 2015). These strong, specific signals mean low concentrations and fewer scans due to the high signal:noise ratio are required per experiments which further increases the efficiency of the method.

Collection of MSRCD measurements are possible by modification of the sample holder at B23, Diamond Light Source by addition of a 1.4 Tesla magnet (Olis™) in which the sample is held for data collection in a known orientation with respect to the magnetic field (e.g. North-South and South-North) therefore two MSRCD spectra are obtained per sample. The final MSRCD spectrum is obtained by subtraction of spectra (S-N) – (N-S) to effectively cancel out and remove normal CD contributions. Measurements are collected in the aromatic region of the near-UV (260-310 nm), and can be collected in the absence of a magnetic field using the non-magnetic sample holder in order to collect standard near-UV spectrum for comparison.

The use of the modified sample holder restricts beam availability to 1 beam therefore for standard near-UV control measurements longer accumulation times may be required; however in the case MSRCD the strong, specific signals obtained relative to conventional CD does not pose a problem for data collection. However, care must be taken with ensuring a consistent orientation of the cell in relation to the propagation of light.

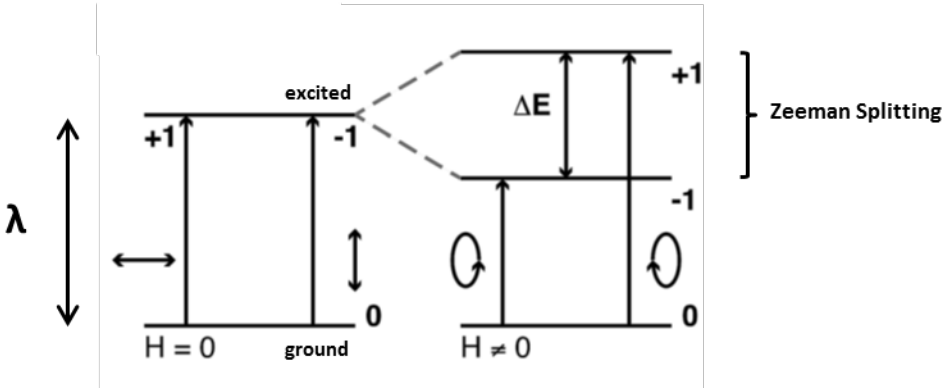

Figure 3-5: Schematic representation of the electronic transitions during MCD of a sample in a magnetic field (H), which is parallel to the direction of light propagation.*Zeeman splitting of an excited state in the presence of a magnetic field (H) produces signals of equal intensity and opposite sign which absorb circularly polarised light differently. Image adapted from Hughes et al., 2015.*

3.3.2.1. Qualitative studies using MSRCD

MSRCD measurements were made in the near-UV region (260-340 nm) at 20 °C in 1 nm increments. A cell of 1 cm pathlength and 2 mm × 2 mm aperture was used and total sample volumes were 100 µl. Settings included 0.5 mm slit width and 1 sec integration time. Three scans were acquired per sample in the presence of a magnetic field (North-South and South-North orientation). Measurements were analysed using the beamline B23 in-house suite of CD Applications programmes, first by determining the buffer subtracted spectra by subtracting appropriate buffers from each component, e.g. North-South (NS) buffer from NS measurements; and South-North (SN) buffer from (SN) measurements. Resulting SN measurements were subtracted from NS measurements for each condition, e.g. SN $VanS_A$ (SN buffer_subtracted) – NS $VanS_A$ (NS buffer_subtracted). Analysed ligands alone were subtracted from the measured spectra, where appropriate.

3.3.2.2. Titrations studies using MSRCD

Titration experiments were performed as described previously (Siligardi *et al.,* 2002; S. G. Patching *et al.,* 2012; Siligardi *et al.,* 2014a). Vancomycin (Sigma) or A2 teicoplanin (Sigma) stock solutions were added incrementally to achieve concentrations of vancomycin ranging from 0.3- to 5- fold molar equivalent in a total added volume that did not exceed 15 % of the original starting volume. Reactions were incubated at 20 °C for 30 minutes after each addition of ligand prior to data collection. 3 scans were collected separately in the NS and SN orientation using a rectangular cell with 10 mm pathlength in the near-UV region (270-325 nm) in 1 nm increments with 1 s integration and 1 mm slit width (equivalent to 1.8 nm bandwidth) in the presence of a magnetic field (1.4 T, OLIS). Difference spectrum was calculated by i) subtraction the relevantly orientated buffers from the equivalent samples, i.e. North-South (NS) buffer from NS samples, etc. ii) NS measurements were subtracted from South-North (SN) measurements (SN-NS) for each sample to ensure a positive value for at 293 nm. Change in CD (mdeg) at specific wavelengths was plotted against corresponding concentration of vancomycin (µM) and fitted with the Hill1 function $y = START + (END - START)\frac{x^n}{k^n + x^n}$ *(OriginLab), where START = start of input data, END = end of input data, k = Michaelis constant, n = cooperative sites* using OriginPro® 9 for K_d determination.

3.3.3. Data Fitting

Functions were applied to data obtained during monitoring of changes in signal at specific wavelengths using Origin Pro, the application of which varied depending on the experimental parameters and the function of change.

3.3.3.1. Gibbs-Helmholtz

During analysis of denaturation studies simplified assumptions are made, using a two-state model of an equilibrium denaturation which states that the protein of interest will exist as either of two states (*Equation 3.3.3.1-1*) and that progression throughout the denaturation conditions, in the case of thermal denaturation studies, transitions from N to D states are as a function of temperature.

$$N \underset{\leftarrow}{\overset{k_d}{\rightarrow}} D \qquad \textit{(Equation 3.3.3.1-1)}$$

Where *N* = native and *D* = denatured.

At the point where an equilibrium between N and D exists (*Equation 3.3.3.1-2*).

$$K_{eq} = \frac{[D]}{[N]} \qquad \textbf{(Equation 3.3.3.1-2)}$$

Application of the Gibbs Free Energy equation (*Equation 3.3.3.1-3*) to *Equation 3.3.3.1-2* results in *(Equation 3.3.3.1-4)*.

$$\Delta G° = -RT \,.\ln K_{eq} \qquad \textbf{(Equation 3.3.3.1-3)}$$

$$K_{eq} = \exp(\frac{-\Delta G_{D-N}}{RT}) \qquad \textbf{(Equation 3.3.3.1-4)}$$

During denaturation studies, obtained signals are sums of the native and denatured states therefore can be expressed as either of *Equation 3.3.3.1-5*, respectively.

$$fN = \frac{1}{K_{eq}+1} \text{ or } fD = \frac{K_{eq}}{K_{eq}+1} \qquad \textbf{(Equation 3.3.3.1-5)}$$

Which when substituted into *Equation 3.3.3.1-2* and rearranged according to *Equation 3.3.3.1-4* while considering the changes in slope for the baselines derived from the intrinsic changes in signals for both the native and denatured states over the course of denaturation experiments to fit chemical denaturation curves gives *Equation 3.3.3.1-6*.

$$\Delta G_{D-N} = m([Denaturant]_{50\%} - [Denaturant] \qquad \textbf{(Equation 3.3.3.1-6)}$$

Where $[Denaturant]_{50\%}$ = concentration of denaturant where 50 % of the population is in the unfolded state; m = slope of the transition.

In the case of thermal denaturation [Denaturant] = temperature (°C)

3.3.3.2. Hill function

In biochemical studies of protein-ligand interactions, it is often seen that binding of one ligand results in the cooperative binding of other molecules (Hill, 1910; Prinz, 2010). The Hill function is used to describe the fraction of molecule saturated by ligand as a function of ligand concentration and is useful to determine the cooperativity of interaction. The n value, otherwise known as the Hill coefficient, infers the cooperativity of an interaction (Weiss 1997). In ligand-binding systems of proteins the Hill function describes for protein (*P*) the number of binding sites (n) occupied by ligand (*L*), which at equilibrium can be expressed as:

$$P + nL \underset{k_d}{\overset{k_a}{\rightleftharpoons}} PL_n \qquad \textbf{(Equation 3.3.3.2-1)}$$

Where k_a = association rate for the protein-ligand complex; k_d = disassociation rate for the protein-ligand complex.

Application of *Equation 3.3.3.2- 1* to the apparent dissociation constant gives *Equation 3.3.3.2-2*.

$$K_d = \frac{k_d}{k_a} = \frac{[P][L]^n}{[PL^n]} \qquad \textbf{(Equation 3. 3.3.2-2)}$$

The fraction of ligand binding sites which are occupied by the ligand [θ] is given by *Equation 3.3.3.2-3*.

$$\theta = \frac{occupied\ binding\ sites}{total\ binding\ sites} = \frac{[PL_n]}{[P]+[PL_n]} \qquad \textbf{(Equation 3.3.3.2-3)}$$

Replacement of $[PL_n]$ with re-arrangement of *Equation 3.3.3.2-2* after simplification gives (*Equation 3.3.3.2-4)*.

$$\frac{[L]^n}{K_{d\,+[L]^n}} \qquad \textbf{(Equation 3.3.3.2-4)}$$

Where K_d = dissociation constant; $[L]$ = ligand concentration; n =number of binding sites for ligands.

3.3.4. Fluorescence Spectroscopy

Proteins have intrinsic fluorescence which can be attributed to the presence of fluorophores including aromatic amino acids (tryptophan, tyrosine, and phenylalanine) and co-factors (e.g. NAD, FAD, FMN and porphyrin rings) which can be monitored by excitation using specific wavelengths. Aromatic amino acids have overlapping excitation spectrum at 280 nm (Fig. 3-6) and although emissions are mostly contributed from tryptophan, individual contributions from tyrosine and to a lesser degree phenylalanine (Appendix, 1.6), in addition to resonance energy transfer from tyrosine and phenylalanine to tryptophan occur (Teale & Weber 1957). As such it becomes necessary to adapt the approach to increase the signal specificity, and one way of doing so in the case of tryptophan monitoring is using higher excitation wavelengths to increase the tryptophan-specific signals.

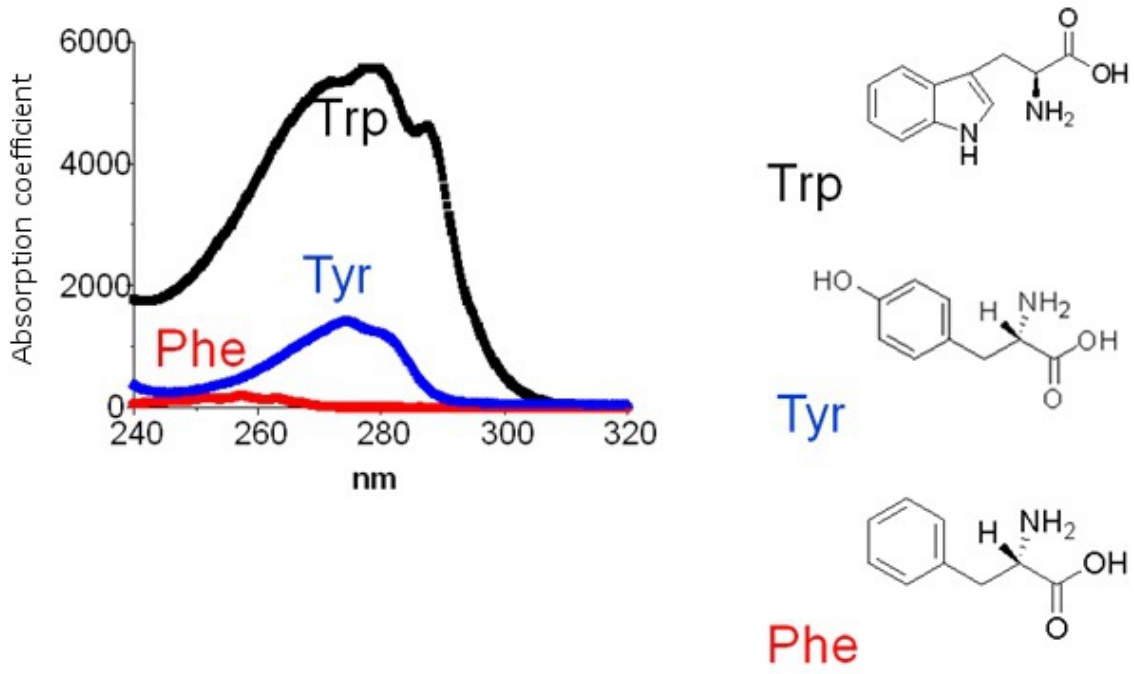

Figure 3-6: Average absorbance spectra for aromatic amino acids tryptophan, tyrosine and phenylalanine. *Image from http://elte.prompt.hu/sites/default/files/tananyagok/IntroductionToPracticalBiochemistry/ch04s06.html.*

Fluorescence spectroscopy is a very sensitive method. Factors such as concentrations of materials and environments of the fluorophore can affect the results. Too high concentrations can lead to an inner filter effect where i) insufficient absorption of excitation light, and ii) reduced detection of emitted fluorescence is caused by shielding in the crowded conditions. The environment of the fluorophore including i) the intrinsic position of the fluorophore e.g. buried or exposed aromatic residue, and ii) the environment of the protein e.g. if the fluorophore is in a polar or apolar environment affects the intensity and maximal wavelength of the emission light. These features make it a useful technique to probe for the specific features of a system of interest and has been a method of choice for many investigations.

As with other spectroscopic techniques low concentrations of fluorophore are required making it an ideal option for investigations of systems where resources are limited, such as the investigation of membrane proteins. However, due to the high sensitivity of the method there is a requirement to ensure correct experimental parameters are, e.g. not using too high concentrations of fluorophore to prevent the excessive absorbance of the excitation light ("inner filter" effect) which can skew experimental results. This is especially import during ligand binding studies where the presence of ligands can cause distortions in the fluorescence emissions, most significant during titration experiments to determine the binding constant for interaction (Birdsall *et al.,* 1983).

Fluorescence spectroscopy studies can be conducted to monitor the interactions of specific amino acids during ligand binding. By using specific excitation wavelengths for the target fluorophore, e.g. 295 nm for tryptophan (Fig. 3-6), the interactions in the presence of ligands can be monitored. Changes including λ_{max} (polarity of the local environment of the fluorophore), intensity (decreasing intensity by a quencher) and shape of peaks resulting from changes in the environment of the fluorophore (Vivian & Callis 2001) can be monitored in the presence of ligands as an indication of ligand binding.

3.3.4.1. Qualitative Fluorescence Spectroscopy

A general schematic for an instrument measuring fluorescence spectroscopy is shown in Fig. 3-7.

Fluorescence spectroscopy was carried out using a Chirascan™-Plus CD Spectrometer (Applied Photophysics) regularly employing a rectangular cell with 1 cm pathlength (1 cm x 1 cm, 4 mm x 4 mm window) at 23 °C. Using 5 nm bandwidth and 600 V, 295 nm excitation wavelength was applied to the sample and emission monitored between 300-500 nm in 1 nm increments.

Samples containing $VanS_A$ in the absence (with addition of equivalent volume of the solvent that the ligand is dissolved in) and presence of ligands (vancomycin (Sigma), teicoplanin (Sigma)) were incubated at 20 °C for 30 minutes prior to data collection.

Data analysis performed using CDApps (Hussain *et al.,* 2015) to obtain values which have been buffer subtracted and dilution-corrected for all components (F values) (protein only, ligand only, protein-ligand). F_o values were determined by normalisation to the initial value for each condition, followed by calculation of F/ F_o using OriginPro® 9. Standard deviation (n=3) shown by error bars.

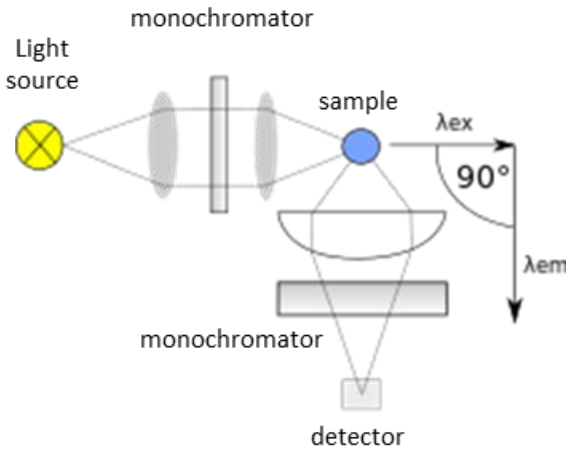

Figure 3-7: A simplified schematic of a fluorescence spectroscopy instrument. *Light from an excitation source passes through a monochromator and strikes the sample. A proportion of the incident light is absorbed by the sample causing some of the molecules in the sample fluoresce. Fluorescence is emitted in all directions, however is only collected 90 ° to the direction of the excitation light to minimise transmitted or reflected light reaching the detector. This fluorescent light passes through a second monochromator before reaching a detector. Image adapted from https://en.wikipedia.org/wiki/Fluorescence_spectroscopy.*

3.3.5. Dynamic Light Scattering (DLS)

DLS is commonly used to monitor the particle size distribution of a solution. The main principles of DLS are based on the Brownian motion of a molecule. When measured at constant temperature over a short period of time a defined pattern of motion can be traced for a molecule (Fig. 3-8) which is related to its size and conformation therefore it is possible to apply statistical methods (intensity correlation, (*Equation 3.3.5-1*) to determine the extent on non-randomness in a data set as a function of time.

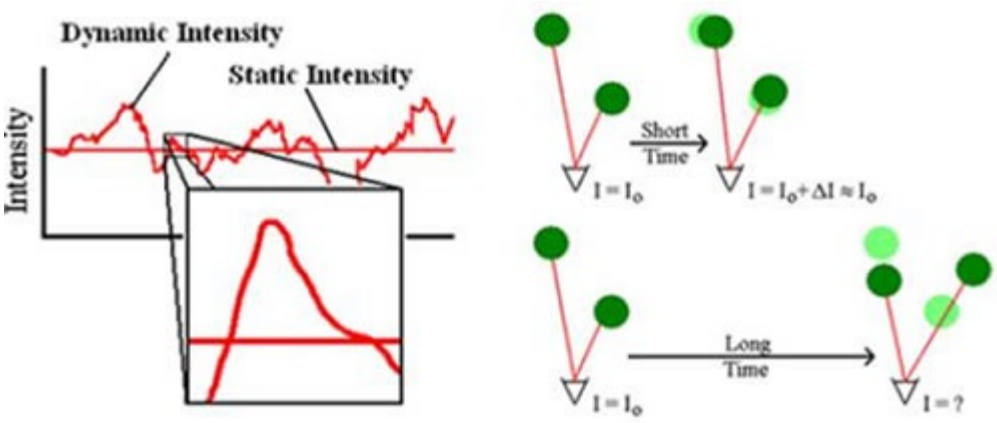

Figure 3-8: Principles of DLS. Brownian motion of a molecule measure over a short period of time (right) has a defined static intensity (left). *Image from http://www.news-medical.net/whitepaper/20141218/Overview-of-Key-Principles-of-Dynamic-Light-Scattering.aspx*

DLS utilises light sources from multiple angles on a sample and monitors the proportion of light scattered back using multiple scatter optics

$$G_\tau = \int_0^\infty I(t)I(t+\tau)dt \qquad \textit{(Equation 3.3.5-1)}$$

For monodisperse samples, the correlation curve can be fitted to a single exponential form (*Equation 3.3.5-2*) using deconvolution algorithms, accounting for the scattering effect for the samples in solution. The scattering vector (q) is shown in *Equation 3.3.5-3*.

$$\int I(t)I(t+\tau)dt = B + Ae^{-2q^2D\tau} \qquad \textit{(Equation 3.3.5-2)}$$

Where *B* = baseline; *A* = amplitude; *D* = diffusion coefficient.

$$q = \frac{4\pi\tilde{n}}{\lambda_\circ}\sin\left(\frac{\theta}{2}\right) \qquad \textit{(Equation 3.3.5-3)}$$

The obtained hydrodynamic radius for the molecule of interest obtained after application of deconvolution algorithms is expressed in (*Equation 3.3.5-4*).

$$R_H = \frac{kT}{6\pi\eta D} \qquad \textit{(Equation 3.3.5-4)}$$

where k = the Boltzmann constant; T = the temperature; η = the dispersant viscosity; *D* = diffusion coefficient.

Routinely, 70 µl of 0.3-0.5 mg/ml of $VanS_A$ in 10 mM HEPES pH 8.0, 20 % (v/v) glycerol, 0.025 % DDM (w/v) was analysed using Disposable Solvent Resistant Micro Cuvettes (ZEN0040, Malvern) in a Zetasizer Nano ZSP (Malvern).

3.4. Results

3.4.1. *Characterisation of the interactions of glycopeptide antibiotics vancomycin and teicoplanin with $VanS_A$*

Type-A vancomycin resistant enterococci exhibit resistance towards both GPAs vancomycin and teicoplanin (whereas type-B resistance is vancomycin resistant and teicoplanin sensitive) therefore this study sought to investigate both antibiotics as potential ligands for the membrane sensor kinase regulating type-A vancomycin resistance in the enterococci.

3.4.1.1. Qualitative screen for binding of glycopeptide antibiotics vancomycin and teicoplanin by $VanS_A$ using Synchrotron Radiation Circular Dichroism in the far-UV region

Initial qualitative screens did not detect any induced change in the secondary structure of $VanS_A$ for either antibiotic as demonstrated through the non-significant differences in the spectrum and SSE for $VanS_A$ under each condition (Fig. 3-9) suggesting the presence of the screened GPAs induced no effect on the secondary fold of the protein. SSE obtained for $VanS_A$ shown in Fig. 3-9 have higher proportion of helical structure relative to predictions based on the secondary structure (Fig. 2-2) which could result from environmental influences such as the buffer conditions. None the less, predictions from amino acid sequences are less reliable relative to secondary structure estimations from CD which have been made based on real protein samples; and the high proportion of helical structure for both cases indicates a strong correlation in helical content which is often expected for membrane proteins as these structures characteristically dominate membrane inserting domains.

As noted in Chapter 2, earlier protein preparations (Fig. 2-12) were less consistent in their folding compared to the later preparations presented in this Chapter (Fig. 3-9) which had higher levels of helical content that were comparable to homology models (Fig. 2-2). These later protein preparations had been purified using optimised methods where factors such as timings for each step, and buffer component concentrations and pH had been determined and become routine.

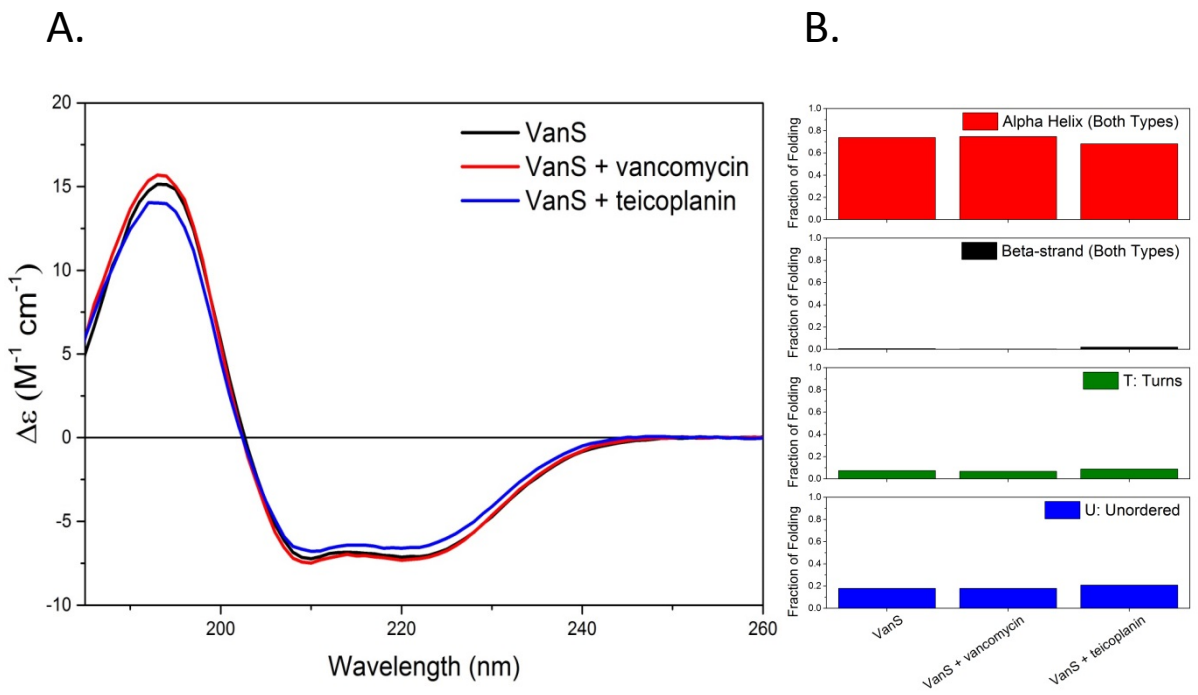

Figure 3-9: Effect of the presence of glycopeptide antibiotics vancomycin and teicoplanin on VanS$_A$ monitored in the far-UV region (185-260 nm). *VanS$_A$ (40 µM) in 10 mM HEPES pH 8.0, 20 % glycerol, and 0.025% DDM was incubated with 5-fold (200 µM) of glycopeptide antibiotic in 10 mM Tris HCl pH 8.0 (or equivalent volume of ligand buffer for no ligand condition) for 30 minutes at room temperature before data collection. Employing 0.05 mm pathlength, 2 scans were collected in 1 nm increments using 1 second integration and 1 mm slit width. (A) Difference spectrum of VanS$_A$ in the far-UV region in the absence (—) and presence of glycopeptide antibiotics vancomycin (—) and teicoplanin (—). (B) Secondary structure estimation using CDApps (Hussain et al., 2015) with CONTILL (Sreerama & Woody 2004), SMP56 (43 soluble, 13 membrane) database. Normalised mean residual standard deviation (NMRSD) is 0.025- 0.049.*

3.4.1.2. Qualitative screen for binding of glycopeptide antibiotics vancomycin and teicoplanin by VanS$_A$ using Synchrotron Radiation Circular Dichroism in the near-UV region

Although no discernible changes were observed in the secondary structure conformation of VanS$_A$ in the presence of the tested GPAs, ligand binding may nonetheless affect local tertiary structures of

$VanS_A$ therefore screens were conducted in the aromatic region of the near-UV to determine their role, if any, in binding by $VanS_A$. During screens in the near-UV region aromatic side chain conformation within the tertiary structure of the protein is required to be in a ligand-accepting orientation, and will ultimately influence the signal observed during CD measurements.

Initial screens revealed broad peaks in the difference spectra for the tyrosine and tryptophan region suggesting roles for both amino acids during GPA binding (Fig. 3-10). The reduction of the induced signal for $VanS_A$ in the presence of both ligands suggests binding occurs in similar mechanisms requiring the same orientation of the aromatic group during binding, and a possible change in conformation of the protein to accommodate this.

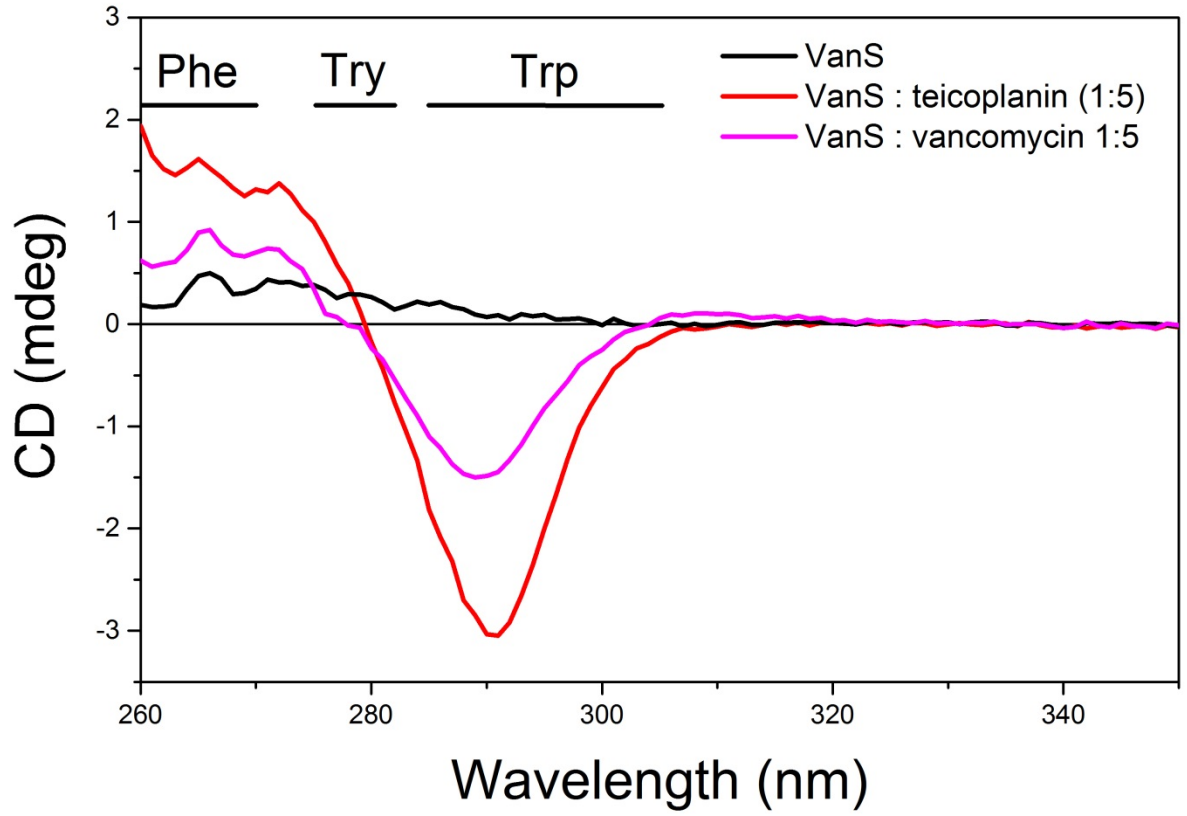

Figure 3-10: Difference spectra of $VanS_A$ in the absence and presence of antibiotic ligands monitored in the near-UV region (260-340 nm).

$VanS_A$ (40 µM) in 10 mM HEPES pH 8.0, 20 % (v/v) glycerol, 0.025% (w/v) DDM was incubated with 5-fold (200 µM) of glycopeptide antibiotic in 10 mM Tris HCl pH 8.0 (or equivalent volume of ligand buffer for no ligand condition) for 30 minutes at 20 °C before data collection. Employing 3 mm pathlength 4 scans were collected in 1 nm increments using 1 second integration and 1 mm slit width.

3.4.1.3. Quantitative characterisation of successful ligand binding using Synchrotron Radiation Circular Dichroism in the near-UV region

3.4.1.3.1. Determination of the binding constant (K_d) for $VanS_A$ with vancomycin using titration methods in the near-UV region

Following the identification of vancomycin as a binding ligand for $VanS_A$ the binding affinity was next to be determined. As described previously (S. Patching *et al.,* 2012; Siligardi *et al.,* 2014a) by monitoring restricted wavelength ranges where large changes in signal are observed, e.g. the aromatic region of the near-UV, it is possible to quantitatively characterise the interaction and determine the binding constant (K_d). Results from CD titration experiments on multiple batches of protein confirmed the binding of vancomycin by tryptophan in $VanS_A$, characterising the binding as moderate affinity (K_d = 75 µM) (Fig. 3-11A) and a Hill coefficient, n, of 1.9 suggesting a cooperativity for the interaction, suggesting the potential for $VanS_A$ to form multimers (most likely dimers) in the presence of ligands as the protein monomer contains one predicted ligand binding site (Fig. 2-2). This concept was introduced in Chapter 2 (2.4.4), and it is worth mentioning the possibility of their formation considering the lower detergent concentrations used during the experiments presented here. However it is necessary to note that as the saturation has not been met for the titration (Fig. 3-11) and standard errors are not presented the obtained K_d and n values should be taken with caution and used as preliminary studies on which to base future experiments to further investigate the system.

Absorbance spectroscopy is a complementary technique which can be simultaneously monitored during CD experiments when using a compatible CD instrument. Data collected supported CD results, reporting a K_d for binding of 85 µM and a change in the microenvironment of aromatic amino acids as a result of antibiotic binding (Xu *et al.,* 2013) (Fig. 3-9B).

High concentrations of detergent can negatively affect the activity of sensor kinase proteins (Ma *et al.,* 2008), therefore we sought to investigate whether the ligand binding activity of $VanS_A$ is also

affected. In the absence of buffer additives, $VanS_A$ bound vancomycin with similar affinity to in the presence of glycerol and DDM (Fig. 3-12A) and was supported by UV absorbance data (Fig. 3-12B) however a second lower affinity binding was shown to occur at higher concentrations of vancomycin, unseen in the presence of glycerol and DDM potentially resulting from low affinity binding to hydrophobic sites.

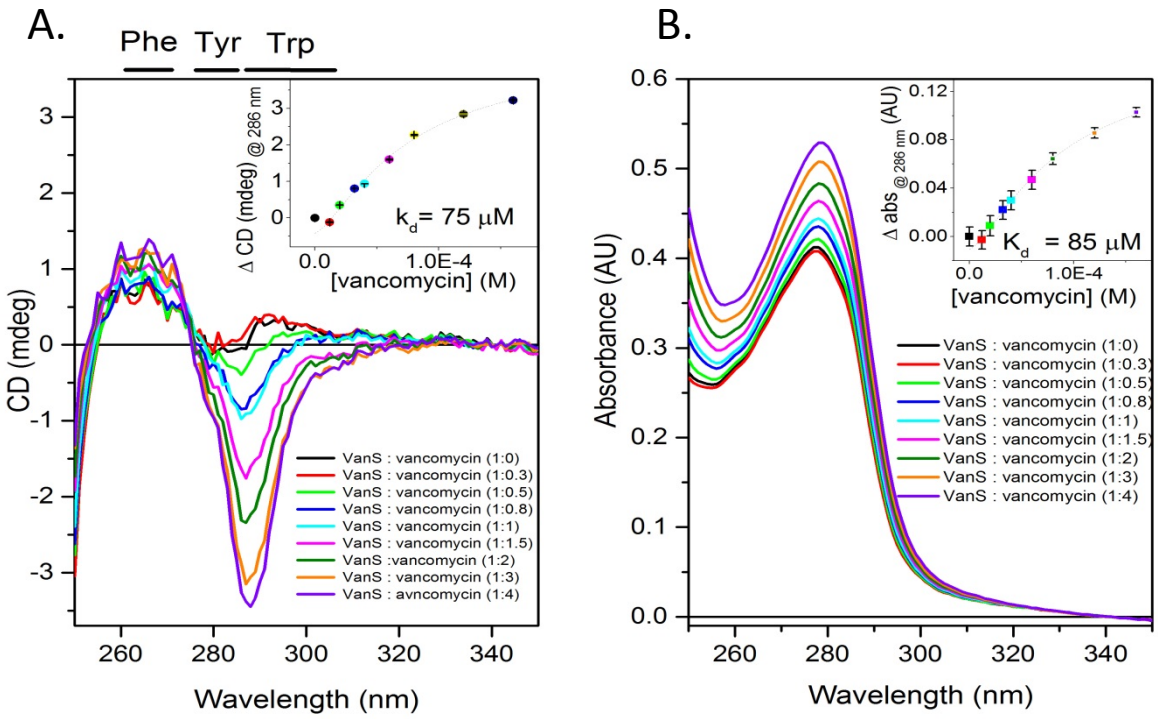

Figure 3-11: Titration of vancomycin against VanS$_A$ in the near-UV region. *VanS$_A$ (40 μM) in 10 mM HEPES pH 8.0, 20 % (v/v) glycerol, 0.025% (w/v) DDM was incubated with incremental volumes of vancomycin stocks in 10 mM HEPES pH 8.0 at 20 °C for 30 minutes after each addition prior to data collection. Employing a rectangular cell of 3 mm pathlength, measurements were taken at 20 °C in the near-UV (260-350 nm) in 1 nm increments using 1 mm slit width (equivalent to 1.8 nm bandwidth) and 1 s integration. Data analysed using CDApps (Hussain et al., 2015) to obtain difference spectrum where all controls (buffers, ligands, etc.) have been subtracted, zeroed at 340-342 nm. Change in signal at 286 nm for (A) CD (mdeg) and (B) absorbance was transferred to OriginPro® 9 and plotted against respective concentration of vancomycin (M) for fitting with the hill1 function to obtain the binding constant* K_d. *Standard deviation (n=4, different batches) shown by error bars. (A, main) Difference CD spectrum of VanS$_A$ during titration experiments; (A, insert) change in CD (mdeg) at 286 nm vs. [vancomycin] (M) fitted with a Hill1 function ; (B, main) difference UV absorbance spectrum of VanS$_A$ in the presence of vancomycin; (B, insert) change in absorbance at 286 nm vs. [vancomycin] (M) fitted with a Hill1 function. Hill function used was* $\theta = \frac{[L]^n}{K_{d\,+[L]^n}}$ *where* K_d *= dissociation constant;* $[L]$ *= ligand concentration;* n *=number of binding sites for ligands.*

3.4.1.3.2. Determination of the binding constant (K_d) for $VanS_A$ of Teicoplanin using titration methods in the near-UV region

Qualitative studies revealed teicoplanin as a binding ligand for $VanS_A$ (Fig. 3-10), therefore the aim of this study was to quantitatively characterise the interaction using previously described methods (Siligardi *et al.,* 2002; S. G. Patching *et al.,* 2012; Siligardi *et al.,* 2014b).

Using these methods, the affinity of $VanS_A$ for teicoplanin was less consistent to determine as different values were obtained using CD (30 µM, Fig. 3-13A) and UV (160 µM, Fig. 3-13B). These differences may be due performing calculations on data which has not reached saturation, therefore should serve as preliminary data for future investigations into the potential differences in binding of teicoplanin and vancomycin by $VanS_A$.

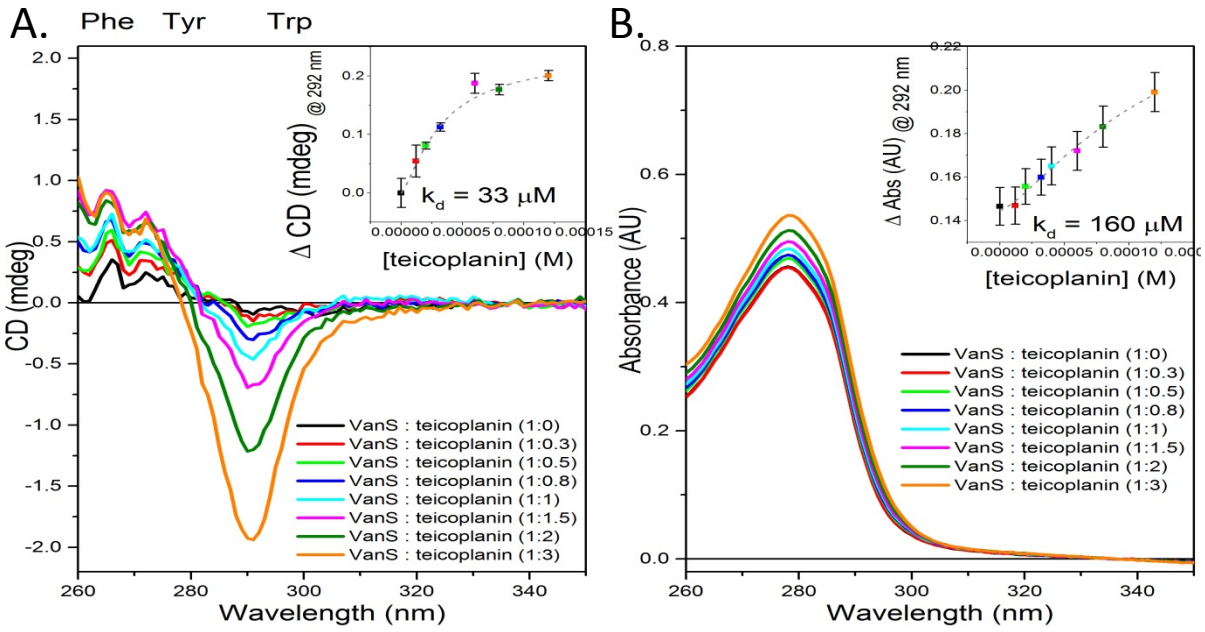

Figure 3-12: CD titration of teicoplanin with $VanS_A$ in 10 mM HEPES pH 8.0, 20 % (v/v) glycerol, 0.025% (w/v) DDM.

40 µM of $VanS_A$ in 10 mM HEPES pH 8.0, 20 % (v/v) glycerol, 0.025% (w/v) DDM was incubated with incrementally increasing concentrations of teicoplanin in 10 mM HEPEPS pH 8.0 at 20 °C for 30 minutes after each addition prior to data collection. Employing 3 mm pathlength rectangular cell, 4 scans were collected at 20 °C in 1 nm increments with 1 s integration time using 2 nm bandwidth. For analysis of (A, main) CD and (B, main) UV absorbance data, difference spectra for each titration point were calculated using CDApps (Hussain et al., 2015), where appropriate controls (baseline buffer, ligands) are subtracted and zeroed at (A, main) 340-342 nm and (B, main) 325-330 nm. (A, main) Data smoothed (Savitzky–Golay filter, 10 points) using OriginPro® 9. Binding constant calculated using OriginPro® 9, plotting (A, insert) change in CD (Δ CD) at 292 nm against the respective concentration of vancomycin (M) at each titration point; and (B, insert) change in absorbance (Δ Abs) at 292 nm against the respective concentration of vancomycin (M) at each titration point. Both were fit with a Hill function $\theta = \frac{[L]^n}{K_{d+[L]^n}}$ where K_d = dissociation constant; $[L]$ = ligand concentration; n =number of binding sites for ligands. Standard deviation (n=4, different batches of protein) shown by error bars.

3.4.1.4. Investigation of the induced fluorescence changes of $VanS_A$ in the presence and absence of glycopeptide antibiotics

Proteins containing intrinsic fluorophores including aromatic amino acids can be monitored using fluorescence spectroscopy. The fluorescence of a folded protein is a mixture of contributions from aromatic residues due to their overlapping absorbance wavelength ranges (Teale & Weber 1957), however using higher excitation wavelengths (e.g. 295 nm for tryptophan, as used in the following experiments) can reduce fluorescence contributions from fluorophores excited by lower wavelengths to enable monitoring of particular amino acids.

3.4.1.4.1. Qualitative study of ligand binding by $VanS_A$ using Fluorescence Spectroscopy

Qualitative studies employing excitation at 295 nm confirmed the role of tryptophan during the binding of GPAs vancomycin and teicoplanin by a blue-shifted fluorescence emission in their presence (Fig. 3-13); the observed quenching resulting from increased electron transfer between tryptophan and solvent as the tryptophan moves into a more polar environment (buried to surface-exposed movement).

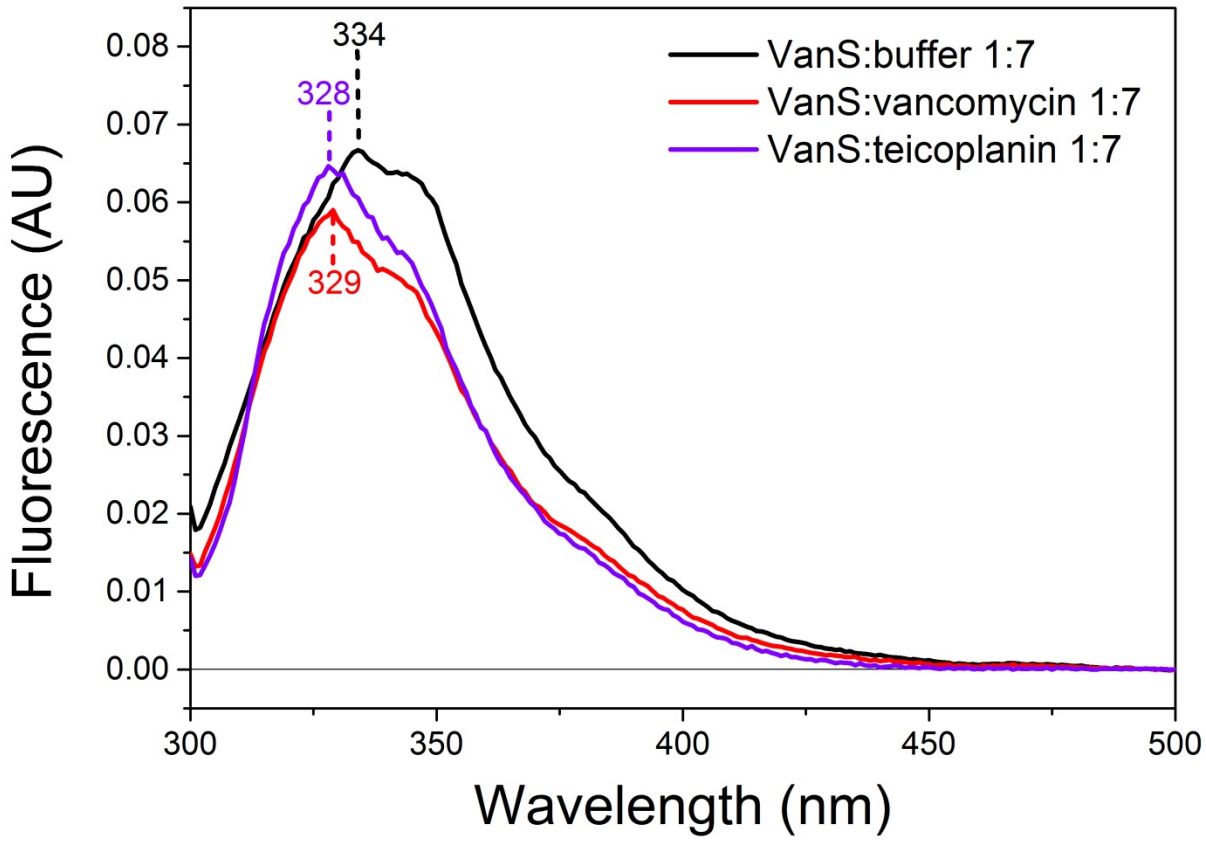

Figure 3-13: Fluorescence emission spectra of $VanS_A$ in the absence and presence of antibiotics (exc. 295 nm).

0.3 mg/ml of $VanS_A$ in buffer (10 mM HEPES pH 8.0, 20 % (v/v) glycerol, 0.025% (w/v) DDM) was incubated in the presence and absence of 5-fold molar equivalent of ligand (in 10 mM HEPES pH 8.0) at 20 °C for 30 minutes prior to data collection. Samples were excited at 295 nm using 5 nm bandwidth, emission was monitored from 300 nm to 440 nm in 1 nm increments.

3.4.1.4.2. Quantitative characterisation of successful ligand binding using Fluorescence Spectroscopy (K_d determination for binding)

Following the assays confirming the role of tryptophan in ligand binding for $VanS_A$, titration experiments were conducted to quantify the binding interaction. Results from these experiments showed quenching of tryptophan fluorescence following addition of ligands to $VanS_A$ (Fig. 3-14A), confirming initial qualitative screens (Fig. 3-13). Differences in the obtained dissociation constant (K_d) for each antibiotic were observed (Fig. 3-14B), supporting previous work suggesting differences in the affinities for each antibiotic (Beauregard *et al.,* 1995). Affinity reported for vancomycin was nearly two-times higher using fluorescence measurements than for CD, most likely a reflection of the sensitivity of the method. For both antibiotics a Hill coefficient, n, was >1 (Teicoplanin = 1.3, Vancomycin = 1.1) indicating a cooperativity for the binding, and as a result suggests the formation of multimeric states (dimers) by $VanS_A$ during binding, as previously suggested by CD titrations (3.4.1.3).

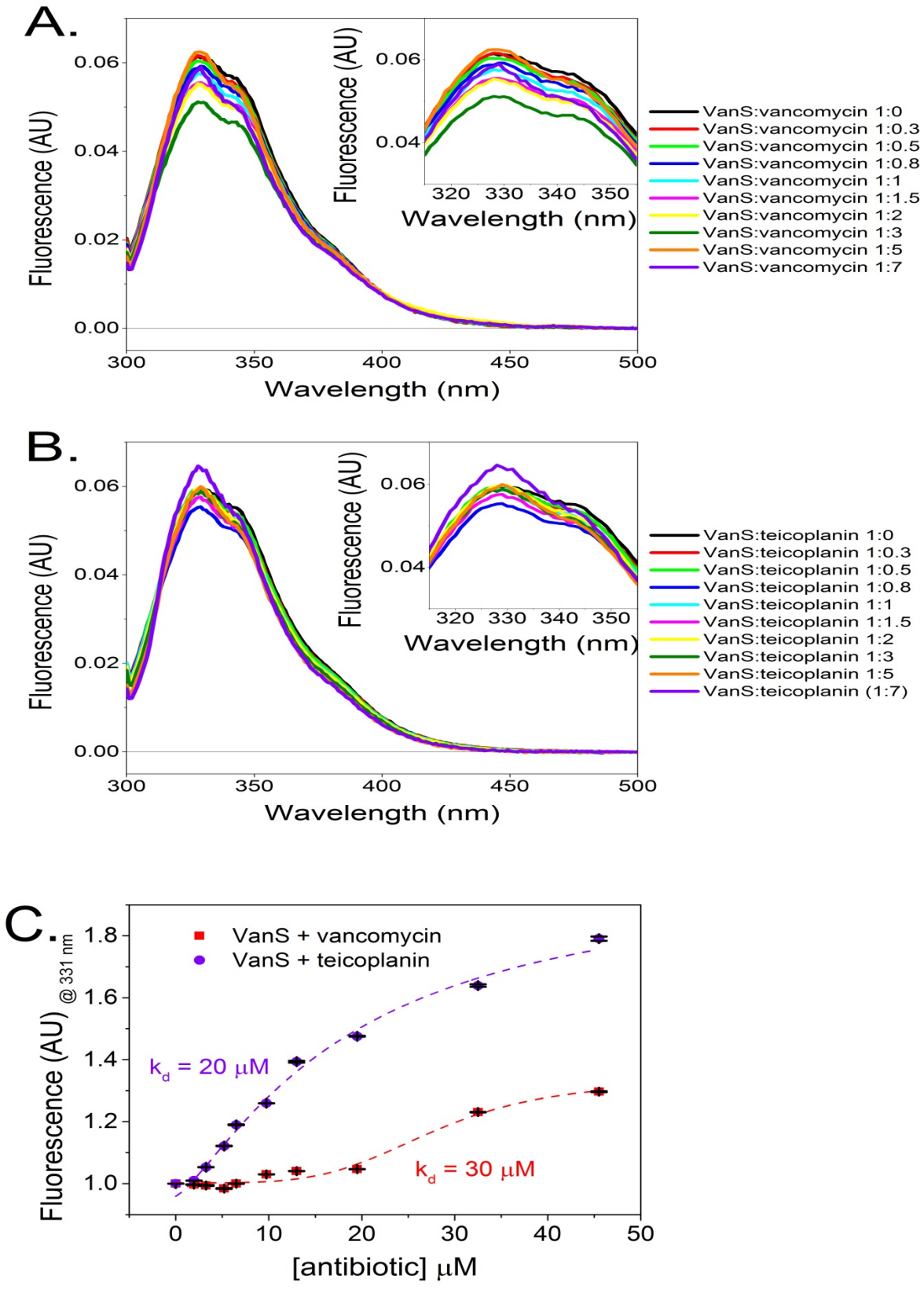

Figure 3-14: Fluorescence titration of $VanS_A$ with glycopeptide antibiotics vancomycin and teicoplanin.

K_d *determination from fluorescence titration of VanS$_A$ in the presence of glycopeptide antibiotics vancomycin and teicoplanin. 0.3 mg/ml of VanS$_A$ in 10 mM HEPEPS pH 8.0, 20 % glycerol (v/v), 0.025 % (w/v) DDM was incubated in incrementally increasing concentrations of antibiotic (0.3 to 7 fold molar equivalent) in 10 mM Tris HCl, or in the case of no-ligand conditions 10 mM Tris HCl only at 20 °C for 30 minutes prior to data collection. Using a rectangular cell with 10 mm pathlength and excitation at 295 nm, 3 scans were collected between 300 – 500 nm in 1 nm increments, 5 nm bandwidth. Emission collected between 300-500 nm in 1 nm increments. Data analysis performed using CDApps (Hussain et al., 2015) to obtain values which have been buffer subtracted and dilution-corrected for all components (F values) (protein only, ligand only, protein-ligand). F_o values were determined by normalisation to the initial value for each condition, followed by calculation of F/ F_o using OriginPro® 9. Fluorescence at 331 nm at each titration point was plotted against concentration of antibiotic and fitted with a Hill function* $\theta = \frac{[L]^n}{K_{d\,+[L]^n}}$ *where* K_d *= dissociation constant;* $[L]$ *= ligand concentration;* n *=number of binding sites for ligands. Standard deviation (n=3, different batches of protein) shown by error bars.*

3.4.1.5. MSRCD study of VanS$_A$ in the presence and absence of ligands

MSRCD is a powerful technique which utilises a strong magnetic field to change the absorbance properties of materials hence can be applied to any material, and can be used to specifically monitor weak signals and transitions obtained using conventional CD (Caldwell *et al.,* 1971). In the case of proteins, signals for tryptophan and tyrosine can be distinguished for individual investigation (Sutherland & Holmquist 1980).

3.4.1.5.1. Qualitative study of ligand binding by VanS$_A$ using MSRCD

CD studies identified roles for tyrosine and tryptophan during the interaction of VanS$_A$ and GPAs vancomycin and teicoplanin (Fig. 3-10) therefore we sought to i) confirm and ii) characterise the interactions of these residues using MSRCD.

MSRCD gives information of the environment of the amino acid (exposure to electron withdrawing of electron donating species) but not the tertiary conformation of the protein (Djerassi *et al.* 1971; Barth *et al.* 1972). In addition to λ_{max} shift, changes in peak intensity can provide information about the changes in the local environment of the amino acid studied (Djerassi *et al.* 1971; Barth *et al.* 1972; Longo *et al*. 2015). Electron withdrawing moieties reduce free higher-energy outer orbital electrons available causing reduced spectral intensities and a blue-shifted λ_{max} whereas electron donating species increase free higher-energy outer orbital electrons and an increased spectral intensity and a red-shifted λ_{max}.

Qualitative screens confirmed the roles of tyrosine and tryptophan during GPA binding, observed as peak shifts relative to VanS$_A$ only conditions (blue-shift for tryptophan, redshift for tyrosine) in the presence of ligands (Fig. 3-15). Given the resolution of measurements (accounting for the 1.8 nm bandwidth used), the significance of the 1 nm shift is questionable, yet the results obtained for tryptophan are in agreement with fluorescence data suggesting a mechanism for the interaction.

Only in the presence of vancomycin was a shift observed in the tryptophan region (Fig. 3-15B) compared to in the tyrosine region where shifts were observed for both GPAs (Fig. 3-15C). Shifted peaks adopted different shapes to non-shifted peaks, signifying broader ranges of excitation wavelengths under the shifted conditions indicative of changes to the electronic transition state and excitation energy requirements of the protein in the presence of the ligands.

Perhaps more significant in Fig. 3-15 are the changes in intensity of the peaks in the presence of the glycopeptide antibiotics. An increase in intensity of the MCD signal was observed in the tryptophan region (Fig. 3-15) suggestive of the movement of the tryptophan into a more electron donating area, potentially signalling the binding of the antibiotic and its donation of electrons. In the tyrosine region, peak intensity reduced (Fig. 3-15), suggestive of the movement of the tyrosine into a more electron withdrawing region, perhaps becoming more solvent-exposed.

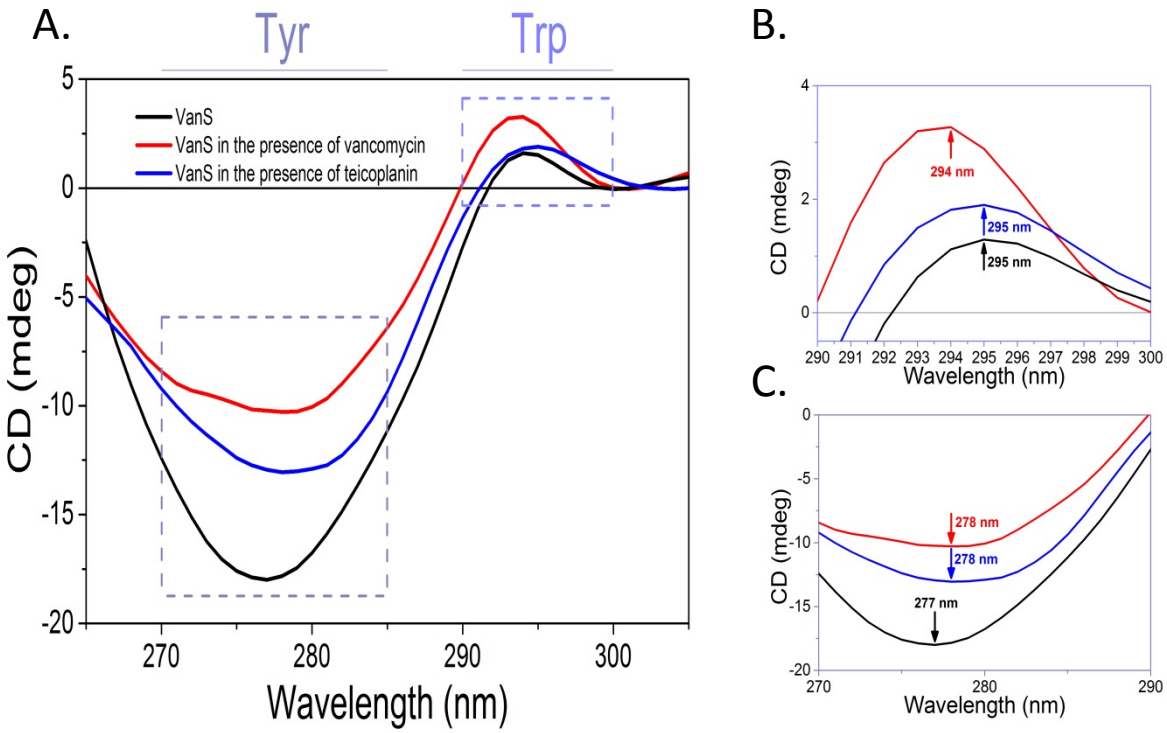

Figure 3-15: Difference MSRCD spectra of VanS$_A$ in the absence and presence of glycopeptide antibiotics vancomycin and A2 teicoplanin.

29 µM of VanS$_A$ (in 10 mM Tris.HCl pH 8.0, 10 % glycerol, 0.025 % DDM) was incubated at 20 °C in the absence or presence of 5-fold molar equivalent of antibiotic in 10 mM Tris. HCl pH 8.0 (or equivalent volume of 10 mM of Tris.HCl for control condition). Employing 1 mm slit width (equivalent to 1.8 nm bandwidth) and a rectangular cell with 10 mm pathlength, 3 scans were collected in the near-UV region (265-330 nm) in the presence of a magnetic field (1.4 T, OLIS) in 1 nm increments with 1 s integration. Measurements were collected separately in the NS and SN orientation of the magnetic field. Difference spectrum was calculated by i) subtraction the relevantly orientated buffers from the equivalent samples, i.e. North-South (NS) buffer from NS samples, etc. ii) NS measurements were subtracted from South-North (SN) measurements (SN-NS) for each sample to ensure a positive value for at 293 nm. A) Displaying 265-330 nm region, B) tyrosine region (270-285 nm), C) tryptophan region (290-300 nm). Data smoothed using Savitzky-Golay (10 pts, VanS$_A$ and VanS$_A$ + vancomycin; 12 pts, VanS$_A$ + teicoplanin).

3.4.1.5.2. Quantitative characterisation of successful ligand binding using MSRCD

After confirming the role of tyrosine and tryptophan during binding of vancomycin and teicoplanin using MSRCD (Fig. 3-16), titration experiments were employed to determine the binding constant (K_d). Monitoring at 294 nm (corresponding to the tryptophan region), the K_d for interactions of tryptophan with ligands was determined for both screened GPAs. During these experiments, tighter binding of antibiotics vancomycin and teicoplanin by tryptophan of $VanS_A$ was demonstrated than previously described using CD, more than 2-fold tighter binding (Figs. 3-16 and 3-17, respectively). These differences could be due to the increased specificity of the signal used to monitor the interaction than conventional CD.

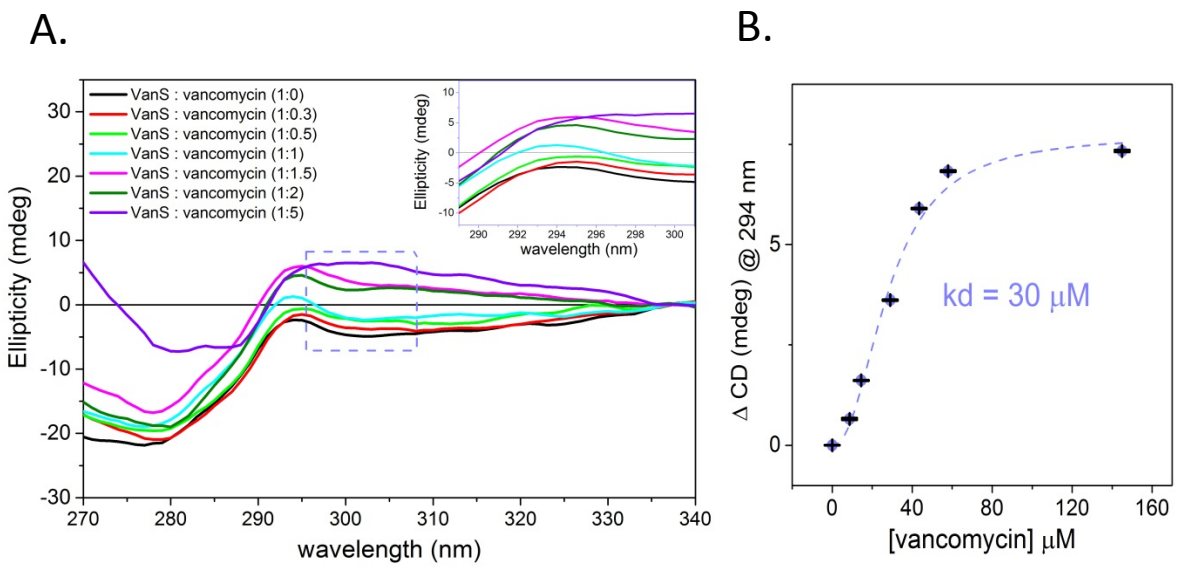

Figure 3-16: Titration of $VanS_A$ with vancomycin using MSRCD.

29 μM of $VanS_A$ was incubated with incremental volumes of vancomycin stock solutions to achieve concentrations of vancomycin ranging from 0.3- to 5- fold molar equivalent in a total added volume that did not exceed 15 % of the original starting volume. Reactions were incubated at 20 °C for 30 minutes after each addition of ligand prior to data collection. 3 scans were collected separately in the NS and SN orientation using a rectangular cell with 10 mm pathlength in the near-UV region (270-325 nm) in 1 nm increments with 1 s integration and 1 mm slit width (equivalent to 1.8 nm bandwidth) in the presence of a magnetic field (1.4 T, OLIS). Difference spectrum was calculated by i) subtraction the relevantly orientated buffers from the equivalent samples, i.e. North-South (NS) buffer from NS samples, etc. ii) NS measurements were subtracted from South-North (SN) measurements (SN-NS) for each sample to ensure a positive value for at 293 nm. (B) Change in CD (mdeg) at 294 nm was plotted against corresponding concentration of vancomycin (μM) and fitted with the Hill1 function $\theta = \frac{[L]^n}{K_{d+[L]^n}}$ *where* K_d *= dissociation constant;* $[L]$ *= ligand concentration;* n *=number of binding sites for ligands using OriginPro® 9 for* K_d *determination. Standard deviation (n=3, different batches of protein) shown by error bars.*

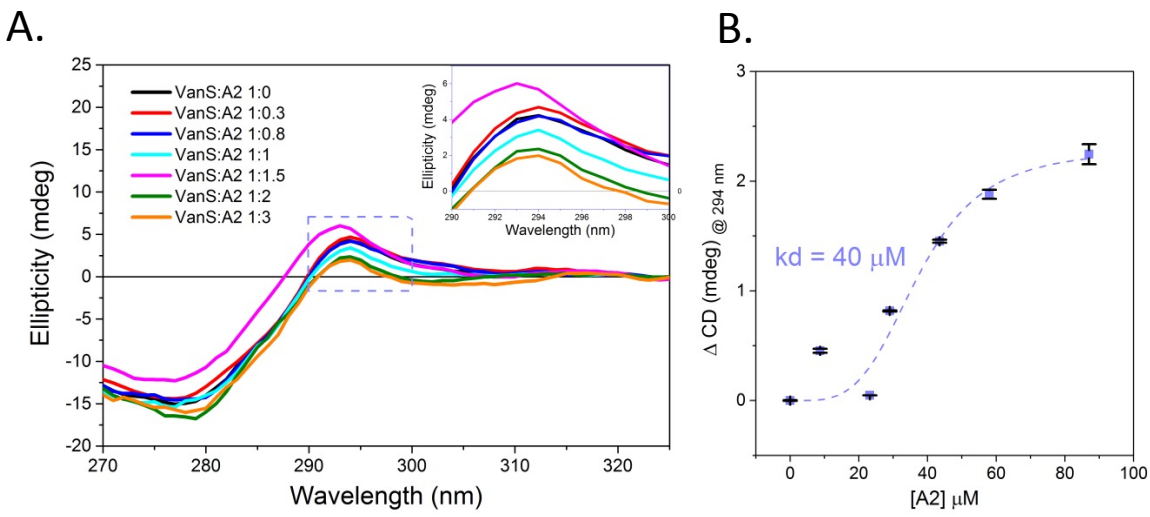

Figure 3-17: Titration of VanS$_A$ with teicoplanin (A2, Sigma) using MSRCD.

(A) difference spectra of MSRCD *data obtained between 160-340 nm (1 nm, 1 second) zeroed at 335 nm for 29 μM VanS$_A$ in the presence of molar equivalent fractions of teicoplanin (described in methods). Difference spectra analysed using CD Apps (Hussain et al., 2015). Magnified spectra of wavelength ranges highlighted in (A) corresponding to tryptophan. (B) Binding analysis using OriginPro® 9 by plotting change in measured absorbance (ΔA (mdeg) v molar fraction of teicoplanin (μM)) at 294 nm was fitted with a Hill function* $\theta = \frac{[L]^n}{K_{d+[L]^n}}$ *where* K_d *= dissociation constant;* $[L]$ *= ligand concentration;* n *=number of binding sites for ligands. Standard deviation (n=3, different batches of protein) shown by error bars.*

3.4.2. Characterisation of the interactions of peptidoglycan components with VanS$_A$

Accumulation of free peptidoglycan precursors in the extracellular environment is a side-effect of the activity of vancomycin (Allen *et al.,* 1996) and had been proposed as an activating signal for the onset of vancomycin resistance (Arthur & Quintiliani 2001), therefore the following study aimed to determine if any peptidoglycan components are indeed ligands for VanS$_A$.

3.4.2.1. Qualitative screen for binding of peptidoglycan components by $VanS_A$ using Circular Dichroism in the far-UV region

Initial screens aiming to identify cell-wall compounds interacting with $VanS_A$ were conducted in the far-UV region. Results from these screens showed no significant difference in the CD spectra in the absence and presence of ligands which was further confirmed by little conformational fold of $VanS_A$ (Fig. 3-18).

Further screens showed small but not significant changes to the secondary fold of $VanS_A$ upon addition of NAG and NAM (Fig. 3-19), furthermore these effects were found to be time-dependent as the effects diminished over time but was recoverable by the addition of freshly prepared NAG (Fig. 3-20) potentially due to NAG degradation.

As described in Chapter 2 detergent concentration can affect the secondary structure of a protein, and was further demonstrated in the protein spectra in Figs. 3-18 and 3-19 which showed decreased helical content in the presence of higher DDM concentration (0.05%) (Fig. 3-18) compared to lower DDM detergent (Fig. 3-19). The CMC for DDM is ~ 0.02% and too high concentrations of detergent may result in detergent-mediated aggregation (Neale et al. 2013) and may explain the longer equilibration period required in higher detergent conditions. Only early protein preparations were produced using higher detergent concentrations which, as discussed in Chapter 2, had lower helical folding potentially due to the use of non-routine methods for protein purification during the optimisation process. The interactions of early preparations with cell wall components are presented in Fig. 3-18 which accounts for the overall differences in the SSE presented in Fig. 3-18, most notably the lower helical content of the protein. Later preparations which had been produced using routine methods and lower detergent concentrations were tested for their interaction with NAG and NAM (Fig. 3-19) and showed similar small changes (<5%) to earlier preparations.

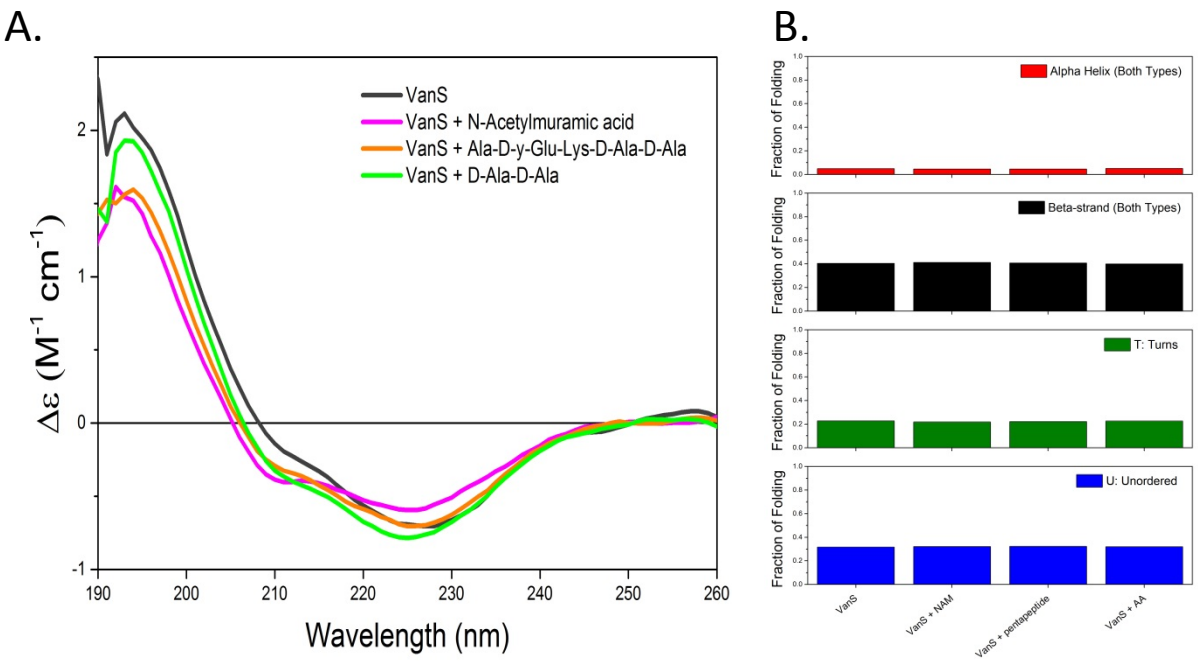

Figure 3-18: Difference spectrum of VanS$_A$ in the absence and presence of cell wall components. *25 µM VanS$_A$ in 10 mM HEPES pH 7.9, 10 % (v/v) glycerol, 0.05 % (w/v) DDM, 100 mM NaCl was incubated at 20 °C for 30 minutes in the absence and presence of 5-fold molar equivalent of cell wall component prepared in ddH_2O before data collection. Employing a rectangular cell with a 10 mm pathlength, 4 scans were taken between 185-260 nm (1 nm increments, 1 second integration), with a slit width of 1 mm (equivalent to 1.8 nm bandwidth). Data was analysed using CDApps (Hussain et al., 2015) to produce difference spectra where all relevant ligands and buffers etc. have been subtracted (A), and secondary structure estimations using CONTILL algorithm (Sreerama & Woody 2004), SMP56 database (43 soluble, 13 membrane) (B). Data zeroed at 248-253 nm. Normalised mean residual standard deviation (NMRSD) is 0.067 – 0.12.*

A. B.

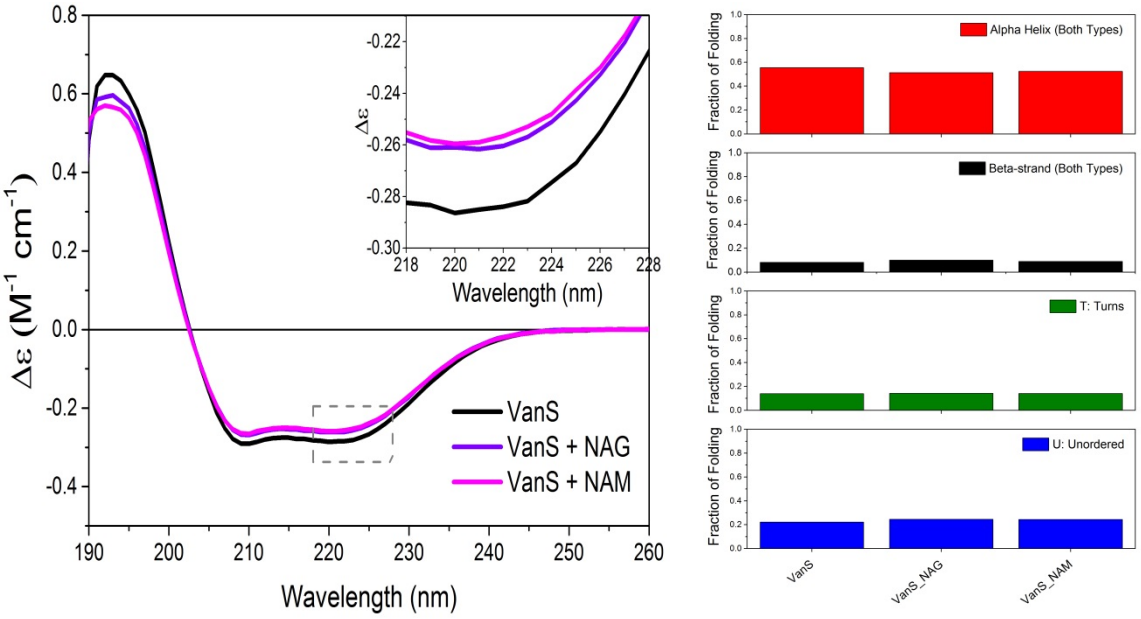

Figure 3-19: Screening of interactions of $VanS_A$ with peptidoglycan components NAG and NAM in the far-UV region. *11 µM of $VanS_A$ in 10 mM HEPES pH 7.9, 10 % (v/v) glycerol, 0.025 % (w/v) DDM was incubated with 5-fold molar equivalent concentration of ligand (N-acetylmuramic acid (NAM), N-acetylglucosamine (NAG)) in 10 mM HEPES pH 8.0 (10 mM HEPES pH 8.0 in no-ligand control conditions) at 20 °C for 30 minutes prior to data collection. Employing a cylindrical cell with a 0.2 mm pathlength, 4 scans were collected in the far-UV region (190-260 nm) in 1 nm increments with 1 s integration at 20 °C. 1 mm slit width (equivalent to 1.8 nm bandwidth) was used throughout. Data was analysed using CDApps (Hussain et al., 2015) to produce difference spectra whereby all controls (buffers, solvents, ligands, etc.) have been subtracted and converted to molar extinction (Δε). Secondary structure estimations performed using CONTILL algorithm (Sreerama & Woody 2004) and SMP56 database (43 soluble, 13 membrane). Data was transferred to OriginPro® 9 for presentation. (A, main) Difference spectrum with (A, insert) enlargement of data in grey box on main graph; and (B) secondary structure estimations of $VanS_A$ in the absence and presence of screened peptidoglycan components. Normalised mean residual standard deviation (NMRSD) is 0.067 – 0.12.*

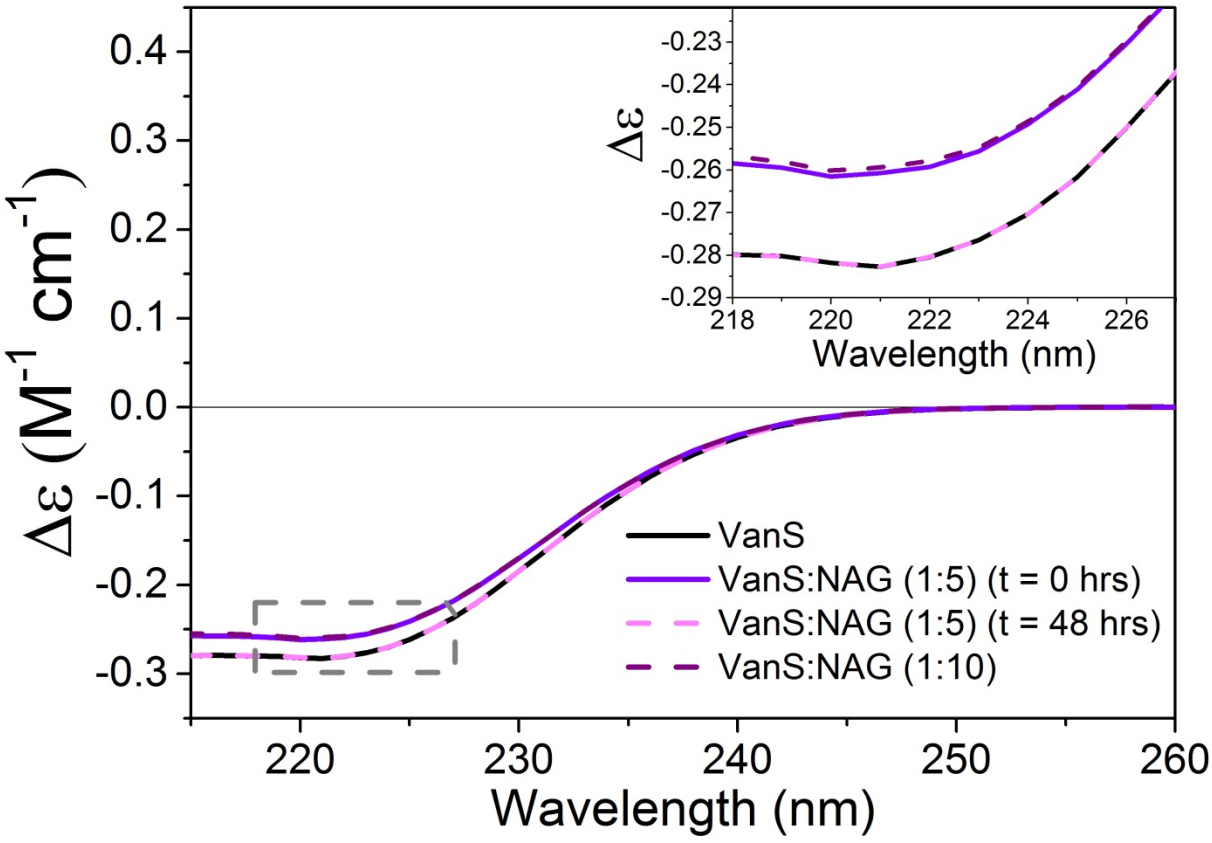

Figure 3-20: Time-dependent loss and recovery of the interaction of NAG with $VanS_A$ in the far-UV region.

11 µM of $VanS_A$ in 10 mM HEPES pH 7.9, 10 % (v/v) glycerol, 0.025 % (w/v) DDM was incubated with 5-fold molar equivalent concentration of ligand in 10 mM HEPES pH 8.0 (10 mM HEPES pH 8.0 in no-ligand control conditions) at 20 °C for 30 minutes prior to data collection. In 10-fold conditions, a further 5-fold molar equivalent of ligand was added to increase the final concentration in the reaction mix to 10-fold. Employing a rectangular cell with a 2 mm pathlength, 4 scans were collected in the far-UV region (215-260 nm) in 1 nm increments with 1 s integration at 20 °C. 1 mm slit width (equivalent to 1.8 nm bandwidth) was used throughout. Data was analysed using CDApps (Hussain et al., 2015) to produce difference spectra whereby all controls (buffers, solvents, ligands, etc.) have been subtracted and converted to molar extinction (Δε). Data was transferred to OriginPro® 9 for presentation. (Main) Difference spectrum of $VanS_A$ in the absence and presence of NAG and (Insert) enlargement of data shown in grey box on main graph.

3.4.2.2. Qualitative screen of binding of peptidoglycan components by $VanS_A$ using Synchrotron Radiation Circular Dichroism in the near-UV region

As with previously described ligand screens throughout this Chapter, 5-fold molar equivalent of cell wall component was screened in the aromatic region of the near-UV (260-305 nm). These measurements showed no aromatic residues of $VanS_A$ were involved in binding of peptidoglycan components (Fig. 3-21) suggesting an alternative mechanism of binding relative to GPAs vancomycin and teicoplanin binding.

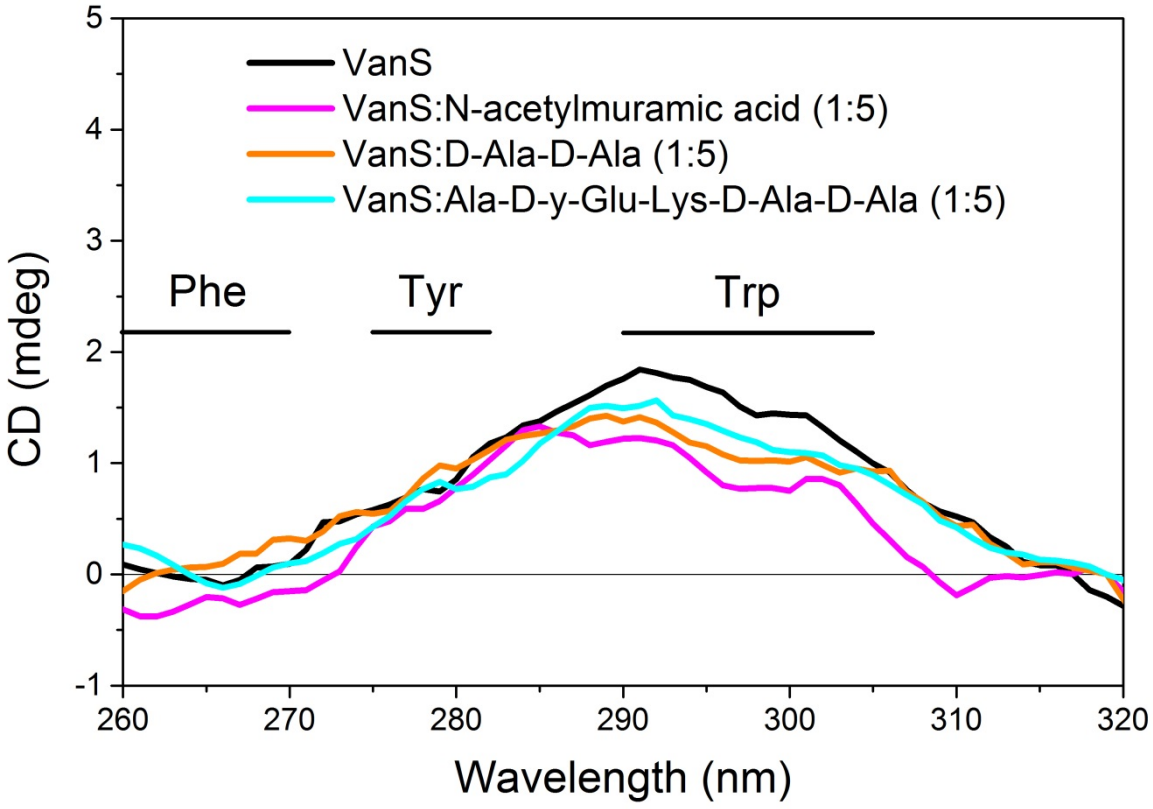

Figure 3-21: Difference spectrum of $VanS_A$, screening the aromatic region of the near-UV region (260-320 nm) in the absence and presence of 5-fold molar equivalent of peptidoglycan components.

$VanS_A$ (20 µM) in 10 mM HEPES pH 7.9, 10 % (v/v) glycerol, 0.025 % (w/v) DDM, 100 mM NaCl was incubated with 5-fold molar equivalent (100 µM) of peptidoglycan components including N-acetylmuramic acid, D-Ala-D-Ala, Ala-D-y-Glu-Lys-D-Ala-D-Ala in 10 mM Tris. HCl pH 8.0 at 20 °C for 30 minutes prior to data collection. 6 scans between 260-350 nm (1 nm increments, 1 second integration) were taken using 10 mm pathlength and 1 mm slit width. Data analysed using CDApps (Hussain et al., 2015) (zeroed 331-332 nm), then transferred to OriginPro for data presentation.

3.4.3. Characterisation of the interactions of sugars and other –OH group containing species with $VanS_A$

Sugar moieties are present in GPAs and peptidoglycan compounds; therefore the interaction of $VanS_A$ with sugars was investigated to determine their role, if any, in the mechanism of binding by $VanS_A$. Glucose isomers were tested to determine if there is an isomeric preference for glucose binding to $VanS_A$.

3.4.3.1. Qualitative screen of binding of sugars and other –OH group containing species by $VanS_A$ using Synchrotron Radiation Circular Dichroism in the far-UV region

D-glucose, the biologically relevant isoform of glucose, was found to bind $VanS_A$ and induce changes to the secondary structure of $VanS_A$. D-glucose is an R-group of vancomycin (Introduction, Fig. 1-1) therefore such findings may have some significance in the binding mechanism between $VanS_A$ and vancomycin therefore comparisons in binding with L-glucose were conducted to test for the specificity of binding by $VanS_A$. Initial qualitative screens revealed both isoforms induced small but non-significant changes in the secondary structure of $VanS_A$ (Fig. 3-22).

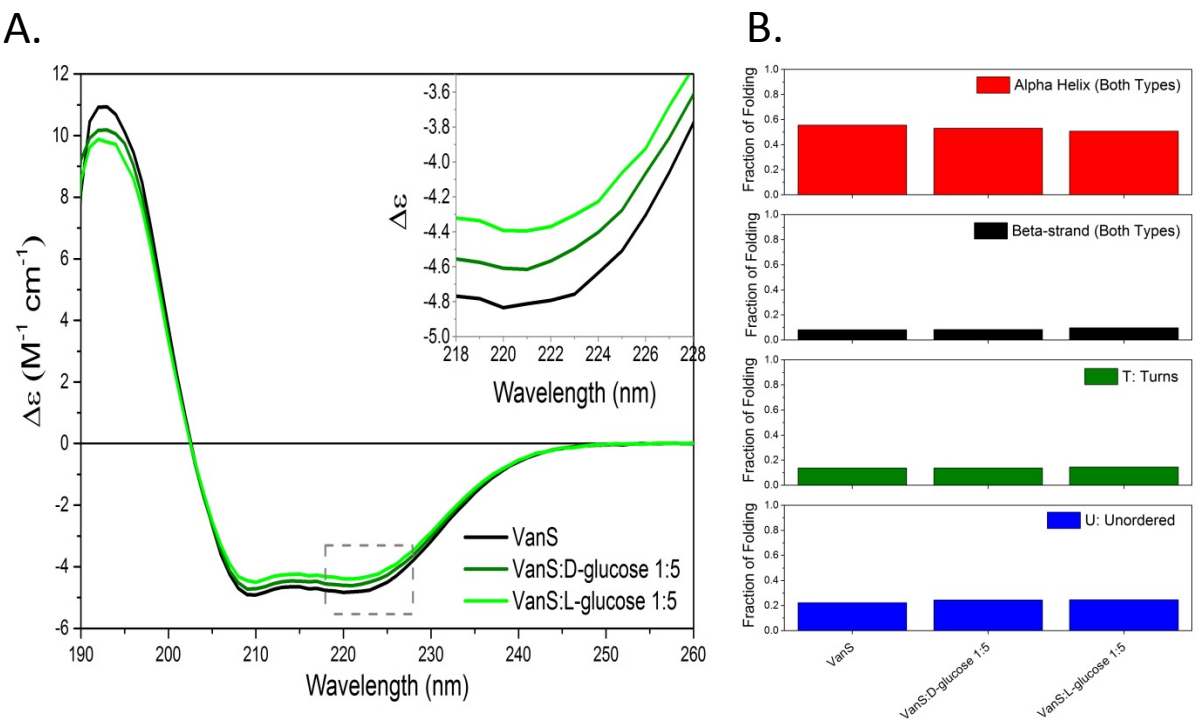

Figure 3-22: VanS$_A$ in the absence and presence of D- and L- glucose.

Screening of the interactions of D- and L-glucose with VanS$_A$ in the far-UV region. 11 µM of VanS$_A$ was incubated with 5-fold molar equivalent concentration of ligand (D-glucose, L-glucose) in 10 mM HEPES pH 8.0 (10 mM HEPES pH 8.0 in no-ligand control conditions) at 20 °C for 30 minutes prior to data collection. Employing a cylindrical cell with a 0.2 mm pathlength, 4 scans were collected in the far-UV region (190-260 nm) in 1 nm increments with 1 s integration at 20 °C. 1 mm slit width (equivalent to 1.8 nm bandwidth) was used throughout. Data was analysed using CDApps (Hussain et al., 2015) to produce difference spectra whereby all controls (buffers, solvents, ligands, etc.) have been subtracted and converted to molar extinction (Δε). Secondary structure estimations performed using CONTILL algorithm (Sreerama & Woody 2004) and SMP56 database (43 soluble, 13 membrane). Data was transferred to OriginPro® 9 for presentation. (A, main) Difference spectrum with (A, insert) enlargement of data in grey box on main graph; and (B) secondary structure estimations of VanS$_A$ in the absence and presence of screened glucose sugars. NMRSD is 0.012 – 0.04.

3.4.3.2. Qualitative screen of binding of sugars and other –OH group containing species by $VanS_A$ using Synchrotron Radiation Circular Dichroism in the near-UV region

Although binding was shown to affect the secondary structure of $VanS_A$, screens were conducted in the near-UV region on the same protein batch to determine if binding affected aromatic residues within the local tertiary structure. These measurements showed binding of sugar-compounds did not involve aromatic residues of $VanS_A$ (Fig. 3-23).

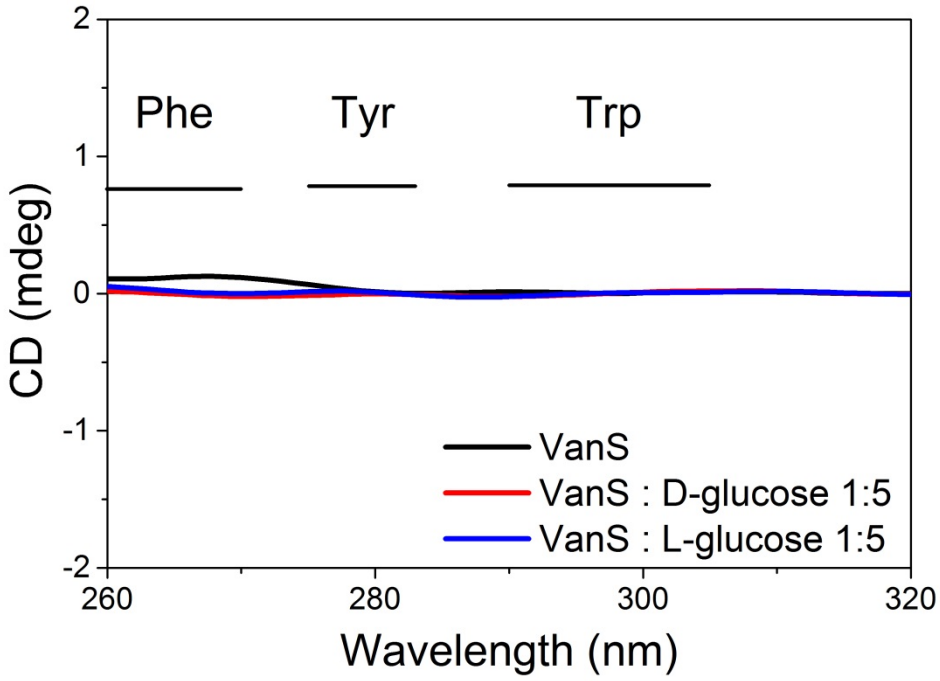

Figure 3-23: Difference spectrum of $VanS_A$ in the presence of glucose enantiomers.

11 µM of $VanS_A$ in 10 mM HEPES pH 8.0, 10 % (v/v) glycerol, 0.025% (w/v) DDM was incubated with 5 fold molar equivalent concentrations of sugar at 20 °C for 30 minutes prior to data collection. Employing a rectangular cell with 2 mm pathlength, 2 scans were collected in the near-UV region (260-320 nm) in 1 nm increments using 1 s integration and 1 nm bandwidth. Data was analysed using CDApps (Hussain et al., 2015) to obtain difference spectrum where all controls (buffers, ligands, etc.) have been subtracted. Data was transferred to OriginPro® 9 for smoothing (12-points Savitzky-Golay) and presentation.

3.4.4. Determination of the effect of the presence of potential ligands on the stability of $VanS_A$ during exposure to extreme experimental conditions, monitored in the far-UV region

Direct measurement of the effects of ligand binding on the secondary and local tertiary structure of a protein of interest are not the only approaches for ligand binding studies. Binding can affect the stability of the protein of interest, therefore complementary studies using the far-UV region to monitor changes in the conformational fold of the protein during exposure to different extreme experimental conditions such as temperature can aid characterisation of protein-ligand interactions.

3.4.4.1. Determination of the melting temperature (T_m) of $VanS_A$ in the presence and absence of potential ligands studied in the far-UV region

Ligand binding can affect the thermostability of a protein of interest; therefore can be exploited as a complementary method for determining ligand-protein interaction, as will be described here. In the absence and presence of screened ligands, $VanS_A$ was incubated at increasing temperatures from 20 °C to 90 °C in 5 °C increments with measurements taken at each temperature. The change in signal at 222 nm was plotted against corresponding temperature for fitting with a Gibbs-Helmotz equation for determination of the melting temperature, the temperature where the protein is at equilibrium state of unfolding 50 % folded : 50 % unfolded (Greenfield 2007).

Experiments investigating the effects of the presence of screened compounds on the thermostability of $VanS_A$ found only the presence of vancomycin caused any significant increase in the thermal stability of $VanS_A$ shown by the differences in the obtained kinetic profile and T_m for $VanS_A$ (Fig. 3-24), supporting the suggestion from near-UV studies identifying vancomycin as a ligand for $VanS_A$.

Furthermore, these results confirmed previous findings indicating the inversely proportional relationship between detergent concentration and protein stability as $VanS_A$ prepared in higher detergent conditions exhibited reduced thermodynamic stability indicated by the differences in the

thermodynamic profile of $VanS_A$ in addition to the different T_m values experimentally obtained (Fig. 3-20).

There are stark differences in the shape of the denaturation curve for higher detergent conditions compared to lower detergent conditions (Fig. 3-24). Lower detergent conditions had higher melting points, and although the stabilisation may have resulted from the lack of destabilising effect from the higher detergent, another explanation for stabilisation could have resulted from dimerisation of $VanS_A$. Dimerisation of $VanS_A$ was suggested as an explanation for the cooperativity of glycopeptide binding to $VanS_A$, and could explain the increased T_m in lower detergent conditions as the increased intrinsic stability of the dimer would make the protein more resistant to thermal denaturation.

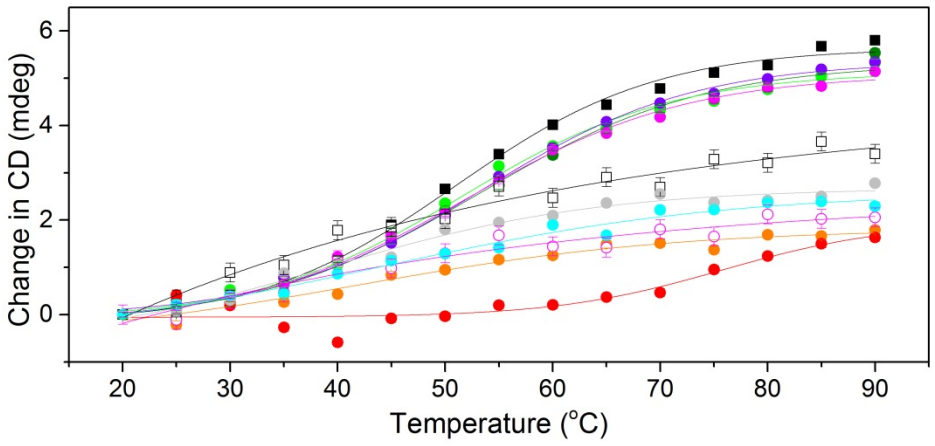

Melting Temperature (Tm) of VanS in the presence of screened ligands (°C)		
VanS 0.025 % DDM	■	51 ± 0.71
VanS + D-glucose 0.025 % DDM	●	53 ± 0.95
VanS + L-glucose 0.025 % DDM	●	52 ± 0.88
VanS + NAG 0.025 % DDM	●	53 ± 0.5
VanS + NAM 0.025 % DDM	●	52 ± 0.63
VanS 0.05 % DDM	□	44 ± 0.71
VanS + D-Ala-D-Ala 0.05 % DDM	●	48 ± 4.07
VanS + NAM 0.05 % DDM	○	44 ± 0.63
VanS + vancomycin 0.05 % DDM	●	79 ± 4.04
VanS + vancomycin + Ala-D-y-Glu-Lys-D-Ala-D-Ala 0.05 % DDM	●	44 ± 2.23
VanS + Ala-D-y-Glu-Lys-D-Ala-D-Ala 0.05 % DDM	●	51 ± 3.23

Figure 3-24: Thermal denaturation profile of $VanS_A$ in the absence and presence of screened ligands in the presence of different compounds in different detergent environments.

$VanS_A$ (0.5 mg/ml) either in 10 mM HEPES pH 8.0, 20 % (v/v) glycerol, 0.025 % DDM (w/v) (■●●●●) or 10 mM HEPES pH 7.9, 10% glycerol (v/v), 100 mM NaCl, 0.05% DDM (w/v) (□●○●●●) was incubated with 5-fold concentrations of ligand prepared in 10 mM Tris.HCl pH 8.0 for 30 minutes at 20 °C in buffer. 0.2 mm pathlength was employed to collect 1 scan at each temperature in the far-UV region (180-260 nm) in 1 nm increments, 1 s integration using 0.5 mm slit width (equivalent to 1.1 nm bandwidth). Analysis was performed using CDApps (Hussain et al., 2015) first to obtain difference spectra for each temperature by the subtraction of relevant buffers and ligand control, followed by the monitoring of the change in CD at 222 nm (□●○●●●) and change in CD (mdeg) at 225 nm (■●●●●). The change in CD (mdeg) at the specified wavelength was plotted against corresponding temperature and fitted using a Gibbs-Helmholtz using OriginPro® 9 to determine the melting temperature (T_m) of $VanS_A$ in each condition (Greenfield 2007). *Error bars displayed (n=3). Standard deviation for melting temperature displayed for T_m in table.*

3.4.5. Determination of the effect of the presence of potential ligands on the size distribution of $VanS_A$

Compared to control conditions tested for the ligands and buffer, it is clear that a detergent micelle had a very small size ~ 1 nm diameter (Figs. 3-25A and 3-25B insert graphs), compared to protein-containing conditions which had peaks ~ 50 nm (Figs. 3-25A and 3-25B main graphs). Screens investigating $VanS_A$ stoichiometry in the presence of a range of compounds showed no change in size-distribution for $VanS_A$ (Fig. 3-25) inferring no ligand-mediated self-association of $VanS_A$ occurred.

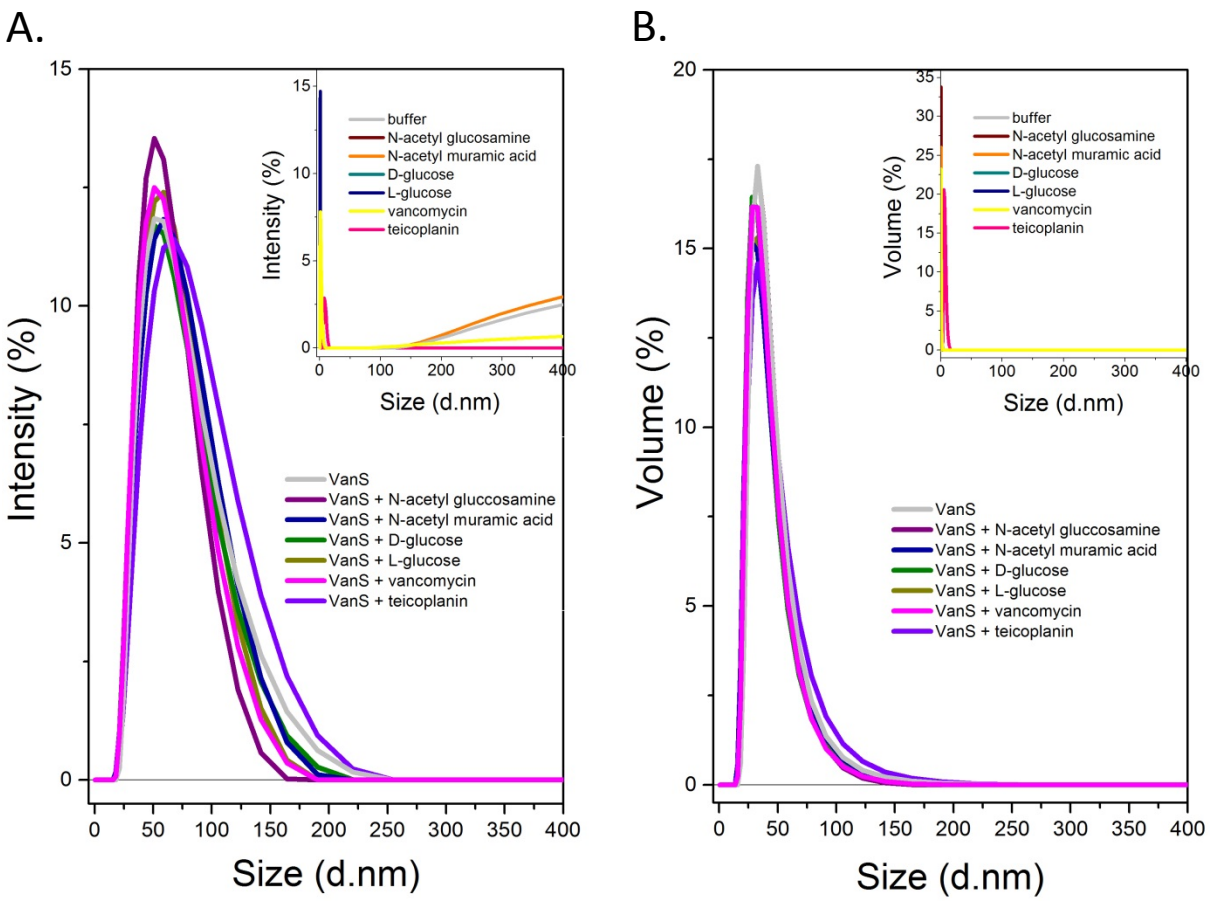

Figure 3-25: DLS spectrum of VanS$_A$ in the presence of screened ligands.

0.5 mg/ml of VanS$_A$ in 10 mM HEPES pH 8.0, 20 % (v/v) glycerol, 0.025 % DDM (w/v) was incubated at 20 °C for 30 minutes in the absence or presence of 5-fold ligands in 10 mM Tris HCl pH 8.0 (in the case of no ligand conditions 10 mM Tris HCl was added only) prior to data collection. Using Disposable Solvent Resistant Micro Cuvettes (ZEN0040, Malvern) in a Zetasizer Nano ZSP (Malvern), samples (70 µl) were analysed using pre-determined programme. Intensity (%) (A and B, respectively) and volume (%) (C and D, respectively) are shown for VanS$_A$ + ligands and ligands only.

3.5. Discussion

This Chapter aimed at identifying and characterising ligands binding to $VanS_A$. For this, Circular Dichroism Spectroscopy (CD) was employed to investigate the structural effects of ligand binding. Successfully identified interactions were further investigated using complementary spectroscopic techniques Magnetic Synchrotron Radiation Circular Dichroism Spectroscopy (MSRCD), UV-Vis absorption, and Fluorescence Spectroscopy (Fluorescence).

Measurements in the far-UV region showed no significant changes in the conformation of $VanS_A$ in the presence of the screened compounds, however thermal melt studies in the presence of the compounds highlighted vancomycin as a potential binding ligand for $VanS_A$ due to the increased melting temperature (T_m) and difference in thermal denaturation profile. Protein preparations used throughout of these experiments contained high proportions of helical structure (Fig. 3-2), in agreement to bioinformatics predictions (Fig. 2-2) suggesting a good basis for the prediction of structure of $VanS_A$ without x-ray crystallography.

Thermal denaturation predictions for $VanS_A$ using the amino acid sequence (Ku *et al.,* 2009) predict a T_m of 55-65 °C. The T_m values obtained for $VanS_A$ in different detergent concentrations during thermal denaturation experiments were below the predicted range (Fig. 3-24) suggesting reduced stability of $VanS_A$ in high concentrations of detergent for protein stability, the T_m decreased from 51 °C to 44 °C (Fig. 3-24) when DDM concentration was changed from 0.025% to 0.05%. This was supported by secondary structure estimations showing increased helical content for $VanS_A$ in lower detergent conditions. Analysis of the denaturation process used a simple two-step model to represent the unfolding process, and although the protein under study has multiple domains this two-step process was chosen for a simpler initial analysis to obtain preliminary information from which more complex models can be applied as more is learned about the system. More rigorous methods could be used to monitor protein unfolding at a later date. Methods such as monitoring the unfolding of specific domains can be monitored (Hussain et al. 2018).

Only in the presence of GPAs vancomycin and teicoplanin was any change observed in the aromatic region of the near-UV (260-310nm), which directly suggested the involvement of tyrosine/tryptophan presented in the tertiary fold of $VanS_A$ during binding. Their roles during binding were confirmed during fluorescence (excitation wavelength 295 nm) and MSRCD experiments which showed a shift in emission peak maximum wavelength (Fig. 3-13) and shift in maximum peak and trough in the presence of the antibiotics (Fig. 3-15), respectively, indicative of a change in the local environment of the fluorophore as a result of antibiotic binding. When further characterised through application of titration methods to CD and UV-vis in the near-UV region, differences were observed in the obtained K_d values for each antibiotic (Figs. 3-11 and 3-12, respectively). Though both methods were in agreement for the determined K_d values for vancomycin, there were discrepancies in the case of teicoplanin. Teicoplanin is a mixture of 9 isomeric compounds (5 major and 4 minor) (Parenti 1986) and the disagreements in K_d for each methods may be a reflection of the binding of different isoforms. Titrations using Fluorescence (Fig. 3-16) and MSRCD (Figs. 3-16 and 3-17) showed tighter binding by tryptophan for both antibiotics, with the differences in affinity using these methods compared to CD reflective of the specificity of the methods for monitoring the interactions of tryptophan during GPA binding. Together the results suggest an important role for tryptophan in ligand binding as interactions characterised were corresponding for this residue suggesting it has a key role in ligand binding.

Literature suggests that the binding of a ligand may result in dimerisation for the enabling of trans-phosphorylation of the dimer for signal relay by the proteins of the two-component system (Wang 2012). Findings presented in this Chapter showed conflicting results. Lower detergent conditions may permit the formation of dimers and was supported by the increased thermal stability of $VanS_A$ in lower detergent conditions (Fig. 3-24) in addition to cooperative binding of vancomycin by $VanS_A$ (Fig. 3-11). DLS experiments showed the presence of screened ligands had no effect on the stoichiometry of $VanS_A$ (Fig. 3-25) which remained as a monomer. The reported assays were conducted in the absence of ATP which may be necessary in addition to ligands to initiate

dimerisation. The discussed discrepancies in the determined state of $VanS_A$ in the presented assays could be due to a small proportion of dimerised $VanS_A$ being present in a majority monomeric state may be because dimer concentrations are below the detection limit of the methods used. If true, this is an important point for consideration with regards to the mechanism of phosphorylation activity of $VanS_A$ which will be discussed in Chapter 4.

CHAPTER 4:
ATTEMPTS TO CHARACTERISE THE ACTIVITY OF $VANS_A$ IN RELATION TO LIGAND BINDING.

4.1. Introduction

This Chapter will explore a variety of methods for the detection and analysis of phosphorylated proteins, comparing their effectiveness at assessing the phosphorylation activities of proteins of the Two-Component Signal Transduction System (TCS) regulating type A vancomycin resistance in enterococci.

Histidine kinases (HKs) are regulatory proteins which are able to regulate their own level of phosphorylation in addition to that of the partner response regulator protein by switching between kinase and phosphatase activities. Monitoring of the autophosphorylation activity of the protein not only confirms the reliability of the purification method as producing pure and active purified protein, but can also be used for ligand binding studies.

More than 50 years since their discovery (Boyer *et al.,* 1962) comparatively less is known about phosphorylated Histidine (pHis) than phosphorylated serine or threonine (Eckhart *et al.,* 1979). One of the challenges faced when investigating the phosphorylation activities of proteins of the TCSs is the comparatively short life-time of the phosphorylated residues which can be explained by the kinetics of the reaction (Trajtenberg et al. 2010) the more negative ΔG value for N-H than O-H (Kee & Muir 2012). This transient behaviour makes investigations of HKs difficult.

In vitro studies have shown HKs of specific TCSs display different activity behaviours (Ma *et al.,* 2008) which can be further changed in the presence of ligands and inhibitors (Potter *et al.,* 2002; Ma *et al.,* 2011). These concepts will be applied to the subsequent investigations of the activities of $VanS_A$, the HK of the TCS regulating type A vancomycin resistance in the enterococci described in this Chapter.

The activating ligand for the onset of A-type vancomycin resistance in enterococci is currently unknown and widely disputed (Kwun *et al.,* 2013; Koteva *et al.,* 2010; Baptista *et al.,* 1996). As such, this Chapter shall discuss work conducted using activity assays to identify interacting ligands

activating or repressing the induction of vancomycin resistance by the TCS regulating A-type vancomycin resistance in the enterococci.

4.2. Working hypothesis

It is hypothesised that screening potential ligands for changes in the autophosphorylation activity of $VanS_A$ will be a valid method for identifying binding activators and repressors of the onset of resistance. Using this key insight, the mechanism for the onset of resistance gene expression will be investigated.

4.3. Methods

4.3.1. $VanS_A$ overexpression and purification

$VanS_A$ overexpression and purification was as previously described (See Chapter 3).

4.3.2. General Activity Assay schematic

Phosphorylation assays undertaken for purified protein preparations of $VanS_A$. Autophosphorylation reactions were undertaken using 60 pmoles of purified protein, which after incubation with ligand (in 10 mm Tris.HCl pH 8.0) or no ligand for the control (10 mM Tris.HCl pH 8.0) for 20 minutes in Assay buffer (50 mM Tris-HCl pH 7.6, 50 mM KCl, 10 mM $MgCl_2$, 1 mM DTT, 50 µm final concentration of ATP was added to initiate the reaction. The reactions were stopped at the appropriate time-point by addition of STOP solution (50 mM Tris.HCl pH 6.8, 2% SDS, 0.005% bromophenol blue, 10% glycerol, 3% β-mercaptoethanol).

4.3.2.1. Phosphorylation activity assays using P^{33}-γ-ATP

Phosphorylation activity assays using P33-γ-ATP were conducted as described above, but the autophosphorylation reactions were initiated by the addition of P33-γ-ATP (185 kBq/5uCi), as described in Potter *et al.,* (2002); Ma *et al.* (2008). Reactions were conducted as above, incubating for a given time and the addition of 1X final concentration of Stop buffer at the desired timepoint. Reactions were separated using SDS-PAGE (5 %/12 %) and the gel dried under vacuum at 80 °C. Film was exposed for between 3 and 10 days before developing and densiometric analysis using a ChemiDoc™ XRS+ and Image Lab™.

4.3.2.2. Activity assays using Phos-tag™ Acrylamide

Autophosphorylation activity assays were conducted under standard conditions, where by the HK was phosphorylated by the addition of ATP. Phos-tag™ Acrylamide gels (5 %/10 %) we made as described by the manufacturer (Wako) but with the addition of 0.1% Ammonium persulfate (APS) rather than the described 0.05% APS. Reactions were separated by running at 30mA/gel until the dye front ran off the gel. For Coomassie stained gels, the gel was placed in 15 ml InstantBlue™ (Expedeon). For Western blots, the gel was incubated in Transfer buffer (25 mM Tris, 200 mM glycine, 20 % methanol) + 10 mM EDTA (pH 8.0) for 10 minutes before incubating in Transfer buffer for 10 minutes, each step with gentle agitation. Blots were performed under standard conditions (90 V, 1 hour), the PVDF membrane was blocked overnight in 10 % (w/v) milk in 1 X TBST (10 mM Tris HCl pH 7.5, 100 mM NaCl, 1 % (v/v) Tween 20). The membrane was probed with Anti-His_6 antibody (INDIA) and developed by incubating with SuperSignal™ West Pico Chemiluminescent Substrate (Thermo Scientific) and exposing to film.

4.3.2.3. Activity assays using Phos-tag™ Biotin BTL-111

Reactions were separated on SDS-PAGE gel electrophoresis (5 %/12 %) at 30 mA/gel before PVDF blotting at 90 V for 1 hour. The protein-blotted membrane was soaked in 1X TBS-T overnight before incubation with (Phos-tag™ Biotin BTL 111)$_4$-(Streptavidin-conjugated HRP) prepared as described by the manufacturer (Wako) for 30 minutes at room temperature. After washing the membrane in 10 % (w/v) milk in 1 X TBST (10 mM Tris HCl pH 7.5, 100 mM NaCl, 1 % (v/v) Tween 20). Chemiluminescence was observed by incubating with SuperSignal™ West Pico Chemiluminescent Substrate (Thermo Scientific) and visualisation using ChemiDoc™ XRS+. Analysis conducted using Image Lab™ (BioRad).

4.3.2.4. Monitoring of kinase activity of $VanS_A$ using R & D systems universal kinase assay kit

Assays were conducted as per the instructions provided in the R & D Systems Universal Kinase Activity Kit (Catalogue # EA004) (R & D), changing the pH to 8.0 due to the tendency of $VanS_A$ to precipitate at pH lower than 8.0. All assays were conducted in 25 mM HEPES pH 8.0, 150 mM NaCl, 10 mM $MgCl_2$, and 10 mM $CaCl_2$. Compatibility checks for the activity of CD39L2 were made in the new conditions. A phosphate standard curve in the new assay conditions was used to determine the conversion factor (CF) for CD39L2 by calculating the slope of OD_{620} x phosphate input (KH_2PO_4). This CF was used in later calculations to determine the amount of PO_4^{2-} produced in later experiments.

For initial ligand and buffer additive screens, $VanS_A$ (0.2 µg) was incubated for 20 minutes prior to the initiation of autophosphorylation by the addition of ATP, after which autophosphorylation was allowed to proceed for 40 minutes before reactions were stopped by the addition of 30 µl Malachite Green Reagent A (ammonium molybdate in 3M sulphuric acid) at t=60. 100 µl d.H_2O was added to each well, followed by 30 µl of Malachite Reagent B (malachite green oxalate and polyvinyl alcohol) and the colour allowed to develop for 20 minutes before determining the optical density at 620 nm.

For kinetics assays, $VanS_A$ (0.2 µg) was incubated with the appropriate ligand (5-fold concentration) in the appropriate buffer condition for 20 minutes prior to initiation of autophosphorylation by the addition of ATP (200 µM) in a final volume of 50 µl as specific time points (e.g. at t=0, final phosphorylation time will be 60 minutes; at t= 20, phosphorylation time will be 40 minutes, etc.) so that when the reactions are stopped at the same time point a full time course is complete. All reactions were stopped by the addition of 30 µl Malachite Green Reagent A (ammonium molybdate in 3M sulphuric acid) at t=60. 100 µl of d.H_2O was added to each well, followed by 30 µl of Malachite Reagent B (malachite green oxalate and polyvinyl alcohol) and the colour allowed to develop for 20 minutes before determining the optical density at 620 nm.

4.4. Results

4.4.1. The use of Phos-tag™ Acrylamide for the investigation of phosphorylation activity of His_6 tagged $VanS_A$

Phos-tag™ acrylamide (PTA) is a novel, non-radioactive system which allows for the separation of phosphorylated and non-phosphorylated proteins using standard SDS-PAGE conditions (Kinoshita *et al.,* 2006), making it an ideal routine method. The Acrylamide method involves preparing acrylamide gels containing PTA in the gels. The presence of PTA in the gels causes a retardation of the migration of phosphorylated protein with respect to non-phosphorylated forms as phosphoryl groups on the phosphorylated protein bind PTA which works to slow the proteins migration (Kinoshita et al. 2006). Standard detection methods for the protein of interest can therefore be employed, such as protein-specific antibodies which should be capable of detecting both dephosphorylated and phosphorylated bands.

Previous work using PTA has utilised the system for the investigation of Serine/Threonine and Tyrosine phosphorylation (Kinoshita *et al.,* 2006). These phosphorylated proteins are generally longer-lived and more stable than phospho-histidine, the biochemically important modification important to the activity of Histidine kinases and phospho-aspartate (Barbieri and Stock 2008) (which are relatively very short-lived and unstable compared to other phosphorylated amino acid). The application of PTA for the investigation of phospho-histidine has been demonstrated (Yamada *et al.,* 2007), so potentially is an appropriate system to investigate the phosphorylation activity changes of $VanS_A$ in response to ligand binding.

Though recent work has validated the use of PTA for the analysis of phospho -histidine and -aspartate (Yamada *et al.,* 2007; Barbieri and Stock 2008) the relatively transient nature of phosphor-histidine and -aspartate, phosphatase activity of these proteins, and few publications reporting PTA data suggest there is still some way before it becomes a reliable routine method for the investigation of two-component systems.

4.4.1.1. Optimisation of the concentration of acrylamide used with Phos-tag™ Acrylamide for the investigation of phosphorylation activity of membrane sensor kinases of two-component systems

The PTA system requires optimisation for the best resolution of phosphorylated from de-phosphorylated forms of the protein of interest (Kinoshita et al., 2006). Initial experiments investigating the migration of $VanS_A$ through SDS-PAGE gels of different concentrations of acrylamide showed 10 % acrylamide gels allowed the optimal migration of $VanS_A$ (Fig. 4-1), and was the concentration which would be used throughout the following experiments.

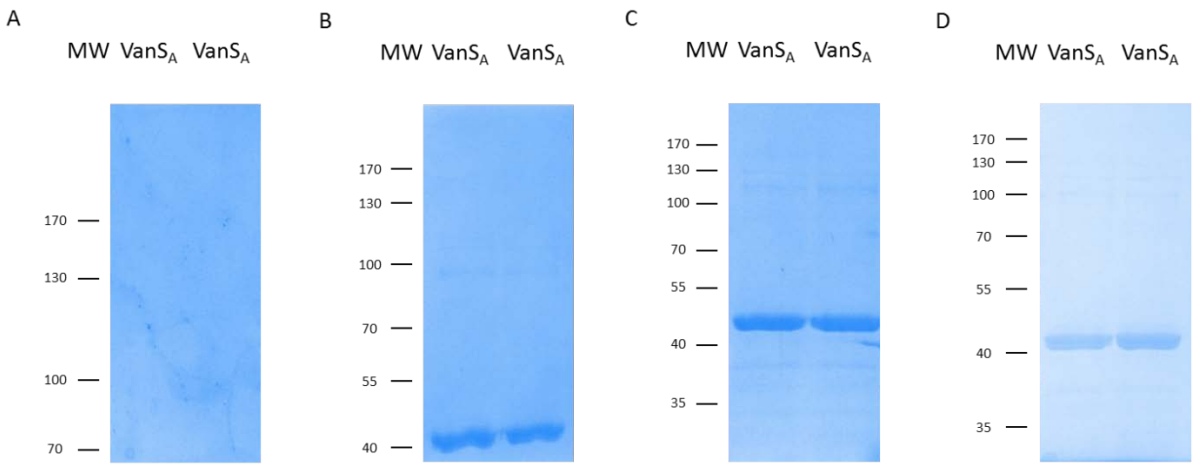

Figure 4-1: Reference migration profiles of VanS$_A$ through SDS-PAGE gels containing different concentrations of acrylamide.

VanS$_A$ (60 pmoles) was run through SDS-PAGE gels with different concentrations of the resolving gel acrylamide A) 6 %, B) 8 %, C) 10 % D) 12 % under standard conditions as described in Methods. Protein was combined with loading buffer (50 mM Tris.HCl pH 6.8, 2% SDS, 0.005% bromophenol blue, 10% glycerol, 3% β-mercaptoethanol) 30 mA/gel until the dye front reached the bottom of the gel. Gels were Coomassie stained (InstantBlue™, Expedeon) and imaged using ChemiDoc XRS+ (BioRad).

In addition to the optimisation of the concentration of acrylamide, the concentration of PTA also requires optimisation. Initial experiments using the previously determined 10 % acrylamide and 50 µM of PTA (the concentration used in pre-cast gels) was adopted as a starting point for the optimisation of PTA concentration. Under these conditions (10 % acrylamide, 50 µM PT acrylamide) resolution of the dephosphorylated and phosphorylated forms of VanS$_A$ was poor (Figs. 4-1D and 4-2) and resolution using different concentrations of PTA did not improve (data not shown), therefore a different approach was taken to improve resolution.

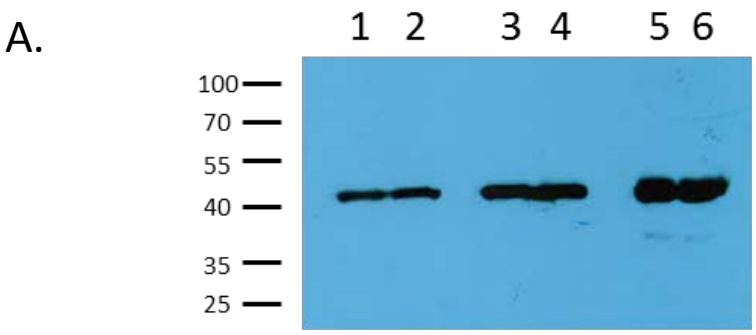

Figure 4-2: Western blot comparing the migration of phosphorylated and native forms of $VanS_A$ through Phos-tag ™ Acrylamide gels. *Assays employing 60 pmoles of $VanS_A$ in final buffer 10 mM HEPES pH 8.0, 10% glycerol, 0.05% DDM were performed as described in Methods. Samples were run through a PTA gel (5%/10% acrylamide, 50 µM PTA) running until the 30 kDa molecular weight marker to the bottom of the gel. Western blot was the performed as described in Methods. Film (ThermoScientific™ CL-XPosure™, ThermoFisher Scientific) was exposed for 15 seconds before developing. (A) Film imaged using ChemiDoc XRS+ (BioRad). (B) Densitometry performed using ImageJ (Schneider et al., 2012; Rasband 1997). Relative Activity (%) calculated relative to $VanS_A$. (1, 2) Freshly prepared $VanS_A$ control assayed in the absence of added ATP; (3, 4) phosphorylation assays conducted for -80 °C stored $VanS_A$ terminated 20 minutes after initiation of phosphorylation by addition of ATP; phosphorylation assays conducted for freshly prepared $VanS_A$ (the same protein preparation used for the control assays (1 and 2) stopped (5) 20 minutes and (6) 40 minutes after addition of ATP.*

Using SDS-PAGE gels of higher concentration (15 %) and running the gel until the 40 kDa molecular weight marker was to the bottom of the gel (because $VanS_A$ consistently migrated relative to the position of the molecular weight markers for 40 and 55 kDa) with the hope of increasing the resolution between the phosphorylated and dephosphorylated forms. Still, under these conditions no distinction between dephosphorylated and phosphorylated forms of $VanS_A$ were observed (Fig.

4-3) unlike what has been previously described for other phosphorylated proteins including phosphor-histidine (Yamada *et al*. 2007; Barbieri & Stock 2008; Kinoshita *et al*. 2009).

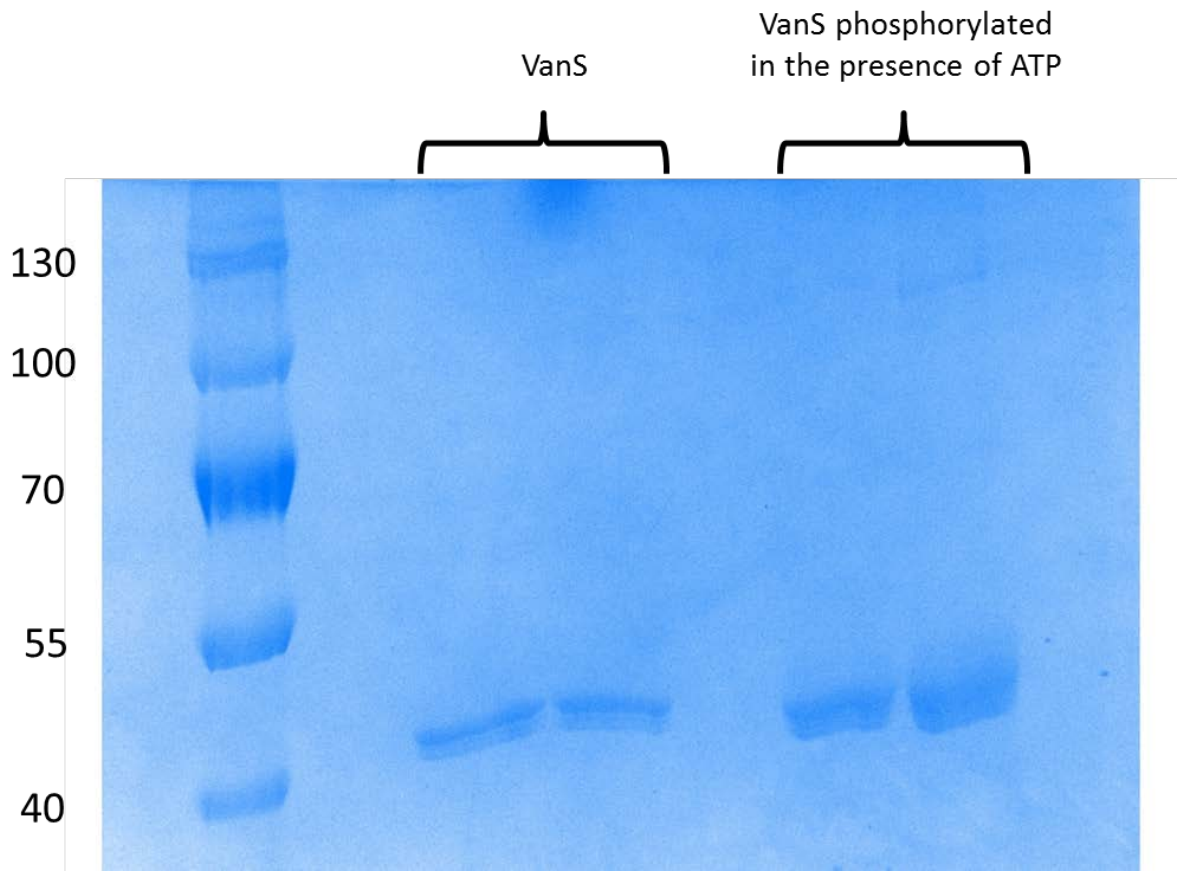

Figure 4-3: Reference migration profiles of VanS$_A$ through SDS-PAGE gels containing different concentrations of acrylamide.*Assays employing VanS$_A$ (60 pmoles) were performed as described in Methods and run through a PTA SDS-PAGE gel (5%/15%, 50 µM PTA) under standard conditions as described in Methods. Protein was combined with loading buffer (50 mM Tris.HCl pH 6.8, 2% SDS, 0.005% bromophenol blue, 10% glycerol, 3% β-mercaptoethanol) and run at 30 mA/gel until the 40 kDa molecular weight marker reached the bottom of the gel. Gels were Coomassie stained (InstantBlue™, Expedeon) and imaged using ChemiDoc XRS+ (BioRad).*

During phosphorylation experiments, the proportion of unphosphorylated and phosphorylated forms of a protein change. When run through a PTA gel, phosphorylated forms are retarded in the

gel (Fig. 4-4B iii) relative to unphosphorylated forms (Fig. 4-4B i). Through a PTA gel, phosphorylation of a protein can be monitored as total protein can be separated into its unphosphorylated and phosphorylated states (Fig. 4-4B ii).

No phosphorylated bands for $VanS_A$ were resolved during PTA time-course experiments. Furthermore the net band intensity for each time-point increased across the time-course (Fig. 4-4A) suggesting either uneven-loading of protein, uneven washing or chemiluminescence substrate binding as this method used protein-specific antibodies to detect the protein of interest.

Large, over-exposed bands were observed (Fig. 4-4A) making quantitative analysing of the bands difficult as reliable comparisons cannot be made. Potential shifting of the film during exposure could account for the overlying bands. These experiments were repeated 4 times with different batches of protein, and each attempt yielded similar results where no band-shift was detected. It is possible that different running conditions were required for better resolved bands such as higher concentration gels and running the gels for longer such to push the known non-phosphorylated band further towards the bottom of the gel.

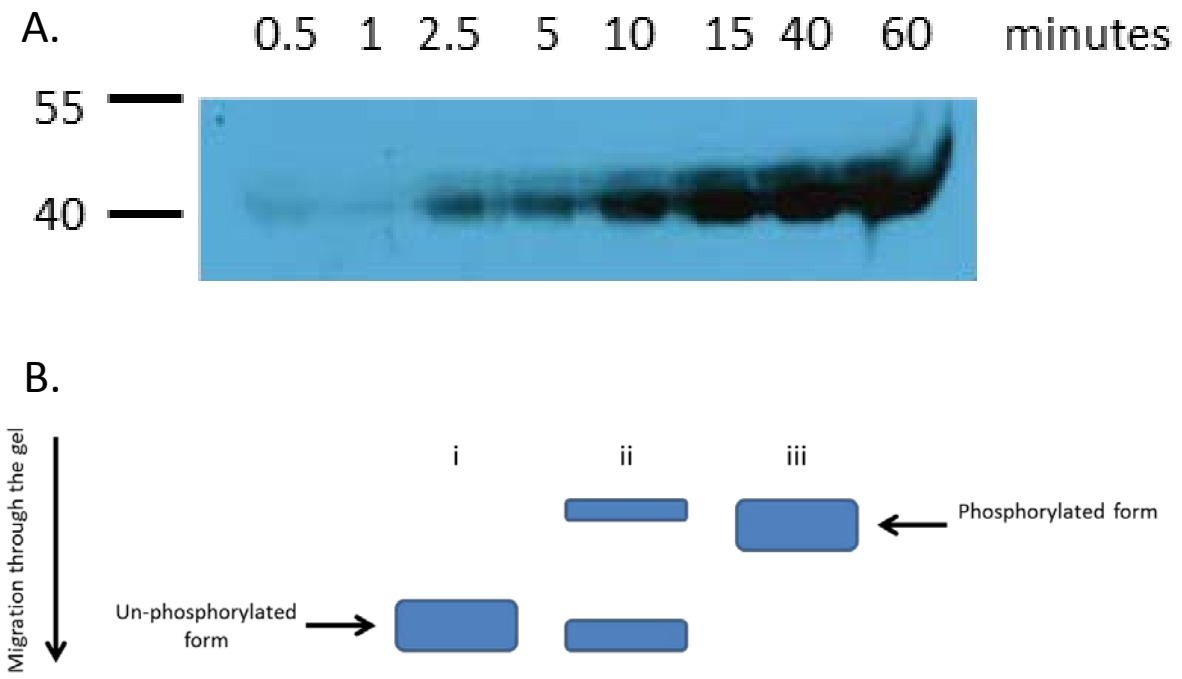

Figure 4-4: Time course of $VanS_A$ autophosphorylation. *$VanS_A$ (600 pmoles in final buffer 10 mM HEPES pH 8.0, 10% glycerol, 0.05% DDM) was phosphorylated by the addition of ATP (500 µM) in a total volume of 135 µl as described in Methods, adapting the method by removing 15 µl aliquots at specified time points. Samples were run through a PTA gel (5%/10 % acrylamide, 50 µM PTA) running until the 30 kDa molecular weight marker to the bottom of the gel. Western blot was the performed as described in Methods. Film (ThermoScientific™ CL-XPosure™, ThermoFisher Scientific) was exposed for 5 seconds before developing. Film imaged using ChemiDoc XRS+ (BioRad). (B) Schematic representation of an ideal PTA gel. Unphosphorylated form of protein (i) runs further through the gel than phosphorylated forms which are retarded in the PTA gel (iii). Proportion of unphosphorylated and phosphorylated protein ratios change for total protein per condition throughout the course of a phosphorylation experiment.*

The effect of the presence of 5-fold concentration of proposed ligands on the autophosphorylation activity of $VanS_A$ 30 minutes after initiation of phosphorylation by the addition of ATP was screened.

Results shown in Fig. 4-5 showed little difference in band intensity for $VanS_A$ and $VanS_A$~P, suggesting the protein was partially phosphorylated before the addition of ATP. In the presence of ligands, the intensity of the band increased overall indicative of the ligands having an effect on overall activity of $VanS_A$, either affecting the rate of phosphorylation, or the overall maximal phosphorylation (V_{max}) for $VanS_A$. Whether this is because of an increase in $VanS_A$~P which had been slightly retarded in the gel relative to $VanS_A$ is difficult to determine as the shift is very small (Fig. 4-5A) and makes analysis difficult for distinguishing the bands and may be corrected by using a higher concentration of acrylamide improve the resolution of the gel. This is a cause for doubt as there is no significant difference in the band intensity for unphosphorylated $VanS_A$ and suggests assay conditions are inefficient and unfavourable for protein phosphorylation. Furthermore, separation of the bands for unphosphorylated and phosphorylated forms are poor, making analysis of the results less reliable.

The upper band appears less intense in the presence of vancomycin compared to A2 teicoplanin (Fig. 4-5) suggesting A2 may be a favoured teicoplanin compound affecting $VanS_A$ activity. Similarly, peptidoglycan components caused similar increases in band intensity (Fig. 4-5) suggesting their presence has an effect on the activity of $VanS_A$.

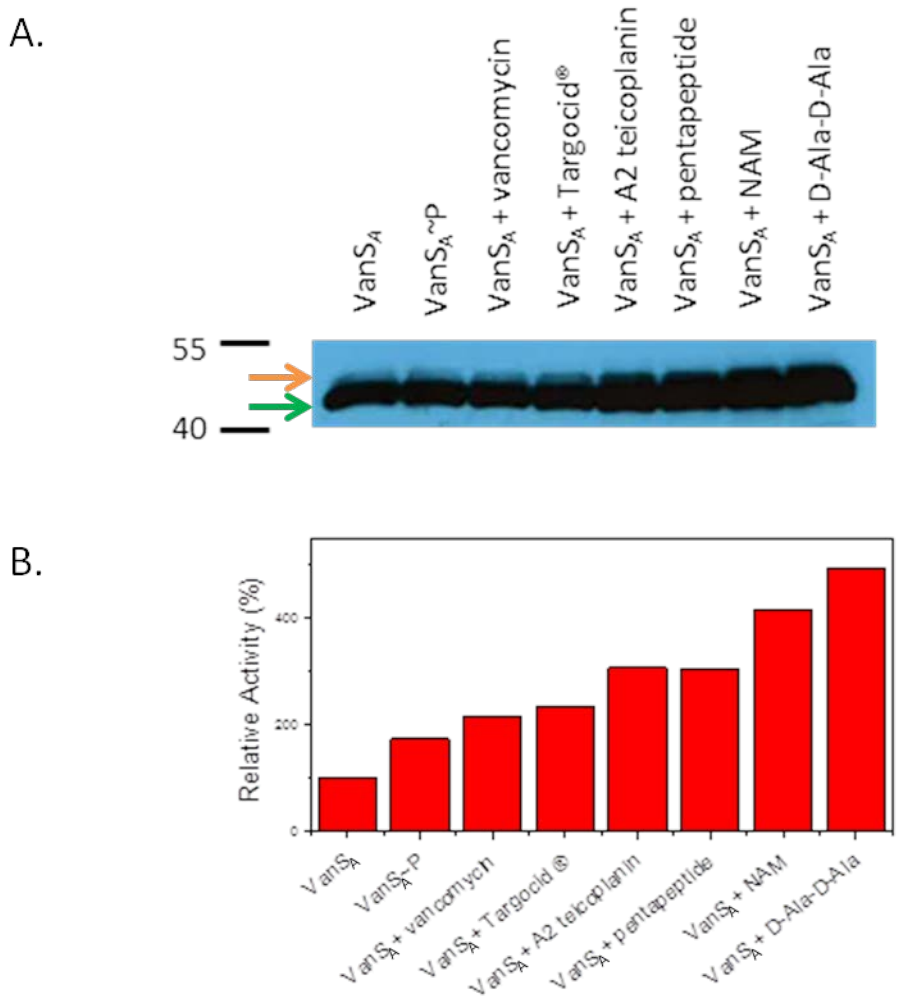

Figure 4-5: Western blot of comparison of autokinase activity of VanS$_A$ in the presence of potential antibiotic and peptidoglycan components separated using Phos-Tag™ Acrylamide.*Assays employing 60 pmoles of VanS$_A$ incubated in the absence or presence of glycopeptide antibiotics or peptidoglycan components (prepared in 10 mM Tris HCl pH 8.0) for 30 minutes at 20 °C were conducted as described in Methods. Samples were run through a PTA gel (5%/10 % acrylamide, 50 µM PTA) running until the 30 kDa molecular weight marker to the bottom of the gel. Western blot was the performed as described in Methods. Film (ThermoScientific™ CL-XPosure™, ThermoFisher Scientific) was exposed for 5 seconds before developing. (A) Film imaged using ChemiDoc XRS+ (BioRad). Unphosphorylated (→) and phosphorylated (→) forms shown. (B) Densitometry performed using ImageJ (Schneider et al., 2012; Rasband 1997) measuring densitometry of the top band.*

Relative Activity (%) calculated relative to $VanS_A$. Phos-tag™ Biotin BTL-111 for the investigation of phosphorylation activity of His_6 tagged $VanS_A$.

Phos-tag™ technology has also been used in the development of non-specific phospho-antibodies that can be used to universally detect phosphorylated proteins by detecting phosphorylated groups (Kinoshita *et al.,* 2012). Using standard SDS-PAGE and Western blot techniques, phosphorylates protein is detected using Phos-tag™ Biotin BTL-111 antibodies therefore they can be used alongside protein-specific antibodies to detect the phosphorylation of a protein of interest.

Little literature is available describing the application of the method for the investigation of phosphorylated protein, especially phospho-histidine and –aspartate, the biologically active forms of proteins of two-component systems. Described here are the attempts to characterise the activities of the histidine kinase of the two-component system regulating A-type vancomycin resistance in enterococci, $VanS_A$ using Phos-tag™ Biotin BTL-111 (PTB-111).

4.4.1.2. Investigation into the autophosphorylation activities of $VanS_A$ in the presence and absence of vancomycin using Phos-tag™ Biotin BTL-111

PTB-111 experiments were difficult to replicate. Often no signal was detected by PTB-111, yet Ponceau staining of the blots showed the presence of protein bands at the predicted molecular weight position suggesting efficient transfer of protein during Western blot and the lack of phosphorylated bands was due to either proportionally little phosphorylated protein present.

Autophosphorylation experiments showed a general trend whereby autophosphorylation of $VanS_A$ increased, plateaued, and decreased over the observed time points, a characteristic which has been seen before (Ma *et al.*, 2008). Maximal phosphorylation was reached by 5 minutes and decreased after 15 minutes (Fig. 4-6A) suggesting either a rapid switch into the autophosphatase mode for $VanS_A$, or that all of the ATP substrate had been used up at this point.

Experiments investigating the phosphorylation kinetics of $VanS_A$ in the presence of vancomycin were not as successful. Less phosphorylation was seen across the blot (Fig. 4-6B) therefore no justified conclusions about the kinetics of $VanS_A$ phosphorylation in the presence of vancomycin can be made.

Overall, the method was unreliable for the analysis of these interactions due to the difficulties associated with obtaining replicable results as often experiments gave no results, as demonstrated in Fig. 4-6. The method requires optimisation for the system under study and current preliminary results should be taken with caution.

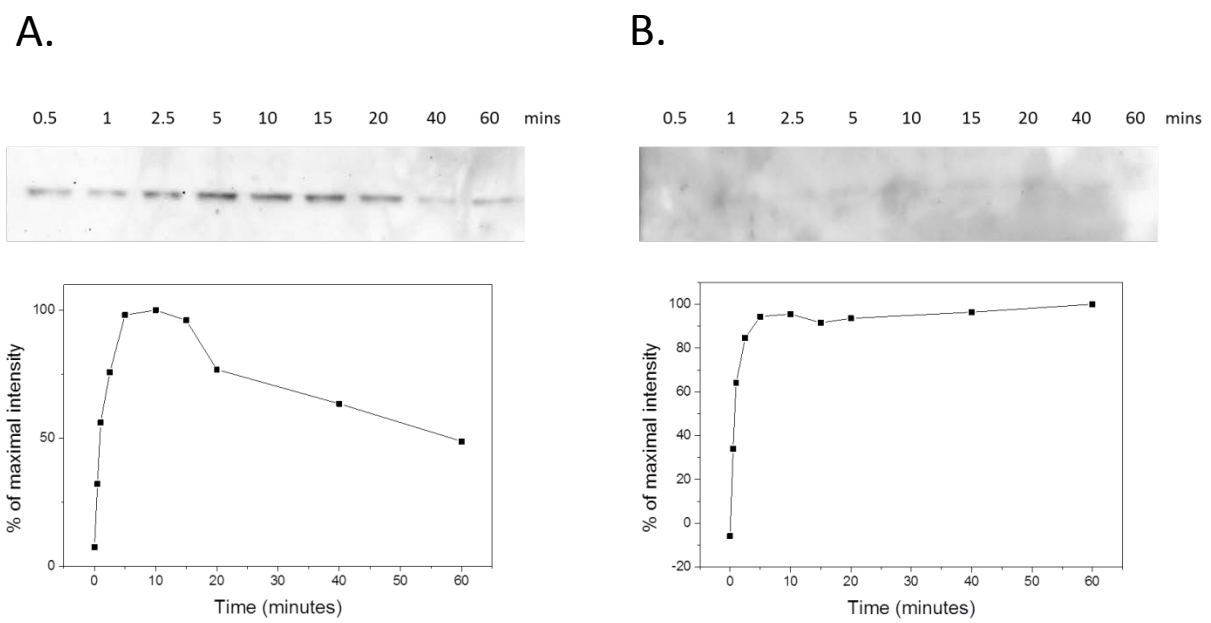

Figure 4-6: Autophosphorylation time course of $VanS_A$ in the presence and absence of vancomycin. *540 pmoles of $VanS_A$ phosphorylated by the addition of a final concentration of 50 µM ATP. 60 pmoles aliquots were removed from the reaction at time points 0.1, 1, 2.5, 5, 10, 15, 20, 40, 60 minutes and stopped by adding 1X final concentration of SDS-loading buffer (50 mM Tris.HCl pH 6.8, 2% SDS, 0.005% bromophenol blue, 10% glycerol, 3% β-mercaptoethanol), as described in Methods. $VanS_A$ was either incubated (A) in the absence of vancomycin (10 mM Tris HCl) or (B) the presence of vancomycin (in 10 mM Tris HCl) in 50 mM Tris-HCl pH 7.6, 50 mM KCl, 10 mM $MgCl_2$, 1 mM DTT. Reactions were resolved through a 5%/12% SDS-PAGE gel under standard conditions as described in Methods. Proteins were Western blotted onto PVDF membrane as described in Methods and probed with (Phos-tag™ Biotin BTL 111)$_4$-(Streptavidin-conjugated HRP) prepared as described by the manufacturer (WAKO) before initiating chemiluminesence using SuperSignal West Pico Chemiluminescent Substrate (Thermo Scientific) and visualising using ChemiDoc XRS+ (BioRad). Images analysed using Image Lab™ to obtain band intensity. Values transferred to Origin®Pro 9 to determine % of maximal intensity and plotted against respective time point (minutes).*

4.4.2. Investigation of the effect of ligand binding and buffer component on the activity of $VanS_A$ using Universal Kinase Assay Kit® (R & D systems)

ADP is often produced as a by-product of kinase activity as the terminal phosphate group is removed and used to phosphorylate the kinase, therefore detecting ADP production can be used to monitor the progression of kinase activity and is the underlying principles for The Universal Kinase Assay Kit® (R & D). Coupling enzyme CD39L2/ENTPD6, a nucleoside phosphohydrolase which preferentially uses ADP as a substrate but is capable of hydrolysing both di- and tri-phosphate nucleotides to the reaction, the kinase reaction can be monitored. During the hydrolysis of ADP by CD39L2/ENTPD6, β-PO_4^{2-} is released; β-PO_4^{2-} production is proportional to ADP production and effectively kinase activity and is detected using Malachite Green. As ATP can be a substrate for CD39L2/ENTPD6 effective coupling is necessary for reliable measurements (Wu 2011). An advantage of this method is it measures the net autophosphorylation activity of the kinase at specific time points, rather than measuring the proportion of phosphorylated protein present at the time point which is a weak and transient state for the protein.

Before assays were undertaken the conversion factor (CF) for CD39L2/ENTPD6 for use in downstream assays was determined (Fig. 4-7). Furthermore trials were conducted to determine the optimum concentration of $VanS_A$ for use in assays. Results showed use of 0.2 µg of $VanS_A$ was deemed the optimal concentration for the assays due to the relatively small variance and in results demonstrated by the small error and the concentration of PO_4^{2-} produced which was similar to values using higher concentrations of kinase (Fig. 4-8) suggestive of more efficient coupling of $VanS_A$ and CD39L2 when using 0.2 µg of $VanS_A$ per assay. Due to the activity of CD39L2, substrate specificity for $VanS_A$ can be shifted from ADP to ATP if there is an excess, as was demonstrated in the results for lower kinase condition. Therefore it was necessary to use conditions where the minimal concentration of kinase was used to effectively couple to CD39L2 and reduce the background ATP contribution.

Relative to the standard curve, results for the phosphorylation of $VanS_A$ was very low at <0.1 (Fig. 4-8) which makes it very difficult to determine the accuracy of the results considering the principles of the Beer-Lambert law described in Chapter 3 where the optimum $OD_{620\ nm}$ will be ~ 0.8. To account for this, reactions could be scaled-up to increase the concentration of ADP to achieve an $OD_{620\ nm}$ closer to 0.8.

Studies using higher concentrations of $VanS_A$ results in reduced coupling activity (Fig. 4-8), therefore increasing the concentration of free ATP available for the coupled $VanS_A$ -CD39L2 could help to achieve this. However it would be important to factor for the potential of CD39L2 to also utilise ATP when determining the optimum concentration of ATP to use.

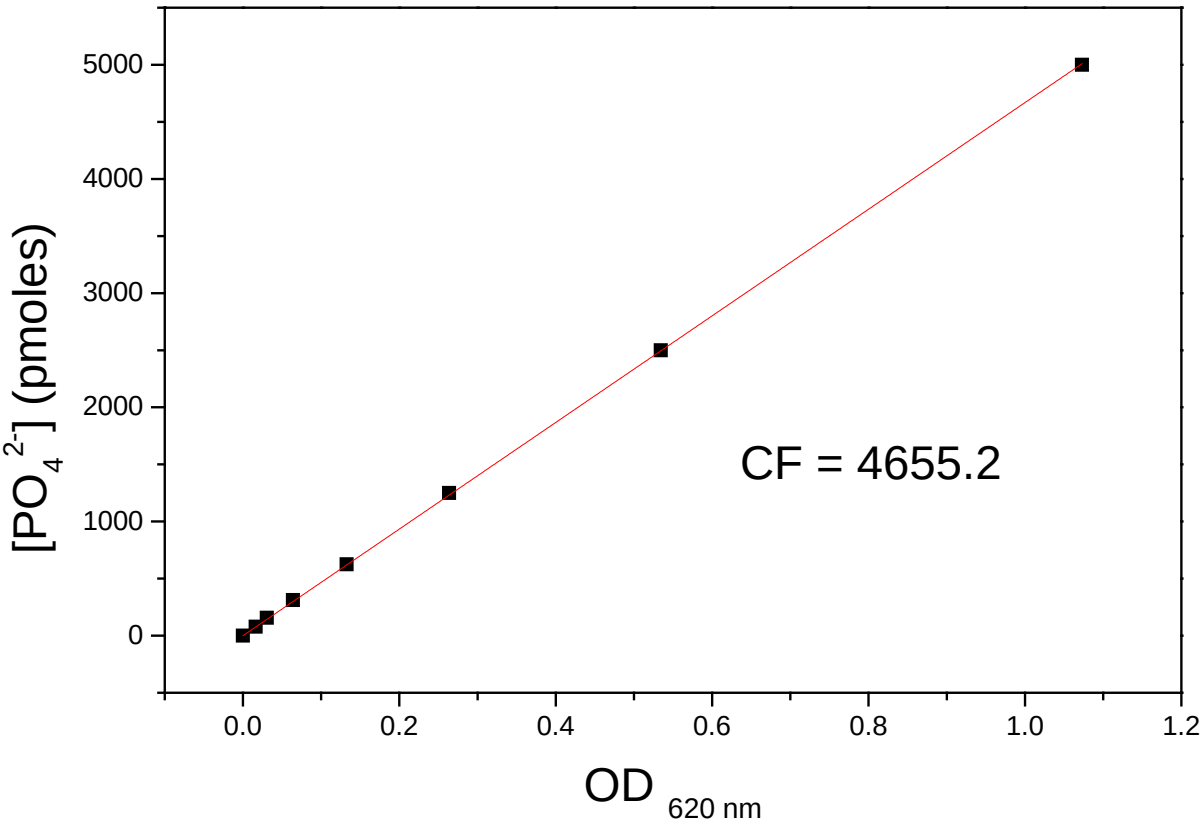

Figure 4-7: A standard curve of $PO4^{2-}$ for the determination of the conversion factor of CD39L2 under new conditions.

As per the instructions for the kit, the OD_{620} nm was used to determine the [$PO4^{2-}$] produced by the phosphatase. *A standard curve of KH_2PO_4 in dH_20 was made by serial 1:1 dilution of phosphate standard from initial 100 µM to 1.5625 µM, and a final negative control containing dH_2O. 50 µl of each dilution was assayed by addition of 30 µl of Malachite Reagent A (ammonium molybdate in 3M sulphuric acid) followed by 100 µl of dH_2O and 30 µl of Malachite Reagent B. Colour was allowed to develop for 20 minutes at 25 °C and the optical density at 620 nm measured. The average of the zero standards was subtracted from average OD measurements and plotted vs. [PO_4^{2-}], fitting with a straight line. The slope of the fitted line is the experimentally determined phosphate conversion factor.*

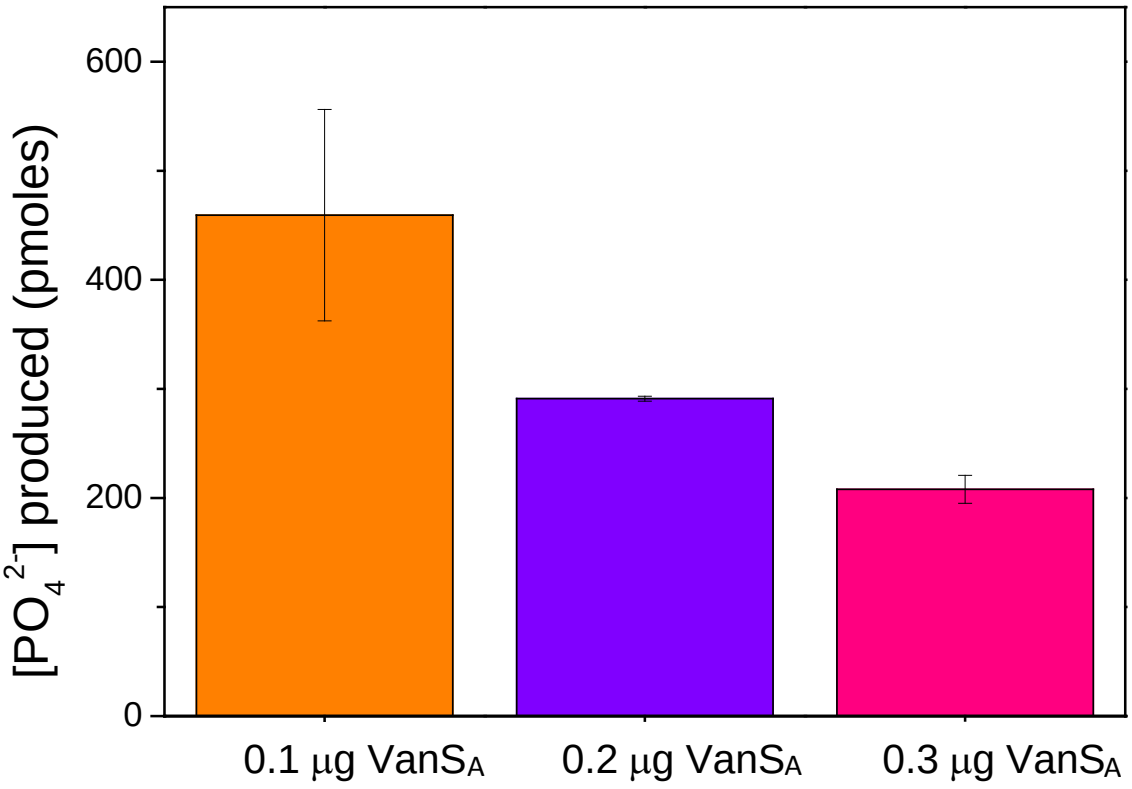

Figure 4-8: Optimisation of the coupling of CD39L2 to $VanS_A$ under new assay conditions. *CD39L2 (0.1 µg) was coupled to different concentrations of $VanS_A$ to determine the optimum conditions for the assays. $VanS_A$ (0.1, 0.2, 0.3 µg) was incubated with 0.1 µg CD39L2 at 25 °C prior the initiation of autophosphorylation assays by the addition of ATP (200 µM) in 10 mM HEPES pH 8.0, 150 mM NaCl, 10 mM $MgCl_2$, 10 mM $CaCl_2$. Autophosphorylation reactions were allowed to progress for 10 minutes before stopping by addition of Malachite reagent A (ammonium molybdate in 3M sulphuric acid). Activity of CD39L2 was visualised as described in the Kinase assay kit and in Methods by measuring the optical density at 620 nm. Negative controls subtracted during analysis and conversion to [PO_4^{2-}] produced using a previously determined conversion factor. Standard deviation displayed (n=3). Assays conducted in duplicate sets of triplicates.*

Initial tests for the effect of the presence of detergent additives on the activity of $VanS_A$ were conducted. Results revealed the presence of higher concentrations of DDM and glycerol both alone and in combination had a significant negative effect on the activity of $VanS_A$. Conversely, although the individual presence of lower concentrations of DDM and glycerol did not significantly affect the activity of $VanS_A$, when assayed in combination $VanS_A$ activity was significantly increased (Fig. 4-9). These results highlight the importance of the considering the experimental conditions when conducting *in vitro* assays which can affect the assayed activity of the system of interest (Figs. 4-9 and 4-10).

Ligand screens were conducted next, aiming to determine the effects of binding of potential ligands on the activity of $VanS_A$. In the presence of glycopeptide antibiotics vancomycin and teicoplanin significant positive effects were observed on the activity of $VanS_A$, compared to peptidoglycan components which produced significant reductions in activity (Fig. 4-10).

Kinetics assays for $VanS_A$ were performed in 10 mM HEPES pH 8.0, 10 % glycerol, 0.025 % DDM (buffer conditions matching the biophysical binding assays discussed in Chapter 3) in the absence and presence of GPAs (Fig. 4-12). The specific conditions (buffer components and ligands) tested were chosen based on initial positive activity screens (Fig. 4-10) and binding studies (Chapter 3). Overall, $VanS_A$ activity in the presence of antibiotics was significantly higher for $VanS_A$ alone (Fig. 4-12), supporting initial screens (Fig. 4-10).

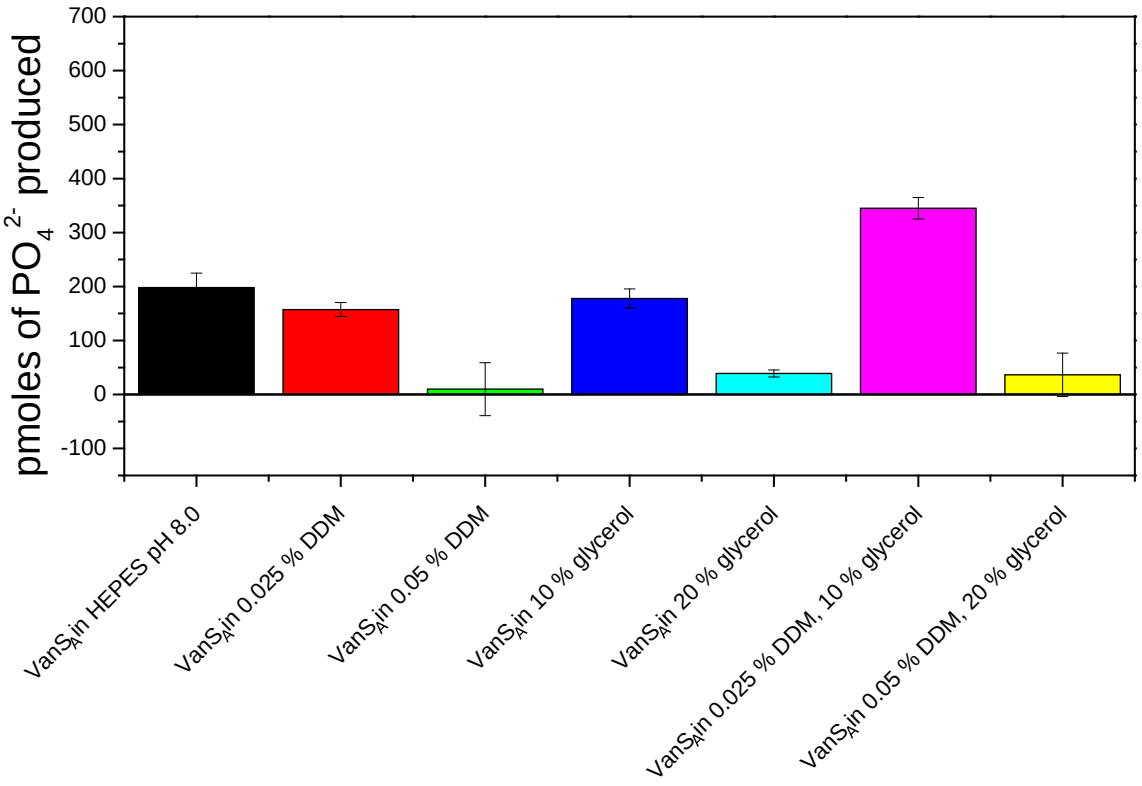

Figure 4-9: pmoles of $PO4^{2-}$ produced by $VanS_A$ in the presence of different buffer additives. *$VanS_A$ (0.2 µg in 10 mM HEPES pH 8.0) was incubated with ligand additives for 20 minutes prior to the initiation of phosphorylation activity by the addition of ATP (200 µM). Reactions were allowed to progress for 40 minutes before stopping by addition of Malachite reagent A (ammonium molybdate in 3M sulphuric acid). Activity of CD39L2 was visualised as described in the Kinase assay kit and in Methods by measuring the optical density at 620 nm. Standard deviation displayed (n=3). Control measurements were performed for each buffer used in the absence protein but presence of ligands to determine their effect on the assay readings. The protein-containing conditions had non-protein containing conditions at the same time-point subtracted.*

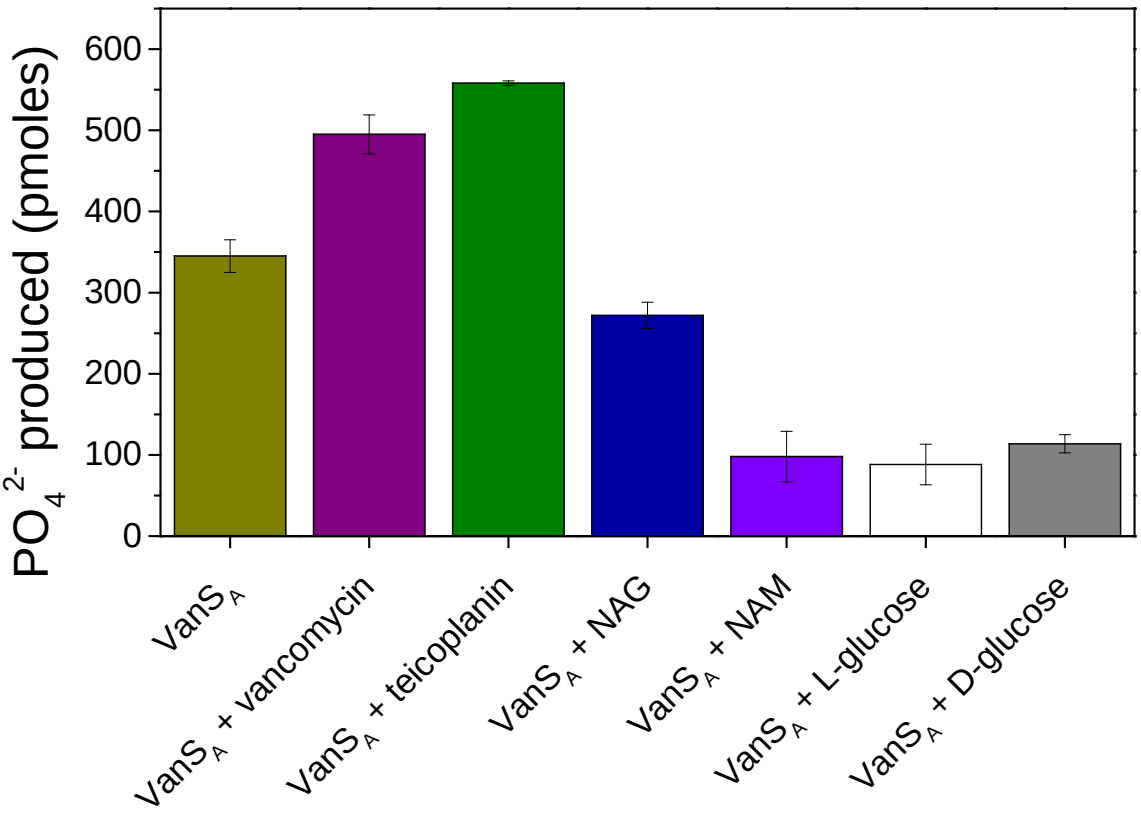

Figure 4-10: Comparison of the change in activity of VanS$_A$ in the presence of screened ligands in two different buffer conditions.

VanS$_A$ (0.2 µg) was coupled to 0.1 µg of CD39L2 prepared in the appropriate buffer condition (10 mM HEPES pH 8.0, 10% glycerol, 0.025% DDM) prior to incubation with 5-fold ligands where appropriate for 20 minutes before initiation of autophosphorylation by the addition of ATP. Autophosphorylation was allowed to proceed for 40 minutes after which the reaction was stopped as described in Methods. Colour was allowed to develop for 20 minutes at 25 °C and the optical density at 620 nm measured. [PO_4^{2-}] was determined as described in the Kinase assay kit and in Methods. Briefly, negative controls (CDC39L2, ATP, no kinase, ligands where appropriate) was subtracted from each reaction to account for background caused by the presence of ATP. [PO_4^{2-}] was calculated using a previously determined conversion factor for the assay conditions. Standard deviations calculated for each condition (n=3) and plotted as error bars.

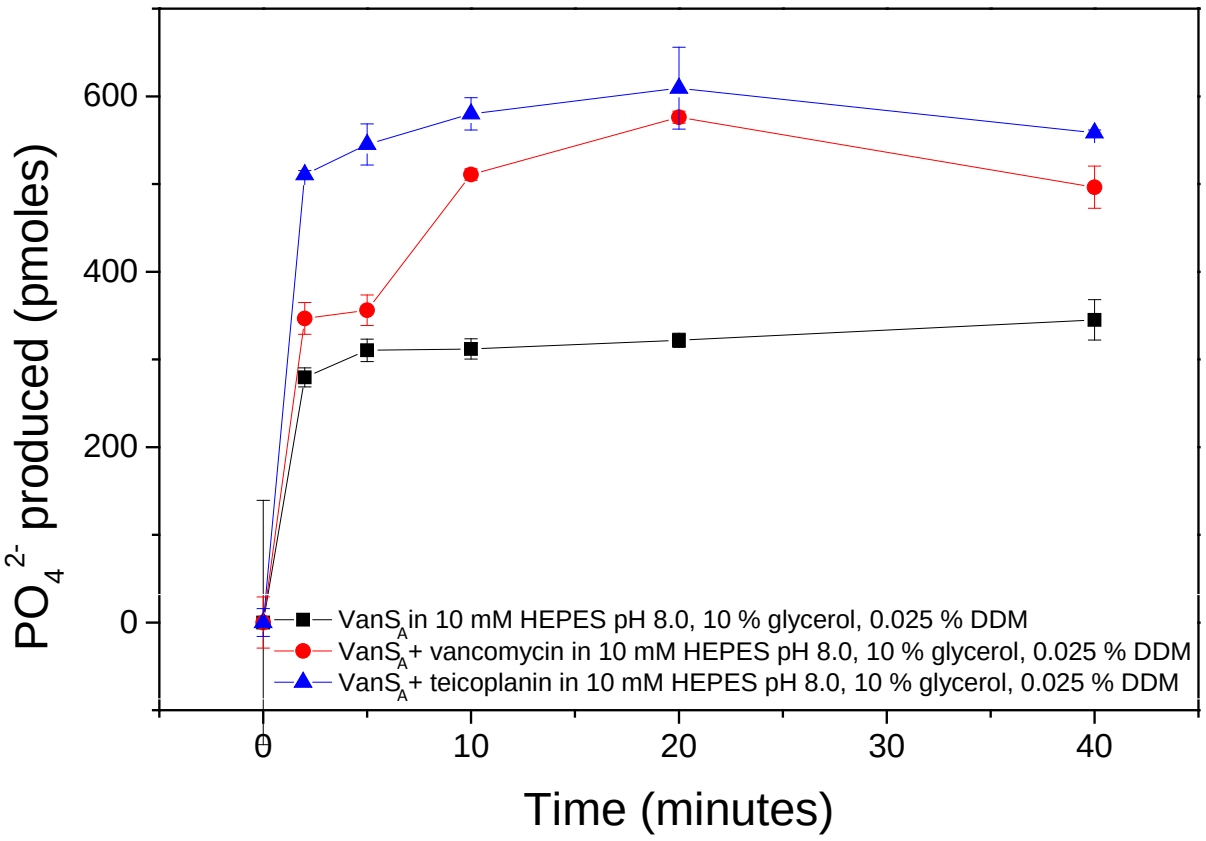

Figure 4-11: Standard curve for the autophosphorylation kinetics of VanS$_A$ in the absence and presence of glycopeptide antibiotics in 10 mM HEPES pH 8.0 assay buffer containing glycerol and DDM detergent additives. *VanS$_A$ (0.2 µg) was coupled to 0.1 µg of CD39L2, incubating with the ligand (1 µg) at 25 °C for 20 minutes prior to the initiation of autophosphorylation by the addition of ATP (200 µM) at the appropriate time point (t=20 for 40 minute condition, t=40 for 20 minute condition, etc. Autophosphorylation was allowed to progress at 25 °C until t= 60 when all reactions were stopped as described in Methods. The colour was allowed to develop for 20 minutes at 25 °C before reading OD at 620 nm. Appropriate negative controls were subtracted from each time-course time-point and the [PO_4^{2-}] for each calculated using a previously determined conversion factor. The amount of PO_4^{2-} produced was plotted for each time point and fitted with a Michaelis-Menten plot (standard deviations shown (n=3)).*

Overall the assay was a useful preliminary study for kinase activity, however a large proportion of kit materials are used for optimisation and control measurements which can be costly and therefore not a viable long-term option as this may out-weigh the routine potential of the kit whose accessibility stems from its ease-of-use and lack of need for specialised equipment, just a plate reader.

4.4.3. Investigation of the effect of ligand binding on the activity of $VanS_A$ using ATP-γ-^{33}P

The use of radiolabelled ATP is routinely used for the direct investigation of the phosphorylation activity of proteins including the investigation of two-component systems due to the high sensitivity of the method which is useful for investigating proteins with relatively short-lived and unstable phosphorylated forms. Previous work utilising this method has shown that the presence of a ligand for the membrane-sensor of a two-component system can result in changes to the phosphorylation activity of the protein (Potter *et al.,* 2006), hence we sought to utilise this quality as a tool to biochemically screen for ligand binding.

The identity of the ligand for $VanS_A$ has been debated, as such we took the approach of screening a range of ligands which have been proposed to serve as activating ligand for $VanS_A$ and have been tested for the structural effects of ligand binding on $VanS_A$ (see Chapter 3), including cell-wall precursors, the antibiotic itself, and antibiotic-cell wall component complex as a thorough screen for the activating species. Initial *in vitro* assays testing the activity of $VanS_A$ in the presence of antibiotic ligands showed the presence of ligands did not significantly affect the activity of the protein, though the presence of both antibiotics resulted in an overall increase in the proportion of phosphorylated protein (Fig. 4-12) which may indicate a potential mechanism for the onset of vancomycin resistance in the presence of GPAs whereby increase phosphorylation activation results in the increased

activation of $VanS_A$ and resulting phosphotransfer to $VanR_A$ for increased expression of vancomycin resistance genes.

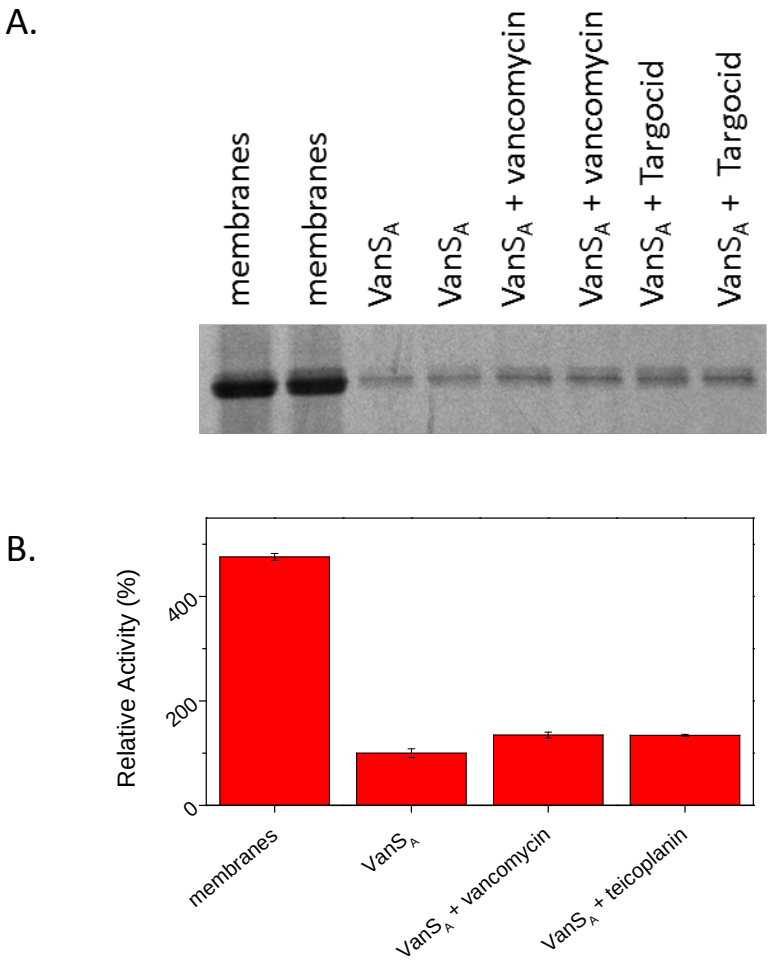

Figure 4-12: Autophosphorylation of $VanS_A$ in mixed E. coli membranes and purified $VanS_A$. *3 µg of membranes containing $VanS_A$ or 60 pmoles of purified $VanS_A$ (in final buffer 10 mM HEPES pH 8.0, 10% glycerol, 0.05% DDM) were incubated at 20 °C for 30 minutes in the absence or presence of antibiotics prepared in 10 mM Tris HCl pH 8.0 (buffer only for controls) before initiation of autophosphorylation by the addition of 50 µM ATP-γ-^{33}P (175.2 kBq) as described in Methods. Reactions were allowed to progress for 40 minutes stopping. Reactions were resolved through a 5%/12% SDS-acrylamide gel under standard conditions as described in Methods before gel drying at 80 °C. The dried gel was exposed to film for 8 days. (A) Developed film imaged using ChemiDoc XRS+ (BioRad), and densitometry performed using ImageJ (Schneider et al., 2012; Rasband 1997). (B) Relative Activity (%) calculated relative to purified $VanS_A$.*

4.4.4. Effect of DDM concentration on the activity of $VanS_A$

As described in the Chapter 2, the presence of DDM and other detergents not explored in this Thesis but described elsewhere (Ma et al. 2008) can prove to be problematic when designing downstream experiments. This is demonstrated throughout this Chapter using different assay methods which showed that assays of $VanS_A$ where higher concentrations of DDM were present resulted in reduced activity of $VanS_A$, and is in agreement with previous studies of other membrane sensor kinases (Ma *et al.,* 2008; Potter *et al.,* 2002). Therefore to test for the effect of detergent on activity assays for $VanS_A$, different concentrations of detergent were assayed. The results demonstrated using ATP-γ-^{33}P (Fig. 4-13) showed the increased activity gained for $VanS_A$ when prepared with lower concentrations of detergent, to a level closer to that of $VanS_A$ in mixed membranes, suggesting too high a concentration of detergent can have adverse effects on the activity of the protein. Although the results were on different gels presented in the figure, these trends were seen on multiple occasions and were supported from results using the Universal Activity Assay kit (R & D systems) (Fig. 4-8) which showed that the presence of higher concentrations of buffer additives glycerol and DDM had a significant negative effect on the activity of $VanS_A$ compared to lower concentrations potentially due to the inhibitory nature of the additives whereby the presence of too high concentrations of detergent and glycerol can prevent the phosphorylation of the protein which has previously been reported for other histidine kinases (Ma et al. 2008).

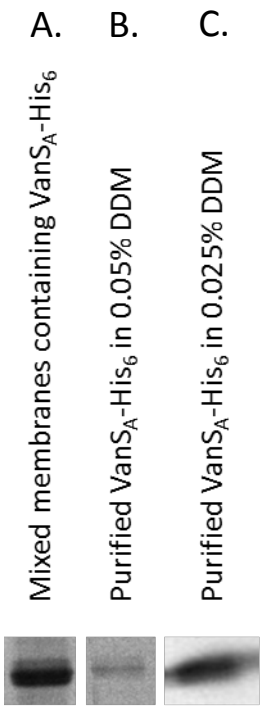

Figure 4-13: Autoradiography of autophosphorylation activity assays of $VanS_A$ purified in different concentrations of DDM detergent, compared to the activity of $VanS_A$ in mixed membranes prior to purification. *$VanS_A$ in membranes (3 µg total protein) and 60 pmoles of purified protein was assayed for autophosphorylation activity by addition of 50 µM ATP-γ-^{33}P and allowing the reaction to proceed for 30 minutes before stopping by the addition of SDS-loading buffer. Reactions were resolved through a 5%/12% SDS-acrylamide gel under standard conditions as described in Methods before gel drying at 80 °C. The dried gel was exposed to film for A) 7-, B) 7-, and C) 8- days. Film imaged using ChemiDoc XRS+ (BioRad). Film imaged using ChemiDoc XRS+ (BioRad).*

4.5. Discussion

4.5.1. Comparison of the assay methods

Results from this Chapter highlight the importance of the compatibility of the system under investigation with the method used to assay. As expected, each method had its own advantages and

disadvantages. In the case of the methods described above, all but R & D systems universal activity assay kit (UAK) monitors the proportion of phosphorylated protein at a snapshot of time. A problem with "snapshot" approaches when investigating less-stable phosphorylated amino acids is (i) kinase and phosphatase activities and (ii) the instability of the phosphor bond can result in reduced phosphorylation detection at specific time points. Comparisons of the results obtained from the methods used throughout the Chapter will be discussed.

Kinase assays conducted using ATP-γ-^{33}P are routine high-resolution and high-sensitivity procedures in many labs, however health and safety regulations regarding the use of radioactive materials can lead to difficulties in the acquisition and disposal of materials in addition to allocation of dedicated lab space. Together, these factors can impede implementing such methods routinely therefore a range of non-radioactive alternative methods have been tested throughout this Chapter to evaluate their assessment of Histidine kinase activity.

Both Phos-tag™ methods tested (acrylamide (PTA) and biotin (PTB-111)) were unreliable, as results were low-resolution (Fig. 4-4) and often irreproducible (Fig. 4-6), requiring multiple optimisations for the system of interest which can be costly in time and resources. Even when higher concentrations of acrylamide and longer gel-running times were used, poor resolution was obtained for the samples (Fig. 4-3). Due to this, the Phos-tag™ methods were deemed as unsuitable for analysis of the activities of $VanS_A$.

UAK differs from other methods tested during this Chapter as is it detects the net ADP produced from the kinase activity of the protein of interest (Wu 2011). Furthermore, assays conducted using UAK were reproducible and the most convenient to perform as few steps and no specialised equipment were required, only a plate reader capable of measuring absorbance at 620 nm which are commonplace in most laboratories. Concentrations of kinase used in the assays were 10-fold lower than those used in other methods described in the Chapter. This, in addition to 4-fold higher concentrations of ATP, allows for the prevention of immediate substrate depletion as the enzyme

utilises ATP and assumes the saturation of all kinases in the reaction for a more efficient analysis of the kinase activity of $VanS_A$.

4.5.2. Discussion of activity changes as a result of assay conditions and ligand presence

4.5.2.1. Buffer conditions

All of the methods used revealed similar characteristic behaviours for the protein, highlighting the effectiveness of non-radioactive alternatives for the assessment of the kinase activity of a protein. Between the methods tested, the kinetics of $VanS_A$ was consistently characterised to have reached maximal autophosphorylation after 10-15 minutes (Figs. 4-4, 4-6 and 4-12) suggesting the potential to reliably interchange methods for the detailed characterisation of a system of interest.

Screens investigating the activity of $VanS_A$ in different buffer systems indicated that the presence of some buffer additives affected the activity of $VanS_A$. The concentration of DDM was shown to affect the activity of $VanS_A$ in an inversely proportional manner, where increasing DDM and glycerol concentrations reduced the kinase activity (Fig. 4-9). Conversely, low concentrations of both DDM and glycerol resulted in increased activity of $VanS_A$ relative to protein in HEPES only (Fig. 4-9) suggesting a preservative or activating action of the buffer components with respect to the activity of $VanS_A$, and has highlighted factors for consideration when planning kinase activity assays. It has previously been reported that higher detergent concentrations can inhibit the activity of sensor kinases of two-component systems (Ma *et al.,* 2008), similar to results reported using different methods in this Chapter (Figs. 4-9 and 4-13).

4.5.2.2. Ligand screens

There were difficulties getting the methods working, as such results investigating the ligand binding qualities of $VanS_A$ were investigated. Form the studies conducted, it was seen that the presence of some ligands affected the activity of $VanS_A$.

Ligand binding studies showed the presence of GPAs vancomycin and teicoplanin have positive effects on the kinase activity of $VanS_A$. Peptidoglycan components were shown to have significant

negative effects on the activity of $VanS_A$ in the presence of DDM and glycerol, yet in the absence of buffer additives glycerol and DDM no significant change was observed, and this behaviour was also observed in the presence of glucose isomers (Fig. 4-10). Together, these results suggest a mechanism whereby vancomycin up-regulates and peptidoglycan down-regulates the kinase activity of $VanS_A$ to enable an induction mechanism where the downstream activity of $VanS_A$ is only required in the incidences where vancomycin is present.

CHAPTER 5:
DISCUSSION

5. Discussion

This Thesis aimed at characterising the activities of $VanS_A$, the sensory histidine kinase of the Two-Component Signal Transduction System (TCS) regulating vancomycin resistance in the enterococci. Applying recombinant membrane protein expression and purification techniques to produce protein, further characterisation of the pure and active protein can be carried out using a range of biophysical methods and *in vitro* phosphorylation activity assays. By doing so, the aim of the Thesis was to characterise the occurrences leading to the onset of vancomycin resistance in the enterococci.

5.1. Proposed mechanism of action for the onset of type A vancomycin resistance in the enterococci

5.1.1. Ligand binding mechanism

This Thesis proposes a mechanism for the onset of type-A vancomycin resistance, whereby the presence of the antibiotic initiated the increase in the phosphorylation activity of $VanS_A$.

This is the first description of the identification of an activating species for $VanS_A$ regulating type A vancomycin resistance in the enterococci. Early studies showed conflicting views on the induction of the *vanA* operon by vancomycin in addition to other glycopeptide (GPA) and non-glycopeptide antibiotics (Allen and Hobbs 1995; Handwerger and Kolokathis 1990; Baptista *et al.,* 1996; Ulijasz *et al.,* 1996). The use of *in vivo* approaches during these early studies to establish an activating mechanism for $VanS_A$ (direct, by the antibiotic itself; or indirect, accumulating peptidoglycan precursors as a result of vancomycin activity; or the vancomycin:peptidoglycan complex) left the identity of the activating ligand for $VanS_A$ of type A vancomycin resistance in the enterococci unresolved. Studies described throughout this Thesis use an *in vitro* approach, utilising purified

$VanS_A$ for the investigation of ligand-induced effects. Such approaches allow for a controlled screening of components interactions to enable a definitive determination of interacting species.

Ligand binding screens using purified $VanS_A$ showed only in the presence of antibiotic ligands were positive changes observed in the aromatic region of the near UV for $VanS_A$, observed by a large peak spanning the tyrosine/tryptophan region of $VanS_A$ (Chapter 3, Fig. 3-10). The role of tryptophan in ligand binding was further supported by magnetic circular Dichroism (MSRCD) and fluorescence spectroscopy (Fluorescence) studies (Chapter 3, Figs. 3-17 and 3-15, respectively). The only tryptophan residue in the amino acid sequence of $VanS_A$ is predicted to lie in the extracellular binding region for $VanS_A$. Furthermore, three tyrosines accompany tryptophan in the predicted extracellular region, supporting CD results emphasising the roles of these residues in ligand binding. Our CD data is supported by previous studies which identified a 4-amino-acid motif (DQGW) from the predicted extracellular binding region of VanSsc (equivalent to the type B $VanS_A$ receptor in soil actinomycetes) to which a vancomycin photoaffinity probe bound (Koteva *et al.,* 2010). Although induction differences have been described for the type A and type B receptors (Arthur and Quintiliani 2001), these results nevertheless suggest an important the role for tryptophan in vancomycin binding and highlight a potential future research target.

Determination of binding constants using CD and UV-vis revealed differences in the values obtained for vancomycin and teicoplanin (Chapter 3, Figs. 3-11 and 3-12). For both antibiotics, the findings should be taken preliminary steps as the findings were obtained at the limit of the methods use, and the lack of error bars cast doubt of the absolute differences in the binding of these antibiotics and makes it difficult to confirm the difference in binding constants. In the case of vancomycin, both CD and UV-vis were in agreement for the determination of the K_d, (Fig. 3-11) compared to teicoplanin which had discrepancies between the methods (Fig. 3-12). Teicoplanin is a mixture of 9 isomeric compounds (5 major and 4 minor) (Parenti 1986) therefore different affinity bindings could be a reflection of the binding of specific isoforms. Future work would include the investigation of the

interactions of the separated isoforms of teicoplanin with $VanS_A$, attempting to further specify the interacting species and therefore a potential biological mechanism. A2 isoforms are the most prominent in teicoplanin mixtures (>95%) (Jehl *et al.,* 2013) whereas A3 teicoplanin has been identified as a degradation product. However it is still possible that a higher affinity ligand/activator is yet to be identified as currently, though teicoplanin binding had a significant first affinity constant, vancomycin on the other hand has only a moderate binding affinity possibly reflecting the higher MIC of vancomycin.

The lack of responses by $VanS_A$ in the presence of peptidoglycan components further supports the mechanism, where by under standard living conditions of the cell in the absence of either antibiotic $VanS_A$ expression is not needed to be induced. Under normal conditions the cells normal cell-wall synthesis machinery is working at a normal rate therefore costly expression of vancomycin resistance genes is not needed and is in fact undesirable for the cell. This also suggest that the peptidoglycan:vancomycin complex is not a major target for $VanS_A$, and may be in important indication of the *in vivo* steps leading to the activation of $VanS_A$ especially when considering that some must be present *in vivo* due to the nature of the action of the drug and the suggestion of an underlying preference for vancomycin as a ligand.

5.2. Evaluation of different methods to assay the phosphorylation activity of $VanS_A$

Throughout Chapter 4, different methods were trialled to determine the phosphorylation activity of $VanS_A$ in the absence and presence of potential ligands with the hope of elucidating the activation mechanism for vancomycin resistance.

The first *in vitro* activity assays conducted on a full-length, intact, active $VanS_A$ are described in Chapter 4. Previous work demonstrated autophosphorylation of VanS and phosphotransfer between the cytosolic portion of $VanS_A$ and intact $VanR_A$ (Wright *et al.,* 1993), therefore studies in this Thesis further investigated the interaction by screening the activity of $VanS_A$ in the presence of ligands, and characterised in the presence of GPAs vancomycin and teicoplanin.

It is hypothesised that in type A resistance systems, vancomycin binding by $VanS_A$ initiates a suppression of phosphatase activity resulting in a net increase in VanR phosphorylation (Hong *et al.,* 2008). Only in the presence of GPAs vancomycin and teicoplanin were increased net phosphorylation levels of $VanS_A$ observed (Chapter 4, Fig. 4-10) yet screens using alternative methods to investigate the phosphorylation levels at a specific time point revealed no significant change in the phosphorylation of $VanS_A$. This could be explained in terms of methodological or biological processes where i) the loss of phosphorylated protein during downstream processing of the experiments resulting from the instability of phospho-Histidine or ii) the conflicting phosphatase activity of $VanS_A$ is up-regulated to match the increased kinase activity in the presence of GPAs which would conflict with previous studies (Hong *et al.,* 2008). These initial results suggest that the phosphorylation rates of $VanS_A$ increased in the presence of GPAs relative to in the absence of the antibiotics (Chapter 4, Fig. 4-11). It would suggest that the phosphatase activity of $VanS_A$ is constitutively active and GPA activation does not affect its activity but instead antibiotic binding affects the kinase activity of $VanS_A$ resulting in an increased rate of phosphorylation which acts to "over-ride" the underlying phosphatase activity. Potential future work could include the use of

phosphatase blockers as a measure of the changes to the rate of phosphorylation in the presence of screened compounds (Karaszkiewicz et al. 2001), which will be discussed in Chapter 7.

$VanS_A$ kinase activity was higher in the presence of teicoplanin than vancomycin however the low OD_{620} produced during the assays casts doubt over the results and indicated that the results should be taken with caution. Binding studies showed affinity differences for each of the antibiotics (Chapter 3, Figs. 3-11 and 3-12), with $VanS_A$ binding teicoplanin with higher affinity than vancomycin. There are proposed differences in the efficiency and mechanism of action for each of the GPAs (Beauregard *et al.,* 1995) where overall teicoplanin was indicated as a more effective antibiotic.

The different activity effects of each antibiotic on $VanS_A$ may be reflective of the reported potency differences *in vivo* of vancomycin and teicoplanin (Chang *et al.,* 2011; Pallanza *et al.,* 1983). By reasoning, the quicker, longer-lived activities of teicoplanin relative to vancomycin may require a more rapid response by $VanS_A$ for activation of resistance gene expression as a means of compensating for the effectiveness of teicoplanin at inflicting cell death. This may be a reflection of the differences in the proposed mechanism of action of teicoplanin (Beauregard *et al.,* 1995) and the binding kinetics experimentally derived from titration experiments which showed a secondary binding in the presence of higher concentrations of teicoplanin. There is evidence for the increased effectiveness *in vivo* of teicoplanin compared to vancomycin; (Pallanza et al. 1983; Arriaga et al. 1990) showed affinity constant was 4 to 5 times higher for teicoplanin than vancomycin – supportive of the binding constants revealed during CD studies.

Literature suggests that the binding of a ligand initiates dimerisation of the sensor kinase which enables trans-phosphorylation of the dimer for signal relay by the proteins of the two-component system (Wang 2012), therefore DLS experiments were conducted to assess the effects of ligand binding on the dimerisation of $VanS_A$. Findings showed the presence of screened ligands had no effect on the homogeneity of $VanS_A$ (Chapter 3, Fig. 3-25) but instead remained as a monomer as

previously determined using SEC-MALS (Chapter 2, Fig. 2-13), though the experiments were conducted in the absence of ATP which may be necessary in addition to ligands to initiate dimerisation and is therefore a point for consideration with regards to the results obtained in Chapter 5 and the overall mechanism of phosphorylation activity of $VanS_A$ in response to ligand binding.

It worth suggesting other, as yet unidentified ligand(s) may be important for the initiation of $VanS_A$, therefore screens of other potential ligands, including the effect of the membrane environment is required.

The methods used were varied, each providing different challenges which require further optimisation. Overall, no method was determined as the overall best method yet similarities in the results were obtained, suggesting a common mechanism in the activity of $VanS_A$ in the absence and presence of screened compounds.

CHAPTER 6:
CONCLUSIONS

6. Conclusions

Antimicrobial resistance is a global concern and the sustained effectiveness of last-line antibiotic vancomycin is at risk against type A resistant enterococci bacteria, the most prominent agent of hospital acquired infections in UK. This Thesis aimed to characterise the binding activities of $VanS_A$, the membrane sensor kinase of the two-component signal transduction system (TCS) regulating vancomycin resistance in the enterococci.

The results so far obtained describe the successful expression and purification for $VanS_A$, in addition to the determination of optimised final buffer conditions for the storage of active and stable protein which was compatible for use in downstream activity and ligand binding studies.

In vitro binding studies for $VanS_A$ using xenon-source and synchrotron radiation circular dichroism showed little protein secondary structure conformational changes in $VanS_A$ when all ligands (glycopeptide antibiotics (GPAs) vancomycin and teicoplanin, peptidoglycan components, and sugars) were screened in the far-UV region. Only in the presence of GPAs vancomycin and teicoplanin were spectral differences observed in $VanS_A$ in the near-UV CD region which suggested a change in the local tertiary structure indicating the roles of aromatic amino acids tryptophan and tyrosine in binding. These roles were later confirmed using magnetic synchrotron radiation circular dichroism and fluorescence spectroscopy. $VanS_A$ displayed different affinities for GPAs vancomycin and teicoplanin 70 µM and 30 and 170 µM, respectively, and binding of ligands did not affect the stoichiometry of $VanS_A$ which maintained its monomeric state in the presence of ligands, Furthermore, *in vitro* kinase activity assays revealed the presence of GPAs increased the rate of phosphorylation of $VanS_A$.

Overall, results described throughout the Thesis identified GPAs vancomycin and teicoplanin as ligands for $VanS_A$ which appear to bind via aromatic amino acids tryptophan and tyrosine with different affinities. Upon interaction with $VanS_A$, an overall increase in phosphorylation of $VanS_A$ is initiated, presumably for activation of *vanA* expression. Of all of the screened ligands described

(GPAs vancomycin and teicoplanin, peptidoglycan components, and sugars) responses were only observed in the presence of GPAs highlighting their roles in the induction of type A vancomycin resistance in the enterococci.

Attempts to evaluate different methods for the assessment of phosphorylation of VanS were carried out, and identified the advantages and disadvantages of each method, with each method requiring optimisation. Of the 4 methods tested R &D gave the most consistent results and did not require specialist equipment or health and safety measures like other methods tested including the use of ATP-γ-^{33}P which requires specialised equipment and rigorous health and safety procedures. Phos-tag™ (PT) methods, both acrylamide and Biotin forms of PT, were tested in Chapter 4 and neither were reliable at giving reproducible results. Overall, flaws were found with each method tested, but R & D was found to be the most dependable and user-accessible kit.

The knowledge acquired thus far and illustrated throughout this Thesis presents a foundation for further understanding the activation mechanism for type A vancomycin resistance and presents a range of methods which can be used to investigate the mechanism. Future work exploring additional aspects of the mechanism of resistance will be described for consideration in the following Chapter.

CHAPTER 7:
FURTHER WORK

7. Further work

7.1. Crystallisation trials for $VanS_A$

Sufficient yields of protein are obtainable for $VanS_A$ using the optimised conditions described in Chapter 2 for use in crystallisation trials. Regularly, yields of 12 mg/ml of $VanS_A$ are required for crystallisation by vapour diffusion (VD) and higher concentrations (~15 mg/ml) are required for lipid cubic phase (LCP). As yet a crystal structure for $VanS_A$ has not been achieved, therefore utilising the highly-pure large-yields of protein, steps should be taken to crystallise $VanS_A$.

Vancomycin and teicoplanin have been identified as the only binding ligands to $VanS_A$ from the selected compounds screened (Chapter 3). Crystallisation trials in the presence of ligands may lead to co-crystallisation of $VanS_A$ with a ligand (Hassell *et al.,* 2007) and such crystals can reveal mechanistic details of the interactions resulting from the protein-ligand interaction.

The suitability of HT-SRCD for use with soluble proteins has been demonstrated (Siligardi and Hussain 2015), therefore this work can expand the application of HT-SRCD for use with membrane proteins in addition to investigating its suitability as a complementary method for screening the effect of crystallisation buffers on the conformation of proteins. Using this approach, all conditions in a standard 96 buffer kit can be screened on a single protein batch in a single experiment.

Often during crystallisation studies, activity of the stock protein is monitored before commencing with crystallisation trials to validate any obtained structures as biologically relevant (Moraes *et al.,* 2014). However, this is a controversial argument as results in Chapter 3 demonstrate how buffer conditions can affect the behaviour of a protein; therefore it is not unreasonable to argue against the assumed extrapolation of conserved activity in each of the different crystallisation conditions. To address this, activity assays can be conducted in the equivalent buffers used during crystallisation trials, possible in the case of $VanS_A$ following optimisation of the universal kinase assay kit (R & D systems) described in Chapter 4. Similar approaches have confirmed the activity and conformation

of proteins *in meso* (lipid cubic phase (Fig. 7-1) relative to the stock protein to verify the effect of the lipid environment on the proteins characteristics reviewed in (Caffrey 2015), yet no comparisons have been made in the presence of the crystallisation buffers. Conducting these experiments will validate crystallisation results as biologically relevant crystal structures of active proteins and provide a richer understanding of the relationship between conditions (e.g. pH or salts, etc.) and the structure/function of a protein.

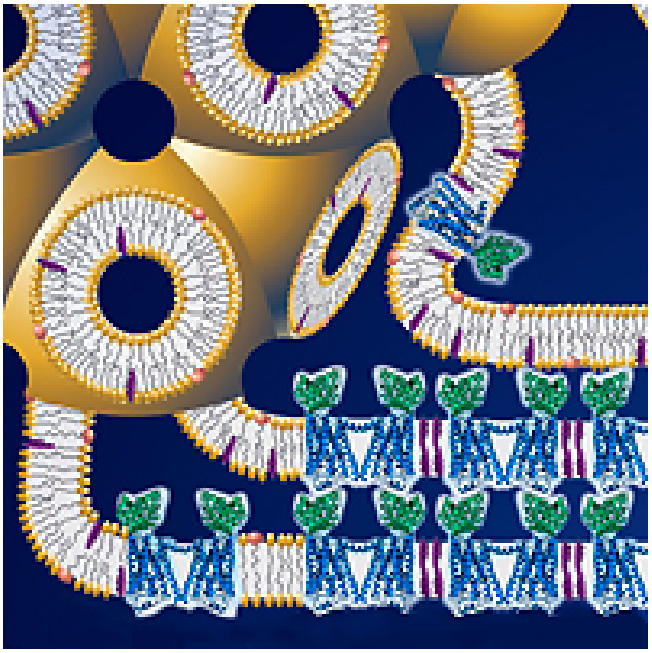

Figure 7-1: Cartoon image of Lipid Cubic Phase.

Lipids assemble into continuous bilayer sheets which form networks of non-intersecting channels. Proteins embed within the lipid bilayers. During in meso crystal formation, proteins pack into highly-ordered arrangements, making both hydrophilic and hydrophobic contacts and reducing solvent contacts. *http://cherezov.usc.edu/resources.htm*

7.2. Phosphotransfer and phosphatase experiments with $VanR_A$

In Chapter 4, the phosphorylation activity of $VanS_A$ was shown to be upregulated in the presence of glycopeptide antibiotics (GPAs) vancomycin and teicoplanin observed by increases in the kinetics for phosphorylation (Chapter 4). Normally phosphorylation of $VanS_A$ is regulated by (i) phosphotransfer to $VanR_A$ for activation of downstream activities, or (ii) phosphatase activity of $VanS_A$ which is able to self-regulate its phosphorylation levels.

Histidine kinases like $VanS_A$ have both kinase and phosphatase activity which are interchangeable depending on the environment and the activity requirements of the protein (Mitrophanov & Groisman 2008; Klumpp & Krieglstein 2002) therefore phosphatase activity may influence the results of phosphorylation activity assays and quantification of the net phosphorylation of a protein under screening conditions. To counteract this problem, as briefly suggested, kinase activity assays could be conducted in the presence of phosphatase inhibitors to monitor the rate of phosphorylation specifically, without the influence of phosphatase activity (Karaszkiewicz et al. 2001).

Phosphotransfer has been demonstrated between the cytosolic portion of $VanS_A$ and full, intact $VanR_A$ (Wright *et al.,* 1993) however the potential effects of the presence of GPAs on this activity have not been investigated. Binding of an activating ligand would be expected to increase the phosphorylation of $VanS_A$ either by increasing the kinase activity or decreasing the phosphatase activity of $VanS_A$ resulting in a net increase in phosphorylation of $VanS_A$. The $VanR_AS_A$ operon is thought to be negatively regulated as only in the presence of $VanR_A$~P is downstream expression activated, therefore it can be assumed that increased phosphorylation of $VanS_A$ (in the presence of an activating ligand would result in increased $VanR_A$~P production for an up regulation of downstream vancomycin resistance gene expression.

In the presence of vancomycin $VanS_A$ phosphatase activity is predicted to be down-regulated, resulting in a net increase on $VanS_A$~P (Hong *et al.,* 2008). Phosphatase activity assays should be

conducted in the absence and presence of vancomycin and teicoplanin in order to define the activation mechanism for vancomycin resistance expression.

7.3. Further ligand screens for $VanS_A$

Binding of both GPAs vancomycin and teicoplanin by $VanS_A$ have been characterised during Chapter 3 showing differences in the affinity for each antibiotic. Furthermore, differences in the effects on the phosphorylation activity of $VanS_A$ were described in Chapter 4 which together suggests different mechanisms for induction of *vanA* by each antibiotic. To further investigate these proposed differences and determine if binding by each antibiotic occurs at the same or different sites competition studies can be conducted using CD (S. Patching *et al.,* 2012) by screening $VanS_A$ in the presence of both vancomycin and teicoplanin to test for differences in binding profiles which have been characterised in Chapter 3.

Telavancin, a new lipoglycopeptide, (semi-synthetic second generation GPA derivative of vancomycin containing a lipid tail (Binda *et al.,* 2014)) has an improved potency and half-life relative to vancomycin (Steed *et al*. 2012) therefore studies applying similar approaches described throughout this Thesis should be conducted to determine the binding characteristics of $VanS_A$ for Telavancin. Results from these studies can enrich the understanding for the recognition moieties in the GPAs used by $VanS_A$. Furthermore, as GPAs differ by the R-group, in the case of vancomycin which is identified by the vancosamine sugar, and teicoplanin a β-D-glucosamine with lipid chains of variable length attached. As these groups are the most variable factors, investigation of their role in ligand recognition by $VanS_A$ can be addressed by screening the sugar and lipid components for interaction with $VanS_A$ using approaches described in Chapter 3.

Non-glycopeptide antibiotics including polymyxin B, robenidine (Lai and Kirsch 1996), moenomycin (Handwerger and Kolokathis 1990), Bacitracin (Allen and Hobbs 1995; Lai and Kirsch 1996) have been shown *in vivo* to induce *vanA* resistance *in vivo* suggesting the antibiotics are not the activating ligands for $VanS_A$ due to the differences in the mode of action for the different classes of antibiotic; conflicting with the findings presented in Chapter 3. Study of the *in vitro* interactions of these antibiotics with $VanS_A$ would directly confirm their activating potential for $VanS_A$.

7.4. Comparison of ligand binding of VanS from type B vancomycin resistant enterococci

Differences in resistance phenotypes are observed for enterococci displaying type A compared to type B resistance; the most recognisable being the differences in susceptibility and resistance towards GPAs vancomycin and teicoplanin displayed by both types of resistant organism. Type A are resistant towards both vancomycin and teicoplanin, and type B resistant to vancomycin but susceptible to teicoplanin and studies investigating the activation of downstream gene expression *in vivo* have confirmed induction is type-specific, i.e. type A is induced by vancomycin and teicoplanin and type B are induced only by vancomycin. Studies have shown binding of a vancomycin-type probe to $VanS_B$ to involve a sequence contain tryptophan (Koteva *et al.,* 2010), and although there is low sequence similarity between type B and type A VanS receptors (16 % similarity, (Hong *et al.,* 2008)), the identification in type B systems and the identification presented in this Thesis (Chapter 3) suggests a key role in for tryptophan in recognition of vancomycin by the VanS receptor. Studies investigating ligand binding by $VanS_B$ may enable the identification of the component(s) (conformation, aromatic residue, etc.) which distinguishes between the types of resistance and have important roles in specifying the differences in resistance and susceptibility to vancomycin and teicoplanin exhibited by each type.

REFERENCES

Agostini, C., Canonica, G. W., and Maggi, E. (2015). European medicines agency guideline for biological medicinal products: a further step for a safe use of biosimilars. Clinical and Molecular Allergy, 13(1), 3.

Allen, N.E. and Hobbs, J.N. (1995). Induction of Vancomycin Resistance in *Enterococcus faecium* by Non-Glycopeptide Antibiotics. FEMS microbiology letters, 132(1–2), pp.107–114.

Allen, N.E., Hobbs, J.N. and Nicas, T.I. (1996). Inhibition of peptidoglycan biosynthesis in vancomycin-susceptible and - resistant bacteria by a semisynthetic glycopeptide antibiotic. Antimicrobial Agents and Chemotherapy, 40(10), 2356–2362.

Arriaga, P., Laynez, J., Menendez, M., Canada, J. and Garcia-Blanco, F. (1990). Thermodynamic analysis of the interaction of the antibiotic teicoplanin and its aglycone with cell-wall peptides. Biochem. J, 265, 69–77.

Arthur, M., Molinas, C., and Courvalin, P. (1992). The VanS-VanR two-component regulatory system controls synthesis of depsipeptide peptidoglycan precursors in *Enterococcus faecium* BM4147. Journal of Bacteriology, 174(8), 2582–2591.

Arthur, M., Reynolds, P. E., Depardieu, F., Evers, S., DutkaMalen, S., Quintiliani, R., and Courvalin, P. (1996). Mechanisms of glycopeptide resistance in enterococci. Journal of Infection, 32(1), 11–16.

Arthur, M., Depardieu, F., Gerbaud, G., Galimand, M., Leclercq, R., and Courvalin, P. (1997). The VanS sensor negatively controls VanR-mediated transcriptional activation of glycopeptide resistance genes of Tn1546 and related elements in the absence of induction. Journal of Bacteriology, 179(1), 97–106.

Arthur, M. and Quintiliani, R. (2001). Regulation of VanA- and VanB-type glycopeptide resistance in enterococci. Antimicrobial Agents and Chemotherapy, 45(2), 375–381.

Attwood, P. V., Piggott, M. J., Zu, X. L., and Besant, P. G. (2007). Focus on phosphohistidine. Amino Acids, 32(1), 145–156.

Baneyx, F. (1999). Recombinant protein expression in *Escherichia coli*. Current Opinion in Biotechnology, 10(5), 411-421.

Bannwarth, M., and Schulz, G. E. (2003). The expression of outer membrane proteins for crystallization. Biochimica et Biophysica Acta (BBA) - Biomembranes, 1610(1), 37–45.

Baptista, M., Depardieu, F., Courvalin, P., and Arthur, M. (1996). Specificity of induction of glycopeptide resistance genes in *Enterococcus faecalis*. Antimicrobial Agents and Chemotherapy, 40(10), 2291–2295.

Barbieri, C.M. and Stock, A.M. (2008). Universally applicable methods for monitoring response regulator aspartate phosphorylation both in vitro and in vivo using Phos-tag-based reagents. Analytical biochemistry, 376(1), 73–82.

Bardone, M. R., Paternoster, M., and Coronelli, C. (1978). Teichomycins, new antibiotics from *Actinoplanes teichomyceticus* nov. sp. II. Extraction and chemical characterization. The Journal of Antibiotics, 31(3), 170–177.

Barna, J., and Williams, D. (1984). The structure and mode of action of glycopeptide antibiotics of the vancomycin group. Annual Review of Microbiology, 38, 339–357.

Barth, G., Voelter, W., Bunnenberg, E. and Djerassi, C. (1972). Magnetic circular dichroism studies. XVII. Magnetic circular dichroism spectra of proteins. New method for the quantitative determination of tryptophan. Journal of the American Chemical Society, 94(4), 1293–1298.

Beauregard, D. a, Williams, D. H., Gwynn, M. N., and Knowles, D. J. C. (1995). Dimerization and membrane anchors in extracellular targeting of vancomycin group antibiotics. Antimicrobial Agents and Chemotherapy. 39(3), 781–785.

Binda, E., Marinelli, F. and Marcone, G. (2014). Old and New Glycopeptide Antibiotics: Action and Resistance. Antibiotics, 3(4), 572–594.

Birdsall, B., King, R. W., Wheeler, M. R., Lewis, C. A., Goode, S. R., Dunlap, R. B., and Roberts, G. C. K. (1983). Correction for light absorption in fluorescence studies of protein-ligand interactions. Analytical Biochemistry, 132(2), 353–361.

Borghi, A., Coronelli, C., Faniuolo, L., Allievi, G., Pallanza, R., and Gallo, G. G. (1984). Teichomycins, new antibiotics from *Actinoplanes teichomyceticus* nov. sp. IV. Separation and characterization of the components of teichomycin (teicoplanin). The Journal of Antibiotics, 37(6), 615–620.

Borghi, A., Antonini, P., Zanol, M., Ferrari, P., Zerilli, L. F., and Lancini, G. C. (1989). Isolation and structure determination of two new analogs of teicoplanin, a glycopeptide antibiotic. The Journal of Antibiotics, 42(3), 361–366.

Boyer, P. D., Deluca, M., Ebner, K. E., Hultquist, D. E., and Peter, J. B. (1962). Identification of phospohistidine in digests from a probable intermediate of oxidative phosphorylation. The Journal of Biological Chemistry, 237, PC3306-PC3308.

Caffrey, M. (2015). A comprehensive review of the lipid cubic phase or in meso method for crystallizing membrane and soluble proteins and complexes. Acta Crystallographica Section F:Structural Biology Communications, 71(Pt 1), 3–18.

Campoli-Richards, D. M., Brogden, R. N., and Faulds, D. (1990). Teicoplanin. A review of its antibacterial activity, pharmacokinetic properties and therapeutic potential. Drugs, 40(3), 449–86.

Cetinkaya, Y., Falk, P., and Mayhall, C. G. (2000). Vancomycin-resistant enterococci. Clinical Microbiology Reviews, 13(4), 686–707.

Chang, S., Sievert, D. M., Hageman, J. C., Boulton, M. L., Tenover, F. C., Downes, F. P., … Fridkin, S. K. (2003). Infection with vancomycin-resistant *Staphylococcus aureus* containing the vanA resistance gene. New England Journal of Medicine, 348(14), 1342–1347.

Chang, Y., Chen, W. C., Hsieh, P. H., Chen, D. W., Lee, M. S., Shih, H. N. and Ueng, S. W. N. (2011). In vitro activities of daptomycin-, vancomycin-, and teicoplanin-loaded polymethylmethacrylate against methicillin-susceptible, methicillin-resistant, and vancomycin-intermediate strains of *Staphylococcus aureus*. Antimicrobial Agents and Chemotherapy, 55(12), 5480–5484.

Columbus, L., Lipfert, J., Klock, H., Millett, I.Doniach, S. and Lesley, S. A. (2006). Expression, purification, and characterization of Thermotoga maritima membrane proteins for structure determination. Protein science : a publication of the Protein Society, 15(5), 961–975.

Courvalin, P. (2006). Vancomycin resistance in Gram-positive cocci. Clinical Infectious Diseases : An Official Publication of the Infectious Diseases Society of America, 42 Suppl 1(Supplement 1), S25-34.

Djerassi, C., Barth, G., Records, R., Bunnenberg, E. and Voelter, W. (1971). Magnetic circular dichroism studies. XII. Determination of tryptophan in proteins. Journal of the American Chemical Society, 93(10), 2545–2547.

Dutta, R., Qin, L., and Inouye, M. (1999). Histidine kinases: diversity of domain organization. Molecular Microbiology, 34(4), 633–640.

Eckhart, W., Hutchinson, M.A. and Hunter, T. (1979). An activity phosphorylating tyrosine in polyoma T antigen immunoprecipitates. Cell, 18(4), 925–933.

Evers, S., Quintiliani, R., and Courvalin, P. (1996). Genetics of glycopeptide resistance in enterococci. Microbial Drug Resistance-Mechanisms Epidemiology and Disease, 2(2), 219–223.

Freeman, D. J., Pattenden, G., Drake, A. F., and Siligardi, G. (1998). Marine metabolites and metal ion chelation. Circular dichroism studies of metal binding to Lissoclinum cyclopeptides. Journal of the Chemical Society, Perkin Transactions 2, 0(1), 129–136.

Gao, R., Mack, T. R., and Stock, A. M. (2007). Bacterial response regulators: versatile regulatory strategies from common domains. Trends in Biochemical Sciences, 32(5), 225–234.

Gerding, D. N. (1997). Is there a relationship between vancomycin-resistant enterococcal infection and Clostridium difficile infection? Clinical Infectious Diseases : An Official Publication of the Infectious Diseases Society of America, 25 Suppl 2(Suppl 2), S206-10.

Gerhard, U., Mackay, J. P., Maplestone, R. A., and Williams, D. H. (1993). The role of the sugar and chlorine substituents in the dimerization of vancomycin antibiotics. Journal of the American Chemical Society, 115(1), 232–237.

Gohon, Y., Vindigni, J.-D., Pallier, A., Wien, F., Celia, H., Giuliani, A., Tribet, C., Chardot, T. and Briozzo, P. (2011). High water solubility and fold in amphipols of proteins with large hydrophobic regions: Oleosins and caleosin from seed lipid bodies. Biochimica et Biophysica Acta (BBA) - Biomembranes, 1808(3), 706–716.

Greenfield, N.J. (2006). Using circular dichroism spectra to estimate protein secondary structure. Nature protocols, 1(6), 2876–2890.

Greenfield, N. J. (2007). Using circular dichroism collected as a function of temperature to determine the thermodynamics of protein unfolding and binding interactions. Nature Protocols, 1(6), 2527–2535.

Greenwood, D. (1988). Microbiological properties of teicoplanin. The Journal of Antimicrobial Chemotherapy, 21 Suppl A(suppl A), 1–13.

Haas, W., Shepard, B. D., and Gilmore, M. S. (2002). Two-component regulator of *Enterococcus faecalis* cytolysin responds to quorum-sensing autoinduction. Nature, 415(6867), 84–87.

Hancock, L., and Perego, M. (2002). Two-Component Signal Transduction in *Enterococcus faecalis*. Journal of Bacteriology, 184(21), 5819–5825.

Hancock, L. E., and Perego, M. (2004a). Systematic inactivation and phenotypic characterization of two-component signal transduction systems of *Enterococcus faecalis* V583. Journal of Bacteriology, 186(23), 7951–7958.

Hancock, L. E., and Perego, M. (2004b). The *Enterococcus faecalis* fsr two-component system controls biofilm development through production of gelatinase. Journal of Bacteriology, 186(17), 5629–5639.

Handwerger, S. and Kolokathis, A. (1990). Induction of vancomycin resistance in *Enterococcus faecium* by inhibition of transglycosylation. FEMS microbiology letters, 58(2), 167–170.

Hassell, A. M., An, G., Bledsoe, R. K., Bynum, J. M., Carter, H. L., Deng, S. J. J., Gampe, R. T., Grisard, T. E., Madauss, K. P., Nolte, R. T., Rocque, W. J., Wang, L., Weaver, K. L., Williams, S. P., Wisely, G. B., Xu, R. and Shewchuk, L. M. (2006). Crystallization of protein-ligand complexes. In Acta Crystallographica Section D: Biological Crystallography. International Union of Crystallography, 72–79.

Henzler-Wildman, K., and Kern, D. (2007). Dynamic personalities of proteins. Nature, 450(7172), 964–972.

Hill, A. V. (1910). The possible effects of the aggregation of the molecules of hæmoglobin on its dissociation curves. The Journal of Physiology, 40(Supplement-Proceedings of the physiological society), pp.iv–vii.

Hiramatsu, K. (1998). Vancomycin resistance in staphylococci. Drug Resistance Updates : Reviews and Commentaries in Antimicrobial and Anticancer Chemotherapy, 1(2), 135–150.

Hoch, J. A. (2000). Two-component and phosphorelay signal transduction. Current Opinion in Microbiology, 3(2), 165–170.

Hofmann, K., and Stoffel, W. (1993). TMbase: A Database of Membrane Spanning Protein Segments. Biological Chemistry, 374, 166.

Hollenbeck, B. L., and Rice, L. B. (2012). Intrinsic and acquired resistance mechanisms in enterococcus. Virulence, 3(5), 421–433.

Hong, H.-J., Hutchings, M. I., and Buttner, M. J. (2008). Vancomycin resistance VanS/VanR two-component systems. Advances in Experimental Medicine and Biology, 631, 200–213.

Hughes, A. J., Rudd, T. R., Wright, G. S. A., Fernig, D. G., Siligardi, G. and Yates, E. A. (2015). Detection of interaction between protein trytophan residues and small or macromolecular ligands by synchrotron radiation magnetic circular dichroism. Anal. Methods, 7(5), 1667–1671.

Hussain, R., Benning, K., Javorfi, T., Longo, E., Rudd, T. R., Pulford, B., and Siligardi, G. (2015). CDApps: integrated software for experimental planning and data processing at beamline B23, Diamond Light Source. Journal of Synchrotron Radiation, 22(2), 465–468.

Hussain, R., Benning, K., Myatt, D., Javorfi, T., Longo, E., Rudd, T. R., Pulford, B. and Siligardi, G. (2015). CDApps: integrated software for experimental planning and data processing at beamline B23, Diamond Light Source. Journal of synchrotron radiation, 22(2), 465–468.

Hussain R., Harding S. E., Hughes C. S., Ma P., Patching S. G., Edara S., Siligardi G., Henderson P. J., Phillips-Jones M. K. (2016). Purification of bacterial membrane sensor kinases and biophysical methods for determination of their ligand and inhibitor interactions. Biochemical Society Transactions, 44(3), 810-823.

Hussain, R. and Siligardi, G. (2016). Characterisation of Conformational and Ligand Binding Properties of Membrane Proteins Using Synchrotron Radiation Circular Dichroism (SRCD). Advances in experimental medicine and biology, 922, 43–59.

Hussain, R., Hughes, C. S.Jávorfi, T., Siligardi, G., Williams, P. and Bonev, B. B. (2018). To Boil an Egg: Substrate Binding Affects Critical Stability in Thermal Unfolding of Proteins. The Journal of Physical Chemistry B, 122(8), 2213–2218.

Javorfi, T., Hussain, R., Myatt, D., and Siligardi, G. (2010). Measuring circular dichroism in a capillary cell using the B23 synchrotron radiation CD beamline at Diamond Light Source. Chirality, 22(1E), E149–E153.

Jehl F., Schramm F., Colombo P. and Brink A.J. (2013). Group A2 Analogs of Innovator Teicoplanin: Variability of their Ratio during Treatment Time Course in Human Blood; Consequences for the Generics. Pharmaceutical Regulatory Affairs, 2(2).

Johnson, W.C. (1985). Circular dichroism and its empirical application to biopolymers. Methods of biochemical analysis, 31, 61–163.

Kahne, D., Leimkuhler, C., Lu, W., and Walsh, C. (2005). Glycopeptide and lipoglycopeptide antibiotics. Chemical Reviews, 105(2), 425-448.

Karaszkiewicz, J.W., Henrich C.J. (2001). Using Protein Kinase and Protein Phosphatase Inhibitors to Dissect Protein Phosphorylation Pathways. Current Protocols in Immunology, Chapter 11(Unit 11.7), 11.7.1-11.7.20.

Kee, J.-M. and Muir, T.W. (2012). Chasing phosphohistidine, an elusive sibling in the phosphoamino acid family. ACS chemical biology, 7(1), 44–51.

Kelly, S. M., and Price, N. C. (2000). The Use of Circular Dichroism in the Investigation of Protein Structure and Function. Current Protein and Peptide Science, 1(4), 349–384.

Kelly, S. M., Jess, T. J., and Price, N. C. (2005). How to study proteins by circular dichroism. Biochimica Et Biophysica Acta-Proteins and Proteomics, 1751(2), 119–139.

Kinoshita, E., Kinoshita-Kikuta, E., Takiyama, K., and Koike, T. (2006). Phosphate-binding tag, a new tool to visualize phosphorylated proteins. Molecular and Cellular Proteomics, 5(4), 749–757.

Kinoshita, E., Kinoshita-Kikuta, E., and Koike, T. (2009). Separation and detection of large phosphoproteins using Phos-tag SDS-PAGE. Nature Protocols, 4(10), 1513–1521.

Kinoshita, E., Kinoshita-Kikuta, E., Sugiyama, Y., Fukada, Y., Ozeki, T., and Koike, T. (2012). Highly sensitive detection of protein phosphorylation by using improved Phos-tag Biotin. Proteomics, 12(7), 932–937.

Kirst, H. A., Thompson, D. G., and Nicas, T. I. (1998). Historical yearly usage of vancomycin. Antimicrobial Agents and Chemotherapy, 42(5), 1303-1304

Klumpp, S. and Krieglstein, J., (2002). Phosphorylation and dephosphorylation of histidine residues in proteins. European journal of biochemistry, 269(4), 1067–71.

Koteva, K., Hong, H.-J., Wang, X. D., Nazi, I., Hughes, D., Naldrett, M. J. and Wright, G. D. (2010). A vancomycin photoprobe identifies the histidine kinase VanSsc as a vancomycin receptor. Nature Chemical Biology, 6(5), 327–329.

Krogh, A., Larsson, B., von Heijne, G., and Sonnhammer, E. L. (2001). Predicting transmembrane protein topology with a hidden markov model: application to complete genomes. Journal of Molecular Biology, 305(3), 567–580.

Ku, T., Lu P., Chan C., Wang T., Lai S., Lyu P., Hsiao N. (2009). Predicting melting temperature directly from protein sequences. Computational Biology and Chemistry, 33(6), pp.445–450.

Kuhlmann, M., and Covic, A. (2006). The protein science of biosimilars. Nephrology, Dialysis, Transplantation : Official Publication of the European Dialysis and Transplant Association - European Renal Association, 21 Suppl 5(suppl_5), v4-8.

Kwun, M. J., Novotna, G., Hesketh, A. R., Hill, L., and Hong, H.-J. (2013). In vivo studies suggest that induction of VanS-dependent vancomycin resistance requires binding of the drug to D-Ala-D-Ala termini in the peptidoglycan cell wall. Antimicrobial Agents and Chemotherapy, 57(9), 4470–4480.

Lai, M.H. and Kirsch, D.R. (1996). Induction signals for vancomycin resistance encoded by the vanA gene cluster in *Enterococcus faecium*. Antimicrobial agents and chemotherapy, 40(7), 1645–1648.

Leclercq, R., Derlot, E., Duval, J., and Courvalin, P. (1988). Plasmid-mediated resistance to vancomycin and teicoplanin in *Enterococcus faecium*. The New England Journal of Medicine, 319(3), 157–161.

Lin, S.H., and Guidotti, G. (2009). Purification of Membrane Proteins. Methods in Enzymology, 463, 619-629.

Liu, J. P., Volk, K. J., Lee, M. S., Pucci, M., and Handwerger, S. (1994). Binding-studies of vancomycin to the cytoplasmic peptidoglycan precursors by affinity capillary electrophoresis. Analytical Chemistry, 66(14), 2412–2416.

Liu, Y.C., Li, Y.S., Lyu, S.Y., Hsu, L.J., Chen, Y.H., Huang, Y.T., Li, T.L. (2011). Interception of teicoplanin oxidation intermediates yields new antimicrobial scaffolds. Nature Chemical Biology, 7(5), 304–309.

Loll, P. J., Miller, R., Weeks, C. M., and Axelsen, P. H. (1998). A ligand-mediated dimerization mode for vancomycin. Chemistry and Biology, 5(5), 293–298.

Longo, E., Hussain, R. and Siligardi, G. (2015). Application of circular dichroism and magnetic circular dichroism for assessing biopharmaceuticals formulations photo-stability and small ligands binding properties. International Journal of Pharmaceutics, 480(1), 84–91.

Lux, R., and Shi, W. (2005). A novel bacterial signalling system with a combination of a Ser/Thr kinase cascade and a His/Asp two-component system. Molecular Microbiology, 58(2), 345-348.

Ma, P., Yuille, H.M., Blessie, V., Gohring, N., IgloI, Z., Nishiguchi, K. and Phillips-Jones, M.K. (2008). Expression, purification and activities of the entire family of intact membrane sensor kinases from *Enterococcus faecalis*. Molecular Membrane Biology, 25(6–7), 449–473.

Ma, P., Nishiguchi, K., Yuille, H. M., Davis, L. M., Nakayama, J., and Phillips-Jones, M. K. (2011). Anti-HIV siamycin I directly inhibits autophosphorylation activity of the bacterial FsrC quorum sensor and other ATP-dependent enzyme activities. FEBS Letters, 585(17), 2660–2664.

Mackay, J. P., Gerhard, U., Beauregard, D. A., Westwell, M. S., Searle, M. S., and Williams, D. H. (1994). Glycopeptide antibiotic activity and the possible role of dimerization: A model for biological signaling. Journal of the American Chemical Society, 116(11), 4581–4590.

Makrides, S. C. (1996). Strategies for achieving high-level expression of genes in *Escherichia coli*. Microbiology Reviews, 60(3), 512–538.

Mascher, T., Helmann, J. D., and Unden, G. (2006). Stimulus perception in bacterial signal-transducing histidine kinases. Microbiology and Molecular Biology Reviews, 70(4), 910–938.

Maslennikov, I., Klammt, C., Hwang, E., Kefala, G., Okamura, M., Esquivies, L. and Choe, S. (2010). Membrane domain structures of three classes of histidine kinase receptors by cell-free expression and rapid NMR analysis. Proceedings of the National Academy of Sciences of the United States of America, 107(24), 10902–10907.

Maule, A. F., Wright, D. P., Weiner, J. J., Han, L., Peterson, F. C., Volkman, B. F., … Peitsch, M. (2015). The Aspartate-Less Receiver (ALR) Domains: Distribution, Structure and Function. PLOS Pathogens, 11(4), e1004795.

Mitrophanov, A. Y., and Groisman, E. A. (2008). Signal integration in bacterial two-component regulatory systems. Genes and Development, 22(19), 2601–2611.

Moraes I., Evans G., Sanchez-Weatherby J., Newstead S., Stewart P. D. (2014). Membrane protein structure determination — The next generation. Biochimica et Biophysica Acta (BBA) - Biomembranes, 1838(1), 78–87.

Nakayama, J., Cao, Y., Horii, T., Sakuda, S., Akkermans, A. D. L., De Vos, W. M., and Nagasawa, H. (2001). Gelatinase biosynthesis-activating pheromone: a peptide lactone that mediates a quorum sensing in *Enterococcus faecalis*. Molecular Microbiology, 41(1), 145–154.

Nakayama, J., Tanaka, E., Kariyama, R., Nagata, K., Nishiguchi, K., Mitsuhata, R., and Sonomoto, K. (2007). Siamycin attenuates fsr quorum sensing mediated by a gelatinase biosynthesis-activating pheromone in *Enterococcus faecalis*. Journal of Bacteriology, 189(4), 1358–1365.

Neale, C., Ghanei, H., Holyoake, J., Bishop, R. E., Privé, G. G., and Pomès, R. (2013). Detergent-mediated protein aggregation. Chem Phys Lipids, 169, 72–84.

Nieto, M., and Perkins, H. R. (1971). Modifications of the acyl-D-alanyl-D-alanine terminus affecting complex-formation with vancomycin. The Biochemical Journal, 123(5), 789–803.

Noble, W. C., Virani, Z., and Cree, R. G. A. (1992). Co-transfer of vancomycin and other resistance genes from *Enterococcus faecalis* Nctc-12201 to *Staphylococcus aureus*. FEMS Microbiology Letters, 93(2), 195–198.

Parenti, F., Beretta, G., Berti, M., and Arioli, V. (1978). Teichomycins, new antibiotics from *Actinoplanes teichomyceticus* nov. sp. I. Description of the producer strain, fermentation studies and biological properties. The Journal of Antibiotics, 31(4), 276–283.

Parenti, F. (1986). Structure and mechanism of action of teicoplanin. The Journal of hospital infection, 7 Suppl A, 79–83.

Patching S. G. Edara S., Ma P., Nakayama J., Hussain R., Siligardi G., Phillips-Jones M. K. (2012). Interactions of the intact FsrC membrane histidine kinase with its pheromone ligand GBAP revealed

through synchrotron radiation circular dichroism. Biochimica et Biophysica Acta, 1818(7), 1595–1602.

Patti, G. J., Kim, S. J., and Schaefer, J. (2008). Characterization of the peptidoglycan of vancomycin-susceptible *Enterococcus faecium*. Biochemistry, 47(32), 8378–85.

Pallanza R., Berti M., Goldstein B. P., Mapelli E., Randisi E., Scotti R., Arioli V. (1983). Teichomycin: In-vitro and in-vivo evaluation in comparison with other antibiotics. Journal of Antimicrobial Chemotherapy, 11(5), 419–425.

Parenti, F. (1986). Structure and mechanism of action of teicoplanin. The Journal of hospital infection, 7 Suppl A, 79–83.

Patching S. G., Edara S., Ma P., Nakayama J., Hussain R., Siligardi G., Phillips-Jones M. K. (2012). Interactions of the intact FsrC membrane histidine kinase with its pheromone ligand GBAP revealed through synchrotron radiation circular dichroism. Biochimica et Biophysica Acta, 1818(7), 1595–1602.

Peng, J., and Xu, J. (2011). RaptorX: exploiting structure information for protein alignment by statistical inference. Proteins, 79 Suppl 1, 161–171.

Perkins, H. R., and Nieto, M. (1974). The chemical basis for the action of the vancomycin group of antibiotics. Annals of the New York Academy of Sciences, 235(1), 348–363.

Pfeiffer, R. R. (1981). Structural features of vancomycin. Review of Infectious Diseases, 3(Supplement), S205–S209.

Pogson, C. J. (2013). Overexpression, purification and ligand interaction studies of intact membrane sensory kinases from enterococci: towards agonist and antagonist screening. University of Central Lancashire.

Pootoolal, J., Neu, J., and Wright, G. D. (2002). Glycopeptide antibiotic resistance. Annual Review of Pharmacology and Toxicology, 42, 381–408.

Potter, C. , Jeong, E. L., Williamson, M. P., Henderson, P. J. F., and Phillips-Jones, M. K. (2006). Redox-responsive in vitro modulation of the signalling state of the isolated PrrB sensor kinase of *Rhodobacter sphaeroides*. FEBS Letters, 580(13), 3206–3210.

Potter, C., Ward, A., and Laguri, C. (2002). Expression, Purification and Characterisation of Full-length Histidine Protein Kinase RegB from *Rhodobacter sphaeroides*. Journal of Molecular Biology, 320(2), 201–213.

Price, M. N., Wetmore, K. M., Deutschbauer, A. M., and Arkin, A. P. (2016). A Comparison of the Costs and Benefits of Bacterial Gene Expression. PLoS ONE 11(10): e0164314.

Prinz, H. (2010). Hill coefficients, dose-response curves and allosteric mechanisms. Journal of Chemical Biology, 3(1), 37–44.

Prodromou C., Siligardi G., O'Brien R., Woolfson D. N., Regan L., Panaretou B., Ladbury J. E., Piper P. W., and Pearl L. H. (1999). Regulation of Hsp90 ATPase activity by tetratricopeptide repeat (TPR)-domain co-chaperones. The EMBO Journal, 18(3), 754–762.

Puttick, J., Baker, E. N., and Delbaere, L. T. J. (2008). Histidine phosphorylation in biological systems. Biochimica et Biophysica Acta, 1784(1), 100-105.

Rasband, W.S. (1997). ImageJ. U. S. National Institutes of Health, Bethesda, Maryland, USA. Available at: https://imagej.nih.gov/ij/index.html.

Rath, A., Glibowicka, M., Nadeau, V. G., Chen, G., and Deber, C. M. (2009). Detergent binding explains anomalous SDS-PAGE migration of membrane proteins. Proceedings of the National Academy of Sciences of the United States of America, 106(6), 1760–5.

Reynolds, P. E. (1989). Structure, biochemistry and mechanism of action of glycopeptide antibiotics. European Journal of Clinical Microbiology and Infectious Diseases, 8(11), 943–950.

Rosano, G. L., and Ceccarelli, E. A. (2014). Recombinant protein expression in *Escherichia coli*: advances and challenges. Frontiers in Microbiology, 5, 172.

Ruckenstein, E., and Shulgin, I. L. (2006). Effect of salts and organic additives on the solubility of proteins in aqueous solutions. Advances in Colloid and Interface Science, 123–126, 97–103.

Saidijam, M., Psakis, G., Clough, J. L., Meuller, J., Suzuki, S., Hoyle, C. J., and Henderson, P. J. F. (2003). Collection and characterisation of bacterial membrane proteins. FEBS Letters, 555(1), 170–175.

Scharf, B. E. (2010). Summary of useful methods for two-component system research. Current Opinion in Microbiology, 13(2), 246-252.

Schlegel, S., Hjelm, A., Baumgarten, T., Vikström, D., and de Gier, J.-W. (2014). Bacterial-based membrane protein production. Biochimica et Biophysica Acta, 1843(8), 1739–1749.

Schneider, C. A., Rasband, W. S., and Eliceiri, K. W. (2012). NIH Image to ImageJ: 25 years of image analysis. Nature Methods, 9(7), 671–675.

Schwaber M. J., Wright S. B., Carmeli Y., Venkataraman L., DeGirolami P. C., Gramatikova A., Perl T. M., Sakoulas G., Gold H. S. (2003). Clinical implications of varying degrees of vancomycin susceptibility in methicillin-resistant *Staphylococcus aureus* bacteremia. Emerging Infectious Diseases, 9(6), 657-664.

Sieradzki, K., Roberts, R. B., Haber, S. W., and Tomasz, A. (1999). The Development of Vancomycin Resistance in a Patient with Methicillin-Resistant *Staphylococcus aureus* Infection. New England Journal of Medicine, 340(7), 517–523.

Sievert, D. M., Ricks, P., Edwards, J. R., Schneider, A., Patel, J., Srinivasan, A., and Suetens, C. (2000). Vancomycin-resistant enterococcal infections. Euro Surveillance : Bulletin Européen Sur Les Maladies Transmissibles = European Communicable Disease Bulletin, 342(10), 710–21.

Siligardi, G., Panaretou, B., Meyer, P., Singh, S., Woolfson, D. N., Piper, P. W., and Prodromou, C. (2002). Regulation of Hsp90 ATPase activity by the co-chaperone Cdc37p/p50cdc37. The Journal of Biological Chemistry, 277(23), 20151–20159.

Siligardi, G., Hussain, R., Patching, S. G., and Phillips-Jones, M. K. (2014). Ligand- and drug-binding studies of membrane proteins revealed through circular dichroism spectroscopy. Biochimica et Biophysica Acta, 1838(1 Pt A), 34–42.

Siligardi, G. and Hussain, R. (2015). CD spectroscopy: an essential tool for quality control of protein folding. Methods in molecular biology (Clifton, N.J.), 1261, 255–276.

Singleton, D. G., Hussain, R., Siligardi, G., Kumar, P., Hrdlicka, P. J., Berova, N. and Stulz, E. (2016). Increased duplex stabilization in porphyrin-LNA zipper arrays with structure dependent exciton coupling. Org. Biomol. Chem., 14(1), 149–157.

Sørensen, H. P., and Mortensen, K. K. (2005). Advanced genetic strategies for recombinant protein expression in *Escherichia coli*. Journal of Biotechnology.

Sreerama, N. and Woody, R.W. (2004). Computation and analysis of protein circular dichroism spectra. Methods in enzymology, 383, pp.318–351.

Srinivasan, A., Dick, J.D. and Perl, T.M. (2002). Vancomycin resistance in staphylococci. Clinical microbiology reviews, 15(3), 430–438.

Stark, M. J. (1987). Multicopy expression vectors carrying the lac repressor gene for regulated high-level expression of genes in *Escherichia coli*. Gene, 51(2–3), 255–67.

Steed, M.E., Vidaillac, C. and Rybak, M.J. (2012). Evaluation of telavancin activity versus daptomycin and vancomycin against daptomycin-nonsusceptible *Staphylococcus aureus* in an in vitro pharmacokinetic/pharmacodynamic model. Antimicrobial Agents and Chemotherapy, 56(2), 955–959.

Stephens, P.J. (1993). Magnetic Circular Dichroism. Annual Review of Physical Chemistry, 48(9), 6144–6151.

Stephenson, K., and Hoch, J. A. (2002). Virulence- and antibiotic resistance-associated two-component signal transduction systems of Gram-positive pathogenic bacteria as targets for antimicrobial therapy. In Pharmacology and Therapeutics 93(2-3), 293-305.

Stevens, R. C. (2000). Design of high-throughput methods of protein production for structural biology. Structure, 8, 177–185.

Sutherland, J.C. and Holmquist, B. (1980). Magnetic circular dichroism of biological molecules. Annual review of biophysics and bioengineering, 9(1), 293–326.

Stock, A. M., Robinson, V. L., and Goudreau, P. N. (2000). Two-component signal transduction. Annual Review of Biochemistry, 69, 183–215.

Sun, G., Birkey, S. M., and Hulett, F. M. (1996). Three two-component signal-transduction systems interact for Pho regulation in Bacillus subtilis. Molecular Microbiology, 19(5), 941–948.

Surade, S., Klein, M., Stolt-Bergner, P. C., Muenke, C., Roy, A., and Michel, H. (2006). Comparative analysis and “expression space” coverage of the production of prokaryotic membrane proteins for structural genomics. Protein Science : A Publication of the Protein Society, 15(9), 2178–2189.

Svetitsky, S., Leibovici, L., and Paul, M. (2009). Comparative efficacy and safety of vancomycin versus teicoplanin: Systematic review and meta-analysis. Antimicrobial Agents and Chemotherapy, 53(10), 4069–4079.

Talley, K., and Alexov, E. (2010). On the pH-optimum of activity and stability of proteins. Proteins, 78(12), 2699–706.

Teale, F.W. and Weber, G. (1957). Ultraviolet fluorescence of the aromatic amino acids. The Biochemical journal, 65(3), 476–82.

Tenover, F. C., Biddle, J. W., and Lancaster, M. V. (2001). Increasing resistance to vancomycin and other glycopeptides in *Staphylococcus aureus*. Emerging Infectious Diseases, 7(2), 327-332.

Thurlow, L. R., Thomas, V. C., Narayanan, S., Olson, S., Fleming, S. D., and Hancock, L. E. (2010). Gelatinase contributes to the pathogenesis of endocarditis caused by *Enterococcus faecalis*. Infection and Immunity, 78(11), 4936–4943.

Trajtenberg, F., Graña, M., Ruétalo, N., Botti, H. and Buschiazzo, A. (2010). Structural and enzymatic insights into the ATP binding and autophosphorylation mechanism of a sensor histidine kinase. The Journal of biological chemistry, 285(32), 24892–24903.

Ulijasz, A.T., Grenader, A. and Weisblum, B. (1996). A vancomycin-inducible lacZ reporter system in Bacillus subtilis: induction by antibiotics that inhibit cell wall synthesis and by lysozyme. Journal of bacteriology, 178(21), 6305–6309.

Vagenende, V., Yap, M. G. S., and Trout, B. L (2009). Mechanisms of protein stabilization and prevention of protein aggregation by glycerol. Biochemistry, 48(46), 11084–11096.

Vivian, J.T. and Callis, P.R. (2001). Mechanisms of Tryptophan Fluorescence Shifts in Proteins. Biophysical Journal, 80(5), 2093–2109.

Walsh, C. T., Fisher, S. L., Park, I. S., Prahalad, M., and Wu, Z. (1996). Bacterial resistance to vancomycin: five genes and one missing hydrogen bond tell the story. Chemistry and Biology, 3(1), 21–28.

Wang, S. (2012). Bacterial Two-Component Systems : Structures and Signaling Mechanisms. Protein Phosphorylation in Human Health, Dr. Cai Huang (Ed.), (Figure 1), 439–466.

Weiss, J.N. (1997). The Hill equation revisited: uses and misuses. FASEB journal : official publication of the Federation of American Societies for Experimental Biology, 11(11), 835–41.

Werner G., Coque T. M., Franz C. M., Grohmann E., Hegstad K., Jensen L., van Schaik W., Weaver K. (2013). Antibiotic resistant enterococci-Tales of a drug resistance gene trafficker. International Journal of Medical Microbiology, 303(6–7), 360–379.

West, A. H., and Stock, A. M. (2001). Histidine kinases and response regulator proteins in two-component signaling systems. Trends in Biochemical Sciences, 26(6), 369–376.

Westwell, M. S., Gerhard, U., and Williams, D. H. (1995). Two conformers of the glycopeptide antibiotic teicoplanin with distinct ligand binding sites. Journal of Antibiotics, 48(11), 1292–1298.

Whitener C. J., Park S. Y., Browne F. A., Parent L. J., Julian K., Bozdogan B., Appelbaum P. C., Chaitram J., Weigel L. M., Jernigan J., McDougal L. K., Tenover F. C., Fridkin S. K. (2004). Vancomycin-resistant *Staphylococcus aureus* in the absence of vancomycin exposure. Clinical Infectious Diseases : An Official Publication of the Infectious Diseases Society of America, 38(8), 1049–55.

Wieland, T., and Attwood, P. V. (2015). Alterations in reversible protein histidine phosphorylation as intracellular signals in cardiovascular disease. Frontiers in Pharmacology, 6, 173.

Wilke, K. E., Francis, S., and Carlson, E. E. (2012). Activity-based probe for histidine kinase signaling. Journal of the American Chemical Society, 134(22), 9150–3.

Wright, G. D., and Walsh, C. T. (1992). D-Alanyl-D-alanine ligases and the molecular mechanism of vancomycin resistance. Accounts of Chemical Research, 25(4), 468–473.

Wright, G. D., Holman, T. R., and Walsh, C. T. (1993). Purification and characterization of VanR and the cytosolic domain of VanS: a two-component regulatory system required for vancomycin resistance in *Enterococcus faecium* BM4147. Biochemistry, 32(19), 5057–5063.

Wright, G. D. (2007). The antibiotic resistome: the nexus of chemical and genetic diversity. Nature Reviews. Microbiology, 5(3), 175–186.

Wrolstad, R. E., Decker, E. A., Schwartz, S. J. and Sporns, P. (2005). Handbook of Food Analytical Chemistry, Water, Proteins, Enzymes, Lipids, and Carbohydrates, John Wiley & Sons.

Wu, Z. L. (2011). Phosphatase-coupled universal kinase assay and kinetics for first-order-rate coupling reaction. PloS One, 6(8), e23172.

Xu, H., Yao, N., Xu, H., Wang, T., Li, G. and Li, Z. (2013). Characterization of the interaction between eupatorin and bovine serum albumin by spectroscopic and molecular modeling methods. International journal of molecular sciences, 14(7), 14185–14203.

Yamada, S., Nakamura, H., Kinoshita, E., Kinoshita-Kikuta, E., Koike, T. and Shiro, Y. (2007). Separation of a phosphorylated histidine protein using phosphate affinity polyacrylamide gel electrophoresis. Analytical biochemistry, 360(1), 160–162.

Yang, Z., Wang, C., Zhou, Q., An, J., Hildebrandt, E., Aleksandrov, L. A., Kappes, J. C., DeLucas, L. J., Riordan, J. R., Urbatsch, I. L., Hunt, J. F. and Brouillette, C. G. (2014). Membrane protein stability can be compromised by detergent interactions with the extramembranous soluble domains. Protein science : a publication of the Protein Society, 23(6), 769–789.

Zanol, M., Cometti, A., Borghi, A., and Lancini, G. C. (1988). Isolation and structure determination of minor components of teicoplanin. Chromatographia, 26(1), 234–236.

APPENDIX

1.1. Sequence of *E. faecium* vanS_A from BM4147 in pTTQ18His

TAGAAGCTTGGCACTGGCCGTCGTTTTACAACGTCGTGACTGGGAAAACCCTGGCGTTACCC
AACTTAATCGCCTTGCAGCACATCCCCCTTTCGCCAGCTGGCGTAATAGCGAAGAGGCCCGC
ACCGATCGCCCTTCCCAACAGTTGCGCAGCCTGAATGGCGAATGGCGCCTGATGCGGTATTT
TCTCCTTACGCATCTGTGCGGTATTTCACACCGCATAAATTCCCTGTTTTGGCGGATGAGAG
AAGATTTTCAGCCTGATACAGATTAAATCAGAACGCAGAAGCGGTCTGATAAAACAGAATTT
GCCTGGCGGCAGTAGCGCGGTGGTCCCACCTGAC
CCGATTCATTAATGCAGAATTAATTCTCATGTTTGACAGCTTATCATCGACTGCACGGTGCA
CCCATGCTTCTGGCGTCAGGCAGCCATCGGAAGCTGTGGTATGGCTGTGCAGGTCGTAAATC
ACTGCATAATTCGTGTCGCTCAAGGCGCACTCCCGTTCTGGATAATGTTTTTTGCGCCGACA
TCATAACGGTTCTGGCAAATATTCTGAAATGAGCTGTTGACAATTAATCATCGGCTCGTATA
ATGTGTGGAATTGTGAGCGGATAACAATTTCACACAGGAAACAGCG

ATGAATTCGCATATGGTTATAAAATTGAAAAATAAAAAAAACGACTATTCCAAACTAGAACG
AAAACTTTACATGTATATCGTTGCAATTGTTGTGGTAGCAATTGTATTCGTGTTGTATATTC
GTTCAATGATCCGAGGGAAACTTGGGGATTGGATCTTAAGTATTTTGGAAAACAAATATGAC
TTAAATCACCTGGACGCGATGAAATTATATCAATATTCCATACGGAACAATATAGATATCTT
TATTTATGTGGCGATTGTCATTAGTATTCTTATTCTATGTCGCGTCATGCTTTCAAAATTCG
CAAAATACTTTGACGAGATAAATACCGGCATTGATGTACTTATTCAGAACGAAGATAAACAA
ATTGAGCTTTCTGCGGAAATGGATGTTATGGAACAAAAGCTCAACACATTAAAACGGACTCT
GGAAAAGCGAGAGCAGGATGCAAAGCTGGCCGAACAAAGAAAAAATGACGTTGTTATGTACT
TGGCGCACGATATTAAAACGCCCCTTACATCCATTATCGGTTATTTGAGCCTGCTTGACGAG
GCTCCAGACATGCCGGTAGATCAAAAGGCAAAGTATGTGCATATCACGTTGGACAAAGCGTA
TCGACTCGAACAGCTAATCGACGAGTTTTTTGAGATTACACGGTATAACCTACAAACGATAA
CGCTAACAAAAACGCACATAGACCTATACTATATGCTGGTGCAGATGACCGATGAATTTTAT
CCTCAGCTTTCCGCACATGGAAAACAGGCGGTTATTCACGCCCCCGAGGATCTGACCGTGTC

CGGCGACCCTGATAAACTCGCGAGAGTCTTTAACAACATTTTGAAAAACGCCGCTGCATACA

GTGAGGATAACAGCATCATTGACATTACCGCGGGCCTCTCCGGGGATGTGGTGTCAATCGAA

TTCAAGAACACTGGAAGCATCCCAAAAGATAAGCTAGCTGCCATATTTGAAAAGTTCTATAG

GCTGGACAATGCTCGTTCTTCCGATACGGGTGGCGCGGGACTTGGATTGGCGATTGCAAAAG

AAATTATTGTTCAGCATGGAGGGCAGATTTACGCGGAAAGCAATGATAACTATACGACGTTT

AGGGTAGAGCTTCCAGCGATGCCAGACTTGGTTGATAAAAGGAGGTCCG**CTGCAG**GCGGTCG

TGGCAGCCACCATCACCATCACCATTAA

Where :

= **pTTQ18His; ATG = start codon; ATCG = vanS$_A$; CTGCAG** = stop codon.

1.2. Amino acid sequence of $VanS_A$ from *E. faecium* BM4147

> 397 aa

MNSHMVIKLKNKKNDYSKLERKLYMYIVAIVVVAIVFVLYIRSMIRGKLGDWILSILENKYD
LNHLDAMKLYQYSIRNNIDIFIYVAIVISILILCRVMLSKFAKYFDEINTGIDVLIQNEDKQ
IELSAEMDVMEQKLNTLKRTLEKREQDAKLAEQRKNDVVMYLAHDIKTPLTSIIGYLSLLDE
APDMPVDQKAKYVHITLDKAYRLEQLIDEFFEITRYNLQTITLTKTHIDLYYMLVQMTDEFY
PQLSAHGKQAVIHAPEDLTVSGDPDKLARVFNNILKNAAAYSEDNSIIDITAGLSGDVVSIE
FKNTGSIPKDKLAAIFEKFYRLDNARSSDTGGAGLGLAIAKEIIVQHGGQIYAESNDNYTTF
RVELPAMPDLVDKRRSAAGGRGSHHHHHH

Where RSMIRGKLGDWILSILENKYDLNHLDAMKLYQYSIRNNID = predicted extracellular ligand-binding domain (TMHMM). Amino acid sequence obtained using Translate tool (http://web.expasy.org/tools/translate/). Transmembrane domains highlighted by XXX. Conserved phosphorylated histidine.

1.3. ProtParam

```
        10          20          30          40          50          60
MNSHMVIKLK  NKKNDYSKLE  RKLYMYIVAI  VVVAIVFVLY  IRSMIRGKLG  DWILSILENK

        70          80          90         100         110         120
YDLNHLDAMK  LYQYSIRNNI  DIFIYVAIVI  SILILCRVML  SKFAKYFDEI  NTGIDVLIQN

       130         140         150         160         170         180
EDKQIELSAE  MDVMEQKLNT  LKRTLEKREQ  DAKLAEQRKN  DVVMYLAHDI  KTPLTSIIGY

       190         200         210         220         230         240
LSLLDEAPDM  PVDQKAKYVH  ITLDKAYRLE  QLIDEFFEIT  RYNLQTITLT  KTHIDLYYML

       250         260         270         280         290         300
VQMTDEFYPQ  LSAHGKQAVI  HAPEDLTVSG  DPDKLARVFN  NILKNAAAYS  EDNSIIDITA

       310         320         330         340         350         360
GLSGDVVSIE  FKNTGSIPKD  KLAAIFEKFY  RLDNARSSDT  GGAGLGLAIA  KEIIVQHGGQ

       370                     380                     390         400
IYAESNDNYT TFRVELPAMP DLVDKRRSAA GGRGSHHHHH H
```

Number of amino acids: 401

Molecular weight: 45764.7

Theoretical pI: 6.28

Amino acid composition:

Ala (A)	30	7.5%
Arg (R)	17	4.2%
Asn (N)	20	5.0%
Asp (D)	31	7.7%
Cys (C)	1	0.2%
Gln (Q)	14	3.5%
Glu (E)	22	5.5%
Gly (G)	18	4.5%
His (H)	14	3.5%
Ile (I)	40	10.0%
Leu (L)	42	10.5%
Lys (K)	31	7.7%
Met (M)	13	3.2%
Phe (F)	12	3.0%
Pro (P)	9	2.2%
Ser (S)	22	5.5%
Thr (T)	18	4.5%
Trp (W)	1	0.2%
Tyr (Y)	21	5.2%
Val (V)	25	6.2%
Pyl (O)	0	0.0%
Sec (U)	0	0.0%
(B)	0	0.0%
(Z)	0	0.0%
(X)	0	0.0%

Total number of negatively charged residues (Asp + Glu): 53

Total number of positively charged residues (Arg + Lys): 48

Atomic composition:

Carbon	C	2058
Hydrogen	H	3276
Nitrogen	N	546
Oxygen	O	603
Sulfur	S	14

Formula: $C_{2058}H_{3276}N_{546}O_{603}S_{14}$

Total number of atoms: 6497

Extinction coefficients:

Extinction coefficients are in units of M^{-1} cm^{-1}, at 280 nm measured in water.

Ext. coefficient	36790
Abs 0.1% (=1 g/l)	0.804, assuming all pairs of Cys residues form cystines

Ext. coefficient	36790
Abs 0.1% (=1 g/l)	0.804, assuming all Cys residues are reduced

Estimated half-life:

The N-terminal of the sequence considered is M (Met).

The estimated half-life is: 30 hours (mammalian reticulocytes, in vitro).
>20 hours (yeast, in vivo).
>10 hours (Escherichia coli, in vivo).

Instability index:

The instability index (II) is computed to be 38.05

This classifies the protein as stable.

Aliphatic index: 105.31

Grand average of hydropathicity (GRAVY): -0.168

ProtParam resources available from ExPASy Bioinformatics Resource Portal at http://web.expasy.org/protparam/

1.4. TMHMM

```
# WEBSEQUENCE Length: 401
# WEBSEQUENCE Number of predicted TMHs:  2
# WEBSEQUENCE Exp number of AAs in TMHs: 42.4730699999999999
# WEBSEQUENCE Exp number, first 60 AAs:  20.73062
# WEBSEQUENCE Total prob of N-in:        0.42707
# WEBSEQUENCE POSSIBLE N-term signal sequence
WEBSEQUENCE     TMHMM2.0        inside       1    22
WEBSEQUENCE     TMHMM2.0        TMhelix     23    45
WEBSEQUENCE     TMHMM2.0        outside     46    81
WEBSEQUENCE     TMHMM2.0        TMhelix     82   101
WEBSEQUENCE     TMHMM2.0        inside     102   401
```

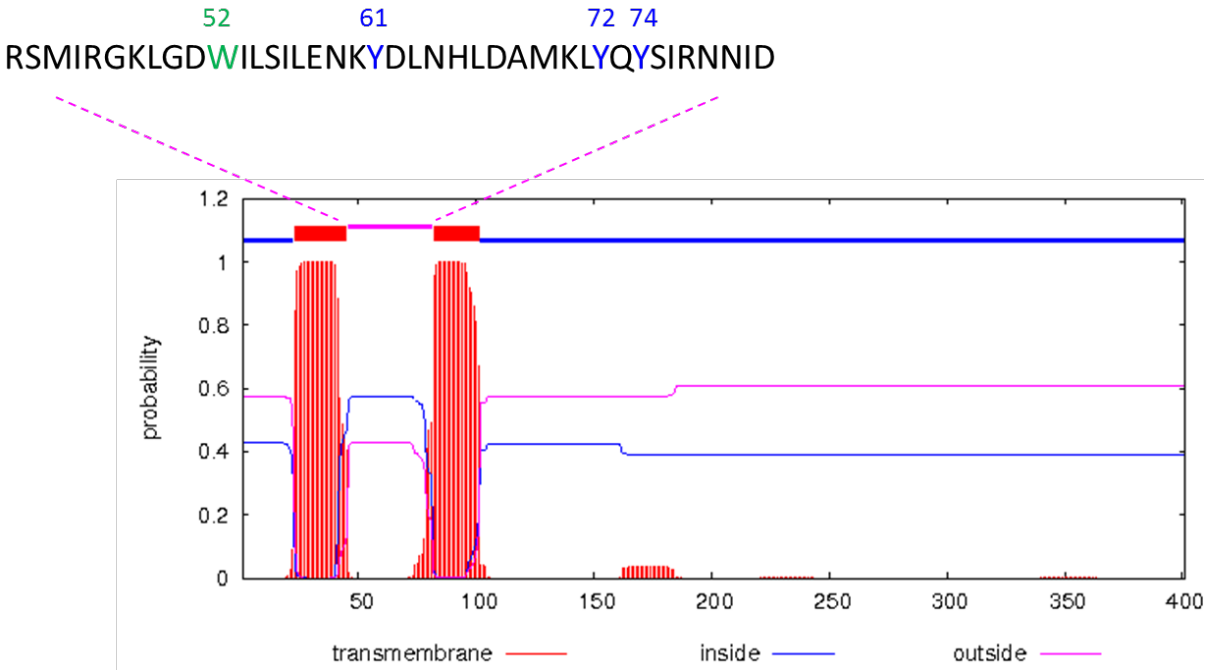

Figure 1.4-1: Predicted transmembrane regions of His_6-tagged $VanS_A$ (TMHMM), showing amino acid sequence for the average region predicted to lie extracellular between the predicted transmembrane regions.

TMHMM resource available at (http://www.cbs.dtu.dk/services/TMHMM-2.0/)

1.5. TMpred

Sequence: MNS...HHH,

length: 401

Prediction parameters: TM-helix length between 17 and 33

TMpred resource available at http://embnet.vital-it.ch/software/TMPRED_form.html

---

1.5.1. Possible transmembrane helices

The sequence positions in brackets denominate the core region.

Only scores above 500 are considered significant.

```
Inside to outside helices :   2 found
      from        to    score center
  23 (  23)  41 (  41)   2584     33
  80 (  82) 101 ( 101)   1854     90

Outside to inside helices :   3 found
      from        to    score center
  25 (  25)  41 (  41)   3023     33
  79 (  82) 100 ( 100)   2357     91
 334 ( 337) 355 ( 355)     66    345
```

1.5.2. Table of correspondences

Here is shown, which of the inside->outside helices correspond to which of the outside->inside helices.

Helices shown in brackets are considered insignificant. A "+"-symbol indicates a preference of this orientation. A "++"-symbol indicates a strong preference of this orientation.

```
          inside->outside | outside->inside
   23-  41 (19) 2584      |    25-  41 (17) 3023 ++
   80- 101 (22) 1854      |    79- 100 (22) 2357 ++
                         |(  334- 355 (22)   66 ++ )
```

1.5.3. Suggested models for transmembrane topology

These suggestions are purely speculative and should be used with **extreme caution** since they are based on the assumption that all transmembrane helices have been found. In most cases, the Correspondence Table shown above or the prediction plot that is also created should be used for the topology assignment of unknown proteins.

```
2 possible models considered, only significant TM-segments used

-----> STRONGLY prefered model: N-terminus inside
 2 strong transmembrane helices, total score : 4941
 # from   to length score orientation
 1   23   41 (19)    2584 i-o
 2   79  100 (22)    2357 o-i
```

------> alternative model

2 strong transmembrane helices, total score : 4877

#	from	to	length	score	orientation
1	25	41	(17)	3023	o-i
2	80	101	(22)	1854	i-o

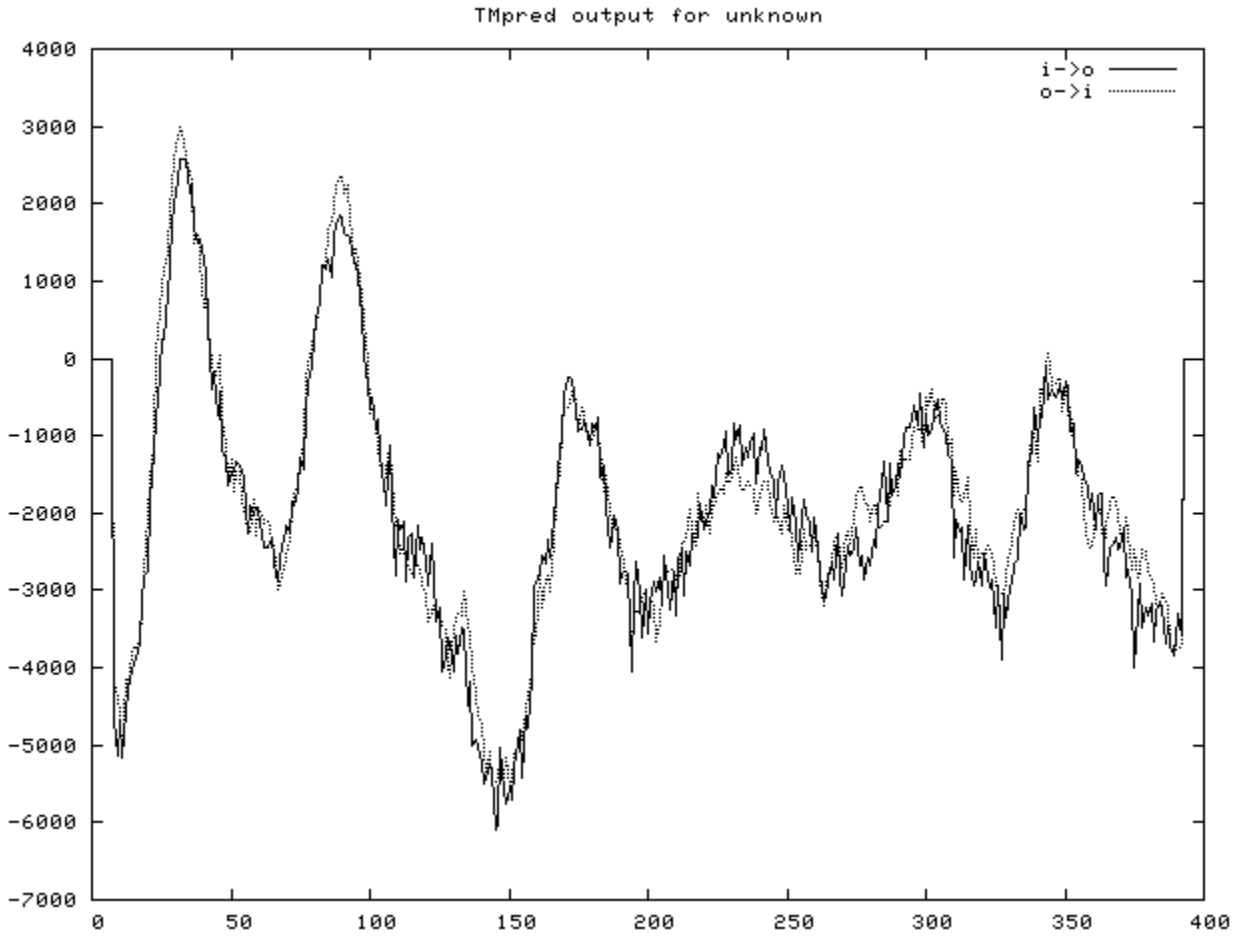

1.6. Fluorescence

	Absorption		Fluorescence	
Amino Acid	**Wavelength (nm)**	**Absorptivity**	**Wavelength (nm)**	**Quantum Yield**
Tryptophan	280	5,600	348	0.20
Tyrosine	274	1,400	303	0.14
Phenylalanine	257	200	282	0.04

Table 1.6-1: Common excitation and emission wavelengths of aromatic amino acids (pH 7.5). Adapted from (Wrolstad *et al*. 2005).

LIST OF PUBLICATIONS

R. Hussain, S. E. Harding, C. S. Hughes, P. Ma, S. G. Patching, S. Edara, G. Siligardi, P. J. F. Henderson, M. K. Phillips-jones (2016). **Purification of bacterial membrane sensor kinases and biophysical methods for determination of their ligand and inhibitor interactions.** Biochemical Society Transactions, (44):810 – 823.

DOI: 10.1042/BST20160023

Mary K. Phillips-jones, Guy Channell, Claire J. Kelsall, Charlotte S. Hughes, Alison E. Ashcroft, Simon G. Patching, Vlad Dinu, Richard B. Gillis, Gary G. Adams, Stephen E. Harding (2017)**. Hydrodynamics of the VanA-type VanS histidine kinase: an extended solution conformation and first evidence for interactions with vancomycin.** Scientific Reports, (7):46180.

DOI: 10.1038/srep46180

C. S. Hughes, E. Longo, M. K. Phillips-jones, R. Hussain (2017). **Characterisation of the selective binding of antibiotics vancomycin and teicoplanin by the VanS receptor regulating type A vancomycin resistance in the enterococci.** Biochimica Et Biophysica Acta (bba) - General Subjects, (1861):1951 – 1959.

DOI: 10.1016/j.bbagen.2017.05.011

C. S. Hughes, E. Longo, M. Phillips-jones, R. Hussain (2017). **Quality control and biophysical characterisation data of $VanS_A$.** Data In Brief, (14):41 – 47.

DOI: 10.1016/j.dib.2017.07.012